Enzyme Active Site Mimics Based on TriAzaCyclophane (TAC)-Scaffolded Peptides and Amino Acid Residues

Nabootsingen van het Actieve Gebied van Enzymen
op Basis van aan TriAzaCyclofaan (TAC)
Gebonden Peptiden en Aminozuur-Residuen

(met een samenvatting in het Nederlands)

Proefschrift

ter verkrijging van de graad van doctor aan de Universiteit Utrecht
op gezag van de rector magnificus, prof.dr. J.C. Stoof,
ingevolge het besluit van het college voor promoties
in het openbaar te verdedigen op
maandag 21 december 2009
des middags te 12.45 uur

door

Hendrik Bauke Albada

geboren op 1 november 1979 te Sneek

Promotor: Prof.dr. R.M.J. Liskamp

Work described in this thesis was financially supported by IDECAT. Printing of this thesis was financially supported by Shimadzu.

Enzyme Active Site Mimics based on TriAzaCyclophane (TAC)-Scaffolded Peptides and Amino Acid Residues

voor mijn ouders

ISBN: 978-90-393-5248-9

Cover design: Sjanet Albada en Bauke Albada

Table of Contents

		page numbers
Chapter 1	*General Introduction on Catalysis, Enzymes, Enzyme Models and Enzyme Mimics*	7-24
Chapter 2	*Synthesis and Analysis of Small and Flexible TAC-based Serine Hydrolase Active Site Mimics*	25-52
Chapter 3	*TAC-Scaffolded Tripeptides as Artificial Hydrolytic Receptors: A Combinatorial Approach Toward Esterase Mimics*	53-72
Chapter 4	*Amide-Bond Cyclized TAC-based Cryptand Molecules Containing all Relevant Components of Serine Hydrolase Active Sites*	73-96
Chapter 5	*1,2,3-Triazole Cyclized TAC-based Cryptand Molecules Containing all Relevant Components of Serine Hydrolase Active Sites*	97-118
Chapter 6	*Metalloenzyme Active Site Mimics Based on Aspartic Acid and Histidine Residues Containing TAC-Scaffolds*	119-144
Chapter 7	*Biomimetic Chemistry of Metalloenzyme Active Site Mimics Based on a TAC-Scaffold Decorated with Aspartic Acid and Histidine Residues*	145-166
Chapter 8	*Application of tris-Histidine Containing TACzymes in Asymmetric Copper(II)-Catalyzed Diels-Alder Reactions and Michael Additions*	167-178
Chapter 9	*Synthesis of Vancomycin-TACzyme Conjugates and Evaluation of their Applicability as Scorpionate Antibiotics*	179-198
Appendix A	*Supramolecular Chemistry of Peptidic TAC-based Amphiphilic Molecules*	199-202
Chapter 10	*Summary and Outlook*	203-210
	Nederlandse Samenvatting	211-218
	List of Abbreviations	219-220
	List of Publications	221
	Curriculum Vitae	223
	Dankwoord	225-228

Chapter 1

General Introduction on Catalysis, Enzymes, Enzyme Models and Enzyme Mimics

Abstract

Ever since the discovery of enzymes and the unraveling of their role as catalysts, scientists have been challenged to mimic their properties. This challenge has been substantially maintained due to the ever increasing knowledge on enzyme mechanisms on one hand, and an expansion of synthetic skills on the other. Knowledge on enzyme mechanisms helps to appreciate the parameters that are important to mimic their properties, whereas synthetic skills are needed in order to incorporate these properties into (an) organic molecule(s). An overview of the main examples of enzyme mimicry is given, followed by an outline of this thesis.

1. Introduction on catalysis and catalysts

The conversion of molecules can be catalyzed by molecular entities. Such a molecular entity is called a catalyst and the assistance itself is called catalysis.[1] To be precise, a catalyst is defined as '*a substance which when present in small amounts increases the rate of a chemical reaction but which is chemically unchanged by the reaction*'.[1] In addition, the process of catalysis is defined as '*the effect produced in facilitating a chemical reaction, by the presence of a substance, which itself undergoes no permanent change*'.[1]

Depending on the catalyst – whether it is a small organic compound or a coordination complex, a metal-containing surface, or a biomolecule – catalysis is usually classified as homogeneous catalysis, heterogeneous catalysis or biocatalysis.[2] Each of these areas has its advantages and disadvantages. For instance, homogeneous catalysts are very powerful at generating selectively new chiral centers, but regeneration of the catalysts is sometimes difficult.[3] On the other hand, heterogeneous catalysts are easily separated from the reactions mixture but are less potent when it comes to stereospecificity.[4] In addition, biocatalysts are extremely active[5] and display the highest selectivity and specificity known, but their stability and reaction scope are usually limited. In view of the unparalled activity and specificity of enzymes in general, it is not surprising that they have served and still serve as a tremendous source of inspiration for the construction of new catalysts.

1.1. Enzymes and enzymatic activity[6]

Enzymes are catalytic proteins and are essential for life. They can be roughly classified as *functional group* enzymes or as *metallo*enzymes. *Functional group* enzymes catalyze reactions only via functional groups present in the side chains of the polypeptide backbone of the enzyme. Alternatively, *metallo*enzymes use some of these functional groups to immobilize metal-ions for catalytic purposes.

Since the discovery of enzymes, ideas about their structure have changed from proteins that have ordered structures[7] to proteins with significant degrees of flexibility.[8] Recently it became clear that enzymes usually display irregular windows of activity.[9] The remarkable properties of enzymes have been attributed to several factors, of which increased reactivity of catalytic groups and transition state stabilization[10] in the microenvironment of the active site are most noteworthy.[11,12] Most enzymes derive the greater part of their catalytic activity by a combination of these and other factors.[13]

Nowadays, it is clear not all factors that contribute to enzymatic catalysis can be included in small synthetic mimics.[14] Whereas our understanding of enzymatic activity has grown enormously over the past decades, the synthesis of reliable enzyme mimics has been slower, although important steps have been taken and novel catalytic entities have been constructed.

2. Mimicry of enzymatic activity and of enzyme active sites[15]

The attempts that have been undertaken to mimic enzymatic activity have covered the entire spectrum of synthetic molecules, ranging from small well-defined designed molecules to large less-defined and heterodisperse polymers. Both *functional group enzymes* and *metalloenzymes* have been mimicked by synthetic molecules, of which several will be mentioned below (*figures 1* and *2*). In general, enzyme mimics can be classified as either bio-inspired or bio-mimetic. The first category refers to mimics that are focused on *achieving the function under ambient conditions*, the second category aims at *close structural mimicry of the active site of an enzyme*.[16] Obviously, the perfect mimic combines the activity of a bio-inspired mimic with the active site resemblance of a bio-mimetic molecular construct.

Even before a crystal structure of a hydrolase - hydrolases are one of the largest categories of functional group enzymes - was described, a few attempts were undertaken to mimic its activity (*figure 1*). For instance, in 1965 Cramer *et al*. decorated a cyclodextrin molecule with imidazole rings and showed an increased rate of hydrolysis of certain esters as result of the presence of the imidazole rings.[17] Soon after the first three-dimensional structures of hydrolytic enzymes were published, the first bio-mimetic molecules of a specific part of, for instance, the Asp-His-Ser[18] catalytic triad emerged.[19] With the dawn of host-guest chemistry, initiated by Pedersen *et al*.[20] and later extended by Lehn *et al*. and Cram *et al*.,[21] principles of supramolecular chemistry were incorporated into enzyme models. For example, Bender *et al*. derivatized cyclodextrin, a known host for small apolar molecules, with an Asp-His dyad earlier used by Bruice *et al*.[22] and Fife *et al*.[19] in order to construct a bio-mimetic molecule of a serine hydrolase.[23] Later, Breslow *et al*. extended the use of cyclodextrin molecules as hosts for substrates which can be hydrolyzed.[24]

A bio-inspired approach was followed by Lehn *et al*. using a crown-ether decorated with cysteine-residues in which hydrolysis of an ester was mediated by the thiolate nucleophiles.[25] In another approach, Diederich *et al*. described the synthesis and evaluation of a macrocyclic host-molecule at the core of which a nucleophilic phenoxy-group was positioned.[26] Around the same time, Cram *et al*. worked extensively on the construction of what has been described 'the ultimate target host'.[27] Even though they never achieved this goal, many insightful discoveries were made along the path that was taken. In addition to the above-mentioned supramolecular approaches - in which cyclodextrins, crown-ethers and related structures were used - Hamilton, Rebek and their co-workers used tweezer-like or tetrapodal constructs, respectively, as catalytic host molecules.[28] Apart from these small-molecule approaches larger constructs like dendrimers, polymers and nanoparticles have also been used.[29] For instance, the group of Reymond used peptide-dendrimers as hydrolysis catalysts (*vide infra*).[30] Also, Kulkarni *et al*. and Suh *et al*. have used molecular imprinted polymers as mimics of

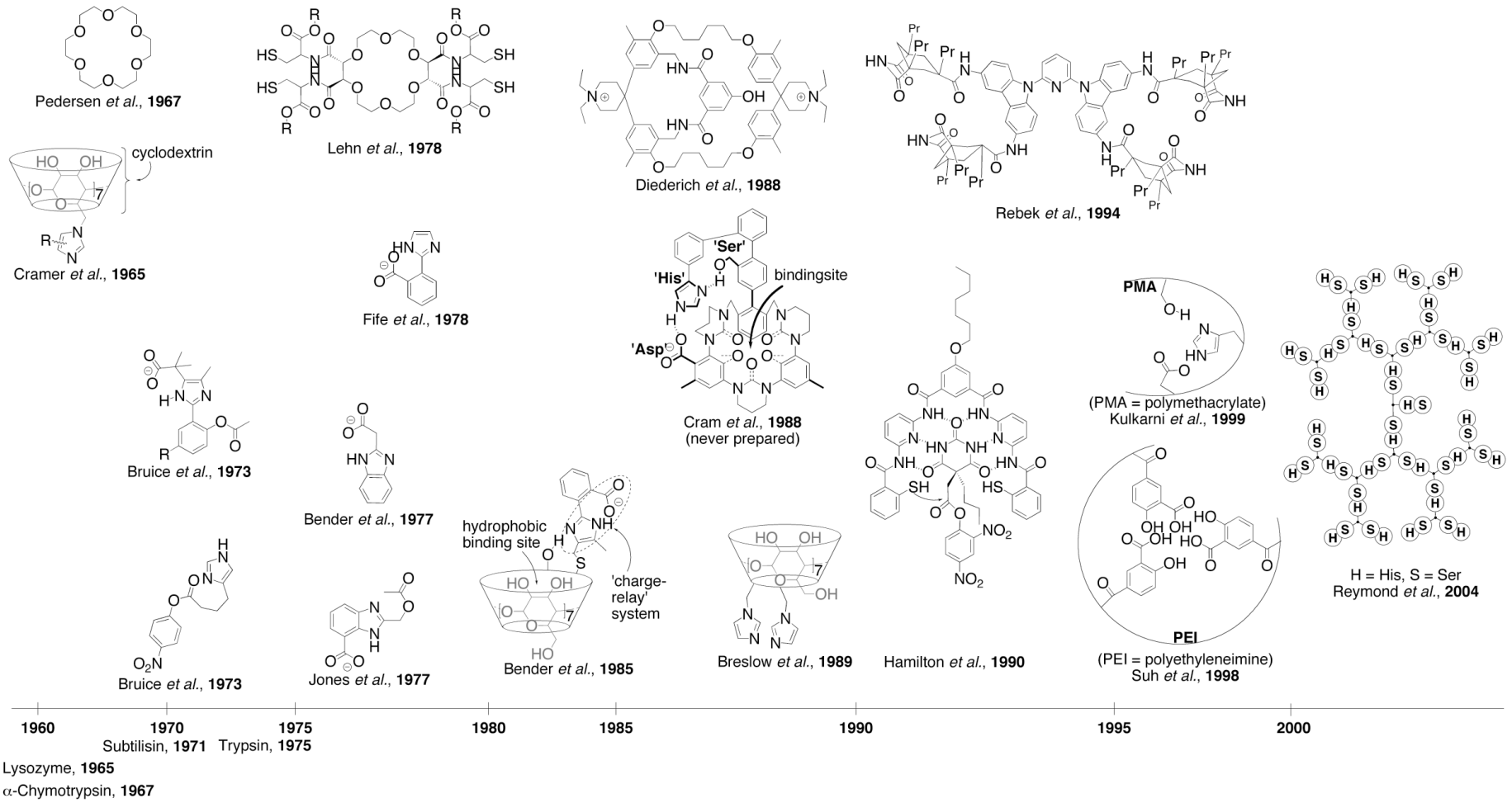

Figure 1. Overview of several synthetic mimics of hydrolytic enzymes.[15,40] The years in which the first X-ray crystal-structure of the mimicked enzymes was reported are indicated below the timeline. The start of supramolecular chemistry is marked by the crown ether described by Pedersen *et al*. in 1967.

hydrolytic enzymes.[31] More recently, gold-nanoparticles decorated with imidazole-carboxylate dyads showed hydrolytic activity towards activated esters.[32]

A similar historical outline can be constructed for metalloenzymes (*figure 2*).[41,33] Whereas mimicry of functional group enzymes relied largely on synthetic organic chemistry, mimicry of metalloenzymes was based mainly on inorganic chemistry methods and methodology in general and in particular coordination chemistry.[34] As was the case for mimics of functional group enzymes, progress in synthetic and analytical techniques resulted in the construction of more sophisticated and more active metalloenzyme mimics.

Remarkably, a few bio-inspired mimics of copper metalloenzymes assisted in the clarification of the mechanism of action of these enzymes even before the crystal-structure of the enzyme was elucidated. For instance, both Karlin *et al*. and Kitajima *et al*. described the synthesis and characterization of a Cu_2O_2-complex and indicated its possible resemblance with the corresponding biological systems.[35] Later, X-ray crystallography indeed showed that a similar Cu_2O_2-core was present in the active site of the common oxygen-carrier hemocyanin.[36] Subsequent work on mimics of this Cu_2O_2-active site strongly indicated that a similar active site had to be present in tyrosinase oxidase and catechol oxidase. Indeed, after cystallization and structural elucidation of the CuO-species of tyrosinase oxidase in 2006[37] and catechol oxidase in 1998[38], this hypothesis was confirmed.

The reverse order of events, in which disclosure of the structure of an enzyme active site predates mimicking attempts occurs more often. However, in almost all cases, a detailed structure of the active site of the enzyme, in some cases together with a substrate derivative, is available before enzyme mimics are studied. A striking example is mimicry of mononuclear non-heme iron active sites.[39]

These active sites, mostly based on the 2-histidine-1-carboxylate triad,[42] have recently been uncovered as a new common motif for the activation of dioxygen.[43] This triad has been discovered in more than 30 different enzymes. Enzymes that contain this triad have been shown to catalyze various processes, including oxidative cleavage of catechols[44], oxidation of carbon-carbon double bonds,[44] oxidation of aliphatic[45] or aromatic[46] CH-groups and oxidative double ring closure[47]. In view of this large range of catalytic transformations, it is not surprising that many model-systems have been described.[39,48] The majority of these models are based on functional groups that act as ligands such as amine-groups, pyridine rings, pyrazole rings or Schiff-base moieties. Even though Nature mostly relies on the imidazole ring of the histidine amino acid residue and the carboxylate functionalities of aspartate and glutamate amino acids, these bio-inspired mimics were capable of catalyzing the oxidation of cyclooctene to either the *cis*-diol or the epoxide.[49] The ratio between cis-diol and epoxide strongly depended on the ligand that was used.

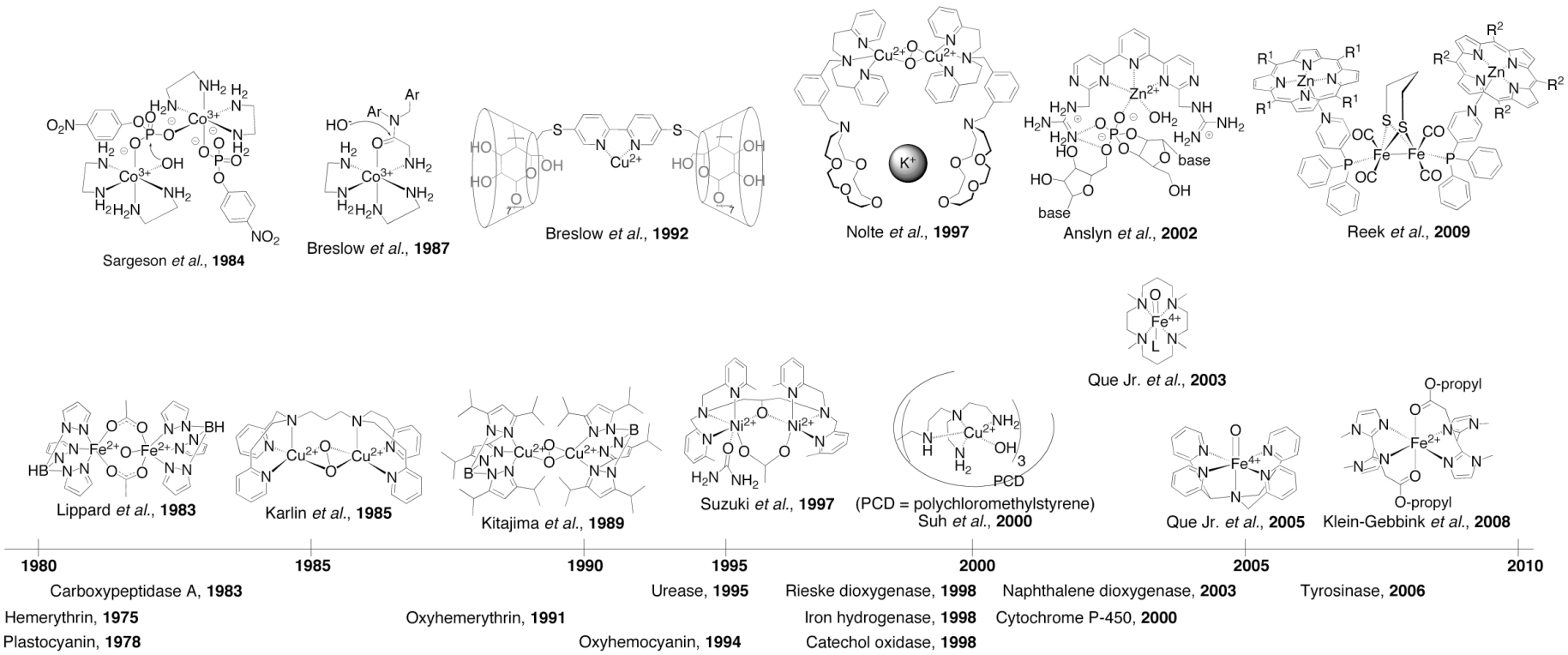

Figure 2. Overview of several synthetic mimics of metalloenzymes.[41] The years in which the first X-ray crystal-structure of the mimicked enzymes was reported are indicated below the timeline.

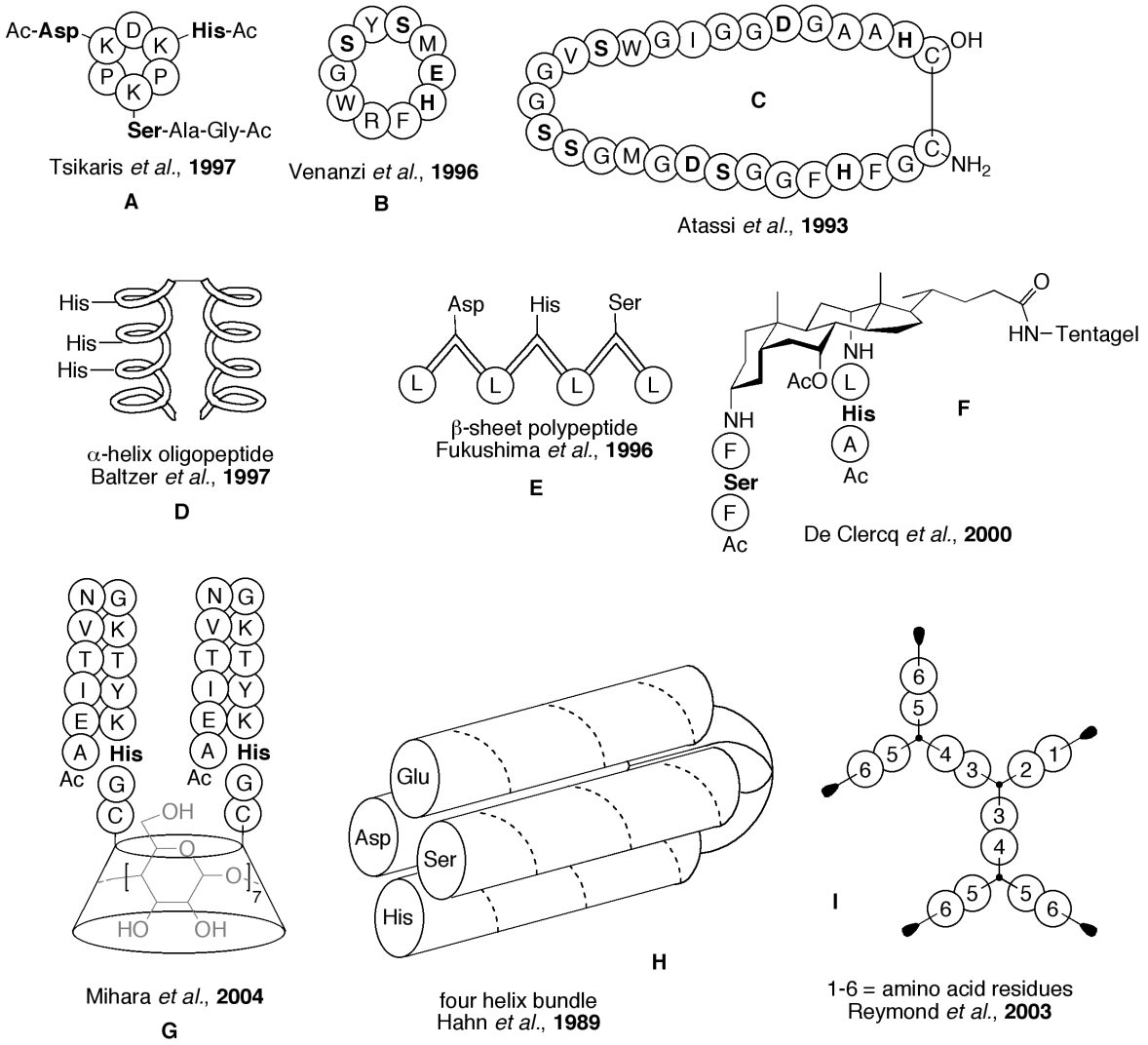

Figure 3. Typical examples of peptides and scaffolded peptides as hydrolase mimics. The mimics of Atassi *et al*. and Hahn *et al*. could not be reproduced.[55] The one-letter code and three letter code for amino acids is given in the list of abbreviations in Appendix C.

Although many models of enzymatic activity or enzyme active sites have been based on synthetic organic molecules, synthetic peptides have also been used to a smaller extent. One main problem with the application of synthetic peptides in the construction of enzyme mimics is the intrinsic flexibility of peptides. This hampers the design and synthesis of a pre-organized structure in which the functional groups are positioned similarly to those of the active site of the enzyme it is supposed to mimic.[50]

2.1. Peptidic constructs as mimics of functional group enzymes

The class of *functional group* enzymes comprising serine hydrolases has received a significant amount of attention for mimicry purposes. The delicately tuned cooperative interaction of the functional groups of the catalytic triad residues has inspired many chemists to construct peptide-based mimics of these enzymes. After discovery of

solid-phase peptide synthesis by Merrifield,[51] the rapid generation of many peptidic constructs became possible. Also, solid-phase split-mix libraries of peptides could be prepared and screened for catalytic properties.[52] Since enzymes are polypeptides, it would be very interesting to determine the extent in which peptides could be used as synthetic mimics of enzymatic activity. In addition, tuning of the catalytic properties is usually more convenient for peptides than for enzymes, which makes this an interesting line of research.

Unfortunately, the earliest attempts to use peptidic constructs as serine hydrolase mimics, although initially promising,[53,54] could not be reproduced and were at least considered as suspicious.[55] Later, other approaches leading to more modest results, *i.e.* hydrolysis of activated esters instead of hydrolysis of amide bonds, were described (*figure 3*). Peptides with α-helix[56] (*figure 3*, **D**) or β-sheet[57] (*figure 3*, **E**) secondary structures showed hydrolytic activity. Cyclic peptides, one with the Asp-His-Ser triad attached onto the cyclic peptide[58] (*figure 3*, **A**) and one with the triad positioned in the ring[59] (*figure 3*, **B**), showed poor hydrolytic activity. Even though the activity of these constructs was low, the ease by which these bio-mimetic systems that contained a high density of functional groups could be synthesized and analyzed illustrated the usefulness and applicability of peptide-chemistry for the construction of enzyme mimics. This was especially evident from the recent research by Reymond *et al.* on hydrolytic peptide dendrimers.[60] By a reliable and rapid method, a large library of potentially catalytic peptide dendrimers was constructed (*figure 3*, **I**), screened and analyzed,[61] revealing peptidic constructs with almost enzyme-like activity-profiles. Unfortunately, these dendrimers were only capable of hydrolysis of activated esters whereas hydrolysis of amide-bonds constructs remained elusive. Finally, scaffolded peptidic constructs (*figure 3*, **F** and **G**) have also been used as serine hydrolase mimics.[62,63] Although these constructs had a poor activity, they represented a novel approach in the construction of peptidic hydrolysis catalysts (*vide infra*).

2.2. Peptidic constructs as mimics of metalloenzymes

As was mentioned above, mimics of metalloenzymes mostly relied on inorganic or organometallic approaches. Nevertheless, some approaches in which peptidic constructs were used as mimics of metalloenzymes have been described.

Peptide-based models, especially scaffolded peptides,[64] have been helpful for elucidation of the role of proteins in tuning the chemical properties of metal centers that are common in metalloenzymes.[65] For instance, Kaiser *et al.* studied helical peptides that were attached to porphyrin as the first generation of models for hemeproteins (*figure 4*, **A**).[66] Hähnel *et al.* attached helical peptides to a RAFT peptide and used this as a water-soluble cytochrome b model protein (*figure 4*, **B**).[67] These constructs have been especially useful in determining the effect of the amino acid sequence on the stability of the model protein, the coordination chemistry of the metal-ion as well

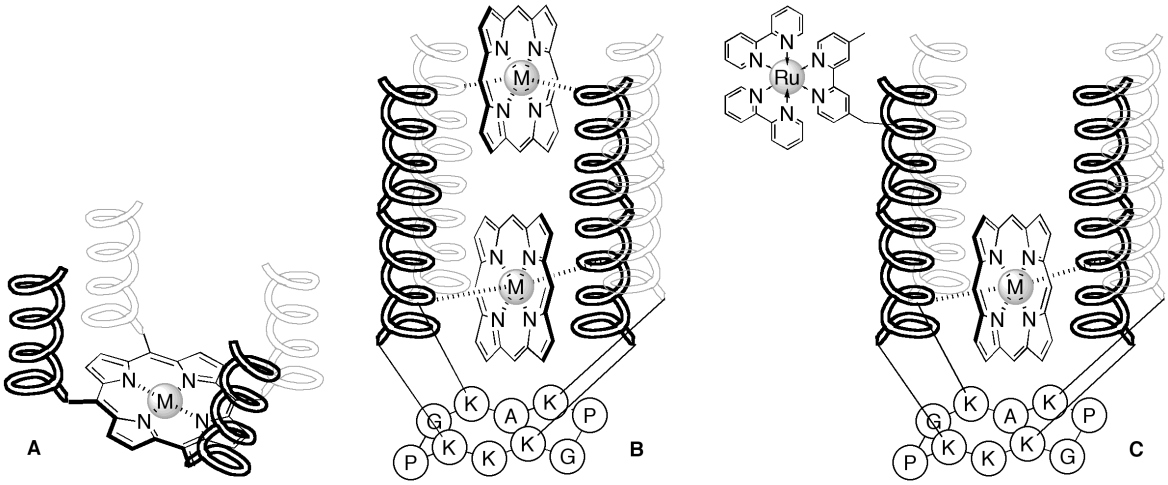

Figure 4. Typical examples of template-assisted synthetic proteins that have been used as enzyme mimics.

as the functional properties of the heme cofactor.[68] The diversity of the scaffold that was used also allowed combinatorial synthesis of model-proteins and screening of the constructs for binding to cofactors like heme groups, Cu(II), flavin or Ru-bipyridine (*figure 4*, **C**).[69] Subsequently, properties like charge transfer, redox potential but also enzymatic activity and folding stability were assessed. This mix of design and combinatorial chemistry proved to be very fruitful and resulted in the construction of Cu(II)-binding model proteins in which the properties of the metal-centre could be modified by subtle changes in the metal-centre flanking helices.[64]

Since metalloenzymes rely on the properties of immobilized metal-ions, which on its turn can be influenced by the surrounding protein scaffold, investigations of model-peptides might lead to a better understanding of the interaction between metal-ion and peptide or protein. As a result of that, improved enzyme mimics or artificial enzymes may be constructed which also might add to our understanding of enzymatic activity.

3. Scaffolded peptides

In the above-mentioned work on metalloenzyme mimicking model proteins, the role of the synthetic scaffold was crucial.[64] This scaffold allowed chemists to replace the bulk of the protein and to study the interaction between metal-ion and protein mimic in great detail.

Several scaffolds have been described in the literature, which can be classified as diversity oriented, pre-organization oriented, or a combination of both (*figure 5*). On one hand, diversity oriented scaffolds allow the introduction of different peptides onto the scaffold molecule. On the other hand, pre-organizing scaffolds are capable of orienting the attached peptides in a convergent manner but do not allow the

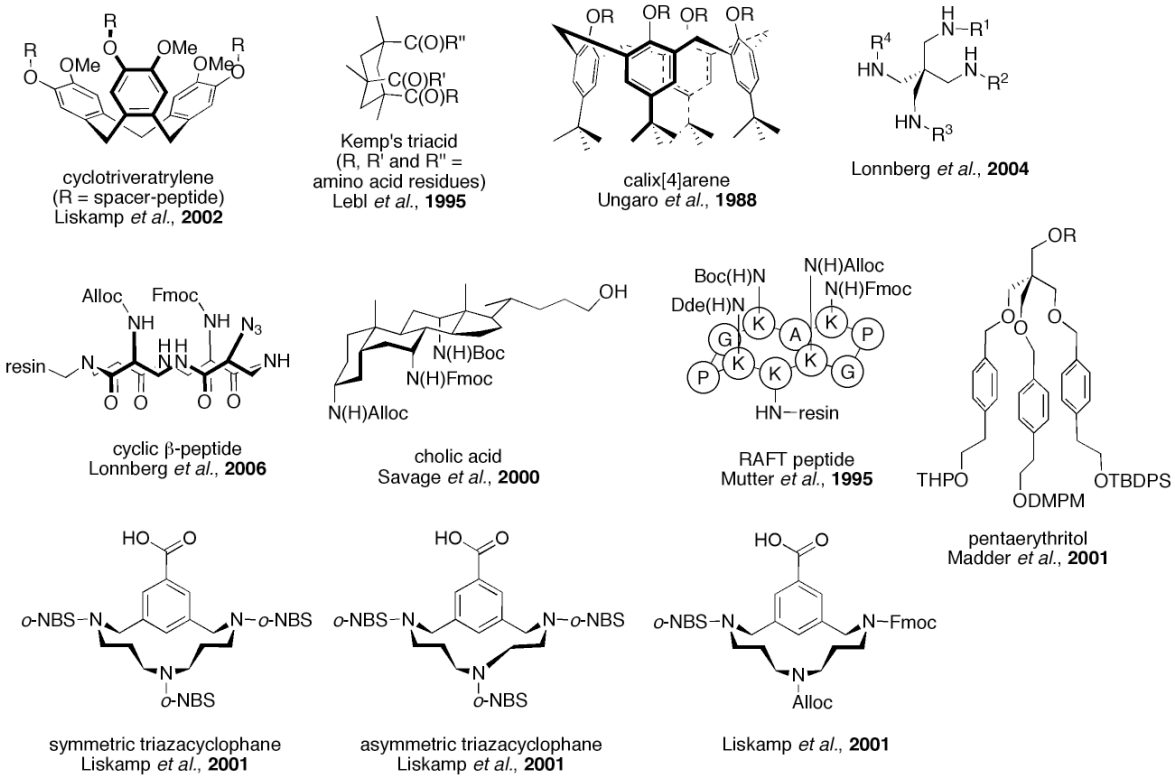

Figure 5. Overview of scaffold molecules that have been used for the attachment of carbohydrate residues, amino acid residues or peptides-chains.[62,64,70]

attachment of different peptides. A combination of both has shown to be very useful in biomimetic chemistry (*vide supra*).

Most of the scaffolds described have only been marginally explored with respect to their applicability in (solid-phase) peptide chemistry. However, a few have proven their value as platforms for the construction of synthetic protein-like structures. For instance, the cyclotriveratrylene (CTV)[71] scaffold has been used as a template for the construction of (synthetic) collagen mimics,[72] synthetic receptors,[73] and for the preparation of trivalent amino acid glycoconjugates.[74] Similarly, calix[4]arene[75] scaffolds have been used for the construction of cyclic-peptide containing constructs[76] and enzyme mimics.[77] The scaffold developed by Madder *et al*. was already published in 2001, and recently the application in the construction of serine hydrolase mimics was described.[78]

Together with applications of the RAFT scaffold described by Mutter *et al*. (*vide supra*),[79] the TAC-scaffold[80] has been one of the most often applied scaffolds in peptide-chemistry. It was initially developed for the construction libraries of tripodal peptidic receptors capable of binding to small fluorescently labeled peptides[81] (*figure 6*, **B** and **D**) or iron(III) ions (*figure 6*, **A**)[82]. These were the first examples in which a scaffold was decorated with different three different peptide-chains and used as receptors for biologically relevant molecular entities. More recently, the TAC-scaffold was used for the construction of a synthetic mimic of cystatin B, which is a protein inhibitor of

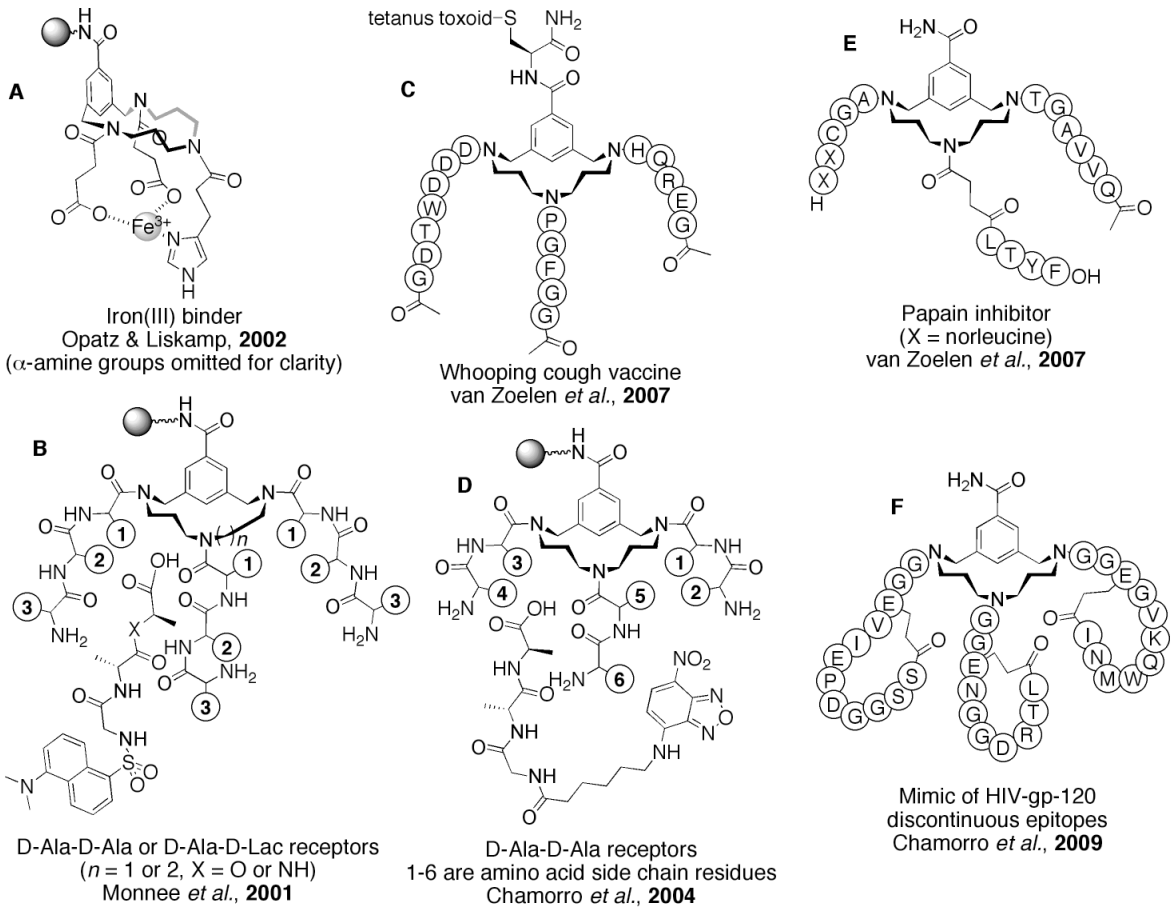

Figure 6. Overview of some applications for TAC-based peptidic constructs.

papain, resulting in a potent inhibitor (*figure 6*, **E**)[83]. Additionally, the TAC-scaffold was used as a platform for the construction of a synthetic vaccine, which generated protective antibodies against whooping cough (*figure 6*, **C**).[84] Even more, the non-stop solid-phase synthesis of a protein mimic containing three peptide loops as a mimic of discontinuous epitopes was recently unclosed (*figure 6*, **F**).[85] These applications revealed the enormous potential of TAC-scaffolded peptides in medicinal chemistry and chemical biology.

Although the TAC-scaffolds have been used in many biologically relevant systems – ranging from the construction of artificial synthetic receptors for peptides of pathogenic organisms to synthetic vaccines – their applicability as scaffolds for the construction of peptide-based enzyme (active site) mimics was unexplored. In this thesis, we describe our efforts toward the construction and analysis of TAC-based peptidic enzyme active site mimics.

4. Outline of the thesis

In this thesis, a symmetrical triazacyclophane (TAC) scaffold will be used in several approaches for the construction of enzyme active sites. TAC-based mimics of functional

group enzymes, especially the serine hydrolases, are described in **chapters 2-5**. In **chapters 6** and **7**, TAC-based mimics of three common metalloenzyme active sites are described. Two novel applications of the TAC-based tris-histidine triad mimic, *i.e.* in asymmetric Cu(II)-catalyzed reactions and in the construction of novel antibiotics, are described in **chapter 8** and **9**, respectively. **Chapter 10** contains a brief description of some interesting results and clues for future applications of TAC-based peptidic constructs in catalysis, drug design and supramolecular chemistry.

In **chapter 2**, three of the smallest possible TAC-based mimics of serine hydrolase active sites are presented. The hydrolytic activity of these three mimics is assessed and shown to be similar to that of 4-methylimidazole. Subsequent NMR-studies of one mimic and two TAC-containing analogues revealed that these small TAC-based constructs were highly flexible. This indicates that the pre-organizing properties of the TAC-scaffold are limited.

In view of the low activity and the flexibility of the constructs, a combinatorial search for artificial synthetic receptors as esterase mimics was employed (**chapter 3**). Inspiration for the construction of the library was obtained from the active sites of serine and cysteine hydrolases as well as from β-lactamases. A library of almost 20,000 potential hydrolysis catalysts was obtained by split-mix synthesis; *N*-terminal amine functionalities were capped with base labile trifluoroacetyl groups. The obtained library was screened for activity using the latent fluorescent substrate 7-acetoxycoumarin. Hits that were visualized by fluorescent microscopy were selected, sequenced by Edman degradation and resynthesized. The activity of the resynthesized members was determined and compared to small analogues. As was the case for the small serine hydrolase active site mimics that were described in **chapter 2**, the hydrolytic activity of the hits that were discovered by this combinatorial approach was also low. Apparently, the extended peptide-chains could not enforce pre-organization to a significant extent.

In order to tackle the problem of flexibility, **chapter 4** and **chapter 5** describe two approached for the construction of TAC-based serine hydrolase mimicking cryptand molecules. In **chapter 4**, amide-bond forming reactions are used to perform the double cyclization reaction. Although the target compound was obtained, the yields were disappointingly low and the activity of the construct could not be determined. Therefore, we shifted our attention from amide-bond to cyclized cryptands to cryptand molecules in which the arms were connected by 1,2,3-triazole rings (**chapter 5**). This double cyclization is achieved by the copper-catalyzed alkyne-azide cycloaddition "click" reaction. We showed that the click reaction could be performed on the solid-support using a test-reaction. The conditions that were successful in this reaction were applied in the double cyclization reaction of the resin-bound cryptand precursor. After cumbersome crucial purification the desired compound was obtained. Again,

the amount of compound that was obtained was too small to determine the structure and activity of the construct.

In **chapter 6** and **7** efforts are described towards the construction of TAC-based mimics of three distinct metalloenzyme active sites. In **chapter 6**, the synthesis of the TAC-based mimics of the frequently occurring 3-histidine, 2-histidine-1-aspartate, and 1-histidine-2-aspartate triad metalloenzyme active sites is described. The interaction of these mimics with Cu(II) in solution are studied using UV-vis spectroscopy and ESI-MS spectrometry. Infrared and Raman analysis of the dried samples provided insight in the changes in functional groups as result of the interaction with Cu(II). From these studies it became clear that TAC-based mimics of metalloenzyme active sites could be prepared. Coordination of the amino acid side-chain functionalities was similar to those in metalloenzymes. Encouraged by these results, we studied the application of these mimics in two important biomimetic reactions (**chapter 7**). The reactions studied are oxygen-binding by Cu(I)-complexes and Fe(II)-H_2O_2 mediated olefin oxidation. UV-vis analysis of the reaction between Cu(I)-complexes and molecular oxygen from the air revealed that oxygen-binding occurred within 15 min. Infrared and Raman spectroscopic analysis of the resulting complexes showed that bis(μ-hydroxo) dicopper(II) complexes were formed. For the Fe(II)-H_2O_2 mediated olefin oxidation, the effect of the TAC-based ligands was only marginal. Again, the large degree of flexibility of these TAC-based constructs might have been the origin of this low effect.

In **chapter 8**, various derivatives of the TAC-based 3-histidine triads are used as chiral ligands in Cu(II)-catalyzed Diels-Alder and Michael addition reactions. For each of the reactions, the substrates were fully converted into the products with enantioselectivities up to approximately 50%. We also show that the chiral induction by these TAC-based ligand systems in these reactions can be tuned by both *N*- and *C*-terminal extensions.

In **chapter 9**, the synthesis and antibacterial activity of conjugates of a TAC-based tris-histidine triad mimic with vancomycin are described. The hydrolytic activity of the constructs could be increased by the attachment of the mimics to a dendrimeric core, which was shown in a model-system. Although the antibacterial activity was lower than that of vancomycin, it could be modulated by the addition of Zn(II).

In **appendix A** we describe the initial results that were obtained for a two TAC-based amphiphilic molecules with respect to their behavior in supramolecular chemistry. We anticipate that these amphiphilic structures can be used as drug-carriers or in the construction of catalytic vesicles. This thesis concludes with a summary and some guidelines for future research (**chapter 10**).

5. Notes and References:

1 See the Oxford English Dictionary at www.eod.com. The word 'catalysis' was used by Berzelius in 1836: '*Many bodies ... have the property of exerting on other bodies an action which is very different from chemical affinity. By means of this action they produce decomposition in bodies, and form new compounds into the composition of which they do not enter. This new power, hitherto unknown, is common both in organic and inorganic nature ... I shall ... call it catalytic power. I shall also call Catalysis the decomposition of bodies by this force.*' (Edin. New Phil. Jrnl. XXI. 223). See also: K.J. Laidler, *Pure & Appl. Chem.* **1996**, *68*, p. 155.

2 R.A. van Santen, P.W.N.M. van Leeuwen, J.A. Moulijn, B.A. Averill (editors), *Catalysis: An Integrated Approach, Second, Revised and Enlarged Edition*, Elsevier, Amsterdam, **1999**.

3 D.J. Cole-Hamilton, *Science* **2003**, *299*, 1702.

4 See: F. Zaera, *Acc. Chem. Res.* **2009**, *42*, 1152. A recent improvement was made using metal-organic frameworks: C.-D. Wu, W. Lin, *Angew. Chem. Int. Ed.* **2007**, *46*, 1075.

5 The uncatalyzed hydrolysis of peptide bonds can take 10-1000 years whereas enzymes can cleave peptide-bonds in milliseconds. See J.M. Berg, J.L. Tymoczko and L. Stryer, *Biochemistry*, 5th edition, **2006**, W.H. Freeman and company, chapter 9.

6 D.E. Metzler, *Biochemistry: The Chemical Reactions of Living Cells*, 2nd edition, Elsevier Academic Press, chapter 9.

7 J.B. Sumner, *J. Biol. Chem.* **1926**, *69*, 435.

8 D.E. Koshland, *Proc. Natl. Acad. Sci., USA* **1958**, *44*, 98. D.E. Koshland, *Nature* **2004**, *432*, 447. A general review on protein-protein interactions: D.D. Boehr, P.E. Wright, *Science* **2008**, *320*, 1429.

9 Q. Chen, R. Groote, H. Schönherr, G.J. Vancso, *Chem. Soc. Rev.* **2009**, *38*, 2671; W. Min, B.P. English, G. Luo, B.J. Cherayil, S.C. Kou, X.S. Xie, *Acc. Chem. Res.* **2005**, *38*, 923.

10 S.D. Lahiri, G. Zhang, D. Dunaway-Mariano, K.N. Allen, *Science* **2003**, *299*, 2067; A. Warshal, P.K. Sharma, M. Kato, Y. Xiang, H. Liu, M.H.M. Olsson, *Chem. Rev.* **2006**, *106*, 3210.

11 D. Ringe, G.A. Petsko, *Science* **2008**, *320*, 1428; D.C. Phillips, *Proc. Natl. Acad. Sci., USA* **1967**, *57*, 484.

12 Additional factors which play a role in enzymatic reactions are: distortion of the substrate (D.L. Pompliano, A. Peyman, J.R. Knowles, *Biochemistry* **1990**, *29*, 3186), the contribution of quantum mechanical tunneling to the rates of enzyme-catalyzed reactions whose mechanisms involve the transfer of hydrogen ions (Z.D. Nagel, J.P. Klinman, *Chem. Rev.* **2006**, *106*, 3095), precise matching of pK_a values of the donor and acceptor atoms in hydrogen bonds that stabilize the transition state, which can lead to short and symmetrical hydrogen bonds of greater-than-normal-strength (W.W. Cleland, P.A. Frey, J.A. Gerlt, *J. Biol. Chem.* **1998**, *273*, 25529; D.A. Kraut, P.A. Sigala, B. Pybus, C.W. Liu, D. Ringe, G.A. Petsko, D. Herschlag, *PLoS Biology* **2006**, *4*, e99, 0501), the role of protein dynamics in aiding the reacting species in crossing the transition-state barrier of the reaction (S. Hammes-Schiffers, S.J. Benkovic, *Annu. Rev. Biochem.* **2006**, *75*, 519; K.A. Henzler-Wildman, V. Thai, M. Lei, M. Ott, M. Wolf-Watz, T. Fenn, E. Pozharski, M.A. Wilson, G.A. Petsko, M. Karplus, C.G. Hübner, D. Kern, *Nature* **2007**, *450*, 838).

13 A. Fehrst, *Enzyme Structure and Mechanism in Protein Science: a Guide to Enzyme Catalysis and Protein Folding*, New York, W.H. Freeman and Company, **1999**; J.R. Knowles, *Nature* **1991**, *350*, 121; T.C. Bruicce, S.J. Benkovic, *Biochemistry* **2000**, *39*, 6267; D.A. Kraut, K.S. Carroll, D. Herschlag, *Annu. Rev. Biochem.* **2003**, *72*, 517; I. Schlichting, J. Berendzen, K. Chu, A.M. Stock, S.A. Maves, D.E. Benson, R.M. Sweet, D. Ringe, G.A. Petsko, S.D. Sligar, *Science* **2000**, *287*, 1615.

14 A.J. Kirby, *Angew. Chem., Int. Ed. Engl.* **1996**, *35*, 707.

15 R. Breslow, *Artificial Enzymes*, 1st ed. Wiley: Weinheim, Germany, **2005**; H. Dugas, *Bioorganic Chemistry:*

A Chemical Approach to Enzyme Action, Springer, New York, 3rd edn., **1996**; P. Ball, *Designing the Molecular World*, Princeton University Press: Princeton, NJ, **1994**, pp. 145-185.

16 S.J. Lippard, *Nature Chemical Biology* **2006**, *2*, 504.

17 F. Cramer, W. Kampe, *J. Am. Chem. Soc.* **1965**, *87*, 1115; F. Cramer, G. Mackensen, *Angew. Chem., Int. Ed. Engl.* **1966**, *5*, 601.

18 M. Paetzel, R.E. Dalbey, *Trends Biochem. Sci.* **1997**, *22*, 29; G. Dodson, A. Wlodawer, *Trends Biochem. Sci.* **1998**, *23*, 347; L. Hedstrom, *Chem. Rev.* **2002**, *102*, 4501.

19 T.H. Fife, R.J. Bambery, B.R. DeMark, *J. Am. Chem. Soc.* **1978**, *100*, 5500; J.B. Jones, K.E. Taylor, *Can. J. Chem.* **1977**, *55*, 1657.

20 C.J. Pedersen, *J. Am. Chem. Soc.* **1967**, *89*, 2495; C.J. Pedersen, *J. Am. Chem. Soc.* **1967**, *89*, 7017.

21 D.J. Cram, J.M. Cram, *Science* **1974**, *183*, 803; D.J. Cram, J.M. Cram, *Acc. Chem. Res.* **1978**, *11*, 8; D.J. Cram, *Science* **1988**, *240*, 760; D.J. Cram, *Angew. Chem. Int. Ed.* **1988**, *8*, 1009.

22 G.A. Rogers, T.C. Bruice, *J. Am. Chem. Soc.* **1973**, *95*, 4452.

23 V.T. D'Souza, M.L. Bender, *Acc. Chem. Res.* **1987**, *20*, 146.

24 R. Breslow, S.D. Dong, *Chem. Rev.* **1998**, *98*, 1997; R. Breslow, *Acc. Chem. Res.* **1995**, *28*, 146.

25 J.-M. Lehn, C. Sirlin, *Chem. Commun.* **1978**, 949.

26 F. Diederich, G. Schürmann, I. Chao, *J. Org. Chem.* **1988**, *53*, 2744.

27 For quote see: Y. Murakami, J. Kikuchi, Y. Hisaeda, O. Hayashida, *Chem. Rev.* **1996**, *96*, 721, see p 751.

28 P. Tecilla, A.D. Hamilton, *J. Chem. Soc., Chem. Commun.* **1990**, 1232; I. Huc. R.J. Pieters, J. Rebek, Jr., *J. Am. Chem. Soc.* **1994**, *116*, 10296.

29 G. Manecke, W. Storck, *Angew. Chem., Int. Ed. Engl.* **1978**, *17*, 657.

30 T. Darbre, J.-L. Reymond, *Acc. Chem. Res.* **2006**, *39*, 925.

31 B.S. Lele, M.G. Kulkarni, R.A. Mashelkar, *Reactive & Functional Polymers* **1999**, *39*, 37; J. Suh, *Acc. Chem. Res.* **2003**, *36*, 562.

32 P. Pengo, S. Polizzi, L. Pasquato, P. Scrimin, *J. Am. Chem. Soc.* **2005**, *127*, 1616.

33 See *Biological Inorganic Chemistry*, edited by I. Bertini, H.B. Gray, E.I. Stiefel, J.S. Valentine, 1st edition, University Science Books, Sausalito, **2007**; D.E. Fenton, *Biocoordination Chemistry*, Oxford University Press, 1st edition, **1995**.

34 D.F. Shriver, P.W. Atkins, *Inorganic Chemistry*, Oxford University Press: Ghent, Belgium, 3rd edition, **1999**.

35 K.D. Karlin, M.S. Haka, R.W. Cruse, Y. Gultneh, *J. Am. Chem. Soc.* **1985**, *107*, 5828; N. Kitajima, K. Fujisawa, Y. Moro-oka, K. Toriumi, *J. Am. Chem. Soc.* **1989**, *111*, 8975.

36 K.A. Magnus, B. Hazes, H. Ton-That, C Bonaventura, J. Bonaventura, W.G.J. Hol, *Proteins: Struct. Funct. Genet.* **1994**, *19*, 302. Hemocyanin: A. Volbeda, W.G.J. Hol, *J. Mol. Biol.* **1989**, *209*, 249

37 Y. Matoba, T. Kumagai, A. Yamamoto, H. Yoshitsu, M. Sugiyama, *J. Biol. Chem.* **2006**, *281*, 8981.

38 T. Klabunde, C. Eiken, J.C. Sacchettini, B. Krebs, *Nat. Struct. Biol.* **1998**, *5*, 1084.

39 M.M. Abu-Omar, A. Loaiza, N. Hontzeas, *Chem. Rev.* **2005**, *105*, 2227; M. Costas, M.P. Mehn, M.P. Jensen, L. Que, Jr. *Chem. Rev.* **2004**, *104*, 939.

40 Y. Murakami, J. Kikuchi, Y. Hisaeda, O. Hayashida, *Chem. Rev.* **1996**, *96*, 721. Trypsin: W. Bode, P. Schwager, *J. Mol. Biol.* **1975**, *98*, 693. Subtilisin: R.A. Alden, J.J. Birktoft, J. Kraut, J.D. Robertus, C.S. Wright, *Biochem. Biophys. Res. Commun.* **1971**, *54*, 337.

41 H.-B. Kraatz, N. Metzler-Nolte, *Concepts and Models in Bioinorganic Chemistry*, Wiley-VCH, Weinheim, Germany, **2006**; Iron hydrogenase: J.W. Peters, W.N. Lanzilotta, B.J. Lemon, L.C. Seefeldt, *Science* **1998**, *282*, 1853; R.J.M. Klein Gebbink, C.F. Martens, M.C. Feiters, K.D. Karlin, R.J.M. Nolte, *Chem. Commun.* **1997**, 389.

42 L. Que, Jr. *Nat. Struct. Biol.* **2000**, *7*, 182.

43 K.D. Koehntop, J.P. Emerson, L. Que, Jr. *J. Biol. Inorg. Chem.* **2005**, *10*, 87.
44 F.H. Vaillancourt, J.T. Bolin, L.D. Eltis, *Crit. Rev. Biochem. Mol. Biol.* **2006**, *41*, 241.
45 B. Yu, W.C. Edstrom, J. Benach, Y. Hamuro, P.C. Weber, B.R. Gibney, J.F. Hunt, *Nature* **2006**, *439*, 879.
46 B. Kauppi, K. Lee, E. Carredano, R.E. Parales, D.T. Gibson, H. Eklund, S. Ramaswamy, *Structure* **1998**, *6*, 571; A. Karlsson, J.V. Parales, R.E. Parales, D.T. Gibson, H. Eklund, S. Ramaswamy, *Science* **2003**, *299*, 1039.
47 N.I. Burzlaff, P.J. Rutledge, I.J. Clifton, C.M.H. Hensgens, M. Pickford, R.M. Adlington, P.L. Roach, J.E. Baldwin, *Nature* **1999**, *401*, 721; P.L. Roach, I.J. Clifton, C.M.H. Hensgens, N. Shibata, A.J. Long, R.W. Strange, S.S. Hasnain, C.J. Schofield, J.E. Baldwin, J. Hajdu, *Eur. J. Biochem.* **1996**, *242*, 736; P.L. Roach, I.J. Clifton, C.M.H. Hensgens, N. Shibata, C.J. Schofield, J. Hajdu, J.E. Baldwin, *Nature* **1997**, *387*, 827.
48 P.C.A. Bruijnincx, G. Van Koten, R.J.M. Klein Gebbink, *Chem. Soc. Rev.* **2008**, *37*, 2716.
49 T.A. Jackson, L. Que, Jr., *Structural and Functional Models for Oxygen-Activating Nonheme Iron Enzymes*, chapter 12, p 259, in *Concepts and Models in Bioinorganic Chemistry*, edited by H.-B. Kraatz, N. Metzler-Nolte, Wiley-VCH, Weinheim, Germany, **2006**.
50 M.J. Corey and E. Corey, *Proc. Natl. Acad. Sci., USA* **1996**, *93*, 11428.
51 R.B. Merrifield, *J. Am. Chem. Soc.* **1963**, *85*, 2149.
52 M.L. Snapper, A.H. Hoveyda, *Combinatorial Chemistry: Practical Approach*, Oxford University Press: Oxford, U.K., **2003**; pp. 433-455.
53 M.Z. Atassi, T. Manshouri, *Proc. Natl. Acad. Sci., USA* **1993**, *90*, 8282.
54 K.W. Hahn, W.A. Klis, J.M. Stewart, *Science* **1990**, *248*, 1544.
55 Contra Atassi: B.W. Matthews, C.S. Craik, H. Neurath, *Proc. Natl. Acad. Sci., USA* **1994**, *91*, 4103; J.A. Wells, W.J. Fairbrother, J. Otlewski, Jr., J. Burnier, *Proc. Natl. Acad. Sci., USA* **1994**, *91*, 4110. Contra Hahn: see ref 50.
56 K.S. Broo, L. Brive, P. Ahlberg, L. Baltzer, *J. Am. Chem. Soc.* **1997**, *119*, 11362; K.S. Broo, H. Nilsson, J. Nilsson, A. Flodberg, L. Baltzer, *J. Am. Chem. Soc.* **1998**, *120*, 4063.
57 Y. Fukushima, *Bull. Chem. Soc. Jpn.* **1996**, *69*, 2269.
58 A. Stavrakoudis, I.N. Demetropoulos, C. Sakarellos, M. Sakarellos-Daitsiotis, V. Tsikaris, *Lett. Pept. Sci.* **1997**, *4*, 481; A. Stavrakoudis, S. Makropoulou, V. Tsikaris, M. Sakarellos-Daitsiotis, C. Sakarellos, I.N. Demetropoulos, *J. Peptide Sci.* **2003**, *9*, 145.
59 R.A. Buono, N. Kucharczyk, M. Neuenschwander, J. Kemmink, L.-Y. Hwang, J.-L. Fauchère, C.A. Vananzi, *J. Computer-Aided Mol. Des.* **1996**, *10*, 213; B. Walse, M. Ullner, C. Lindbladh, L. Bülow, T. Drakenberg, O. Teleman, *J. Computer-Aided Mol. Des.* **1996**, *10*, 11.
60 A. Clouet, T. Darbre, J.-L. Reymond, *Angew. Chem. Int. Ed.* **2004**, *43*, 4612; A. Clouet, T. Darbre, J.-L. Reymond, *Biopolymers* **2006**, *84*, 114; D. Lagnoux, E. Delort, C. Douat-Casassus, A. Eposito, J.-L. Reymond, *Chem. Eur. J.* **2004**, *10*, 1215; E. Delort, T. Darbre, J.-L. Reymond, *J. Am. Chem. Soc.* **2004**, *126*, 15642; C. Douat-Casassus, T. Darbre, J.-L. Reymond, *J. Am. Chem. Soc.* **2004**, *126*, 7817; E. Delort, N.-Q. Nguyen-Trung, T. Darbre, J.-L. Reymond, *J. Org. Chem.* **2006**, *71*, 4468.
61 N. Maillard, A. Clouet, T. Darbre, J.-L. Reymond, *Nature Protoc.* **2009**, *4*, 132.
62 H. De Muynck, A. Madder, N. Farcy, P.J. De Clercq, M.N. Pérez-Payán, L.M. Öhberg, A.P. Davis, *Angew. Chem. Int. Ed.* **2000**, *39*, 145; A. Madder, L. Li, H. De Muynck, N. Farcy, D. van Haver, F. Fant, G. Vanhoenacker, G. Sandra, A.P. Davis, P.J. De Clercq, *J. Comb. Chem.* **2002**, *4*, 552.
63 H. Tsutsumi, H. Ikeda, H. Mihara, A. Ueno, *Bioorg. Med. Chem. Lett.* **2004**, *14*, 723.
64 Y. Singh, G.T. Dolphin, J. Razkin, P. Dumy, *ChemBioChem* **2006**, *7*, 1298.
65 F. Nastri, A. Lombardi, L.D. D'Andrea, M. Sanseverino, O. Maglio, V. Pavone, *Biopolymers (Peptide Science)* **1998**, *47*, 5; L. Regan, *Trends Biochem. Sci.* **1995**, *20*, 280; B.R. Ginbey, F. Rabanal, P.L. Dutton, *Curr. Opin. Chem. Biol.* **1997**, *1*, 537; W.F. DeGrado, C.M. Summa, V. Pavone, F. Nastri, A. Lombardi,

Annu. Rev. Biochem. **1999**, *68*, 779; A. Lombardi, C.M. Summa, S. Geremia, L. Randaccio, V. Pavone, W.F. DeGrado, *Proc. Natl. Acad. Sci., USA* **2000**, *97*, 6298.

66 T. Sasaki, E.T. Kaiser, *J. Am. Chem. Soc.* **1989**, *111*, 380; T. Sasaki, E.T. Kaiser, *Biopolymers* **1990**, *29*, 79.

67 H.K. Rau, W. Hähnel, *J. Am. Chem. Soc.* **1998**, *120*, 468; H.K. Rau, N. DeJonge, W. Hähnel, *Proc. Natl. Acad. Sci., USA* **1998**, *95*, 11526.

68 M. Fahnenschmidt, R. Bittl, E. Schlodder, W. Hähnel, W. Lubitz, *Phys. Chem. Chem. Phys.* **2001**, *3*, 4082.

69 W. Hähnel, *Mol. Diversity* **2004**, *8*, 219; H.K. Rau, N. DeJonge, W. Hähnel, *Angew. Chem. Int. Ed.* **2000**, *39*, 250; R. Schnepf, P. Hörth, E. Bill, K. Wieghart, P. Hildebrandt, W. Hähnel, *J. Am. Chem. Soc.* **2001**, *123*, 2186.

70 Lönnberg: P. Virta, M. Leppänen, H. Lönnberg, *J. Org. Chem.* **2004**, *69*, 2008; P. Virta, M. Karskela, H. Lönnberg, *J. Org. Chem.* **2006**, *71*, 1989. P. Kocis, O. Issakova, N.F. Sepetov, M. Lebl, *Tetrahedron Lett.* **1995**, *36*, 6623; X.-T. Zhou, A. Rehman, C. Li, P.B. Savage, *Org. Lett.* **2000**, *2*, 3015.

71 A. Collet, *Tetrahedron* **1987**, *43*, 5725.

72 E.T. Rump, D.T. Rijkers, H.W. Hilbers, P.G. de Groot, R.M.J. Liskamp, *Chem. Eur. J.* **2002**, *18*, 4613.

73 C. Chamorro, R.M.J. Liskamp, *J. Comb. Chem.* **2003**, *5*, 794; C. Chamorro, R.M.J. Liskamp, *Tetrahedron* **2004**, *60*, 11145.

74 J. van Ameijde, R.M.J. Liskamp, *Org. Biomol. Chem.* **2003**, *1*, 215.

75 M.A. McKervey, M.-J. Schwing-Well, E. Arnaud-Neu, *Comprehensive Supramolecular Chemisty*, Pergamon, Oxford, **1996**, Vol. 1, Chapter 15, p. 537; A. Pochini, R. Ungaro, *Comprehensive Supramolecular Chemisty*, Pergamon, Oxford, **1996**, Vol. 2, Chapter 4, p. 103; A. Ikeda, S. Shinkai, *Chem. Rev.* **1997**, *97*, 1713; Y.K. Agramal, H. Bhatt, *Bioinorg. Chem. Appl.* **2004**, *2*, 237.

76 H.S. Park, Q. Lin, A.D. Hamilton, *J. Am. Chem. Soc.* **1999**, *121*, 8.

77 P. Molenveld, J.F.J. Engbersen, H. Kooijman, A.L. Spek, D.N. Reinhoudt, *J. Am. Chem. Soc.* **1998**, *120*, 6726.

78 A. Gea, N. Farcy, N. Roqué I Rossell, J.C. Martins, P.J. De Clercq, A. Madder, A. *Eur. J. Org. Chem.* **2006**, 4135; S. van der Plas, A. Gea, S. Figaroli, P.J. De Clercq, A. Madder, *Eur. J. Org. Chem.* **2008**, 1582.

79 P. Dumy, I.M. Eggleston, S. Cervigni, U. Sila, X. Sun, M. Mutter, *Tetrahedron Lett.* **1995**, *36*, 1255.

80 The synthesis of the orthogonally protected TAC-scaffold is described in: T. Opatz, R.M.J. Liskamp, *Org. Lett.* **2001**, *3*, 3499.

81 M.C.F. Monnee, A.J. Brouwer, L.M. Verbeek, A.M.A. van Wageningen, R.M.J. Liskamp, *Bioorg. Med. Chem. Lett.* **2001**, *11*, 1521; C. Chamorro, J.-W. Hofman, R.M.J. Liskamp, *Tetrahedron* **2004**, *60*, 8691.

82 T. Opatz, R.M.J. Liskamp, *J. Comb. Chem.* **2002**, *4*, 275.

83 D.J. van Zoelen, M.R. Egmond, R.J. Pieters, R.M.J. Liskamp, *ChemBioChem* **2007**, *8*, 1950.

84 M. Hijnen, D.J. van Zoelen, C. Chamorro, P. Van Gageldonk, F.R. Mooi, G. Berbers, R.M.J. Liskamp, *Vaccine* **2007**, *25*, 6807.

85 C. Chamorro, J.A.W. Kruijtzer, M. Farsaraki, J. Balzarini, R.M.J. Liskamp, *Chem. Commun.* **2009**, 821.

Chapter 2

Synthesis and Analysis of Small and Flexible TAC-based Serine Hydrolase Active Site Mimics

Abstract

Three small TAC-based serine hydrolase active site mimicking structures have been prepared by solid-phase peptide chemistry using an orthogonally protected TAC-scaffold. Analysis of the kinetic parameters showed that these compounds were poor hydrolysis catalysts. NMR studies of the constructs revealed the presence of several conformers, which originated mainly from the presence of tertiary amide-bonds between the amino acids and the scaffold. Also, this flexibility of the scaffold prevented further structural characterization of the constructs. NMR analysis of smaller constructs showed that it is very unlikely that these flexible molecules have any preferred three-dimensional structure, thereby limiting a possible cooperation between attached functional groups, which is needed for enhanced hydrolytic activity.

1. Introduction

1.1. Active site structure and mechanism of serine hydrolases

Hydrolytic enzymes catalyze their reactions by the cooperative action of well-positioned functional groups present on the side-chains of certain amino acid residues.[1] For instance, serine proteases – and more generally serine hydrolases – use cooperativity between the hydroxyl group of a serine residue, the imidazole ring of a histidine residue as well as the carboxylate functionality of an aspartate residue for cleaving peptide bonds.[2] Such an arrangement of three cooperating residues that are crucial for catalysis is denoted a catalytic triad and is found in the active site.[3]

In the mechanism of catalysis, a reactive serine side-chain oxygen-nucleophile is generated (*vide infra*) which reacts with a substrate leading to formation of the amine-part of the substrate and an acyl-enzyme intermediate (*equation 1*).[2,4] This intermediate is subsequently hydrolyzed to the corresponding free enzyme and carboxylic acid part of the substrate. The nucleophilic serine side-chain residue is a very characteristic feature of serine proteases[5], is important for successful enzyme active site mimicry[6] and the target of many inhibitors.[7]

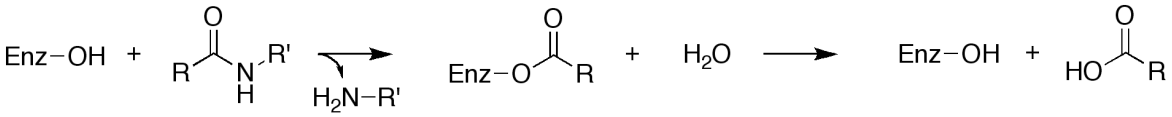

Equation 1. Reaction equation of the enzymatic hydrolysis of a peptide-bond.

Activation of the serine hydroxyl group in the active site of serine proteases is achieved by a combination of factors that have extensively been described in literature.[2] This activation is mainly due to formation of a hydrogen bond between the basic histidinyl imidazole ring and the serine hydroxyl proton (*figure 1*).[8] As result of this hydrogen bond, electronic density of the O-H bond is shifted towards the O-atom of the hydroxyl group, rendering it more nucleophilic. The increased nucleophilicity is even more enhanced by the usually hydrophobic cavity of the active site.[2,4] Upon attack of this activated oxygen atom of the serine side-chain on the carbonyl carbon atom of the substrate, the active site histidine residue becomes protonated, generating a positive charge on the imidazole ring. In many cases, this positive charge is stabilized by the negative charge of a nearby aspartate side-chain.[9] Serine activation is indeed one of the most important factors for the activity as was shown by site-directed mutagenesis studies on subtilisin, a bacterial serine protease. From this study it became apparent that the relative order of importance of the catalytic triad residues is: Ser > His > Asp.[10] The significant reduction in activity that accompanied substitution of even the least important residue Asp illustrates how well interactions in the active site of

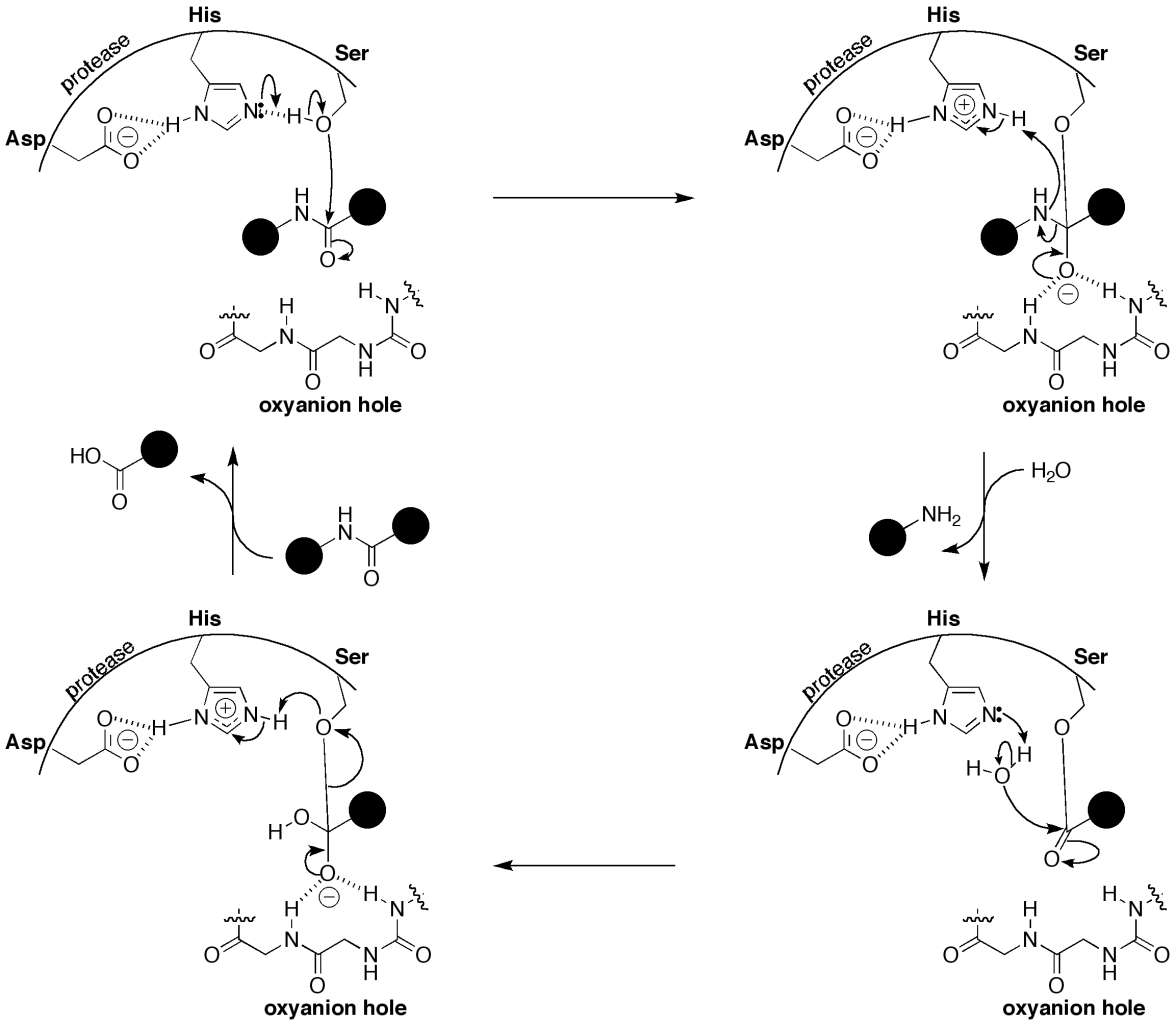

Figure 1. Schematic representation of the catalytic cycle of a serine protease.

subtilisin have been fine-tuned for hydrolyzing its substrate. As a result, mimicry of these active sites is a tremendous challenge.[11]

1.2. Small peptide-base mimics of serine hydrolases

The general occurrence of serine hydrolases in Nature, together with their importance in biological systems and their intriguing mechanism of action, has enticed chemists to mimic their activity using synthetic constructs. Although many small synthetic organic molecules have been attempted for this purpose,[4,12] peptide-based mimics of serine hydrolases deserve special attention. By using the exact same components that Nature uses for the construction of the active site, the use of peptide-based mimics allows the incorporation of important backbone-functionalities like amide NH- and CO-groups.[13] Two attempts described in literature will be briefly mentioned here.[14]

In the first attempt, a cyclic peptide was synthesized in which catalytic triad mimicking side-chain functionalities were directly incorporated into the backbone of the cyclic peptide (*figure 2*, left).[15] In the second attempt, the backbone of the

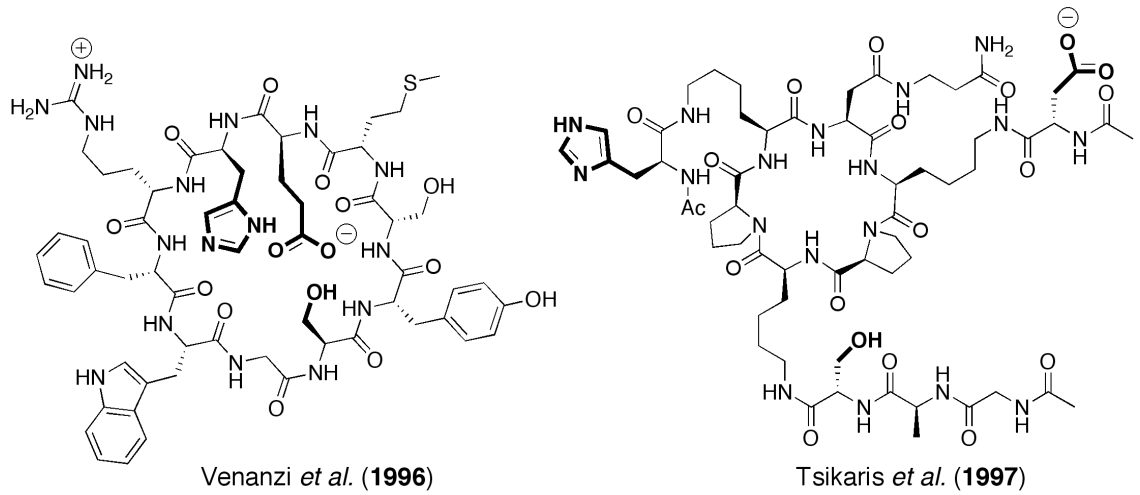

Figure 2. Structures of two peptide-based serine hydrolase catalytic triad mimics. The functionalities that mimic the active site residues are depicted in bold.

cyclic peptide served as a scaffold to attach the required residues (*figure 2*, right).[16] Both of these molecules were only moderately active with respect to hydrolysis of a *para*-nitrophenol ester,[17] illustrating the difficulties that will be encountered when one whishes to pursue the mimicry of serine hydrolase active sites. Especially, the flexibility and concomitantly poor pre-organization of the functionalities was mentioned as reason for the low activity.

Although small-organic molecules that can be used as scaffolds for the construction of peptide-based constructs have been described,[18] their application in the construction of serine hydrolase active site mimics has been limited.[6] Nevertheless, analysis of small serine hydrolase active site mimicking triads based on a scaffold molecule can provide valuable information on the applicability of that scaffold for the construction of enzyme active site mimics. Based on this information, necessary modifications might be rationalized and incorporated into the structure of the mimics. In the research described in this chapter we explore the applicability of an orthogonally protected triazacyclophane (TAC)-scaffold for the construction of serine hydrolase mimics.

1.3. Diverse applications of TAC-scaffold containing peptidic constructs

Since we were anticipating a variety of applications of a small synthetically accessible

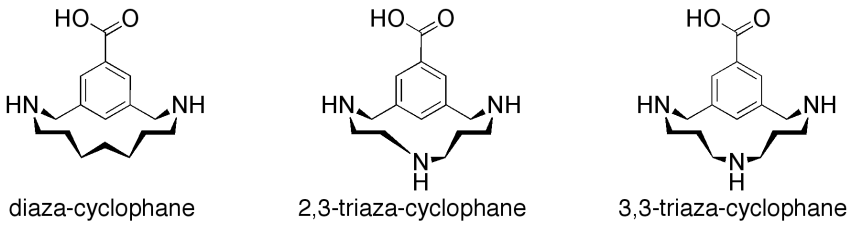

Figure 3. Three aza-cyclophane scaffolds synthesized in our group.

and tunable scaffold-molecule, especially in the field of biomimetic chemistry, our group has designed and synthesized several aza-cyclophane molecules (*figure 3*). Initially, these scaffolds were used in our group for the construction and identification of artificial peptide-based binders for biological relevant moieties like bacterial cell-wall D-Ala-D-Ala/Lac-OH sequences[19] and Fe(III).[20] Later, the symmetrical triazacyclophane (TAC)-scaffold was also used as a platform for the construction of peptide-based enzyme inhibitors[21] and synthetic vaccines.[22] In addition, we were interested in exploring the possibilities of the application of the TAC-scaffold in the construction of enzyme active site mimics. By studying the smallest possible Asp-His-Ser triad containing TAC-scaffold – those in which each amine of the scaffold is decorated with one *N*-terminally acetylated amino acid – we hoped to gain insight in the ability of these molecules to catalyze hydrolysis by means of cooperating functional groups.

2. Synthesis and analysis of flexible TAC-based serine hydrolase active site mimics

2.1. Synthesis of HOC(O)-TAC(*o*-NBS/Alloc/Fmoc)

Synthesis of the semi-orthogonally protected TAC-scaffold was done according to the procedures we have described earlier (*scheme 1*).[23] First, 3,5-dimethylbenzoic acid **1** was converted into the corresponding methyl ester. After this, radical bromination on the benzylic positions was performed using NBS and AIBN under influence of light,[24] which yielded bisbromide **2**.

For the synthesis of the amine-part of the scaffold we used triamine **3**. First, monoprotected triamine **4** was prepared using *o*-NBS-Cl and an excess of triamine **3**. After this, the remaining primary amine was protected using ethyl trifluoroacetate in the presence of one equivalent of water, to facilitate formation of TFA-salt **5**. This protonated secondary amine was protected using Alloc-Cl in the presence of $NaHCO_3$, to yield the fully protected triamine **6**. Tedious column chromatography afforded pure protected triamine **6**.

Cyclization of bisbromide **2** with protected triamine **6** was achieved using Cs_2CO_3 and TBAB, which gave fully protected TAC-scaffold **7a**. This monomeric compound could be separated from a dimeric species **7b** by two subsequent cumbersome column chromatographic steps. Saponification of the methyl ester and concomitant hydrolysis of the trifluoroacetyl-amide was achieved using Tesser's base.[25] This afforded compound **8**, of which the free amine was protected using Fmoc-OSu and Et_3N. Column chromatography afforded pure final protected TAC-scaffold **9**.

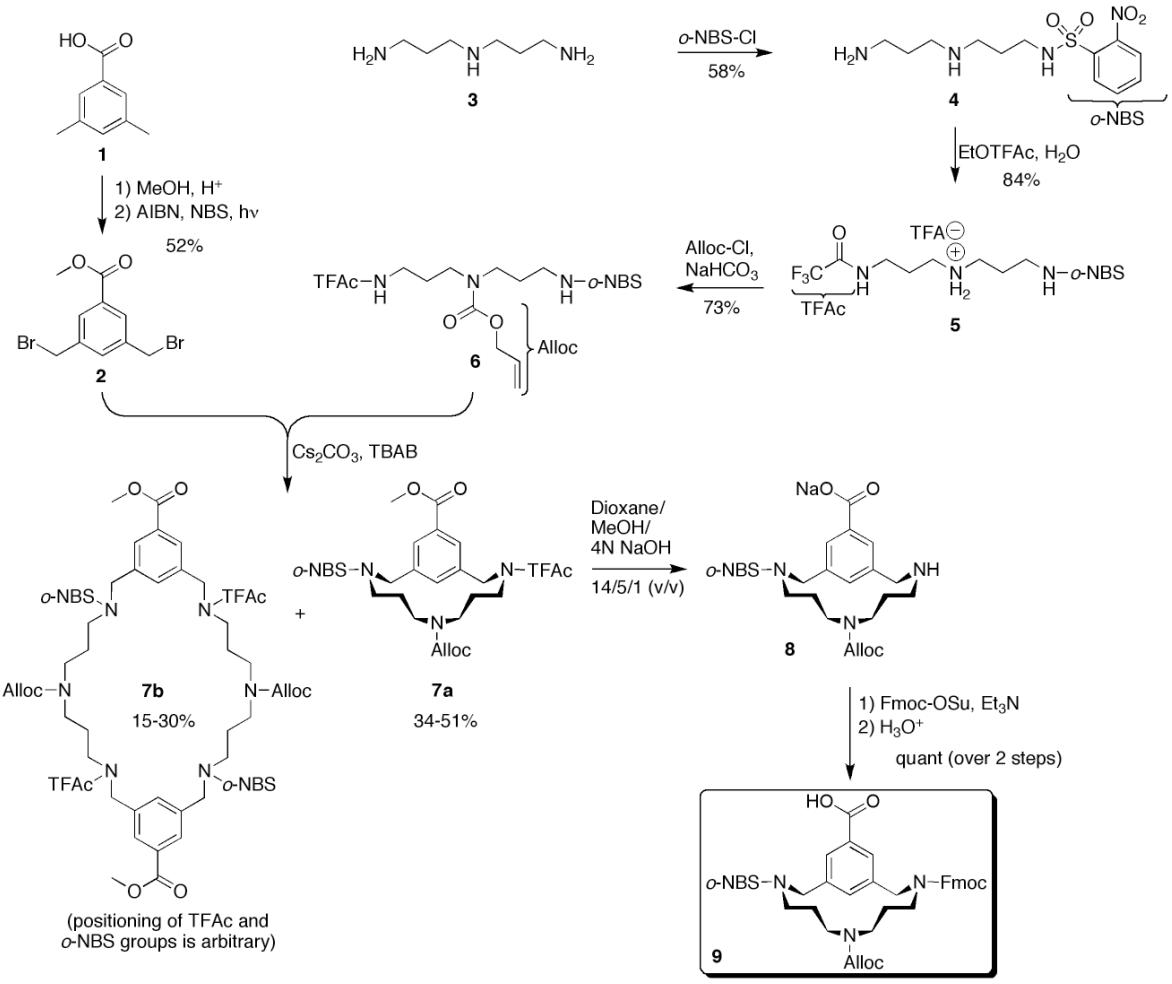

Scheme 1. Synthesis of the *o*-NBS/Alloc/Fmoc-protected TAC-scaffold **9**.

2.2. X-ray crystal-structure of TAC-scaffold 9

Fortunately, product **9** crystallized from EtOAc and a structure was obtained by single crystal X-ray diffraction (*figure 4*). The availability of this structure allowed some interesting observations. First, the aromatic ring is positioned almost perpendicular to the plane of the amine-containing aliphatic ring (*figure 4*, right). In addition, a plane of symmetry is present through the C1 and C4 atoms of the aromatic ring as well as the middle nitrogen atom of the triazacyclophane-ring (*figure 4*, left). It should be noted, however, that the structure of the TAC-scaffold and resulting molecular constructs are most likely less defined in solution (*vide infra*).

2.3. Synthesis of three small TAC-based mimics of the active site of serine hydrolases

Three small TAC-based mimics of serine hydrolase active sites were prepared using solid-phase synthesis (*scheme 2*). For this, the amine of PS S RAM resin **10** was deprotected using piperidine, after which scaffold **9** was attached using BOP and

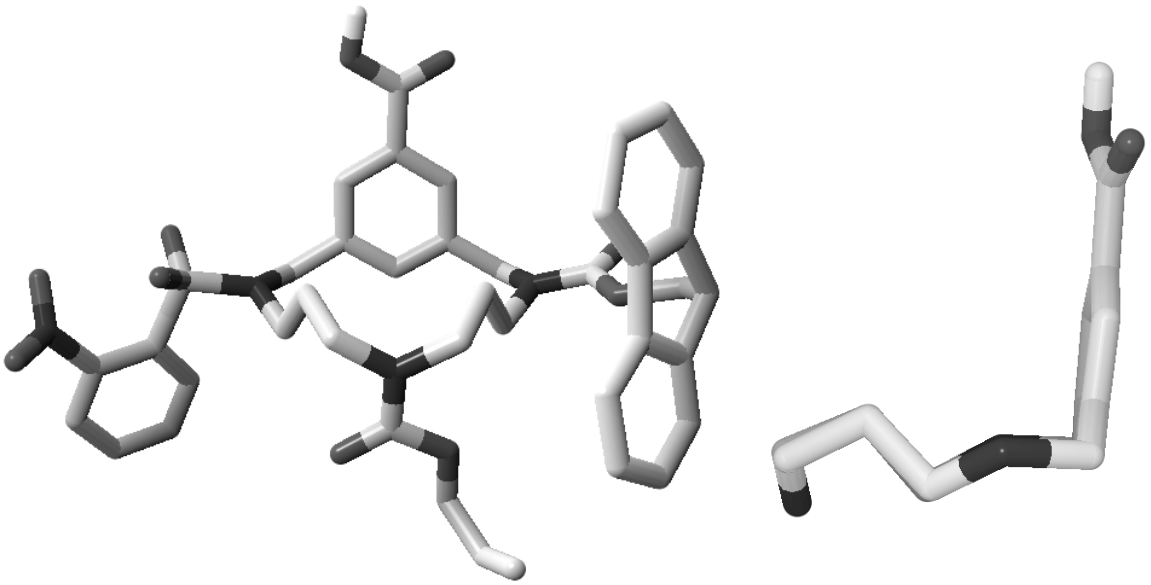

Figure 4. Front (*left*) and side view (*right*, protecting groups are omitted for clarity) of the X-ray crystal structure of TAC-scaffold **9**.

D*i*PEA. Any remaining amines were permanently protected with an acetyl-group and the loading of the resin with scaffold **9** was determined using Fmoc-quantification. This method is based on the detection of a piperidine-benzofulvene adduct, which results from piperidine affected Fmoc-removal and can be detected at 301 nm (*figure 5*). Resin-bound scaffold **11** was used to construct three different Asp-His-Ser containing receptors.

For the synthesis of these receptors, the batch of resin-bound scaffold **11** was divided into three equal portions. To each of the portions a different amino acid of the Asp-His-Ser catalytic triad was attached, using Fmoc-Asp(O*t*Bu)-OH, Fmoc-Ser(*t*Bu)-OH or Fmoc-His(Trt)-OH as amino acid building blocks, and BOP and D*i*PEA as coupling reagents. The Fmoc-group was substituted for the permanent protecting acetyl group, thereby also mimicking the peptide-backbone. This resulted

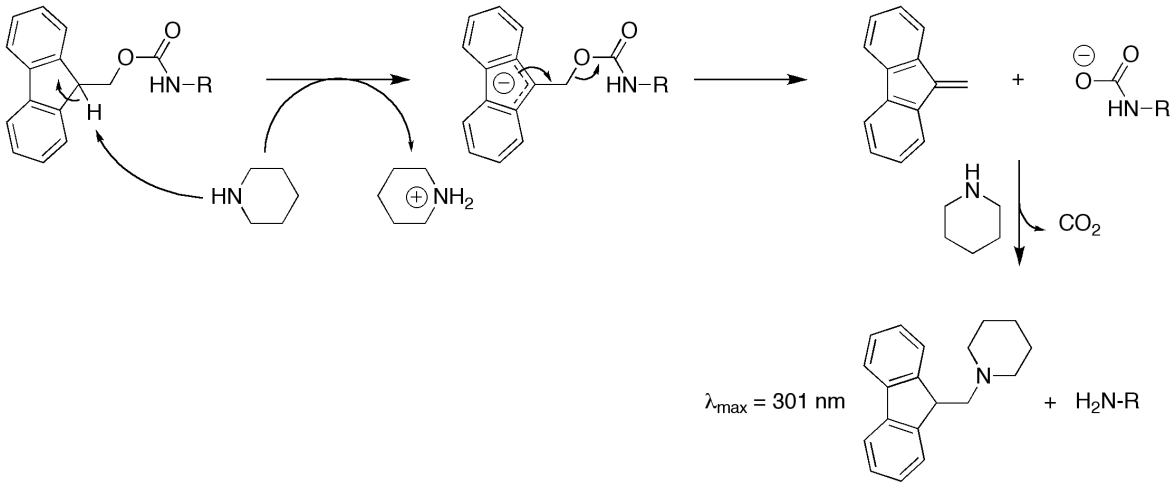

Figure 5. Fmoc cleavage by piperidine.

in resin-bound precursors **12a-c**. After removal of the *o*-NBS-protecting group, one of the remaining two amino acids was coupled using the same procedure as

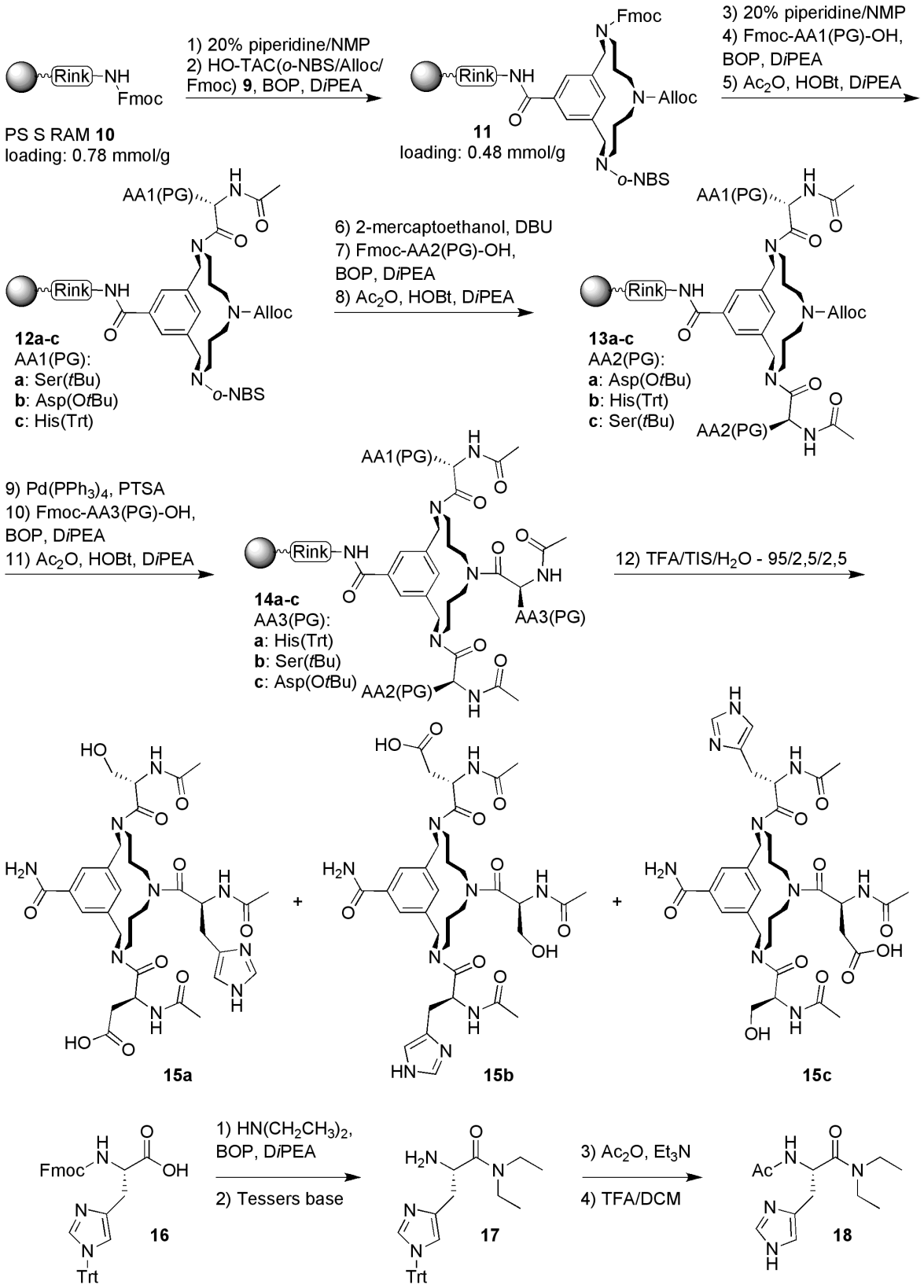

Scheme 2. Solid-phase synthesis of three Asp-His-Ser containing TAC-based receptors **15a-c** (PTSA = anilinium *p*-toluenesulfinate) and synthesis of reference catalyst **18**.

for coupling of the first amino acids. Again, the α-amine was protected using the acetyl group, leading to precursors **13a-c**. Removal of the Alloc-group was effected by freshly prepared $Pd(PPh_3)_4$ in the presence of anilinium *p*-toluenesulfinate as a scavenger. The third arm was constructed in the same way as the other two arms using the one remaining amino acid, resulting in three fully protected resin-bound receptors **14a-c**. Cleavage and deprotection of the side-chain functionalities resulted in three different TAC-based receptors **15a-c**. These were obtained by purification using column chromatography, in a yield of 23% (**15a**), 42% (**15b**) and 37% (**15c**).

Receptors **15a-c** combine some features that are thought to be crucial for hydrolysis: possible oxyanion stabilization by hydrogen bond donors from secondary amide bonds, possible π-π stacking between the aromatic ring of the TAC-scaffold and that of the substrate, and nucleophilic attack of either the serine hydroxyl functionality or the histidine imidazole moiety.

By comparing the activity of receptors **15a-c** with Ac-His-diethylamide (Ac-His-dea) **18** and 4-methylimidazole (4-MeIm), we hoped to gain insight in the relative activity of the TAC-based Asp-His-Ser triad mimics. For this purpose, Ac-His-dea **18** was synthesized from Fmoc-His(Trt)-OH **16** starting with BOP-mediated coupling of diethylamine and removal of the Fmoc-group (*scheme 3*). After this, the α-amino group was acetylated and the trityl protecting group on the imidazole ring was removed using 5% TFA in DCM. Ac-His-dea **18** was purified by column chromatography.

2.4. Hydrolytic activity of Asp-His-Ser containing receptors 15a-c, 4-MeIm and Ac-His-dea 18

Hydrolytic activity of receptors **15a-c** was assessed by measuring the rate of hydrolysis of 4-nitrophenyl acetate, a substrate that is often used in hydrolysis studies (*figure 6*). For this, solutions containing 1 mM of receptor **15a-c** and 2.5-12.5 mM substrate were mixed and the formation of the *para*-nitrophenolate anion was spectroscopically determined.

The rate of hydrolysis was determined by measuring the steepest increment of the first 10 measurements, which correspond to the first 10 minutes of the measurement. This resulted in an apparent rate (V_{app}) given in mOD/min. From this V_{app}, the rate of hydrolysis in absence of a catalyst was subtracted (V_{uncat}) yielding V_{net}. This rate in mOD/min was converted into the rate in μM/min using the appropriate calibration curves. The obtained V_{net} was used in the program GraphPad Prism to generate V_{net}/[S]-curves. Typical examples of the obtained curves are given in *figure 7* (measured at pH 7.0). From these curves, V_{max} and K_M were calculated using the formula $V_{max}=(V_{net}\times[S])/(K_M+[S])$, which is known as the Michaelis-Menten equation.[26] K_M is found at $V_{max}/2$ and is a measure for the affinity of the catalyst for the substrate. The obtained V_{max} was used to calculate the k_{cat} using $k_{cat} = V_{max}/[cat]$. This k_{cat} is the turnover number and is a measure for the efficiency of the catalyst. By calculating the

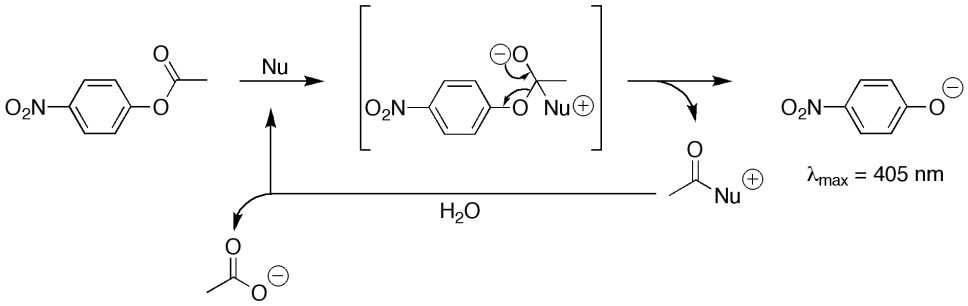

Figure 6. Hydrolytic reaction used to study the catalytic activity of the synthesized receptor molecules.

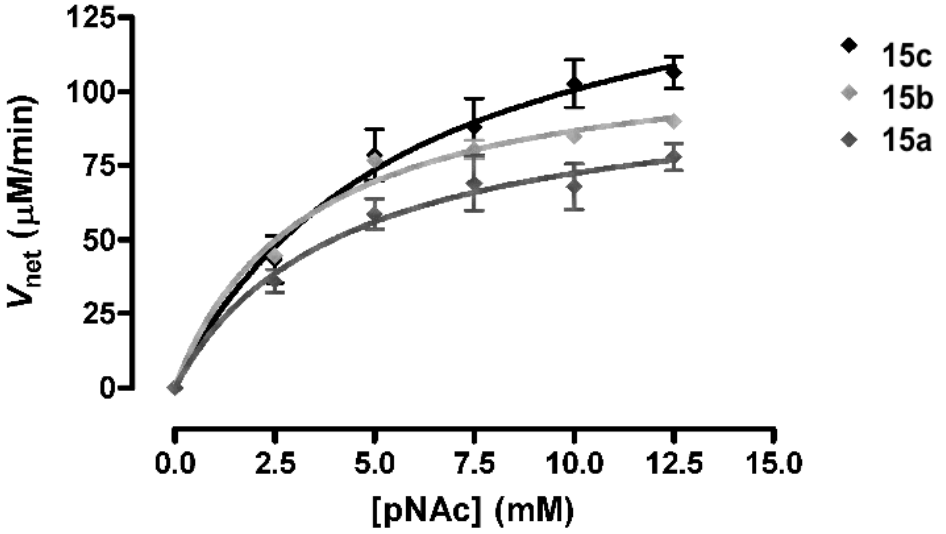

Figure 7. V_{net}/[pNAc]-curves for 0.1 mM of the three Asp-His-Ser containing TAC-scaffolds **15a-c** (at pH 7.0).

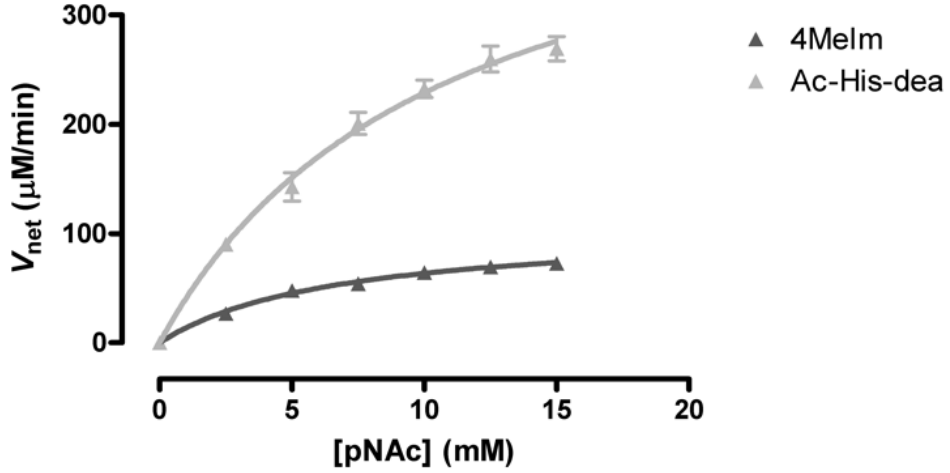

Figure 8. V_{net}/[pNAc]-curves for 1 mM of 4-MeIm and Ac-His-dea **18** (at pH 7.0).

specificity or performance constant k_{cat}/K_M, some insight can be obtained with respect to the performance of the catalyst.[27] A high value of this constant identifies a catalyst with high performance concerning the reaction measured. From these kinetic studies it immediately became clear that the hydrolytic activity of receptors **15a-c** was low

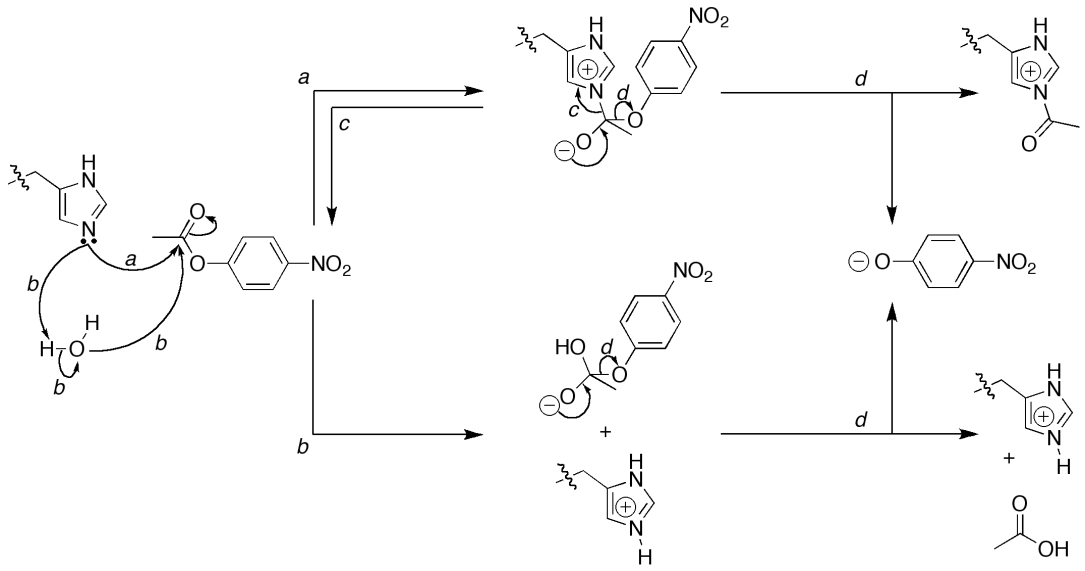

Figure 9. Histidinyl imidazole acting as a nucleophile (route a) or as a general base (route b) in the catalytic hydrolysis of pNAc.

Table 1. Kinetic parameters of the synthesized receptors **15a-c**, 4-MeIm and Ac-His-dea **18** for the hydrolysis of pNAc. Values were obtained using 0.1 mM receptor **15a-c** or 1 mM reference catalyst, 2.5-12.5 mM substrate, 20 mM Bis-Tris buffer (pH 7.0) and DMSO as cosolvent.

(*table 1*).

Catalyst	k_{cat} **(10^{-3} min^{-1})**	K_M **(mM)**	k_{cat}/K_M **(10^{-3} $min^{-1}\cdot mM^{-1}$)**
Receptor **15a**	102 ± 13	4.1 ± 1.5	24.9
Receptor **15b**	115 ± 6	3.3 ± 0.5	34.8
Receptor **15c**	160 ± 14	5.9 ± 1.2	27.1
Ac-His-dea **18**	471 ± 29	10.6 ± 1.3	44.4
4-MeIm	106 ± 5	--	--

[a] k_{cat} was measured as result of the presence of DMSO.

Some important conclusions can be derived from these data. In general, the activity was low, as can be concluded from comparing the activity of the receptors with those of reference catalysts **18** and 4-methylimidazole. Also, low K_M-values illustrate poor substrate binding ability of these constructs. Nevertheless, despite the low activity a significant difference was observed between receptor **15c** on one hand and receptors **15a** and **15b** on the other. The synthetic receptor (**15c**) with the aspartate residue on the middle position showed the highest activity. This might point to a weak cooperativity between the groups responsible for the hydrolytic reaction, in this case between the histidinyl imidazole and the aspartate carboxylate. Based on the observed low activity, hydrolysis most likely resulted solely from the histidine residue, reacting as a nucleophile or as a general base (*figure 9*). The absence of a significant cooperativity between functional groups probably originated from the flexibility of these receptors.

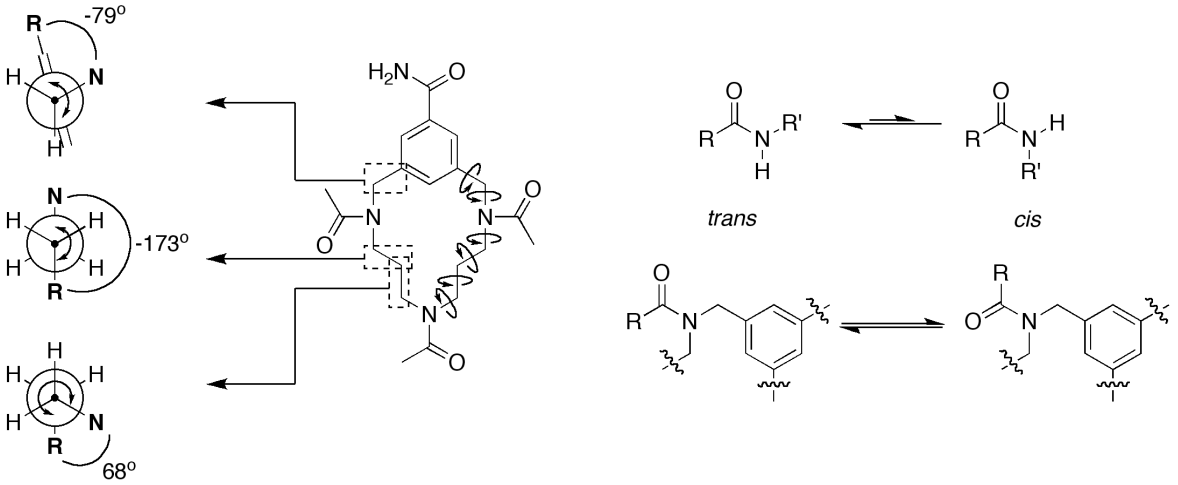

Figure 10. Overview of the rotatable bonds in acylated TAC-molecules. Newman projections (*left*) of the aliphatic cyclic part of the scaffold indicate approximate orientations of substituents as present in the X-ray crystal structure of **9** (*figure 4*). Curved arrows indicate rotatable bonds in the TAC-scaffold. On the *right*, secondary and tertiary amide bond *cis* or *trans* conformations are depicted.

In order to obtain some insight in the flexibility of our receptors **15a-c** and related molecular constructs in solution, several NMR studies were performed. We hoped that the results of these NMR-studies might provide valuable clues for improvement of the activity of these molecules.

3. NMR analysis of Asp-His-Ser containing TAC-based receptors

A high degree of flexibility in a potential catalytic system often lowers its substrate-binding ability and reduces the chance of cooperative interactions between functional groups.[2,4] The major origins of flexibility of the TAC-based constructs are illustrated in *figure 10*. The flexibility of TAC-based constructs is mainly caused by rotation around single bonds of the 14-membered triazacyclophane ring and to a lesser extent by rotation about the tertiary amide bonds between the amino acids and the scaffold. As a result a substantial number of conformers is present. For instance, the three tertiary amide bonds between scaffold and amino acid residues, each in the *cis* or *trans* conformation (*figure 10*, bottom right), may result in the presence of eight (2^3) different rotameric species.

To determine to what extent these factors affected the structure of receptors **15a-c**, preliminary NMR-studies were performed. One receptor, receptor **15a**, was studied in more detail using NMR spectroscopy at elevated temperatures. It was expected that conclusions concerning this receptor may be translated to the other two receptors. Since this was the first time that small TAC-based constructs were used as potential catalysts, we assumed that results obtained this preliminary conformational analysis could provide clues for further optimization of TAC-based serine hydrolase mimics.

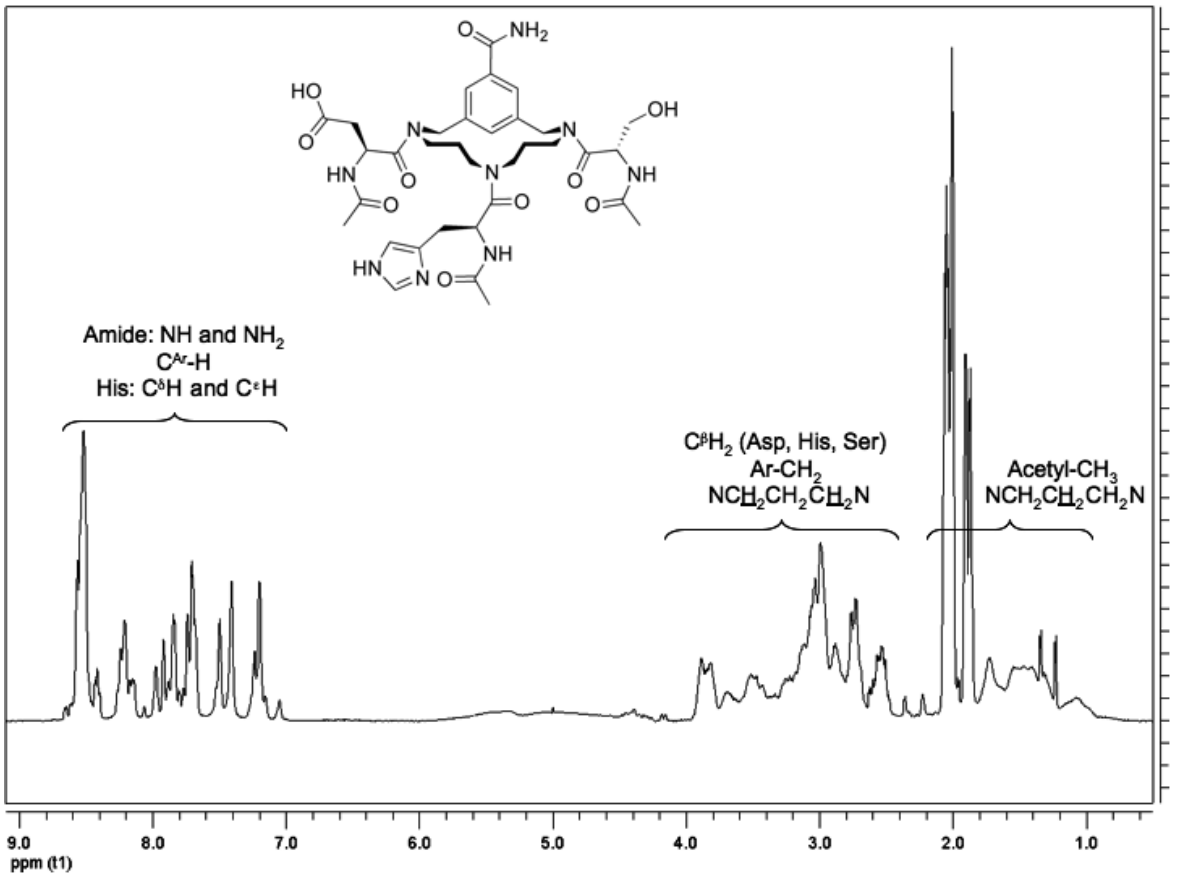

Figure 11. Full-width 500 MHz ^{1}H NMR spectrum of receptor **15a** at 5 °C. C$^{\alpha}$-protons (typically at 4.5-5.0 ppm) are not visible due to suppression of the water peak.

3.1. One-dimensional ^{1}H-NMR-analyses of receptor 15a

For this, 5 mg of receptor **15a** was dissolved in 10% (v/v) D_2O in H_2O (*figure 11*). This receptor was chosen since the arrangement of amino acids – Asp-His-Ser – matches the arrangements in which they occur in serine hydrolase active sites (*cf. figure 1*).

From this spectrum it immediately became clear that several conformational isomers of one compound were present in the solution of receptor **15a**. This was especially clear from the signals of the acetyl-groups at approximately 2 ppm. Although three acetyl-groups were present in the **15a**, at least nine peaks were observed in the spectrum. Due to the presence of these conformational isomers, detailed assignment of all peaks was not possible. Usually, peaks originating from rotamers merge into one peak as the temperature of the sample increases. Since TLC and HPLC analyses showed that a single compound was present, we conducted a temperature annealing experiment to determine whether these multiple signals indeed originated from several conformations. Especially signals originating from acetyl-groups proved to be useful in analyzing changes in rotamer distribution as a result of increasing the temperature (*figure 12*).

Initially, at least nine signals originating from the acetyl groups were observed

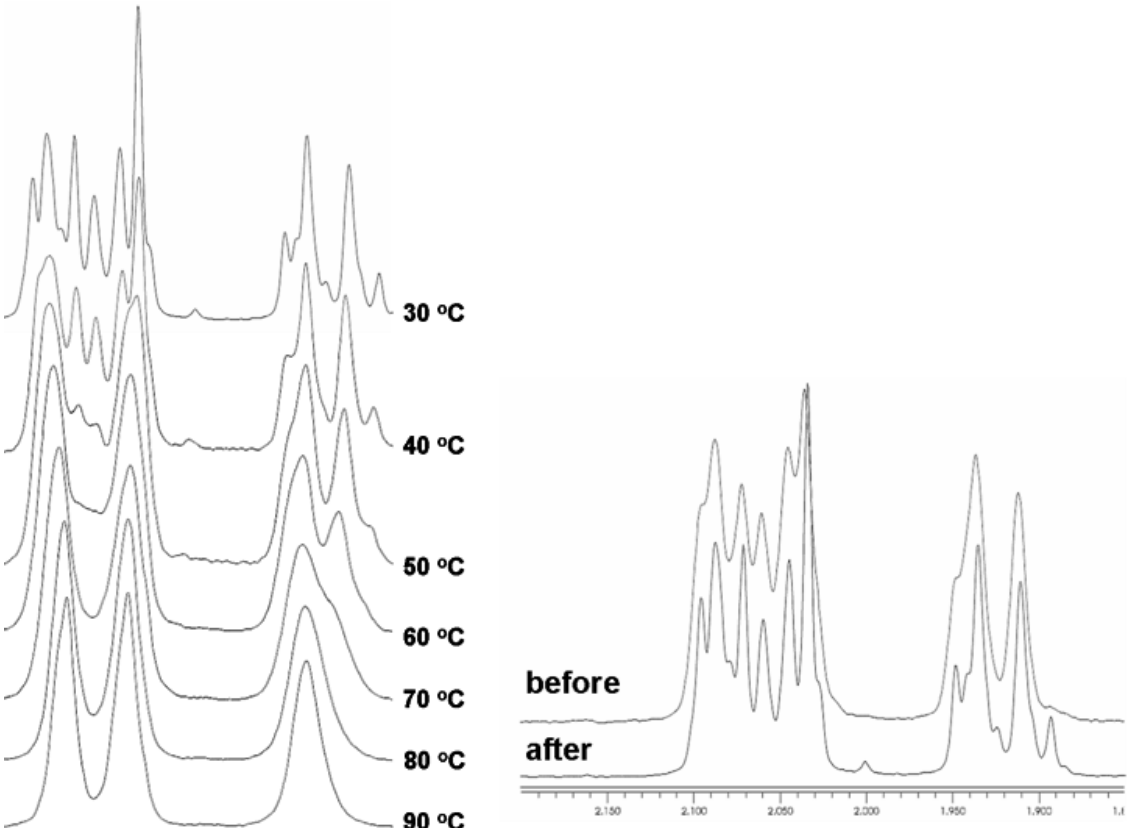

Figure 12. Shifts of acetyl methyl-group signals of **15a** (1.89-2.11 ppm) as result of temperature decrease from 90 to 30 °C (*left*). Differences in peaks before and after annealing are also shown (*right*, both at 30 °C).

(*figure 12*, right top spectrum). Upon heating of the sample, one peak for each acetyl-group was observed in NMR. Subsequent cooling of the sample led again to reappearance of more signals. For instance, below 80 °C, a shoulder emerged at the most isolated acetyl group (*figure 12*, left). When returning to 30 °C at least 15 different signals originating from the acetyl groups were present, indicating the presence of more distinct conformations than before the annealing experiment (*figure 12*, right lower spectrum).

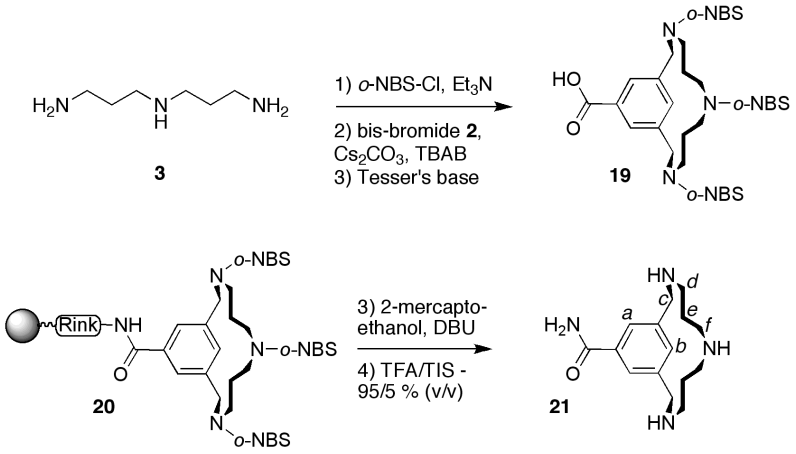

Scheme 4. Synthesis of TAC-scaffold **21**.

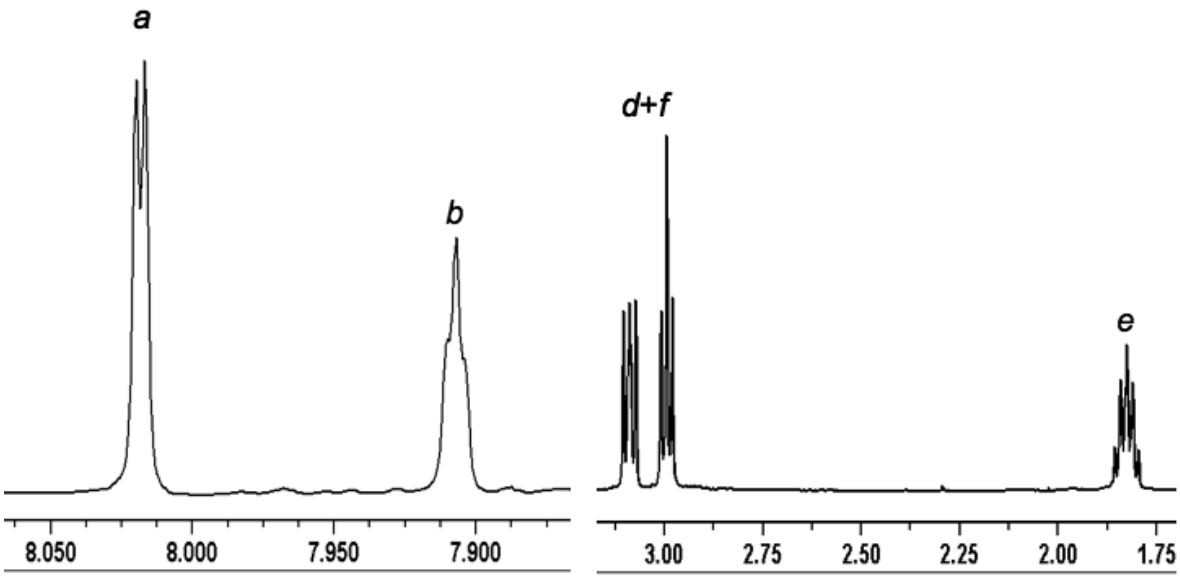

Figure 13. Aromatic (*left*) and aliphatic (*right*) part of a 500 MHz ^{1}H NMR spectrum of scaffold **21** in D_2O. Assignments are given (protons at ***c*** are not shown).

3.2. ^{1}H-NMR analysis of simple TAC-constructs: not-acylated and mono-acylated TAC-scaffolds

Due to the complexity of the spectra obtained for tri-acylated TAC-scaffolds, one non- and one mono-acylated construct were also prepared and analyzed. For construction of the non-acylated scaffold, resin-bound TAC(*o*-NBS)$_3$ scaffold **20** was used (*scheme 4*). This TAC-scaffold was prepared from triamine **3** using *o*-NBS-Cl and Et_3N. Fully protected triamine was cyclized with bis-bromide **2** and after saponification scaffold **19** was obtained. After attachment to a Rink-linker containing resin, the *o*-NBS protecting groups were removed by a thiolate nucleophile and the product was cleaved from the resin. Purification and desalting were performed by column chromatography. From the ^{1}H NMR spectrum of TAC-scaffold **21** (*figure 13*) it could be concluded that this compound was present in one conformation or that the different conformations interchanged rapidly.

Mono-acylated scaffold **27** was prepared starting from HOC(O)-TAC(Fmoc/Alloc/Fmoc) **23**. Scaffold **23** was prepared by protecting the two primary amine functionalities in amine **3** with TFAc-groups using ethyl trifluoroacetate in refluxing MeCN, followed by introduction of the Alloc-group, to afford protected triamine **22** (*scheme 5*). This was cyclized with bis-bromide **2** in the presence of Cs_2CO_3 and TBAB. After cyclization, the methyl ester and TFAc-amides of the product were hydrolyzed using Tesser's base.[25] The resulting two benzylic amine-groups were protected with an Fmoc-group and scaffold **23** was obtained in an overall yield of 10%.

Scaffold **23** was attached to resin-bound Rink amide linker using BOP and D*i*PEA (*scheme 6*). After this, Fmoc-protected amines of **24** were converted into TFAc-

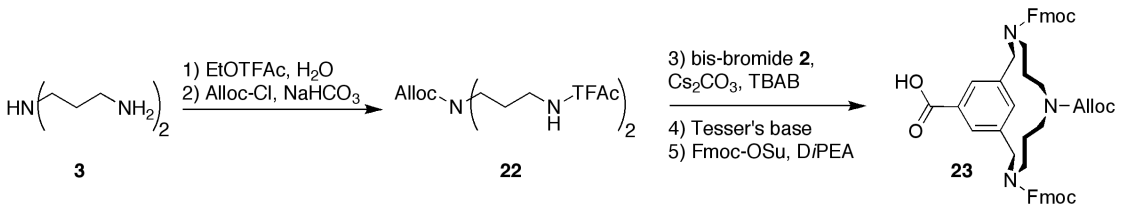

Scheme 5. Synthesis of scaffold **23**.

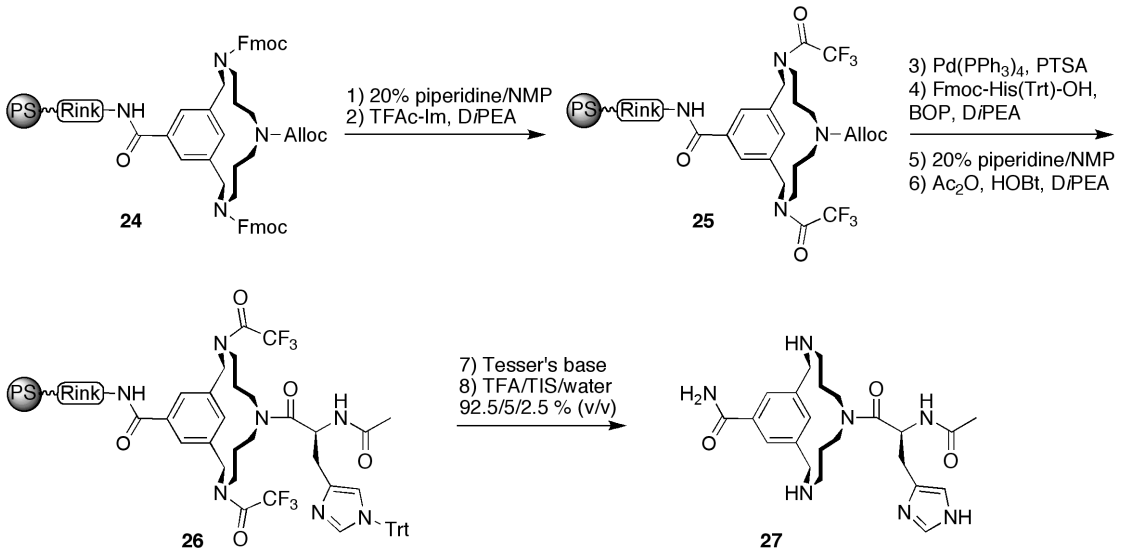

Scheme 6. Solid-phase synthesis of mono-acylated TAC-scaffold **27**.

protected amines, followed by removal of the Alloc-group from **25** and subsequent coupling of Fmoc-His(Trt)-OH. The *N*-terminal Fmoc-group was removed and replaced by an acetyl group using a standard capping reagent. The obtained resin-bound construct **26** was subjected to hydrolysis of the TFAc-groups using Tesser's base,[25] after which product **27** was liberated by acidic cleavage. Product **27** was purified by preparative HPLC and analyzed by ESI-MS, HPLC and ^{1}H NMR.

Upon acylation of the TAC-scaffold with the histidine residue, resulting in compound **27**, the flat nature of the amide-bond resulted in a loss of symmetry of the triazacyclophane ring: one TAC NCH_2-group may be closely in space to the carbonyl oxygen atom, whereas the other TAC NCH_2-group may be close to the side-chain of the histidine residue. It was expected that the different chemical environment influence the methylene-groups that are in close proximity of the acylated amine. However, it remained to be seen whether the effect was visible in the signals of the remainder of the azacyclophane ring, including the more remote benzylic protons, which showed three sets of signals (*figure 14*).

From these analyses it immediately became apparent that elucidation of the structures of such flexible constructs was difficult using NMR. The presence of multiple probably rapid inter-converting conformations prevented this.

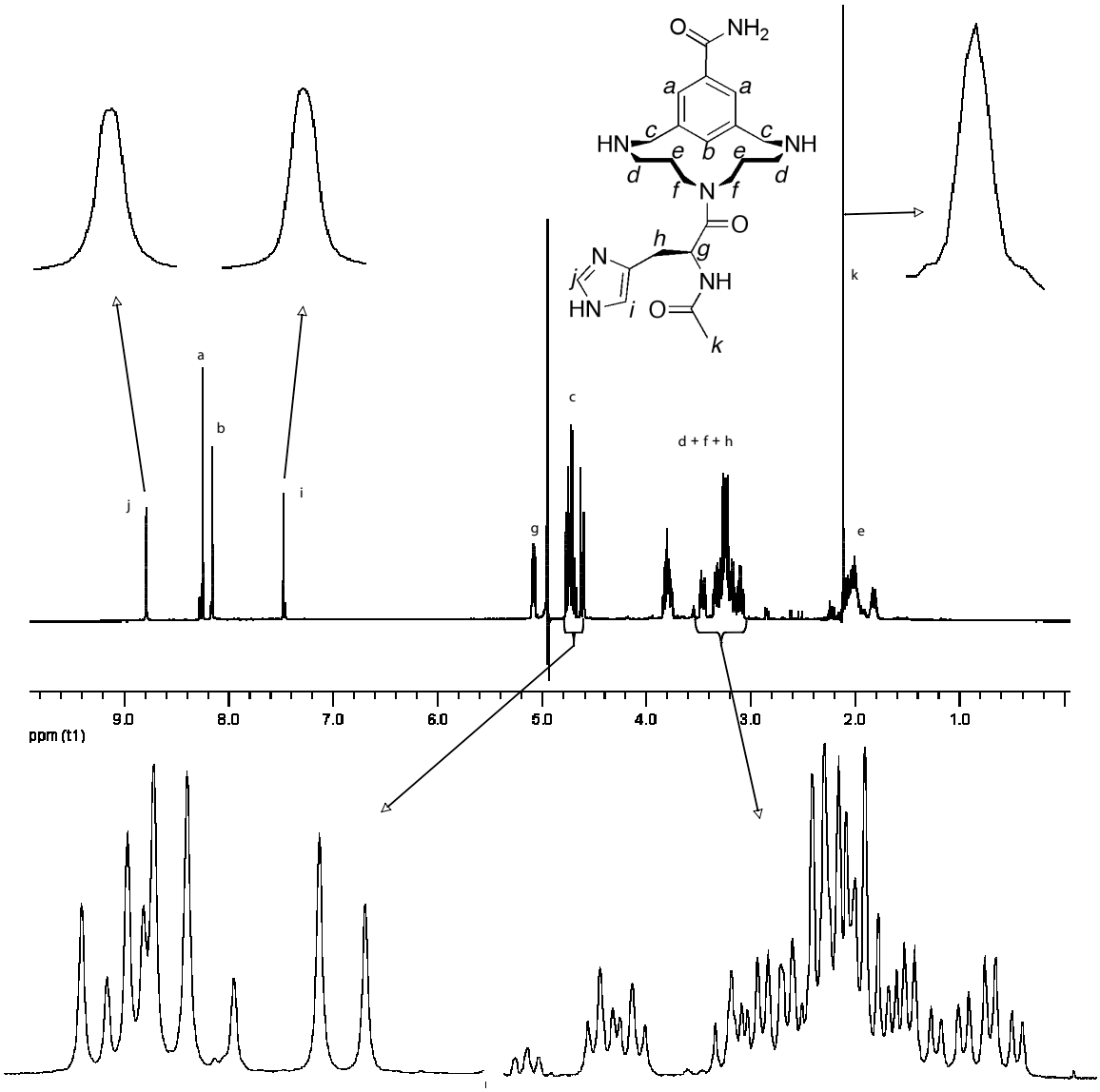

Figure 14. Top spectrum: 900 MHz ^{1}H NMR spectrum of **27** (see inserted structure) in D_2O. Inserts show the presence of single peaks for His-C$^{\varepsilon}$H, His-C$^{\delta}$H and Acetyl-CH_3. Lower spectra: zoomed spectra of the two Ar-CH_2N groups (left) and the four NCH_2 groups (right).

4. Discussion and Conclusions

From past attempts it was already known that both structural and functional mimicry of serine hydrolase active sites by peptidic constructs is not straightforward. Nevertheless, in the process of constructing true active site mimics the analysis of novel simple serine hydrolase catalytic triad containing constructs is a crucial step. This can provide crucial insights into the changes that have to be implemented in order to ultimately obtain a true structural and functional mimic. The synthesis and analysis of these simple TAC-based constructs has been described in this chapter.

It should be emphasized that this was the first time that TAC-based serine hydrolase active site mimics have been constructed and that the structure and activity of those mimics have been studied in detail. The synthetic accessibility of an orthogonally

protected TAC-scaffold was utilized for the construction of these small mimics. This resulted in three different mimics, each with a slightly different activity towards the hydrolysis of 4-nitrophenyl acetate. Although the activities were similar or better than that of 4-methylimidazole, it was much less than that of the histidine amino acid derivative Ac-His-diethylamide, a mimic of TAC-bound histidine. This indicated that the synthesized TAC-based serine hydrolase mimics were not very active in the hydrolysis of the substrate, and therefore poor functional mimics of serine hydrolase active sites.

In an attempt to unravel the origin of the poor hydrolytic activity, the constructs were subjected to several NMR studies. All three TAC-based constructs showed the presence of multiple conformations. A more detailed analysis of one of the three constructs, in which the residues were positioned in the arrangement as in the enzyme active site, showed that at least three conformations were visible. Moreover, after temperature annealing, five conformations could be inferred from the presence of at least fifteen distinct acetyl-CH_3 signals. Clearly, when catalysis depends on the cooperation between amino acid residue side chains, flexibility of the construct that contains these residues may hamper the catalytic activity. Also, the presence of multiple conformations prevented a full characterization of the structure of the TAC-based constructs. The origin of several conformations lies in the flexibility of the TAC-scaffold as well as cis/trans isomerization of the tertiary amides. Even a mono-acylated TAC-scaffold showed already a fairly complex NMR spectrum, indicating that acylation of the scaffold resulted the loss of symmetry and the presence of several conformations of the triazacyclophane ring.

It appeared that attachment of amino acid residues of the catalytically active amino acids of serine hydrolase active sites onto a TAC-scaffold in itself is not sufficient to successfully mimic the activity of the enzyme. Considering the flexibility of the TAC-based constructs and the proposed needed pre-organization of the functionalities, the low observed activity was not surprising. Thus, further adaptations need to be made in order to come up with functional mimics of serine proteases. Fortunately, the TAC-scaffold and the peptide chemistry used to construct these TAC-based enzyme active site mimics offered ample possibilities to impose the mimicry of enzyme active sites. Approaches towards this will be described in subsequent chapters.

5. Experimental Section

Chemicals were obtained from commercial sources and used without further purification. Reactions were performed at room temperature. Solution phase reactions were monitored by TLC analysis and R_f-values were determined on Merck pre-coated silica gel 60 F-254 (0.25 mm) plates. Spots were visualized with UV-light. Solid-phase synthesis was carried out in plastic syringes with PE frit (20 μm), Applied Separations Inc., distributed by Alltech Applied Science Group (Hoogeveen, The Netherlands). Column chromatography was carried out using Silica-P Flash silica gel (60 Å; particle size 40-63 μm; Silicycle). Electrospray Ionisation mass spectrometry (ESI-MS) was performed on a Finnigan LCQ Deca XP MAX LC/MS system. HPLC was performed on a Shimadzu Class-VP automated high performance liquid system, using an analytical reverse-phase column (Alltima, C_8, 300 Å, 5 μm, 250 × 4.6 mm) and a UV-detector (operating at 220 and 254 nm) as well as an ELSD-detector. Elution was realized using a gradient from water:MeCN:TFA – 95:5:0.1 % (v/v) to MeCN:water:TFA – 95:5:0.1 % (v/v) in 20 min and at a flow rate of 1 mL/min.

Methyl 3,5-dimethyl benzoate

3,5-dimethyl benzoic acid **1** (75 g, 0.5 mol) was dissolved in MeOH (1250 mL). To this, concentrated sulfuric acid (96%; 2 mL) was added. The mixture was refluxed over the weekend, subsequently neutralized by 2N NaOH and concentrated *in vacuo*. The crude product was dissolved in EtOAc (250 mL) and washed with 5% $NaHCO_3$ (2 × 150 mL), water (150 mL) and brine (150 mL). The organic phase was dried on Na_2SO_4, filtered and condensed using a rotary evaporator. Drying *in vacuo* afforded 79 g of clear crystals (yield: 96%). R_f = 0.85 (1% MeOH in DCM (v/v)). ^{1}H-NMR (300 MHz, $CDCl_3$, TMS): δ 2.36 (s, 6H, Ar-CH_3), 3.90 (s, 3H, C(O)OCH_3), 7.19 (s, 1H, C^4H), 7.66 (s, 2H, C$^{2,6}H$). ^{13}C-NMR (75 MHz, $CDCl_3$, APT): δ 21.0 (ArCH$_3$), 51.8 (OCH$_3$), 127.1-137.8 (C^{Ar}), 167.2 (C=O).

Methyl 3,5-bis(bromomethyl)benzoate 2

Methyl 3,5-dimethyl benzoate (16.4 g, 100 mmol) was dissolved in methyl formate (150 mL). In this mixture, *N*-bromosuccinimide (39.2 g, 220 mmol) was suspended and a catalytic amount of AIBN was added (100 mg). The reaction mixture was exposed to light (100 W) and refluxed until completion (after approx. 3.5 h). The cooled reaction mixture was filtered, condensed and the residue dissolved in Et_2O (150 mL). The precipitated succinimide was removed by filtration and the solution was washed with $Na_2S_2O_5$ (10% (w/w) 2 × 100 mL) and brine (1 × 100 mL). Drying over Na_2SO_4 and evaporation of the solvent gave the desired after crystallization from Et_2O and Et_2O-hexanes. Several batches of product **2** were obtained as white needles Yield: 17.3 g (54 mmol, 54%). R_f = 0.66 (EtOAc:hexanes – 3:1 (v/v)). ^{1}H-NMR (300 MHz, $CDCl_3$, TMS): δ 3.94 (s, 3H, C(O)OCH_3), 4.50 (s, 4H, Ar-CH_2Br), 7.62 (s, 1H, C^4H), 8.00 (s, 2H, C$^{2,6}H$). ^{13}C-NMR (75 MHz, $CDCl_3$, APT): δ 31.8 (CH$_2$Br), 52.4

(OCH_3), 130.0-138.9 (C^{Ar}), 165.8 (C=O).

Mono-*o*-NBS protected bis(3-aminopropyl)amine 4

A solution of *o*-NBS-Cl (31.7 g, 143 mmol) in DCM (200 mL) was added to a cooled (0 °C) solution of bis(3-aminopropyl)amine **3** (200 mL, 1.43 mol) in DCM (250 mL). This mixture was allowed to react at room temperature for 45 min after which water (300 mL) was added and the organic phase removed. To the water layer 1N HCl (100 mL) was added and products were extracted with DCM (250 mL). To the aqueous phase NH_4Cl (50 g) was added as a concentrated aqueous solution followed by extraction with DCM (2 × 100 mL). After concentration *in vacuo*, mono-*o*-NBS protected triamine **4** was obtained after column chromatography. By-products were first eluted using a gradient of 10% to 40% MeOH in DCM. The desired mono-protected triamine was then eluted with MeOH containing 1% Et_3N. Yield: 26.32 g (83 mmol, 58% from *o*-NBS-Cl). R_f = 0.44 ($CHCl_3$:MeOH:25% NH_4OH (aq) – 8:4:1.5 (v/v/v)). ^{1}H-NMR (300 MHz, DMSO-d_6, TMS): δ 1.41-1.54 (d of quint, 4H, $CH_2CH_2CH_2$), 2.40-2.47 (q, 4H, $NHCH_2CH_2$), 2.52-2.57 (t, 2H, NH_2CH_2), 2.90-2.95 (t, 2H, *o*-NBS-$NHCH_2$), 3.66 (s, 3H, N*H*), 7.79-7.96 (m, 4H, C^{Ar}-*H*).

***o*-NBS/TFAc-protected triamine 5**

Mono-*o*-NBS protected triamine **4** (19.6 g, 62 mmol) was dissolved in dry MeCN (3Å, 220 mL). To this, 2.5 equiv ethyl trifluoroacetate (18.5 mL, 155 mmol) and 1 equiv of water (1.12 mL; 62 mmol) were added, after which the mixture was stirred overnight under reflux. The resulting mixture was concentrated under reduced pressure resulting in a yellow solid of high purity, as judged by TLC. Yield: 27.42 g (52 mmol, 84%). R_f = 0.20 (10% MeOH in DCM (v/v) and 1 drop of Et_3N). ^{1}H-NMR (300 MHz, DMSO-d_6, TMS): δ 1.75-1.83 (d of quintets, 4H, $CH_2CH_2CH_2$), 2.90 (br s, 4H, $NHCH_2CH_2$), 2.96-2.99 (q, 2H, *o*-NBS-$NHCH_2$), 3.23-3.29 (q, 2H, TFAc-$NHCH_2$), 7.87-8.03 (m, 4H, C^{Ar}-*H*), 8.27 (t, 1H, *o*-NBS-N*H*), 8.59 (br s, 2H, NH_2), 9.56 (t, 1H, TFAc-N*H*). ^{13}C-NMR (75 MHz, $CDCl_3$, APT): δ 25.1 and 26.2 ($CH_2CH_2CH_2$), 36.6 (CH_2NH-TFAc), 40.1 (CH_2NH-*o*-NBS), 44.4-44.6 ($NH_2(CH_2)_2$), 110.2-123.0 (d of q, $^2J_{C\text{-}F}$ 298 and 288 Hz, 2 × CF_3), 124.5, 129.5, 132.7, 134.1 (C^{Ar}H), 132.6, 147.8 (C^{Ar}), 155.8-157.2 and 158.7-159.1 (d of q, $^3J_{C\text{-}C\text{-}F}$ 32 and 36 Hz, 2 × C(O)CF_3). ^{19}F-NMR (282 MHz, $CDCl_3$): δ -74.0 and -74.8 (NC(O)CF_3 and F_3CC(O)O).

***o*-NBS/Alloc/TFAc-protected triamine 6**

Triamine **5** (13.2 g; 25 mmol) was dissolved in a mixture of dioxane (125 mL) and water (125 mL). A solution of $NaHCO_3$ (8.4 g, 100 mmol) in water (100 mL) was added to this organic phase. The mixture was cooled on ice after which a solution of Alloc-Cl (3.2 mL; 30 mmol) in dioxane (70 mL) was added dropwise. The ice-bath was removed and the mixture was stirred at room temperature for 2 h. After completion of the reaction water (400 mL) was added and

the crude product was extracted with DCM (400 and 200 mL). The combined organic phase was dried over Na_2SO_4, concentrated *in vacuo* and purified by column chromatography (eluent: EtOAc/hexanes – 1/1). The desired product was obtained as a yellow oil. Yield: 12.26 g (24.7 mmol, 99%). R_f = 0.54 (EtOAc:hexanes – 2:1). ^{1}H-NMR (300 MHz, $CDCl_3$): δ 1.73 (br m, 4H, $CH_2CH_2CH_2$), 3.04-3.11 (q, ^3J 6.6 and 6.4 Hz, 2H, *o*-NBS-NHCH_2), 3.27 (br s, 6H, NCH_2CH_2), 4.54-4.55 (d ^3J 5.2 Hz, 2H, OCH_2), 5.16-5.27 (m, 2H, =CH_2), 5.54 + 6.14 (2 s, 0.66 and 0.34 H, *o*-NBS-N*H*), 5.80-5.93 (m, 1H, =C*H*-), 6.94 + 7.93 (2 s, 0.32 and 0.68 H, TFAc-N*H*), 7.70-8.09 (m, 4H, C^{Ar}-*H*). ^{13}C-NMR (75 MHz, $CDCl_3$, APT): δ 26.8, 28.4, 36.0, 36.9, 40.9, 43.8 (*C*H_2 in triamine), 66.5 (O*C*H_2), 110.1-121.6 (q, $J_{C\text{-}F}$ 287 Hz, *C*F_3), 118.2 (=*C*H_2), 125.2, 130.8, 132.7, 133.7 (C^{Ar}H), 132.3 (=*C*H-), 133.4, 147.9 (C^{Ar}), 156.5-157.9 (q, $J_{C\text{-}C\text{-}F}$ 36.6 Hz, *C*(O)CF_3 and N*C*(O)O). ^{19}F-NMR (282 MHz, $CDCl_3$): δ -76.5 (NHC(O)C*F*$_3$). ESI-MS: *m/z* 519.85 (calculated: 519.12 for $[M+Na]^+$).

MeOC(O)-TAC(*o*-NBS/Alloc/TFAc) 7a

Triamine **6** (5.6 g, 11.3 mmol) was dissolved in MeCN (3Å, 1 L). To this were added tetrabutylammonium bromide (TBAB) (3.6 g, 11.3 mmol), bis-bromide **2** (3.6 g, 11.3 mmol) and Cs_2CO_3 (14.7 g, 45 mmol). The resulting mixture was refluxed for 1 h after which TLC analyses indicated complete conversion of the starting materials. After this, ca 50% of the solvent was removed by evaporation under reduced pressure. To the concentrated mixture was added a solution of $KHSO_4$ (9.8 g, 72 mmol) in water (350 mL). From this acidic mixture the products were extracted using DCM (2 × 200 mL). The organic phase was washed with brine (100 mL), dried over Na_2SO_4 and concentrated *in vacuo*. Yield: 3.82 g (5.8 mmol, 51%). R_f = 0.38 (eluent: EtOAc:hexanes – 2:1). ^{1}H-NMR (300 MHz, $CDCl_3$): δ 1.32-1.65 (d quint, 1H and 3H, $CH_2CH_2CH_2$), 2.88-3.47 (m, 8H, NCH_2), 3.93-3.95 (d, $\delta_{T=25}$ 6.3 Hz, 3H, OCH_3), 4.46-4.78 (m, 6H, ArCH_2N and OCH_2), 5.15-5.25 (m, 2H, =CH_2), 5.80-5.90 (m, 1H, =C*H*-), 7.67-8.07 (m, 7H, C^{Ar}-*H*). ^{19}F-NMR (282 MHz, $CDCl_3$): δ -67.66 and -68.75 ($\delta_{T=25}$ 308 Hz, NC(O)C*F*$_3$). ESI-MS: *m/z* 657.15 (calculated: 657.18 for $[M+H]^+$), 678.70 (calculated: 679.18 for $[M+Na]^+$). Dimeric species **7b** eluted after monomer **7a**. Yield: 1.84 g (1.4 mmol, 25%). R_f = 0.26 (eluent: EtOAc:hexanes – 2:1). ^{1}H-NMR (300 MHz, $CDCl_3$): *δ* 1.64-1.86 (d br s, 2H and 6H, $CH_2CH_2CH_2$), 3.08-3.34 (m, 16H, NCH_2), 3.88-3.93 (q, 6H, OCH_3), 4.43-4.69 (m, 12H, ArCH_2N and OCH_2), 5.13-5.25 (m, 4H, =CH_2), 5.80-5.87 (m, 2H, =C*H*-), 7.54-7.96 (m, 14H, C^{Ar}-*H*). ^{19}F-NMR (282 MHz, $CDCl_3$): δ -68.61, -68.67, -69.19, -69.27 (NC(O)C*F*$_3$). ESI-MS: *m/z* 1351.05 (calculated: 1351.35 for $[M+K]^+$), 1335.55 (calculated: 1335.35 for $[M+Na]^+$), 1313.30 (calculated: 1313.35 for $[M+H]^+$).

HOC(O)-TAC(*o*-NBS/Alloc/Fmoc) 9

Fully protected TAC-scaffold **7a** (3.3 g, 5.1 mmol) was dissolved in Tesser's base (177 mL, dioxane:methanol:4N NaOH – 14:5:1 (v/v)) and allowed to react overnight at room

temperature. The resulting solution of **8** was neutralized using 1N HCl and concentrated under reduced pressure. The crude product was dissolved in 100 mL acetonitril:water – 1:1 (v/v) and the pH of the solution was adjusted to 9.5 using Et_3N. A solution of Fmoc-OSu (1.9 g; 5.6 mmol) in acetonitril (10 mL) was added and the pH of the mixture was maintained between 8.5-9.0 using Et_3N. After ca 90 min, the reaction was complete and acidified using 1N HCl. Water (350 mL) was added and the product was extracted with EtOAc. The collected organic layers were dried over Na_2SO_4, concentrated *in vacuo* and the product was purified by column chromatography (eluent: EtOAc:hexanes – 2:1 (v/v) and a trace of AcOH). After concentration of the fractions, the product was obtained as an off-white foam. Yield: 3.56 g (4.6 mmol, 91%). R_f = 0.15 (EtOAc:hexanes – 2:1, 1% AcOH). ^{1}H-NMR (300 MHz, $CDCl_3$): δ 0.95-1.28 (br m, 3H and 1H, $CH_2CH_2CH_2$), 2.33-3.27 (br m, 8H, NCH_2), 4.24-4.73 (br m, 9H, OCH_2CH and $ArCH_2N$), 5.16-5.23 (br d, 2H, $=CH_2$), 5.84 (br s, 1H, =CH-), 7.22-8.03 (m, 15H, C^{Ar}-H), 10.52 (br s, 1H, COOH). ^{13}C-NMR (75 MHz, $CDCl_3$, APT): δ 27.8 ($CH_2CH_2CH_2$), 45.2-48.4 (NCH_2CH_2), 47.3 (Fmoc-CH), 53.0 and 53.8 ($Ar\text{-}CH_2N$), 65.8 (Alloc-OCH_2), 67.2 (Fmoc-OCH_2), 117.4 ($=CH_2$), 119.9-148.3 (C^{Ar} and =CH-), 155.7 (NC(O)O), 169.9 (COOH). ESI-MS: *m/z* 769.50 (calculated: 769.25 for $[M+H]^+$).

$Pd(PPh_3)_4$ and **anilinium *p*-toluenesulfinate (PTSA)**: according to a literature procedure.[28]

Standard solid-phase peptide synthesis procedures

Generally, 6 mL of solvent was used for each gram of resin. After each reaction, a standard washing protocol is followed (*vide infra*).

- Fmoc-deprotection: 20% piperidine/NMP (2 × 8 min).
- Coupling: was performed using 4 equiv Fmoc-AA(PG)-OH, 4 equiv BOP, and 8 equiv D*i*PEA in NMP in syringes placed on a shaker (18 h).
- Capping of amines: using a standard capping reagent consisting of 0.5 M acetic anhydride, 0.125 M D*i*PEA and 0.015 M HOBt in NMP (2 × 10 min).
- Washing: NMP (3 × 2 min) and DCM (3 × 2 min).
- Coupling, deprotection and capping was monitored using the Kaisertest[29] (for primary amines) or chloranil[30] test (for secondary amines).

Asp-His-Ser triad containing TAC-molecules 15a-c

For these syntheses, three batches of each 0.5 g of PS S RAM loaded with TAC(Fmoc/Alloc/*o*-NBS) scaffold **9** (loading = 0.57 mmol/g) were used. In a parallel synthesis, all three combinations of receptors were prepared using Fmoc-Ser(*t*Bu)-OH (440 mg, 1.1 mmol, 4 equiv), Fmoc-Asp(O*t*Bu)-OH (472 mg, 1.1 mmol, 4 equiv), and Fmoc-His(Trt)-OH (711 mg, 1.1 mmol, 4 equiv), respectively, together with BOP (507 mg) and D*i*PEA (400 mL). The end deprotection and cleavage conditions are described in the standard procedures section.

Column purification of the cleaved products (eluent: $CHCl_3$:MeOH:25% NH_4OH – 8:4:1.5 (v/v)) afforded:

TAC(SerAc/HisAc/AspAc) 15a: yield: 48.8 mg (65.8 μmol, 23%). ESI-MS: *m/z* 742.30 (calculated: 742.35 for $[M+H]^+$). HPLC (C_8): t_R = 14.57 min (92% $\lambda_{254\ nm}$; 100% ELSD), 14.78 min (8% $\lambda_{254\ nm}$).

TAC(AspAc/SerAc/HisAc) 15b: yield: 88.1 mg (118.8 μmol, 42%). ESI-MS: *m/z* 742.25 (calculated: 742.35 for $[M+H]^+$). HPLC (C_8): t_R = 14.55 min (100% $\lambda_{254\ nm}$; 100% ELSD).

TAC(HisAc/AspAc/SerAc) 15c: yield: 78.2 mg (105.5 μmol, 37%). ESI-MS: *m/z* 742.30 (calculated: 742.35 for $[M+H]^+$). HPLC (C_8): t_R = 14.52 min (85% $\lambda_{254\ nm}$; 94% ELSD), 13.88 min (8% $\lambda_{254\ nm}$; 3.2% ELSD) and 14.85 min (7% $\lambda_{254\ nm}$; 3.2% ELSD).

Lyophilization of these three constructs from water (pH 7.0) gave white solids.

Ac-His-dea 18

Fmoc-His(Trt)-OH **16** (1 mmol, 620 mg) was dissolved in DCM and 1 equiv BOP (442 mg) and 2 equiv D*i*PEA (348 μL) were added. To this solution, a solution of 1 equiv diethylamine (104 μL) in 10 mL of DCM was added slowly. After completion of the reaction (ca 2 h), the mixture was concentrated under reduced pressure. ^{1}H-NMR ($CDCl_3$): δ 1.00-1.05 + 1.14-1.26 (2 × 3H, dt, 2 × CH_2CH_3), 2.80-3.00 (2H, dq, $C^{\beta}H_2$), 3.16-3.23 + 3.43-3.47 (4H, dm, NCH_2), 4.08-4.27 (3H, dm, Fmoc-$CHCH_2$), 4.87-4.90 (1H, q, $C^{\alpha}H$), 5.75-5.78 (1H, d, C(O)N*H*), 6.61 (1H, s, $C^{\delta}H$), 7.07-7.74 (24H, m, Trt-C*H* + Fmoc-$C^{Ar}H$).

To the crude product, 25 mL of Tesser's base (1,4-dioxane/MeOH/4N NaOH – 14/5/1) was added and the solution was stirred for 30 min at room temperature. The basic mixture was acidified with excess of 1N $KHSO_4$ and washed with diethylether. After this, the aqueous phase was adjusted to basic pH (~ 12) by addition of 4N NaOH and H-His(Trt)-diethylamide **17** was extracted with EtOAc. This organic phase was concentrated *in vacuo* and the product was dissolved in DCM (30 mL) and 1.5 equiv Et_3N (418 μL) together with 1.5 equiv Ac_2O (284 μL) were added. The mixture was stirred overnight and concentrated under reduced pressure. The product was dissolved 1N $KHSO_4$ and extracted from the aqueous phase by repeated extractions with EtOAc. The collected organic layers were washed with brine, dried over Na_2SO_4 and concentrated *in vacuo*. ^{1}H-NMR ($CDCl_3$): δ 1.00-1.04 + 1.16-1.21 (2 × 3H, dt, 2 × CH_2CH_3), 1.90 (3H, s, Ac-CH_3), 2.77-2.98 (2H, dq, $C^{\beta}H_2$), 3.13-3.30 + 3.40-3.47 (4H, dm and m, NCH_2), 5.10-5.13 (1H, q, $C^{\alpha}H$), 6.58 (1H, d, $C^{\delta}H$), 6.63-6.65 (1H, d, C(O)N*H*), 7.08-7.15 (6H, m, Trt-$C^{2,6}H$), 7.26-7.29 (1H, d, $C^{\varepsilon}H$), 7.29-7.34 (12H, m, Trt-$C^{3,4,5}H$).

Removal of the trityl-protecting group was performed by dissolving the product in 5% TFA/DCM. After concentration, the crude material was dissolved in 1N $KHSO_4$ and washed with DCM. To the aqueous solution of the product, $NaHCO_3$ (s) was added until pH ~ 9 (pH paper) and the product was extracted by repeated washings with EtOAc. A final purification by column chromatography (10-20 % MeOH/DCM gradient) afforded pure Ac-His-

diethylamide **18** as a colorless oil. Yield (overall): 9.5 mg (3.8 μmol, 4%). R_f (20% MeOH/DCM) = 0.56. ^{1}H-NMR ($CDCl_3$): δ 1.07-1.16 (6H, dt, J = 6.9 and 7.2 Hz, 2 × CH_2CH_3), 1.99 (3H, s, Ac-CH_3), 2.93-3.09 (2H, dq, J = 6.3 and 8.5 Hz, $C^{\beta}H_2$), 3.16-3.36 + 3.45-3.54 (4H, dm, NCH_2), 5.06-5.13 (1H, q, J = 6.6 and 8.3 Hz, $C^{\alpha}H$), 5.8 (1H, br, Im-N*H*), 6.83 (1H, s, $C^{\delta}H$), 6.94-6.97 (1H, d, J = 8.3 Hz, C(O)N*H*), 7.56 (1H, s, $C^{\varepsilon}H$). ^{13}C-NMR (APT, DMSO-d_6): δ 12.8-14.2 (d, CH_2CH_3), 22.3 (C(O)CH_3), 29.8 (C^{β}), 41.1 (CH_2CH_3), 48.3 (C^{α}), 117.1 (C^{δ}), 127.7 (C^{γ}), 134.4 (C^{ε}), 168.6 (*C*(O)N), 170.1 (*C*(O)NH). ESI-MS: *m/z* 253.46 (calculated: 253.17 for $[M+H]^+$); 275.59 (calculated: 275.15 for $[M+Na]^+$); 527.35 (calculated: 527.32 for $[2M+Na]^+$).

Hydrolysis experiments

To analyze the hydrolytic properties of the synthetic receptors under identical conditions, hydrolysis was performed in 96-well plates. For this, the synthesized receptors or reference catalysts were dissolved in DMSO to a concentration of 0.1 mM and 1 mM, respectively, and 4-nitrophenyl acetate was dissolved in a mixture of DMSO/buffer – 2/3 (v/v) to a concentration of 25 mM. For the buffer 20 mM Bis-Tris (pH 6.0 and 7.0) was used. All measurements were carried out with a total volume of 50 μL (5 μL "catalyst" + 5-25 μL substrate solution + 40-20 μL buffer). The reaction was monitored for 2 hours and initial rates were calculated using the steepest increment over five measurements in the first ten minutes. This increment (mOD/min) was given by the software (Full Mode-KC4 (Version 3.4 (Rev 21)) software (BioTek instruments); data point resolution was set at 2 nm). This rate v (mOD/min) was converted into the rate in μM/min using the appropriate calibration curves made from solutions of 4-nitrophenol in 50 μL buffer/DMSO mixtures. All hydrolytic reactions were performed in duplo. After subtraction of the background hydrolysis, the obtained V_{net}(μM/min)/[S] (mM)-values were processed using GraphPad Prism 4. V_{max} and KM were calculated using the nonlinear fit model of the program, which relies on the formula $V_{max} = V_{net} \times [pNAc])/(K_M+[S])$. The turnover ($k_{cat}$) number was calculated by V_{max}/[cat].

Tri-*o*-NBS protected bis(3-aminopropyl)amine

A mixture of Et_3N (8.36 mL, 60 mmol) and bis(3-aminopropyl)amine **3** (2.83 mL, 20 mmol) in DCM (60 mL) was cooled on ice. To this, a solution of *o*-NBS-Cl (15.54 g, 70 mmol) in DCM (60 mL) was added dropwise. The mixture was stirred at room temperature until completion. The formed precipitate was removed by filtration and the solution was condensed in vacuo, which resulted in yellow oil. Pure product was obtained by column chromatography by eluting with a gradient from DCM to 0.75% MeOH in DCM. Yield: 6.8 g (10.0 mmol, 50%). R_f = 0.23 (2% MeOH in DCM (v/v)). ^{1}H-NMR (300 MHz, $CDCl_3$, TMS): δ 1.80-1.85 (m, 4H, $CH_2CH_2CH_2$), 3.10-3.17 (m, 4H, $NHCH_2$), 3.35-3.40 (t, J 6.9 Hz, 4H, NCH_2), 5.57-5.61 (t, J 6.3 Hz, 2H, N*H*), 7.61-8.12 (m, 12H, $C^{Ar}H$). ^{13}C-NMR (75 MHz,

$CDCl_3$): δ 28.8 ($CH_2CH_2CH_2$), 40.7 (NCH_2), 45.4 ($NHCH_2$), 124.3-147.9 (C^{Ar}).

The **HOC(O)-TAC(*o*-NBS)$_3$** scaffold **19** was prepared according to a literature procedure.[20]

Non-acylated TAC-scaffold 21

Removal of the *o*-NBS-protecting groups on resin bound *o*-NBS-protected TAC-scaffold **20** was achieved using 2-mercaptoethanol (11.7 mL of a 0.5 M solution in DMF) and DBU (438 μL) (3 × 30 min). The deprotected TAC-scaffold was cleaved from the resin using TFA:TIS – 95:5 (v/v). The product was concentrated in vacuo and purified by column chromatography (eluent: $CHCl_3$:MeOH:25% NH_4OH (aq) – 70:25:5 % (v/v)). ESI-MS: *m/z* 277.15 (calculated: 277.20 for $[M+H]^+$). Yield: 38.8 mg (140 μmol, quant). NMR was measured by dissolving 5.1 mg of 21 in approx. 800 μL D_2O *figure 14*).

Bis(3-(TFAc)aminopropyl)(Alloc)amine 22

Bis(3-aminopropyl)amine **3** (5 mL, 35 mmol) and water (630 μL; 35 mmol) were added to 100 mL MeCN (stored on 3Å molsieves). To this solution, ethyl trifluoroacetate (13.2 mL, 105 mmol) was added and the mixture was refluxed for 2 days. The mixture was concentrated under reduced pressure, which resulted in the formation of a white solid. The solid was dissolved in 60 mL dioxane and 60 mL water and $NaHCO_3$ (11.8 g, 140 mmol) was added. To this mixture, a solution of Alloc-Cl (4.5 mL, 42 mmol, 1.2 equiv) in dioxane (30 mL) was added slowly. The reaction was allowed to proceed overnight, after which the mixture was concentrated in vacuo. To the residue water was added and the product was extracted using DCM. The DCM extract was dried over Na_2SO_4, filtered and concentrated under reduced pressure. A colorless oil was obtained that crystallized under vacuum to a white solid. Yield: 14.3 g (35 mmol, quantitative). R_f = 0.45 (5% MeOH in DCM). ^{1}H-NMR (300 MHz, $CDCl_3$, TMS): δ 1.76 (s, 4H, $CH_2CH_2CH_2$), 3.30-3.32 (s, 8H, NCH_2), 4.56-4.58 (d, *J* 5.8 Hz, 2H, OCH_2), 5.20-5.31 (m p, 2H, $=CH_2$), 5.82-5.93 (m, 1H, =CH-), 7.18 and 8.03 (ds, 2H, N*H*-TFAc). ^{13}C-NMR (75 MHz, $CDCl_3$, APT): δ 27.5 ($CH_2CH_2CH_2$), 36.1 (NCH_2), 43.8 ($NHCH_2$), 66.7 and 67.0 (OCH_2), 113.9 and 114.6 and 117.7 ($C(O)CF_3$), 118.5 ($=CH_2$), 132.1 (=CH-), 156.6-158.1 (C=O). ^{19}F-NMR (282 MHz, $CDCl_3$): δ -76.56, -76.34 (d, *J* 63 Hz, $C(O)CF_3$).

MeOC(O)-TAC(TFAc/Alloc/TFAc)

Protected triamine **22** (4.1 g, 11 mmol), bis-bromide **2** (3.2 g, 11 mmol), TBAB (3.2 g, 11 mmol) and Cs_2CO_3 (14.3 g, 44 mmol) were added to 500 mL MeCN (3Å). The mixture was refluxed until completion of the reaction and then condensed to half of its original volume. $KHSO_4$ (9.0 g, 66 mmol) in water (250 mL) was added and the products were extracted

using DCM (2 × 250 mL). This organic phase was washed with brine and dried over Na_2SO_4. After filtration and condensing the filtrate, the obtained product was purified by column chromatography (eluent gradient: DCM:hexanes:EtOAc – 80:1:9 to 80:9:1) and obtained as off-white foam. Yield: 3.1 g (5.4 mmol, 49%). R_f = 0.32 (5% MeOH in DCM). ESI-MS: *m*/*z* 568.20 (calculated: 568.18 for $[M+H]^+$). ^{1}H-NMR (300 MHz, $CDCl_3$, TMS): δ 1.26-1.63 (m p, 4H, $CH_2CH_2CH_2$), 2.87-3.49 (m p, 8H, NCH_2CH_2), 3.91-3.96 (t, *J* 4.68 and 5.78 Hz, 3H, OCH_3), 4.49-4.51 (m, 2H, OCH_2), 4.68-4.79 (m p, 4H, Ar-CH_2N), 5.17-5.28 (m p, 2H, =CH_2), 5.81-5.92 (m, 1H, =C*H*-), 7.50-8.07 (m p, 3H, C^{Ar}H).

HOC(O)-TAC(Fmoc/Alloc/Fmoc) 23

This scaffold was prepared from the fully protected monomeric scaffold analogous to the preparation of scaffold **9**. The desired product was obtained as a white solid by precipitation from THF using Et_2O. Yield: 2.9 g (3.6 mmol, 20%). HPLC (C_8): t_R = 24.98 min. ESI-MS: *m*/*z* 806.60 (calculated: 806.34 for $[M+H]^+$). ^{1}H-NMR (300 MHz, $CDCl_3$, TMS): δ 1.05-1.35 (d br s, 4H, $CH_2CH_2CH_2$), 2.5-3.4 (m br p, 8H, NCH_2CH_2), 4.24-4.63 (m br p, 12H, Ar-CH_2N and OCH_2 and Fmoc-C*H*), 5.16-5.25 (m p, 2H, =CH_2), 5.83-5.92 (m, 1H, =C*H*-), 7.3-7.9 (m p, 19H, $C^{Ar}H$). ^{13}C-NMR (75 MHz, THF-d_8, APT): δ 29.6 ($CH_2CH_2CH_2$), 46.0 and 47.7 (NCH_2CH_2), 48.6 (Fmoc-*C*H), 53.5 (Ar-CH_2N), 66.2 (Alloc-OCH_2 and Fmoc-OCH_2), 117.1 (=CH_2), 120.9-145.6 (C^{Ar} and =*C*H-), 155.9 and 157.0 (N*C*(O)O), 167.4 (*C*(O)OH).

Mono-acylated TAC-scaffold 27

For this synthesis, three equivalents of scaffold **23** were used for attachment to PS S RAM in the presence of 3 and 6 equiv of BOP and D*i*PEA, respectively. Any remaining amines were capped using a solution of Ac_2O/HOBt/DiPEA in NMP. After this, the Fmoc-groups were replaced by the trifluoroacetyl-groups using subsequently 20% piperidine in NMP and a mixture of trifuoroacetyl-imidazole (20 equiv, 355 µL) and D*i*PEA (20 equiv, 543 µL) in NMP. The Alloc-group of **25** was removed using Pd^0 in the presence of the scavenger anilinium *p*-toluenesulfinate. After this, Fmoc-His(Trt)-OH (387 mg) was coupled using BOP (276 mg) and D*i*PEA (217 µL). The Fmoc-group was replaced by the acetyl-group by treatment of the resin subsequently with 20% piperidine in NMP and a solution of Ac_2O, HOBt and D*i*PEA in NMP. Now, one portion of resin **26** was used for the construction of mono-acylated TAC-scaffold **27**. This portion of resin was treated with Tesser's base[25] followed by cleavage of compound **27** using TFA:TIS:water – 92.5:5:2.5 (v/v). The product was precipitated by cold (-20 °C) MTBE:*n*-hexane – 1:1 (v/v). Purification by preparative HPLC afforded mono-acylated scaffold **27**. Yield: 14.5 mg (19.4 µmol, 25%). ESI-MS: *m*/*z* 478.15 (calculated: 478.26 for $[M+Na]^+$). HPLC (C_8): t_R = 14.17 min.

6. Notes and References

1 See *Handbook of Proteolytic Enzymes*, eds. A.J. Barrett, N.D. Rawling, J.F. Woessner, New York, Elsevier Academic Press, **2004**, vol. 2.

2 A. Fehrst, *Enzyme Structure and Mechanism in Protein Science: a Guide to Enzyme Catalysis and Protein Folding*, New York, W.H. Freeman and Company, **1999**; M. Paetzel, R.E. Dalbey, *Trends Biochem. Sci.* **1997**, *22*, 29; G. Dodson, A. Wlodawer, *Trends Biochem. Sci.* **1998**, *23*, 347; L. Hedstrom, *Chem. Rev.* **2002**, *102*, 4501.

3 J.M. Berg, J.L. Tymoczko and L. Stryer, *Biochemistry*, 5th edn, New York, W.H. Freeman and company, **2006**.

4 H. Dugas, *Bioorganic Chemistry: A Chemical Approach to Enzyme Action*, Springer, New York, 3rd edn., **1996**.

5 D.H. Williams, E. Stephens, D.P. O'Brien, M. Zhou, *Angew. Chem. Int. Ed.* **2004**, *43*, 6596.

6 M.J. Corey and E. Corey, *Proc. Natl. Acad., Sci. USA* **1996**, *93*, 11428.

7 J.C. Powers, J.L. Asgian, Ö. Dogan Ekici, K. Ellis James, *Chem. Rev.* **2002**, *102*, 4693.

8 C.N. Fuhrmann, M.D. Daugherty, D.A. Agard, *J. Am. Chem. Soc.* **2006**, *128*, 9086.

9 B. Schiøtt, *Chem. Commun.* **2004**, 498; G.A. Rogers, T.C. Bruice, *J. Am. Chem. Soc.* **1974**, *96*, 2473.

10 P. Carter, J.A. Wells, *Nature* **1988**, *332*, 564.

11 M.J. Corey, E. Corey, *Proc. Natl. Acad. Sci., USA* **1996**, *93*, 11428.

12 R. Breslow, *Artificial Enzymes*, Wiley, Weinheim, 1st edn. 2005; A.J. Kirby, *Angew. Chem., Int. Ed. Engl.* **1996**, *35*, 707; V.T. D'Souza, M.L. Bender, *Acc. Chem. Res.* **1987**, *20*, 146; R. Breslow, *Acc. Chem. Res.* **1995**, *28*, 146.

13 For instance, the amide-NH group of the active site serine residue often assists in oxyanion stabilization of the reaction intermediate. See ref 2.

14 Asp-His-Ser containing β-sheet: Y. Fukushima, *Bull. Chem. Soc. Jpn.* **1996**, *69*, 2269.

15 R.A. Buono, N. Kucharczyk, M. Neuenschwander, J. Kemmink, L.-Y. Hwang, J.-L. Fauchère, C.A. Vananzi, *J. Computer-Aided Mol. Des.* **1996**, *10*, 213. See also B. Walse, M. Ullner, C. Lindbladh, L. Bülow, T. Drakenberg, O. Teleman, *J. Computer-Aided Mol. Des.* **1996**, *10*, 11.

16 A. Stavrakoudis, I.N. Demetropoulos, C. Sakarellos, M. Sakarellos-Daitsiotis, V. Tsikaris, *Lett. Pept. Sci.* **1997**, *4*, 481; A. Stavrakoudis, S. Makropoulou, V. Tsikaris, M. Sakarellos-Daitsiotis, C. Sakarellos, I.N. Demetropoulos, *J. Peptide Sci.* **2003**, *9*, 145.

17 Venanzi's mimic hydrolyzed Boc-Phe-pNP with $k_{cat} = 0.35 \pm 0.03$ min^{-1} and Tsikaris' mimic hydrolyzed Boc-Ala-pNP with $k_{cat} = 0.414$ min^{-1}.

18 For example see: cyclo-β-tetrapeptide: P. Virta, M. Karskela, H. Lönnberg, *J. Org. Chem.* **2006**, *71*, 1989. Pentaerythritol: A. Gea, N. Farcy, N. Roqué I Rossell, J.C. Martins, P.J. De Clercq, A. Madder, *Eur. J. Org. Chem.* **2006**, 4135. Steroidal: H. De Muynck, A. Madder, N. Farcy, P.J. De Clercq, M.N. Pérez-Payán, L.M. Öhberg, A.P. Davis, *Angew. Chem. Int. Ed.* **2000**, *39*, 145; A. Madder, L. Li, H. De Muynck, N. Farcy, D. van Haver, F. Fant, G. Vanhoenacker, G. Sandra, A.P. Davis, P.J. De Clercq, *J. Comb. Chem.* **2002**, *6*, 552. Kemps triacid: P. Kocis, O. Issakova, N.F. Sepetov, M. Lebl, *Tetrahedron Lett.* **1995**, *36*, 6623. Various amine-functionalized small symmetrical molecules: C. Guarise, L.J. Prins, P. Scrimin, *Tetrahedron* **2006**, *62*, 11670.

19 C. Chamorro, J.-W. Hofman, R.M.J. Liskamp, *Tetrahedron* **2004**, *60*, 8691; M.C.F. Monnee, A.J. Brouwer, L.M. Verbeek, A.M.A. van Wageningen, R.M.J. Liskamp, *Bioorg. Med. Chem. Lett.* **2001**, *11*, 1521.

20 T. Opatz, R.M.J. Liskamp, *J. Comb. Chem.* **2002**, *4*, 275.

21 D.J. van Zoelen, M.R. Egmond, R.J. Pieters, R.M.J. Liskamp, *ChemBioChem* **2007**, *8*, 1950.

22 M. Hijnen, D.J. van Zoelen, C. Chamorro, P. van Gageldonk, F.R. Mooi, G. Berbers, R.M.J. Liskamp, *Vaccine* **2007**, *25*, 6807.
23 T. Opatz, R.M.J. Liskamp, *Org. Lett.* **2001**, *3*, 3499.
24 R. Bruckner, *Advanced Organic Chemistry: Reaction Mechanisms*, Burlington (USA), Harcourt/Academic Press, **2002**, pp. 28-31.
25 G.I. Tesser, I.C. Balvert-Geers, *Int. J. Pept. Protein Res.* **1975**, *7*, 295.
26 L. Michaelis, M.L. Menten, *Biochem. Z.* **1913**, *49*, 333.
27 D. Koshland, *Bioorg. Chem.* **2002**, *30*, 211.
28 S. Komiya, *Synthesis of Organometallic Compounds*, **1997**, John Wiley & Sons Ltd. England.
29 E. Kaiser, R.L. Colescott, C.D. Bossinger, P.I. Cook, *Anal. Biochem.* **1970**, *34*, 595.
30 T. Vojkovsky, *Pept. Res.* **1995**, *8*, 236.
31 M.C.F. Monnee, A.J. Brouwer, R.M.J. Liskamp, *QSAR Comb. Sci.* **2004**, *23*, 546.

Chapter 3

TAC-Scaffolded Tripeptides as Artificial Hydrolytic Receptors: A Combinatorial Approach Toward Esterase Mimics

Abstract

In this chapter we present the first library (19,683 members) of tripodal synthetic receptor molecules containing three different, temporarily *N*-terminal protected peptidic arms capable of performing hydrolytic reactions. For the construction of the peptidic arms three different sets of amino acids were used, each focused on one part of the catalytic triad as is found in several families of hydrolytic enzymes. *N*-termininal amine groups were temporarily protected by trifluoroacetyl groups. Screening was performed with the known esterase substrate 7-acetoxycoumarin, which upon hydrolysis gave the fluorescent 7-hydroxycoumarin, leading to fluorescence of beads containing a hydrolytically active synthetic receptor. Although many synthetic receptors contain catalytic triad combinations, apparently only a few showed hydrolytic activity. Sequence analysis of the active receptors revealed that substrate cleavage was mediated by lysine (non-catalytic) or histidine (catalytic) residues. Kinetic analysis of resynthesized receptors showed that catalysis depends mainly on the number of histidine residues and was not assisted by significant substrate binding.

Parts of this chapter have been published: H.B. Albada and R.M.J. Liskamp, *J. Comb. Chem*. **2008**, *10*, 814.

1. Introduction

Artificial synthetic receptor molecules that possess catalytic properties are among the most interesting and challenging molecules to be designed and synthesized.[1] The combination of substrate binding and catalytic activity makes them not only interesting as catalytic species in their own respect, they also may be helpful in understanding of enzymatic activity. Therefore, it is not surprising that enzymes have been a tremendous source of inspiration in the development of small synthetic constructs capable of performing catalytic reactions.[2] Especially the selectivity and turn-over shown by enzymes[3] has been extremely inspiring and has posed an ever present challenge of mimicry their behavior. Among all enzymes, serine hydrolases have received above average amount of attention from chemists who embarked on attempts to mimic their activity.

So far, the response to this challenge of mimicking enzymatic activity has resulted in very diverse synthetic systems ranging from complicated designed molecules with pre-organized functionalities,[4] especially by Cram *et al*.,[5] to polymers randomly decorated with functional groups that are also present in catalytic sites of enzymes.[6] Within these approaches, peptide based mimetics are particularly interesting[7] since their functional groups are exactly identical to their enzymatic counterparts.[8] Combinatorial approaches might be especially useful in the discovery of novel peptide based catalysts,[9] or enzyme active site mimics, since a broad spectrum of molecular diversity becomes available in which subtle molecular interactions can be generated beyond prediction.[10] With respect to this it should be mentioned that only two combinatorial approaches have been reported so far in which hydrolytic activity towards ester bonds could be attributed to the combination of several functionalities of the side chains of amino acids. Firstly, the group of Reymond has shown impressive hydrolytic properties of peptidic dendrimers containing the serine protease catalytic triad aspartate-histidine-serine and serine-histidine dyads.[11] Their system showed astonishing hydrolytic activity and demonstrated unambiguously that dendrimers obtained by combinatorial approaches were 2-10 times more active than previously designed dendrimers.[12] Secondly, using small synthetic tweezer-like receptors, De Clercq *et al*. have shown that scaffolds containing two parallel tripeptides were able to cleave ester bonds, although catalysis has not been demonstrated.[13] Recently, they described an initial study on the application of an orthogonally protected tripodal synthetic receptor for the synthesis of serine protease mimics and other constructs.[14]

Encouraged by our results in the area of scaffolded peptides[15] towards selective binding of biological relevant molecules[16] and ions[17], and more recently as mimetics of type-3 copper binding sites in proteins, especially enzymes,[18] we decided to explore the properties of TAC-based peptidic receptors with respect to hydrolytic activity. These investigations might lead to peptide-based hydrolase mimics that rely on cooperation of peptidic arms as a result of attachment to a suitable scaffold. In

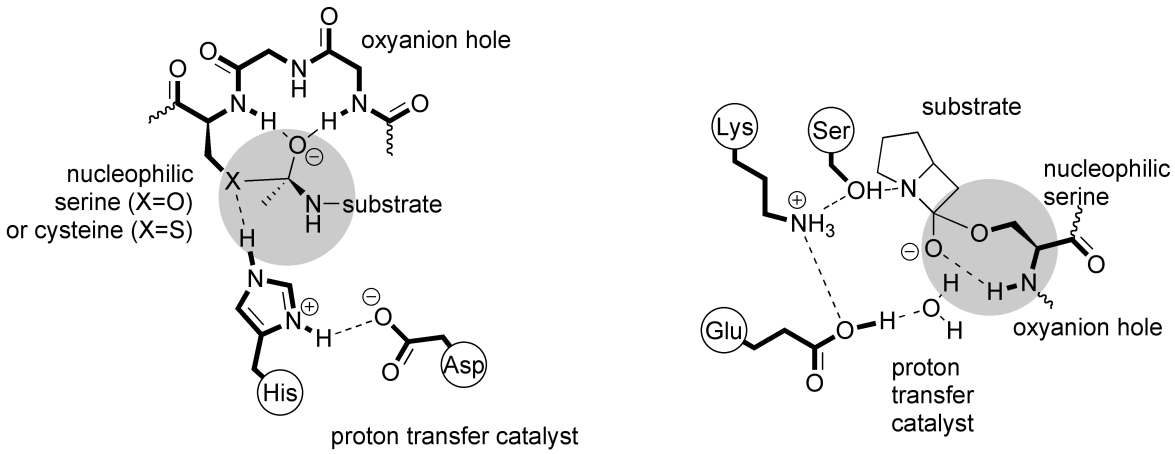

Figure 1. The most important components of the active sites of cysteine or serine proteases (*left*) and β-lactamases or DD-peptidases (*right*). For clarity, the tetrahedral intermediate of the enzyme-bound substrate stabilized by the oxyanion hole is highlighted by the grey circle, residues of to the enzyme are depicted in bold.

addition, we anticipated that our system with three different peptidic arms attached to one scaffold could shed more light on the requirements for small systems to serve as mimics of hydrolytic enzymes. Also, the presence of multiple functional amino acid residues that are also found in numerous enzymes active sites other than hydrolytic enzymes, can lead to catalytic receptors capable of reactions other than hydrolysis.

As far as hydrolysis by functional group enzymes is concerned, it is well-known that the activity is mainly determined by the cooperation between conformationally pre-organized acidic, basic and nucleophilic residues (Asp-His-Ser/Cys in serine or cysteine proteases, and Lys-Glu-Ser in β-lactamases and DD-peptidases[19,20]) (*figure 1*). Based on this knowledge we decided to decorate the semi-orthogonally protected triazacyclophane (TAC)-scaffold with the hydrolytically important residues that are found in the active sites of these three classes of enzymes. By selecting these residues, we created a very biased library that should allow screening for subtle arrangements of functional side chains within our synthetic receptors, possibly leading to hydrolysis. Incorporation of all these residues was deemed to be important due to the relative unknown properties of TAC-scaffolded receptors with respect to hydrolysis. Findings described in this paper can be used to create more advanced and focussed libraries.

2. Synthesis of the Library

The aim of this study was to investigate possible hydrolytic activity of scaffolded peptides, with the ultimate goal to identify potential functional mimetics of hydrolytic enzymes. To achieve this, the three different amine functionalities of the TAC-scaffold were decorated with three different tripeptide arms, using three different sets of amino acids – the chemsets. These three different chemsets enabled post-screening characterization of each of the arms in the active receptors by on-bead

Edman degradation.[21] This direct identification of the amino acids present in the active receptors circumvents the use of potentially interfering tags. The amino acids used in each arm corresponded to the nucleophilic, basic or acidic part of the catalytic triad. In addition, one non-functional hydrophobic amino acid in each set was introduced. These hydrophobic amino acids may provide a hydrophobic binding environment for the substrate. Therefore, the used chemsets were Cys/Ser/Phe for the arm containing the nucleophile, *i.e.* the nucleophilic set, His/Lys/Leu for the arm containing the base, *i.e.* the basic set, and Asp/Glu/Ile for the arm containing the acid, *i.e.* the acidic set. The resulting library was prepared by split-mix synthesis and contained theoretically 19,683 (3^9) different members of which one receptor contains only hydrophobic residues and of which 512 receptors contain only functional amino acids. A receptor in which three amino acids are specifically assigned to three positions, for instance with the serine, histidine and aspartate catalytic triad residues attached directly to the TAC-scaffold, is present in 729 (3^6) variations.

The orthogonally protected TAC-scaffold was synthesized as was described before.[22] For preparation of the library by split-mix synthesis, the scaffold was attached first to the Argogel-NH_2® resin by a BOP/D*i*PEA coupling yielding **1** (*scheme 1*). After removal of the Fmoc (9-fluoromethylmethoxycarbonyl) group from **1**, using piperidine in NMP, the resin was split into three equal portions. To each portion one of the three amino acids from chemset **2** (Fmoc-His(Trt)-OH {*1*}, Fmoc-Lys(Boc)-OH {*2*}, Fmoc-Leu-OH {*3*}) was coupled using BOP/D*i*PEA. After coupling, the three portions of resin were mixed into one portion and the Fmoc-group was removed using piperidine. Again, the resin was divided and the coupling, mixing, deprotection procedure was repeated twice. After coupling of the last amino acid, the Fmoc-group was removed and the liberated α-amine was protected by the base labile trifluoroacetyl group to yield chemset **3**. This temporary *N*-terminal protection was introduced in order to avoid acylation of the α-amine during the screening and prevent involvement of charged *N*-termini in the hydrolytic reaction. Removal of the *o*-NBS (*ortho*-nitrobenzenesulfonyl) group from **3** was accomplished by β-mercaptoethanol and DBU in DMF. For the construction of the second arm, the nucleophilic chemset **4** (containing Fmoc-Ser(*t*Bu)-OH {*1*}, Fmoc-Cys(Trt)-OH {*2*} and Fmoc-Phe-OH {*3*}) was used in three sequential split-mix steps followed by Fmoc-group removal and trifluoroacetylation. This afforded chemset **5**. After this, the Alloc (allyloxycarbonyl) group was removed by Pd^0 and the third arm was constructed using chemset **6**, consisting of Fmoc-Asp(O*t*Bu)-OH {*1*}, Fmoc-Glu(O*t*Bu)-OH {*2*}, and Fmoc-Ile-OH {*3*}. Removal of the *N*-terminal Fmoc-group was followed by trifluoroacetylation and the side-chain protecting groups were removed using an acidic cleavage cocktail. The presence of *N*-terminal TFAc-protecting groups on chemset **7** was verified by resistance of the receptors towards Edman-degradation.

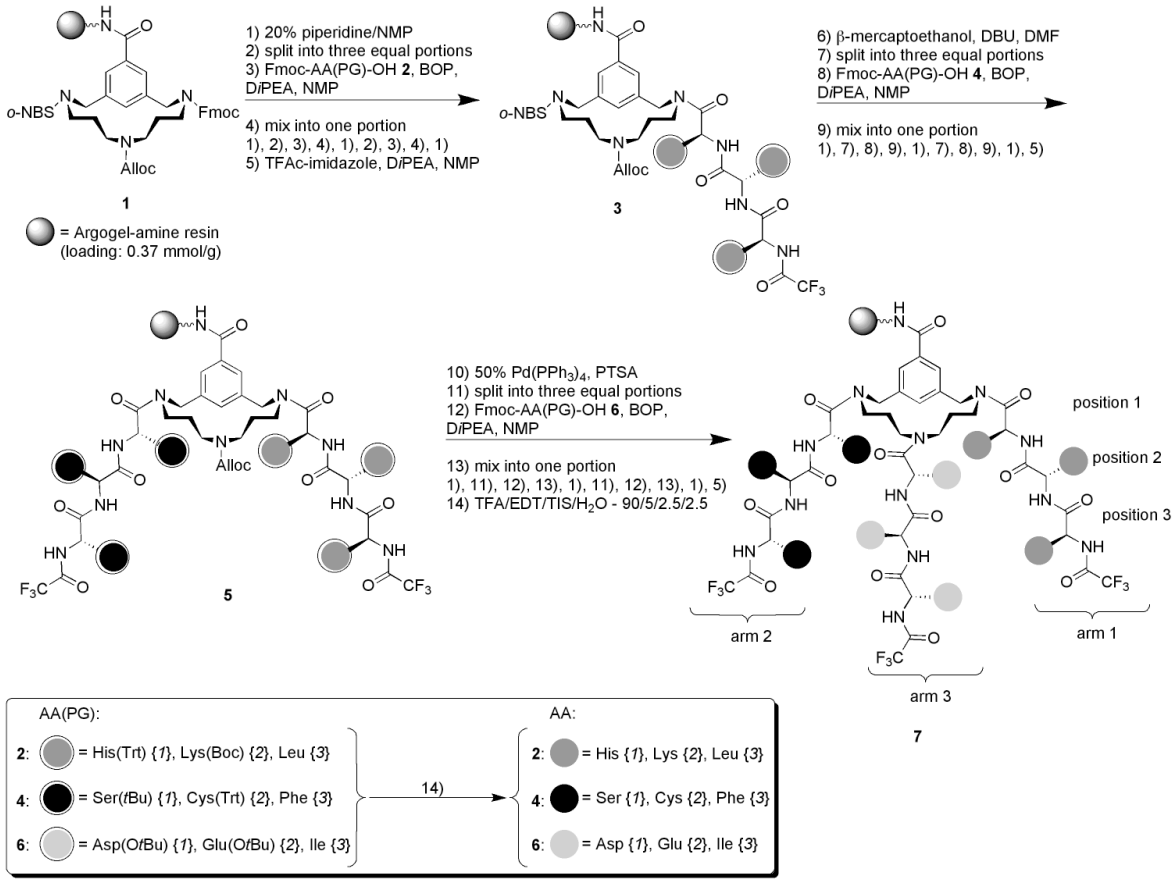

Scheme 1. Synthesis of the 19,683 membered library in which each arm of the synthetic receptor contains residues found in a particular part of several catalytic triads of hydrolytic enzymes (PTSA = anilinium *p*-toluenesulfinate).

3. Screening of the Library and Sequence Analysis of Hits

For screening of the library, to assess hydrolytic activity of resin-bound receptors, the method published by Reymond *et al.*[11a] was used. This method involved incubation of a monolayer of receptor-containing beads with a solution of a latent fluorescent substrate in a 20 mM Bis-Tris (pH 6.0) buffer on a Petri-dish. Diffusion of the fluorescent hydrolysis product is assumed to be limited by the microenvironment created by the polymer network of the resin, resulting in a build-up of fluorescence on the active receptor-containing bead. Although the screening was initially performed with several substrates,[23] the substrate that gave the best results so far was the 7-acetoxycoumarin ester. Upon hydrolysis of this substrate, the fluorescence of resulting 7-hydroxycoumarin produced a clearly identifiable blue fluorescent coloration of the bead containing the hydrolytically active receptors, which could easily be observed using a fluorescent microscope (*figure 2*).

Successive increasing concentrations of substrate were applied in order to find supposedly less hydrolytically active synthetic receptors. Fluorescent beads were picked, transferred into a micro tube and immediately treated, subsequently with a

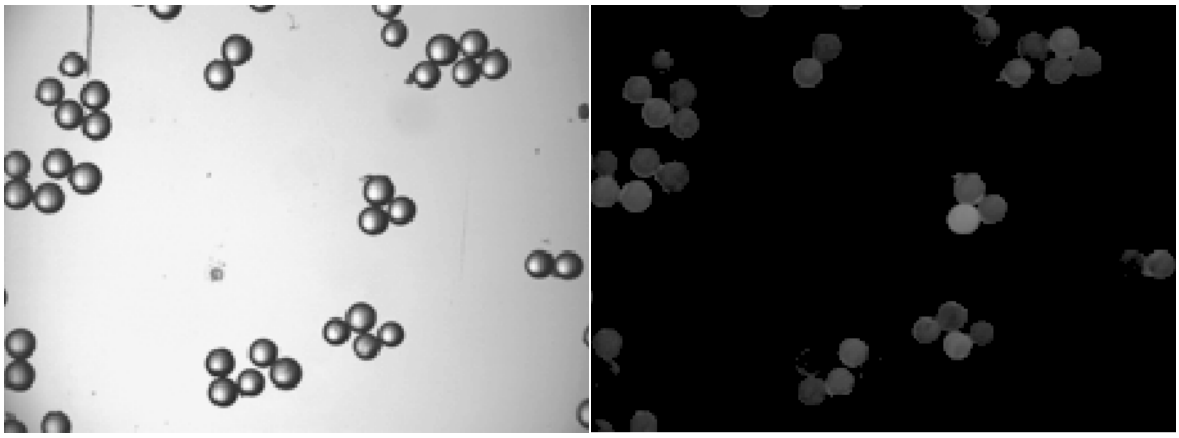

Figure 2. Clear distinction between a bead containing and beads lacking fluorescent hydrolyzed product (λ_{ex}: 330 nm; λ_{em}: 460 nm). Pictures obtained from beads illuminated by visible (left) and UV (λ_{ex}: 340-380 nm) light (right).

solution of acrylamide, a cysteine alkylating agent,[24] and Tesser's base.[25] The latter reagent was needed for removal of the trifluoroacetyl groups, in order to allow on-bead Edman-degradation.

From the Edman-degradation results it immediately became clear that signals originating from the nucleophilic arm did not show the presence of any cysteine residues. Also, in some degradation cycles no signals were observed corresponding to any of the other amino acids positioned in this arm. Even more, when the library was subjected to a solution of Ellman's reagent,[26] no significant coloration of the beads or solution was seen, indicating that no cysteine thiols were present in the library. Therefore, it was assumed that the cysteine residues were oxidized to the corresponding disulfide bridges, even in cases where an odd number of cysteine residues were present on the receptor. To test this, disulfide bridges were reduced to their thiol counterparts using 1,4-dithiotreitol (DTT).[27] After extensive washing with NMP under inert atmosphere the Ellman test indeed showed a strong coloration of the beads and solution, indicating that cysteine residues were regenerated. Cystine and cysteine residues cannot be detected by Edman degradation[28] and the absence of signals corresponding to acrylamide derivatized cysteine was explained by oxidation of cysteine residues. Therefore, although signals originating from cysteine-derivatives were absent in Edman-degradation profiles, the presence of cysteine residues was assumed when none of the other two possible amino acid phenyl-thiohydantoin derivatives, *i.e*. derived from serine or phenylalanine, showed up in the analyses. In *table 1* these residues are indicated by "*Cys*".

Some general observations can be derived from these screening results. First of all, the arm that contains residues which are known to be least important for hydrolysis mediated by serine hydrolases[29] – the middle arm with the acidic residues – showed the highest consistency with respect to the found residues by Edman degradation: the receptors preferably contain carboxylate residues. In addition, these receptors seem

Table 1. Edman degradation results of found hits from screening of the library with 40-800 μM 7-acetoxycoumarin solution in 20 mM Bis-Tris buffer (pH 6.0). *Cys* indicates positions of oxidized cysteine residues; bold numbers refer to resynthesized receptors (*scheme 2*).

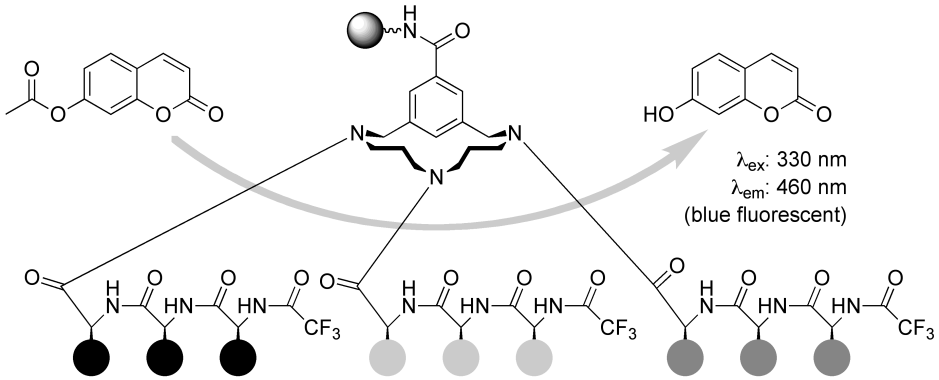

Entry	[S][a]	F.I.[b]									
1	40	+	Phe	Phe	Phe	Glu	Asp	Glu	Lys	Leu	Lys
2	40	+	*Cys*	*Cys*	Ser	Asp	Asp	Asp	Lys	Lys	Lys
3	40	+	Phe	Phe	Ser	Glu	Asp	Asp	Lys	Leu	Leu
4	40	+	*Cys*	Phe	Phe	Glu	Asp	Asp	Leu	His	Leu
5	100	++	Ser	Phe	Phe	Asp	Ile	Asp	His	His	Lys
6	100	+	*Cys*	*Cys*	*Cys*	Ile	Asp	Ile	Lys	Leu	His
7[c] (**11c**)	200	-	*Cys*	*Cys*	Ser	Glu	Ile	Glu	His	His	His
8	400	+	*Cys*	*Cys*	Ser	Asp	Asp	Glu	His	Leu	Leu
9 (**11d**)	400	++	*Cys*	*Cys*	Phe	Asp	Asp	Glu	His	His	His
10 (**11b**)	800	++	Phe	Phe	Phe	Ile	Asp	Asp	His	Leu	Leu
11	800	+	Phe	Phe	Ser	Asp	Asp	Asp	Leu	Leu	Lys

Notes: [a] substrate concentration in (μM); [b] Fluorescence Intensity as estimated by eye; [c] non-fluorescent bead as a negative control.

to prefer aspartate over glutamate. Secondly, despite the relatively low pH (6.0) at which the screening was performed, lysine residues were found, especially at low concentrations of screening substrate (*table 1*, entries 1-3 and 10). Although β-lactamases and DD-peptidases hydrolyse their substrate using a Lys-Glu-Ser triad, receptors decorated with these triads did not show catalytic turnover. Instead, the lysine ε-amine reacted as nucleophile – even though the pH was far below the pK_a of the ε-amine (pK_a ~10.5)[30] – resulting in aminolysis of the substrate.[31] However, increasing the substrate concentration to 100-800 μM revealed the preference of histidine over of lysine residues in the basic arm of the synthetic receptors (*table 1*, entries 7-10). Thirdly, the found hits also showed that histidine residues seem to be more important for hydrolysis than serine residues. Although enzymes hydrolyze ester bonds by means of direct attack of an activated serine or cysteine residue on the carbonyl carbon atom,[3] it is known that histidine residues themselves can also react as a nucleophile.[1a,2b] Even more, it has been reported that cooperation of histidine

with other histidine residues[6b,c,7i,j,11d,f] or carboxylate containing residues[32] can be significantly rate enhancing. Both of these combinations are present in the hits and might have been responsible for the observed ester hydrolysis.

4. Resynthesis and Hydrolytic Activity of Hits

As was mentioned above, fluorescence of beads containing hits with lysine residues probably originated from aminolysis of the subtrate,[31] which is a non-catalytic process. Since we were interested in catalysis, hits containing lysine residues were not considered for resynthesis.[33] With respect to this, two hits (entry 9 (**11d**) and 10 (**11b**), *table 1*), together with the negative control (entry 7 (**11c**), *table 1*) and the receptor containing only non-functional amino acids (referred to as receptor **11a**), were resynthesized in order to assess their hydrolytic properties in more detail (*scheme 2*). This kinetic analysis is crucial to validate the screening results and to gain a better understanding of the hydrolytic properties of these molecules, which might allow further improvements of the mimics.

Synthesis of the non-resin bound receptors was performed on TentaGel S RAM resin, a resin which is decorated with an acid-labile Rink-amide linker. The same protocol used for the construction of the library was also used in these syntheses (*scheme 2*), although now the products were cleaved from the resin. Receptors **11a** and **11b** yielded products of high purity[34]. Since we assumed the presence of intramolecular disulfide bonds in receptors **11c** and **11d**, cysteine containing receptors **11c'** and **11d'** were subjected to overnight intra-molecular disulfide formation using a dilute solution of the receptor in 20% DMSO in water (pH ~ 7). The reaction mixture was concentrated and pure cystine containing receptors **11c** and **11d** were obtained by preparative reversed phase HPLC.

For assessment of the hydrolytic activity of the resynthesized receptors, we studied the hydrolysis rate of 4-nitrophenyl acetate.[35] This substrate was used in view of the relatively small difference between the absorption spectrum of 7-hydroxycoumarin and 7-acetoxycoumarin, which was used for screening. During this analysis it was observed that the rate of hydrolysis at pH 6 was too low to obtain any reliable kinetic data, although a significant amount of hydrolyzed product was observed after the time interval of 90 minutes in which the screening was performed. However, at pH 7 reliable kinetic data were obtained. Together with analysis of these receptors, the rate of hydrolysis without catalyst and in the presence of 4-methylimidazole (4-MeIm, a histidine side-chain mimic) and Ac-His-diethylamide (Ac-His-dea **14**, a mimic of a histidine residue bound to a secondary amine of the TAC-scaffold) were measured (*table 2* and *scheme 2*). The synthesis of reference catalyst Ac-His-dea **14** was described in chapter 2.

The rate of hydrolysis in the presence of catalysts **11a-d**, **14** and 4-MeIm was determined by measuring the steepest increment of the first 10 measurements, which

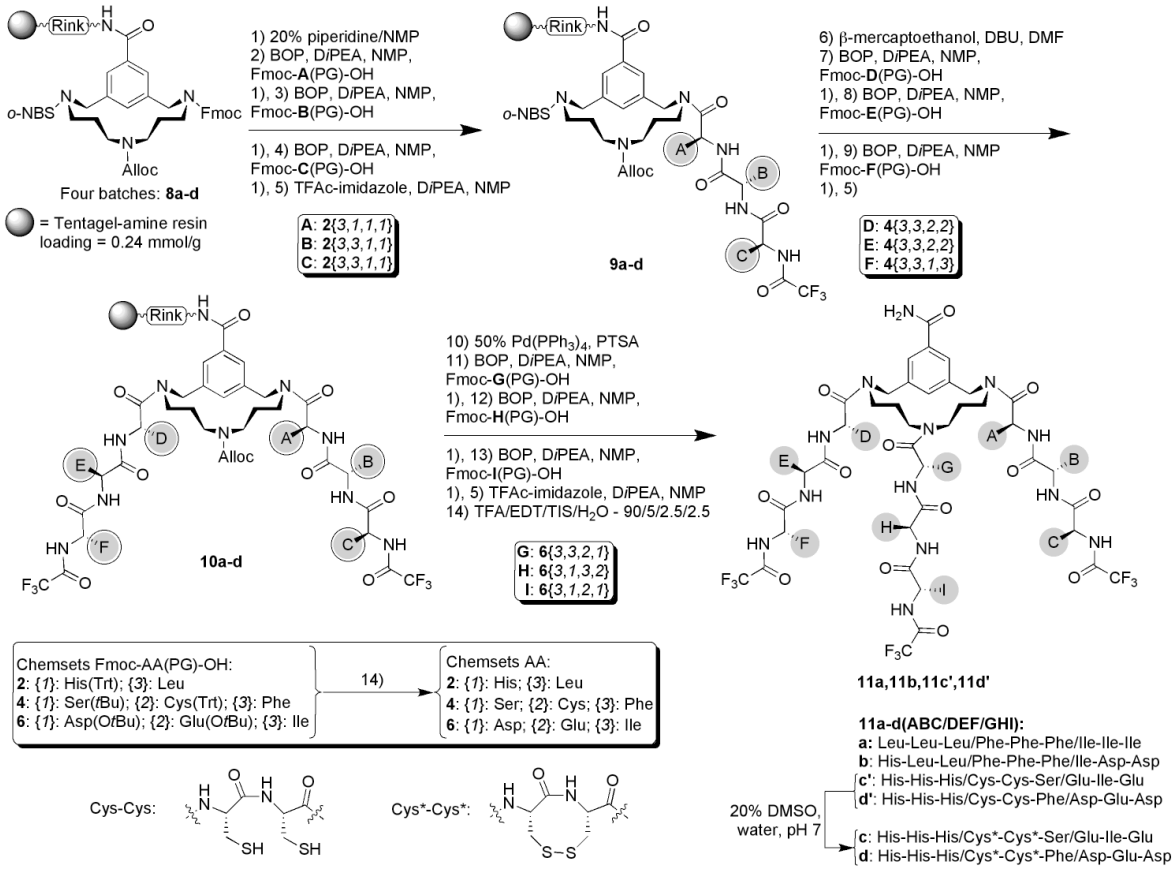

Scheme 2. Synthesis of resynthesized hydrolytic receptors (**11a-d**). Chemset numbering **#{a,b,c,d}**: **#** = number of chemset (**2**, **4** or **6**); **a**-**d** refer to the particular amino acid of the specified chemset used for the synthesis of receptor **a**, **b**, **c**, or **d**. The circles around the shadings in **9a-d** and **10a-d** symbolize the protected nature of the side-chain functionalities, they are unprotected in **11a-d'**.

correspond to the first 10 minutes of the measurement. This resulted in an apparent rate (V_{app}) given in mOD/min. From this V_{app}, the rate of hydrolysis in absence of a catalyst (V_{uncat}) was subtracted yielding V_{net}. This rate in mOD/min was converted into the rate in µM/min using the appropriate calibration curves (*figure 3*). From these curves, V_{max} and K_M were calculated using the formula $V_{max} = (V_{net} \times [S])/(K_M + [S])$, which is known as the Michaelis-Menten equation (*table 2*).[36] K_M is found at $V_{max}/2$ and is a measure for the affinity of the catalyst for the substrate. From the obtained V_{max} the k_{cat} was calculated using $k_{cat} = V_{max}/[cat]$. This k_{cat} is the turnover number and is a measure for the efficiency of the catalyst. By calculating the specificity or performance constant k_{cat}/K_M, some insight can be obtained with respect to the performance of the catalyst.[37] A high value of this constant identifies a catalyst with high performance concerning the reaction measured.

Although a linear correlation between rate of hydrolysis and substrate concentration was expected for these small hydrolysis catalysts,[1a,3,11,12] slightly curved lines were observed. Whereas some affinity for the substrate by Ac-His-dea **14** can be envisioned, based on hydrophobic interactions between catalyst and substrate, significant binding by 4-MeIm is very unlikely. The most likely cause of the observed non-linearity is

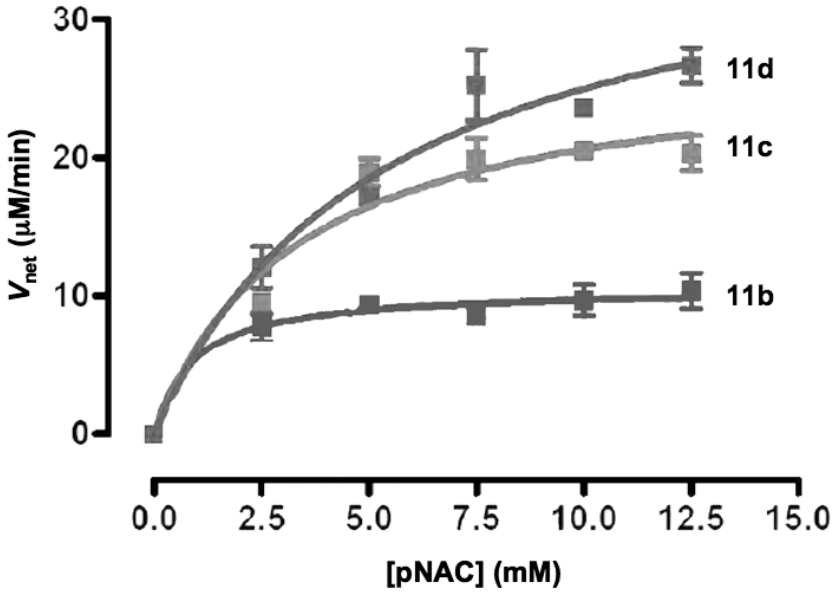

Figure 3. V_{net}/[pNAc]-curves for the three resynthesized receptors **11b-d**. *Conditions*: ~ 0.1 mM receptor, 2.5-12.5 mM substrate, 20 mM Bis-Tris buffer (pH 7.0) at 25 °C.

the presence of different amounts of DMSO at different concentrations of substrate. Due to the limited solubility of the substrate in water, DMSO had to be used as a co-solvent: at higher concentrations of substrate, more DMSO had to be used (up to 36% at 15 mM pNAc). It is known from literature that higher concentrations of DMSO can have a negative effect on the rate of hydrolysis of esters.[38] Although this artifact limits comparison of the observed rates with other studies in which different[7e,f] co-solvents have been used, these curves can be used to value the activity of the catalytic receptors and imidazole derivatives, which were tested under identical solvent-conditions.

Apparently, the screening resulted in the identification of a false negative, receptor **11c**, and at this stage the origin of this false negative is not clear. Nevertheless, important information can be obtained from the results shown in *table 2*. Firstly, a correlation is present between the number of histidine residues and the rate of hydrolysis: more histidine residues result in higher hydrolytic activity (receptors **11c** and **11d** *vs*. receptor **11b**). This is consistent with observations of other groups.[6,7i,j,11,12] Secondly, when compared to compound **14**, the activity of the receptors is at best similar in case of the most active receptor, which is disappointingly low. Thirdly, a significant difference is found between the catalytic activity of the two most active receptors (**11c** and **11d**), each containing three histidine residues in the basic arm. Apparently, variations in the other two arms have an influence on the kinetic parameters of the receptor. These variations can result in a more nucleophilic species, the presence of a hydrophobic substrate binding-site close to the nucleophile or even an oxyanion stabilizing moiety opposite to the attacking nucleophile. Fourthly, the high values of the Michaelis constant (K_M) show that these systems do not display significant affinity for the substrate. Only receptor **11b** showed some substrate binding, most

Table 2. Kinetic parameters of the resynthesized receptors **11a-d**. Values for the two reference catalysts were described in detail in chapter 2.

Catalyst	k_{cat} **(10^{-3} min^{-1})**	K_M **(mM)**	k_{cat}/K_M **($min^{-1}\cdot mM^{-1}$)**
receptor **11a** 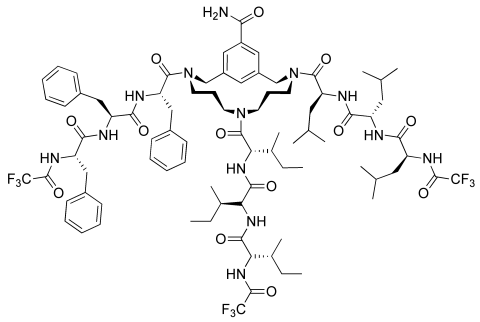	--	--	--
receptor **11b** 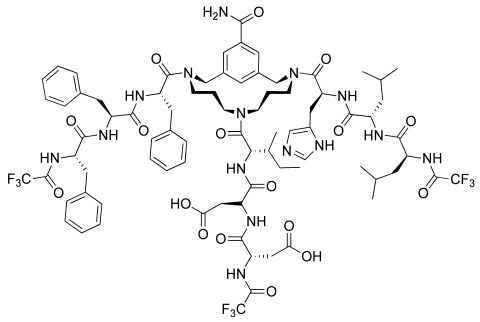	113 ± 7	0.9 ± 0.4	0.126
receptor **11c** 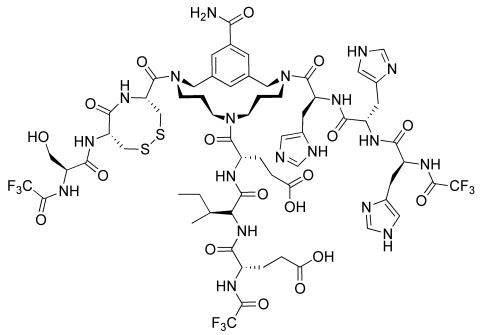	332 ± 47	3.4 ± 1.5	0.098
receptor **11d** 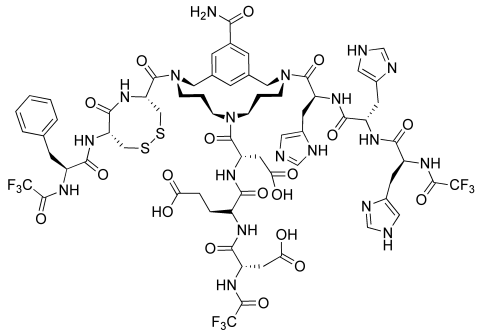	462 ± 65	5.4 ± 1.8	0.086
4-MeIm	106 ± 5	--	--
Ac-His-dea **14**	471 ± 29	10.6 ± 1.3	0.044

likely originating from the hydrophobic residues present in the receptor. Despite the higher substrate binding ability of this receptor, the activity is not comparable to the mimic of the histidine-residue in this system, Ac-His-dea. This might be due to reduced accessibility of the imidazole ring as result of the bulkiness of surrounding amino acid residues. Poor substrate binding ability by these TAC-based receptors is also concluded from the specificity constant k_{cat}/K_M: **11b** shows the highest and **11d** the lowest value, although the low values of this constant do not reveal impressive specific activity by any of these constructs. Lastly, even though 4-MeIm is abundantly used in the literature as a reference catalyst,[11,12] it appeared that 4-MeIm is not a reliable mimic of histidine based hydrolysis catalysts, although it might be used as a mimic of a histidine side-chain. When compared with Ac-His-dea, it is clear that not only the imidazole-ring is involved in catalysis, but that the backbone of the histidine residue assists in the hydrolytic cleavage of the substrate.

5. Discussion and Conclusions

Here, we describe the solid-phase preparation of a 19,683 membered library of tripodal peptide-based synthetic receptors, which might act as potential functional mimics of hydrolytic enzymes. This library was aimed at the identification of TAC-scaffolded receptors containing functional amino acids capable of hydrolyzing activated ester bonds. The availability of a sizable library allows, in principle, the evaluation of many combinations of (functional) amino acids. For this purpose, amino acids found in catalytic triads of hydrolytic enzymes were attached onto the TAC-scaffold and the *N*-terminal amines were temporarily protected by the trifluoroacetyl group. This protection prevented *N*-terminal acylation during screening as well as possible interference of charged *N*-termini with catalysis. Determination of the peptide sequence of resin-bound receptors was achieved by on-bead Edman degradation after removal of the trifluoroacetyl group. Since no tags were used for decoding of the selected hits, the observed activity was solely due to the amino acid sequences present on the TAC-scaffold. Although screening with low concentrations of 7-acetoxycoumarin substrate gave almost exclusively hits containing the β-lactamase triad Ser-Glu/Asp-Lys, at higher concentrations hits were found containing the serine protease triad Asp-His-Ser. Unfortunately, cysteine residues in the synthetic receptors were easily oxidized and could not be made available as nucleophiles during the screening. Resynthesis and analysis of the kinetic data of a few receptors identified by the screening showed that the catalytic activity of the receptors is most likely the result of the nucleophilicity of histidinyl imidazole rings and is only assisted by low substrate binding capacity. An increasing number of histidine residues led to higher hydrolytic activity. Apparently, subtle differences in the other arms had significant effect on the hydrolytic activity of the receptor. This might point to the possibilities offered by these TAC-scaffolded peptides to display catalytic activity and to tune the catalytic properties by small

changes in the arms of the receptors. Comparison of the activity of the catalytic receptors with two reference catalysts containing the imidazole ring, 4-MeIm and Ac-His-dea, showed that the activity of the most active receptor was comparable with that of Ac-His-dea.[39] In addition, it was observed that for hydrolysis reactions Ac-His-dea is a more reliable mimic of the histidine residue than the often-used reference compound 4-methylimidazole. Based on these results more focused libraries might be prepared, containing also amino acid residues capable of binding the substrate, in addition to the catalytically active amino acid residues. With respect to this, future combinatorial approaches towards peptide based hydrolytic receptors are best served when cysteine and lysine residues are replaced by other residues and when an Ac-His-amide derivative is used as a reference catalyst.

Although the catalytic activity of our synthetic receptor was low, this work shows that a multitude of diverse synthetic catalytic receptor molecule combinations can be conveniently synthesized and subjected to versatile screening procedures.[40] Even more, subtle changes in the amino acids of the arms can have pronounced effect on the catalytic activity, an observation that might encourage further research to be dedicated to the application of scaffolded peptides as catalysts. With this respect we envision the application of such novel peptide-based scaffolded receptor molecules in future catalytic studies focused on other catalytic reactions.

6. Experimental Section

General information

Chemicals were obtained from commercial sources and used without further purification. Reactions were performed at room temperature. Solution phase reactions were monitored by TLC analysis and R_f-values were determined on Merck pre-coated silica gel 60 F-254 (0.25 mm) plates. Spots were visualized with UV-light. Solid-phase synthesis was carried out in plastic syringes with PE frit (20 μm), Applied Separations Inc., distributed by Alltech Applied Science Group (Hoogeveen, The Netherlands). Column chromatography was carried out using Silica-P Flash silica gel (60 Å; particle size 40-63 μm; Silicycle). Electrospray Ionisation mass spectrometry (ESI-MS) was performed on a Finnigan LCQ Deca XP MAX LC/MS system. HPLC was performed on a Shimadzu Class-VP automated high performance liquid system, using an analytical reverse-phase column (Alltima, C_8, 300 Å, 5 μm, 250 × 4.6 mm) and a UV-detector (operating at 220 and 254 nm) as well as an ELSD-detector. Elution was realized using a gradient from water:MeCN:TFA – 95:5:0.1 % (v/v) to MeCN:water:TFA – 95:5:0.1 % (v/v) in 20 min and at a flow rate of 1 mL/min.

Standard procedures

Generally, ca 6 mL of solvent was used for each gram of resin.

- Fmoc-deprotection was performed using a 20% piperidine in NMP solution (2×8 min).
- Coupling (18 h) was performed using 4 equiv Fmoc-AA(PG)-OH, 4 equiv BOP, and 8 equiv D*i*PEA in NMP. The syringes were placed on a shaker.
- Capping of amines was carried out using a capping reagent consisting of 0.5 M acetic anhydride, 0.125 M D*i*PEA and 0.015 M HOBt in NMP (2×10 min).
- Washing: standard washing with NMP (3×2 min) and DCM (3×2 min).
- Coupling, deprotection and capping was monitored using the Kaisertest[41] (for primary amines) or chloranil[42] test (for secondary amines).

Preparation of the library

Prior to coupling 1 g of Argogel-NH_2® resin (0.37 mmol/g, 65 – 125 mesh, average bead diameter 178 μm) was washed with 0.1 M HOBt in NMP and 15% D*i*PEA in NMP (each for 15 minutes) and washed with NMP and DCM. To this resin were added 715 mg (0.9 mmol, 2.5 equiv) HO-TAC(Fmoc/Alloc/*o*-NBS), 411 mg (0.9 mmol, 2.5 equiv) BOP, and 322 μL (1.85 mmol, 5 equiv) D*i*PEA in 10 mL NMP. After capping of any remaining amine functionalities the resin was dried under *vacuo* and the loading of the resin was determined to be 0.29 mmol/g.[43]

From half of the total amount of resin, the Fmoc-group was removed using the standard Fmoc-deprotection protocol and the resulting resin was divided into three equal portions. To each of the portions Fmoc-His(Trt)-OH, Fmoc-Lys(Boc)-OH or Fmoc-Leu-OH was

coupled using the standard coupling method in a volume of 3 mL NMP. The syringes with the reaction mixture were placed on a shaker for 18 h after which the resin was washed using standard washing protocols. Completion of the coupling was determined by means of the chloranil test. The loading of each portion of the resin was determined and corrected for the added weight. Each of the resulting resins had a loading of 0.27 mmol/g. After pooling of the resins, the Fmoc-group was removed and the resin mixture was again divided into three equal portions. The procedure described above, involving the coupling of one of the three amino acids to each portion, was repeated twice. After this, the *N*-terminal Fmoc-group was removed from the resulting scaffolded tripeptide and the α-aminegroup was protected with the trifluoroacetyl group using 248 μL D*i*PEA (20 equiv, 0.713 mmol) and 163 μL 1-(trifluoroacetyl)imidazole (20 equiv) in NMP. The reaction was allowed to proceed for 18 h under gentle shaking. The resin was washed with NMP and DCM (each 3×2 min) and completion of protection of the first arm was shown by a negative Kaiser test.

Prior to the removal of the *o*-NBS-group, the resin was thoroughly washed with DMF in order to remove all DCM. After this, the *o*-NBS-group of the scaffold was removed using 1.43 mL 0.5 M 2-mercaptoethanol in DMF (10 equiv, 0.713 mmol) and 53 μL DBU (5 equiv, 0.356 mmol) (2×30 min).[44] After deprotection, the resin was washed using DMF (3×2 min) and DCM (3×2 min). A positive chloranil test showed the presence of a secondary amine. The resin was divided into three equal portions to each of which one of the amino acids of Fmoc-Cys(Trt)-OH, Fmoc-Ser(*t*Bu)-OH or Fmoc-Phe-OH was attached using the standard coupling procedure. The synthesis of this, so called "nucleophilic", arm was completed as described for the first, so called "basic", arm.

Subsequently, the Alloc-group was removed using 50% $Pd(PPh_3)_4$ (41 mg) in the presence of 20 equiv of anilinium *p*-toluenesulfinate as a scavenger (378 mg) in NMP. The reaction was carried out for 18 h under a gentle stream of Argon and liberation of the amine was apparent from the chloranil test. Prior to the standard washing protocol, the resin was washed extensively with a 20 mM solution of the sodium salt of diethyldithiocarbamic acid. The construction of the third, so called "acidic", arm was carried out using the same procedure as for the other two arms, using the amino acids Fmoc-Asp(O*t*Bu)-OH, Fmoc-Glu(O*t*Bu)-OH and Fmoc-Ile-OH. After Fmoc-deprotection of the tripeptide and trifluoroacetylation of the *N*-terminal amine, the fully protected library was obtained. Deprotection of the side-chains was carried out using an acidic cleavage cocktail of TFA/EDT/TIS/H_2O – 90/5/2.5/2.5 (%) for 3 hours. The resin was thoroughly washed with NMP and DCM – until no EDT could be smelled – and was stored under Argon.

Resynthesis of the hits from screening, *i.e.* receptors 11a-d

Resynthesis of the receptors was carried out analogously to the procedure used for the construction of the library. After the deprotection and cleavage, the receptors containing the

two cysteine residues (**11c** and **11d**) were subjected to disulfide bridge formation. This could be achieved by overnight reaction of 1 mM solutions of the receptors **11c'** and **11d'** in 20% DMSO/water at pH ~ 7. After this, the reaction mixture was condensed in vacuum at 40 °C and the crude mixture was purified by preparative-HPLC. The products were analyzed by MS and the combined fractions containing the products were lyophilized. MS-analysis of resynthesized receptors:
receptor **11a**: *m/z* 1685.35 (calculated: 1684.85 for $[M+H]^+$)
receptor **11b**: *m/z* 1711.95 (calculated: 1712.71 for $[M+H]^+$).
receptor **11c**: *m/z* 1638.62 (calculated: 1638.52 for $[M+H]^+$).
receptor **11d**: *m/z* 1686.36 (calculated: 1686.49 for $[M+H]^+$)

7-acetoxycoumarin ester: synthesis was performed according to the literature.[45]

Screening of the library
Prior to screening, the library was washed with 25% D*i*PEA (1×10 min) under nitrogen in order to remove the TFA-salts that were left after deprotection, followed by NMP (3×2 min, 6 mL each time), DCM (2×2 min, 6 mL each time), MeCN (2×2 min, 6 mL each time) and water (2×2 min, 6 mL each time). Amino acid side-chain amine, carboxylic acid and imidazole functionalities were protonated or deprotonated, respectively, by incubation with 20 mM Bis-Tris (pH 6.0) buffer overnight. The buffer was removed, the resin quickly rinsed with MeCN and poured into a Petri-dish using DCM. This created upon evaporation of the DCM a perfect monolayer, necessary for screening. The library was treated with a small amount of MeCN in order to remove residual DCM. After evaporation of all MeCN a substrate solution in the buffer – a stock-solution of the substrate in MeCN was diluted a 1000-fold with the buffer to the appropriate concentration – was applied and incubated with the resin on the Petri-dish for 90 minutes. Blue fluorescent beads, indicating hydrolysis by synthetic receptors, were visualized under a fluorescent microscope. Fluorescent beads were picked and processed further in micro tubes (100 μL). Prior to subsequent screenings, the library was washed in a syringe with frit using MeCN, NMP and MeCN. Beads were again poured into the Petri-dish according to the procedure mentioned above.

Post-screening alkylation of cysteine residues and removal of the trifluoroacetyl group
This was performed in order to prepare the library for on-bead Edman sequencing. Cysteine residues were alkylated by treatment of the bead with a 2 M solution of acrylamide in 0.3 M Tris buffer (pH 8.3) for 2 hours in the dark at room temperature under Argon. After alkylation, excess of reagents was removed by washing with water (3 times), ether (once), DCM (once) and MeOH (twice). Removal of *N*-terminal trifluoroacetyl-groups was performed by treatment with Tesser's base[25] (overnight) and subsequent washing with water (twice). After

this, beads were subjected to on-bead Edman sequencing.

1,4-Dithiotreitol (DTT) reduction of cysteine residues

A solution of 17.1 mg (111 μmol, ~ 3 equiv/Cys) DTT was dissolved in a minimum amount of 0.3 M Tris-buffer (pH 8.3). This was added to the library and allowed to react for 30 minutes. During disulfide reduction, the beads turned slightly brown. The DTT solution was removed by filtration and the resin was washed with 1 mL aqueous 0.1 M EDTA solution in 2 mL NMP (2 × 2 min), this resulted in complete decoloration of the beads. After this, the beads were extensively washed with NMP under inert atmosphere.

Ellman's test for free thiol groups

The dry resin was swelled in DCM and washed twice with MeCN followed by a quick rinse with water. A solution of 3 mM EDTA in a 200 mM NaOAc (pH = 8.0) buffer was added and allowed to react for 5 minutes. The solution was removed by suction and the beads were treated with a 20 mM 5,5'-dithio-bis(2-nitrobenzoic acid) (DTNB) solution in 50 mM phosphate buffer (pH = 7.0) under a gentle stream of nitrogen. DTT treated resin showed an immediate color change to yellow (due to the formation of the thiolate anion) upon treatment with Ellman's reagent. Resin not treated with DTT did not undergo this color change. The resulting mixed cysteine-Ellman reagent disulfides could again be reduced by DTT, resulting in a strongly yellow colored solution, indicating regeneration of cysteine residues.

The synthesis of Ac-His-dea **14** has been described in **chapter 2**.

Hydrolysis study

To analyze the hydrolytic properties of the synthetic receptors under identical conditions, hydrolysis was performed in 96-well plates. For this, the synthesized receptors or reference catalysts were dissolved in DMSO to a concentration of 0.1 mM and 1 mM, respectively, and 4-nitrophenyl acetate was dissolved in a mixture of DMSO/buffer – 2/3 (v/v) to a concentration of 25 mM. For the buffer 20 mM Bis-Tris (pH 6.0 and 7.0) was used. All measurements were carried out with a total volume of 50 μL (5 μL "catalyst" + 5-25 μL substrate solution + 40-20 μL buffer). The reaction was monitored for 2 hours and initial rates were calculated using the steepest increment over five measurements in the first ten minutes. This increment (mOD/min) was given by the software (Full Mode-KC4 (Version 3.4 (Rev 21)) software (BioTek instruments); data point resolution was set at 2 nm). This rate *v* (mOD/min) was converted into the rate in μM/min using the appropriate calibration curves made from solutions of 4-nitrophenol in 50 μL buffer/DMSO mixtures. All hydrolytic reactions were performed in duplo. After subtraction of the background hydrolysis, the obtained V_{net}(μM/min)/[S](mM)-values were processed using GraphPad Prism 4. V_{max} and

K_M were calculated using the nonlinear fit model of the program, which relies on the formula $V_{max} = V_{net} \times [pNAc])/(K_M+[S])$. The turnover ($k_{cat}$) number was calculated by $V_{max}/[cat]$.

7. References and Notes

1 See for instance: a) R. Breslow, *Artificial Enzymes*, Wiley, Weinheim, 1st edn., **2005**; b) H. Dugas, *Bioorganic Chemistry: A Chemical Approach to Enzyme Action*, Springer, New York, 3rd edn., **1996**; c) P. Ball, *Designing the Molecular World*, Princeton University Press, **1994**, pp. 145-185; d) L.F. Lindoy, *The Chemistry of Macrocyclic Ligand Complexes*, Cambridge University Press, **1989**, pp. 136-173; e) Y. Murakami, J. Kikuchi, O. Hayashida, *Chem. Rev.* **1996**, *96*, 721.

2 a) A.J. Kirby, *Angew. Chem., Int. Ed. Engl.* **1996**, *35*, 707; b) V.T. D'Souza, M.L. Bender, *Acc. Chem. Res.* **1987**, *20*, 146; c) R. Breslow, *Acc. Chem. Res.* **1995**, *28*, 146; d) J.B. Jones, K.E. Taylor, *Can. J. Chem.* **1977**, *55*, 1653.

3 A. Fehrst, *Enzyme Structure and Mechanism in Protein Science: a Guide to Enzyme Catalysis and Protein Folding*, New York, WH Freeman and Company, **1999**.

4 A. Madder, P.J. De Clercq, *J. Org. Chem.* **1998**, *63*, 2548.

5 D.J. Cram, *Angew. Chem., Int. Ed. Engl.* **1988**, *8*, 1009; D.J. Cram, *Science* **1988**, *240*, 760.

6 a) I.M. Klotz, G.P. Royer, I.S. Scarpa, *Proc. Natl. Acad. Sci., USA* **1971**, *2*, 263; b) J. Suh, *Acc. Chem. Res.* **2003**, *36*, 562; c) J. Suh, *Synlett* **2001**, *9*, 1343.

7 a) M.Z. Atassi, T. Manshouri, *Proc. Natl. Acad. Sci., USA* **1993**, *90*, 8282. However, claims could not be confirmed: b) B.W. Matthews, C.S. Craik, H. Neurath, *Proc. Natl. Acad. Sci., USA* **1994**, *91*, 4103; c) J.A. Wells, W.J. Fairbrother, J. Otlewski, M. Laskowski Jr., J. Burnier, *Proc. Natl. Acad. Sci., USA* **1994**, *91*, 4110; d) D.R. Corey, M.A. Phillips, *Proc. Natl. Acad. Sci., USA* **1994**, *91*, 4106. Cyclic peptide as scaffold: e) A. Stavrakoudis, I.N. Demetropoulos, C. Sakarellos, M. Sakarellos-Daitsiotis, V. Tsikaris, *Lett. Pept. Sci.* **1997**, *4*, 481; f) A. Stavrakoudis, S. Makropoulou, V. Tsikaris, M. Sakarellos-Daitsiotis, C. Sakarellos, I.N. Demetropoulos, *J. Peptide Sci.* **2003**, *9*, 145. Aggregating α-helices containing Ser-His-Asp catalytic triad: g) K.W. Hahn, W.A. Klis, J.M. Stewart, *Science* **1990**, *248*, 1544. Reinvestigation of claims in this paper could not reproduce the claimed activity: h) M.J. Corey, E. Corey, *Proc. Natl. Acad. Sci., USA* **1996**, *93*, 11428. α-helices containing topological neighboring histidine residues: i) K. Broo, L. Brive, P. Ahlberg, L. Baltzer, *J. Am. Chem. Soc.* **1997**, *119*, 11362; j) K.S. Broo, H. Nilsson, J. Nilsson, A. Flodberg, L. Baltzer, *J. Am. Chem. Soc.* **1998**, *120*, 4063.

8 a) A. Berkessel, *Curr. Opin. Chem. Biol.* **2003**, *7*, 409; b) Y. Li, Y. Zhao, S. Hatfield, R. Wan, Q. Zhu, X. Li, M. McMills, Y. Ma, J. Li, K.L. Brown, C. He, F. Liu, X. Chen, *Bioorg. Med. Chem.* **2000**, *8*, 2675.

9 See for instance: a) C.A. Lewis, A. Chiu, M. Kubryk, J. Balsells, D. Pollard, C.K. Esser, J. Murry, R.A. Reamer, K.B. Hansen, S.J. Miller, *J. Am. Chem. Soc.* **2006**, *128*, 16454; b) M.B. Fierman, D.J. O'Leary, W.E. Steinmetz, S.J. Miller, *J. Am. Chem. Soc.* **2004**, *126*, 6967; c) D.J. Guerin, S.J. Miller, *J. Am. Chem. Soc.* **2002**, *124*, 2134; d) G.T. Copeland, S.J. Miller, *J. Am. Chem. Soc.* **2001**, *123*, 6496; e) C. Schmuck, J. Dudaczek, *Org. Lett.* **2007**, *9*, 5389; f) J.D. Revell, H. Wennemers, *Curr. Opin. Chem. Biol.* **2007**, *11*, 269; g) H. Wennemers, *Comb. Chem. High Througput Screen.* **2001**, *4*, 273.

10 M.L. Snapper, A.H. Hoveyda, *Combinatorial Chemistry: practical approach*, Oxford University Press, Oxford, **2003**, pp. 433-455.

11 a) A. Clouet, T. Darbre, J.-L. Reymond, *Angew. Chem. Int. Ed.* **2004**, *43*, 4612; b) A. Clouet, T. Darbre, J.-L. Reymond, *Biopolymers (Peptide Science)* **2006**, *84*, 114; c) D. Lagnoux, E. Delort, C. Douat-Casassus, A. Eposito, J.-L. Reymond, *Chem. Eur. J.* **2004**, *10*, 1215; d) E. Delort, T. Darbre, J.-L. Reymond, *J. Am. Chem. Soc.* **2004**, *126*, 15642; e) C. Douat-Casassus, T. Darbre, J.-L. Reymond, *J. Am. Chem. Soc.* **2004**,

126, 7817; f) E. Delort, N.-Q. Nguyen-Trung, T. Darbre, J.-L. Reymond, *J. Org. Chem.* **2006**, *71*, 4468; g) T. Darbre, J.-L. Reymond, *Acc. Chem. Res.* **2006**, *39*, 925.

12 A. Eposito, E. Delort, D. Lagnoux, F. Djojo, J.-L. Reymond, *Angew. Chem. Int. Ed.* **2003**, *42*, 1381.

13 a) H. De Muynck, A. Madder, N. Farcy, P.J. De Clercq, M.N. Pérez-Payán, L.M. Öhberg, A.P. Davis, *Angew. Chem. Int. Ed.* **2000**, *39*, 145; b) A. Madder, L. Li, H. De Muynck, N. Farcy, D. van Haver, F. Fant, G. Vanhoenacker, G. Sandra, A.P. Davis, P.J. De Clercq, *J. Comb. Chem.* **2002**, *6*, 552.

14 a) A. Gea, N. Farcy, N. Roqué I Rossell, J.C. Martins, P.J. De Clercq, A. Madder, *Eur. J. Org. Chem.* **2006**, 4135; b) S. Van der Plas, A. Gea, S. Figaroli, P.J. De Clercq, A. Madder, *Eur. J. Org. Chem.* **2008**, 1582.

15 a) M.C.F. Monnee, A.J. Brouwer, L.M. Verbeek, A.M.A. van Wageningen, R.M.J. Liskamp, *Bioorg. Med. Chem. Lett.* **2001**, *11*, 1521; b) D.W.P.M. Löwik, M.D. Weingarten, M. Broekema, A.J. Brouwer, W.C. Still, R.M.J. Liskamp, *Angew. Chem. Int. Ed.* **1998**, *37*, 1846.

16 a) C. Chamorro, J.-W. Hofman, R.M.J. Liskamp, *Tetrahedron* **2004**, *60*, 8691; b) C. Chamorro, R.M.J. Liskamp, *Tetrahedron* **2004**, *60*, 11145; c) M. Hijnen, D.J. van Zoelen, C. Chamorro, P. van Gageldonk, F.R. Mooi, G. Berbers, R.M.J. Liskamp, *Vaccine* **2007**, *25*, 6807; d) D.J. van Zoelen, M.R. Egmond, R.J. Pieters, R.M.J Liskamp, *ChemBioChem* **2007**, *8*, 1950.

17 T. Opatz, R.M.J. Liskamp, *J. Comb. Chem.* **2002**, *4*, 275.

18 H.B. Albada, F. Soulimani, B.M. Weckhuysen, R.M.J. Liskamp, *Chem. Commun.* **2007**, 4895.

19 a) M. Paetzel, R.E. Dalbey, *Trends Biochem. Sci.* **1997**, *22*, 29; b) G. Dodson, A. Wlodawer, *Trends Biochem. Sci.* **1998**, *23*, 347.

20 M. Nukaga, K. Mayama, A.M. Hujer, R.A. Bonomo, J.R. Knox, *J. Mol. Biol.* **2003**, *328*, 289.

21 a) P. Edman, *Acta. Chem. Scand.* **1950**, *4*, 283; b) P. Edman, G. Begg, *Eur. J. Biochem.* **1967**, *1*, 80; c) R.A. Laursen, *Eur. J. Biochem.* **1971**, *20*, 89. Sequencing of peptoid peptidomimetics by Edman degradation: d) A. Boeijen, R.M.J. Liskamp, *Tetrahedron Lett.* **1998**, *39*, 3589.

22 T. Opatz, R.M.J. Liskamp, *Org. Lett.* **2001**, *3*, 3499.

23 7-acetoxy-*N*-methylquinolinium iodide was also tested but it proved to be too unstable for these studies, see also F. Caturla, J. Enjo, M.C. Bernabeu, S. Le Serre, *Tetrahedron* **2004**, *60*, 1903. Screening with 7-octanoyl-oxycoumarin did not yield significantly different receptor molecules; no increased hydrophobic recognition was seen.

24 Non-derivatized cysteine residues cannot be observed in Edman-degradation cycles: D.C. Brune, *Anal. Biochem.* **1992**, *207*, 285 and ref. 28. Two alkylating agents were tested: acrylamide and iodoacetamide. Acrylamide proved to be the most useful since the retention time of the acrylamide alkylated cysteine is 7.15 minutes. The acetamide alkylated cysteine residue had a retention time of 6.57 minutes, which was close to the 6.45 minutes of glutamic acid.

25 G.I. Tesser, I.C. Balvert-Geers, *Int. J. Pept. Protein Res.* **1975**, *7*, 295.

26 G.L. Ellman, *Archives of Biochemistry and Biophysics* **1959**, *82*, 70.

27 J. Butler, S.P. Spielberg, J.D. Schulman, *Anal. Biochem.* **1976**, *75*, 674.

28 M. Friedman, L.H. Krull, J.F. Cavins, *J. Biol. Chem.* **1970**, *245*, 3868.

29 P. Carter, J.A. Wells, *Nature* **1988**, *332*, 564.

30 See *The Merck Index*, 13th edition, **2006**, p. MISC-60. At pH 6.0 still 20 ppm of the lysine residues is unprotonated, leaving them nucleophilic towards reaction with the carbonyl of the substrate. Nevertheless, Edman sequencing did not show signals of acetylated lysine residues, since the amount of this residue is below the detection limit of the method. Due to highly fluorescent character of 7-hydroxycoumarin, even small traces of aminolyzed substrate can be observed causing fluorescence of beads containing the lysine residues.

31 a) L.N. Vakhitova, V.A. Savelova, F.Ya. Burdina, I.A. Belousova, A.F. Popov, *Rus. J. Org. Chem.* **2003**, *39*, 968; b) J. Suh, S.S. Hah, H.L. Lee, *Bioorg. Chem.* **1997**, *25*, 63; c) A.C. Satterthwait, W.P. Jencks, *J.*

Am. Chem. Soc. **1974**, *96*, 7018.
32 P. Pengo, S. Polizzi, L. Pasquato, P. Scrimin, *J. Am. Chem. Soc.* **2005**, *127*, 1616.
33 Entry 4 was not selected due to the presence of an odd number of cysteine residues.
34 It should be mentioned that the total number of synthetic steps for the synthesis of the library and the resynthesized receptors is 27. The isolated yield of receptors **11a** and **11b** was 18-22%, which corresponds to an average yield of 94% per step; yields of **11c** and **11d** were lower due to the extra steps needed in the synthesis.
35 The use of two different substrates, one to meet screening conditions and another to meet the conditions needed for determination of catalytic parameters, is not uncommon. See for instance: C. Schmuck, J. Dudaczek, *Org. Lett.* **2007**, *9*, 5389.
36 L. Michaelis, M.L. Menten, *Biochem. Z.* **1913**, *49*, 333.
37 D. Koshland, *Bioorg. Chem.* **2002**, *30*, 211.
38 For a review on the effect of water-organic solvent mixtures on kinetics: A.J. Parker, *Chem. Rev.* **1969**, *69*, 1. More specific on the effect of DMSO on hydrolysis: M.S. Metwally, *React. Kinet. Catal. Lett.* **1992**, *47*, 319.
39 It should be noted that peptides cleaved from the resin were isolated as TFA-salts after lyophilization. Receptors **11b** (one histidine residue), **11c** and **11d** (each containing three histidine residues) – assuming the presence of one TFA counterion per histidine residue – therefore have a molecular weight of 1826.73, 1980.62 and 2028.62, respectively. Using these values, the molarity of catalyst in the hydrolysis studies becomes then 93.7, 82.7 and 83.1 μM, respectively. These values were used in the calculation of the k_{cat} (100 μM was used for receptor **11a**).
40 Other substrates might be screened by this library. Also, addition of transition metals might facilitate reactivity. See for instance: a) A. Berkessel, D.A. Hérault, *Angew. Chem. Int. Ed.* **1999**, *38*, 102; b) O. Lavastre, F. Bonnette, L. Gallard, L. *Curr. Opin. Chem. Biol.* **2004**, *8*, 311.
41 E. Kaiser, R.L. Colescott, C.D. Bossinger, P.I. Cook, *Anal. Biochem.* **1970**, *34*, 595.
42 T. Vojkovsky, *Pept. Res.* **1995**, *8*, 236.
43 Using a slightly modified procedure of: W.C. Chan, P.D. White, *Fmoc Solid Phase Peptide Synthesis: a practical approach*, Oxford University Press, New York, **2000**, pp. 62-63.
44 Loading $f = [A_{300} \times 1.28]/[m_{resin}\ (mg)]$. Corrected loading $f' = [1000 \times f]/[1000 - (FW_{added} \times f)]$.
45 See for instance T. Fukuyama, C.-K. Jow, M. Cheung, *Tetrahedron Lett.* **1995**, *26*, 6373.
46 A slightly modified procedure was used, of: X. Ren, X. Chen, K. Peng, X. Xie, Y. Xia, X. Pan, *Tetrahedron Asymmetry* **2002**, *13*, 1799.

Chapter 4

Amide-Bond Cyclized TAC-Based Cryptand Molecules Containing all Relevant Components of Serine Hydrolase Active Sites

Abstract

In this chapter, several attempts to construct *N*-terminally bis-cyclized TAC-based serine hydrolase catalytic triad residue containing receptors are described. Cyclization was performed by construction of a peptide bond using one bis-amine and two flanking carboxylic acid moieties. In a first attempt, the amine functionalities were protected as azides and the carboxylic acid moieties as trimethylsilylethyl-esters. In a more advanced approach, amine functionalities were protected by the trimethylsilylethyloxy carbonyl group, allowing simultaneous *C*- and *N*-terminus deprotection. In both attempts, cyclization appeared to be very difficult, yielding only a small amount of desired product. The ^{1}H-NMR spectrum was very complex, which indicated the presence of several conformations. Unfortunately, the amount synthesized was too small for hydrolysis experiments, preventing assessment of the effect of the rigidification on the activity.

1. Introduction on pre-organization in *functional group* enzymes

Enzymes often catalyze reactions by the cooperative action of a few well-positioned functional groups present on the side-chains of amino acids.[1] These functional groups are present in the so-called active site of the enzyme, which is a highly optimized environment for a particular reaction.[2] One of the functions of the protein surrounding the active site of an enzyme is to position the catalytically crucial functional groups in such a way that highly reactive functionalities are generated.[1,3] It is therefore not surprising that catalytically active residues are usually found in highly conserved regions of the protein[4] and are often less mobile than non-catalytic residues.[5]

The similarity of the pre-organization of functional groups can be illustrated by the positions of the active site residues of serine hydrolase catalytic triads present in several enzymes (*figure 1*). Even though these enzymes hydrolyze different acyl-containing substrates, *i.e.* peptide bonds and esters,[6] the positioning of the functionalities of the catalytic triads is virtually identical.

1.1. Pre-organization and catalytic activity of enzyme mimics

It has been suggested that a high degree of pre-organization of functionalities is also crucial for the realization of true enzyme mimics, in particular those that can also cleave amide bonds.[12] Whereas most man-made hydrolysis catalysts were only active against (activated) ester bonds, hydrolysis of amide bonds was not achieved for a long time. In fact, one of the main objections concerning the limited activity of many hydrolase mimics is that they were only active towards reactive substrates, formulated as the '*p*-nitrophenol ester syndrome'.[13] For the hydrolysis of the activated esters often used in hydrolysis studies the presence of an imidazole ring is usually sufficient, circumventing the necessity of functional group cooperation to the same extent as is found in active sites of hydrolytic enzymes.

Whereas hydrolase mimicry produced numerous esterase mimics, the first organic artificial proteinase was not published until 1998. By means of molecular imprinting

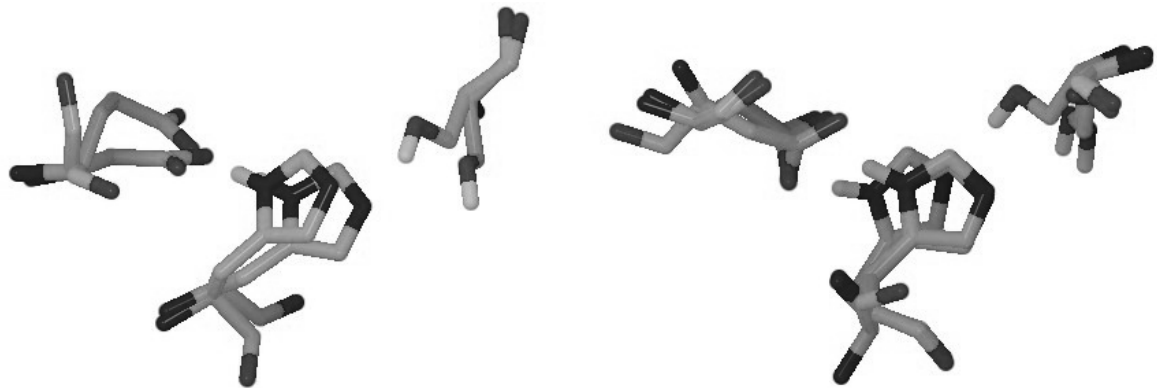

Figure 1. Overlay of several serine hydrolase catalytic triads. Lipase[7] and acetyl choline esterase[8] (left), subtilisin,[9] trypsin[10] and γ-chymotrypsin[11] (right).

Suh *et al*. produced an aspartic protease mimic of which the active site contained three convergent salicylate residues on a polyethylenimine (PEI) network.[14] In the presence of this artificial proteinase, the half-life of γ-globulin was 1 h (at pH 7 and 50 °C). For comparison, random decoration of PEI with salicylates resulted in very low activity, indicating that proteolytic activity of the artificial enzyme arose from collaboration between proximal salicylates. This example showed that a cooperative interaction between functional groups in enzyme mimics is crucial for hydrolysis of stable bonds like amide bonds (*vide infra*).

In contrast, small (FW<1000) synthetic molecules containing all relevant components of serine protease active sites in a pre-organized fashion were never realized. A model proposed by Cram – until now not synthesized – is an outstanding example of this (*figure 2*). This model was the ultimate goal of a long lasting interest in the synthesis and analysis of host-molecules for certain guest-molecules.[15] In fact, host-guest chemistry describes basic principles that underline the field of biomimetic chemistry, especially enzyme mimicry.[16]

Already in 1967, Pedersen *et al*. showed that crown ethers have a high affinity for certain cations.[17] Later, Cram *et al*. discovered that chiral crown ethers selectively bind one isomer of certain amino acid derivatives and thereby mimic stereospecific binding often found in enzymes.[15] Whereas Pedersen *et al*. pioneered the field of host-guest chemistry by his description of crown ethers, Cram *et al*. and Lehn *et al*. extended this concept by designing polycyclic compounds, resulting in more pre-organized hosts

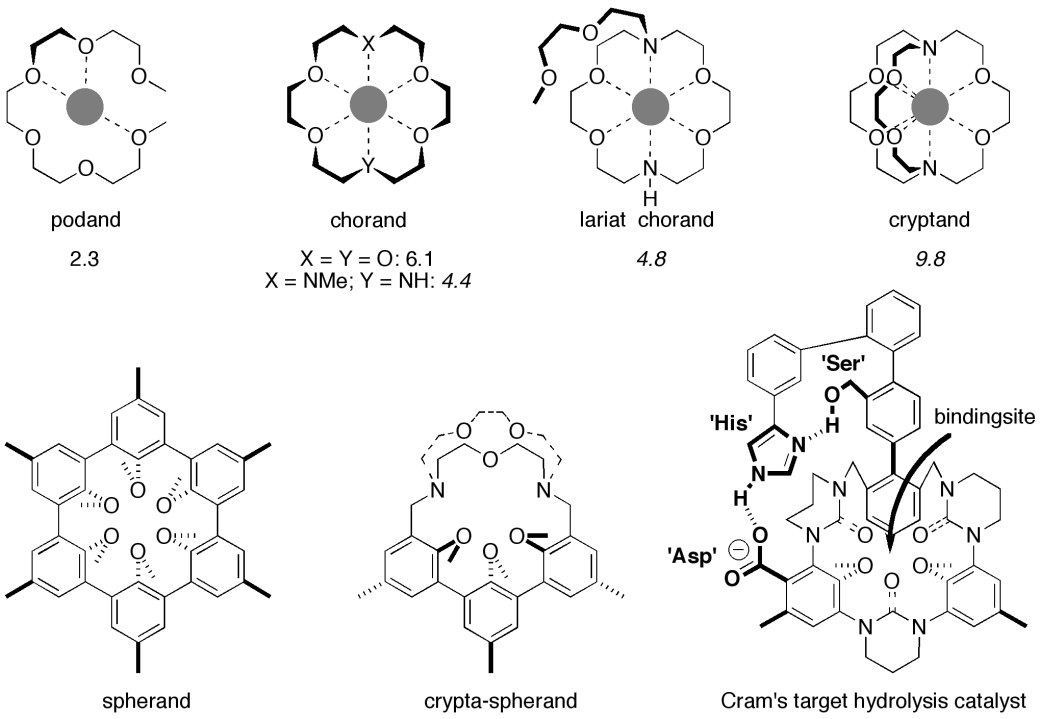

Figure 2. Top four structures show five distinct hosts for potassium cations; values below the complexes are logK_a values of the hosts for potassium (in MeOH or 95% MeOH in water (*values in italic*)). The lower three structures show two even more pre-organized hosts and Cram's proposed serine hydrolase mimic.

with even more affinity for a guest (*figure 2*).[18] More recently, covalently cyclized cage molecules and some guests have been studied: cyclotriveratrylene (CTV) for Xe,[19] nitrogen-bridged macrocycles for cations and anions,[20] hemicarcerands and fullerenes for gas molecules,[21] pyrrolo-tetrathiafulvalene for chloroform,[22] and cyclophanes for anionic chromophores[23]. In addition, some self-assembling cage molecules or capsules formed by coordination complexes have been described.[24] The group of Rebek Jr. developed self-assembling capsule molecules capable of binding guests[25] and catalyzing reactions[26]. He also showed the important principle of convergent functional groups in catalysis.[27]

Based on these considerations and findings, together with the observed low activity of previously synthesized TAC-based serine hydrolase constructs, we anticipated that the synthesis of rigid constructs could lead to more active serine hydrolase mimicking molecules (*figure 3*). Enhanced activity might originate from cooperation of functional groups and/or from enhanced affinity for a substrate caused by the presence of a binding pocket as in a baseball-glove. In addition to this, the number of synthetic peptidic cryptands presented in literature is very limited, which added to our desire to study such molecules.[28]

So far, TAC-based receptor molecules were all based on the attachment of linear or cyclic peptides onto the scaffold, generating relatively flexible constructs.[30] In one occasion, a dipodal or tweezer-like receptor was cyclized at the *N*-terminus using ring-closing metathesis, thereby increasing the affinity for a guest with a factor of 6.[31] Therefore, imposing constraints on tripodal TAC-scaffolded amino acids or peptides may result in pre-organization of functional groups and as a consequence the catalytic activity originating from the cooperation of functionalities may take place or is enhanced.[32] However, rigidification of TAC-based constructs may also lead to aberrant pre-organization of functionalities,[31] *e.g.* on the outside of the caged structure.

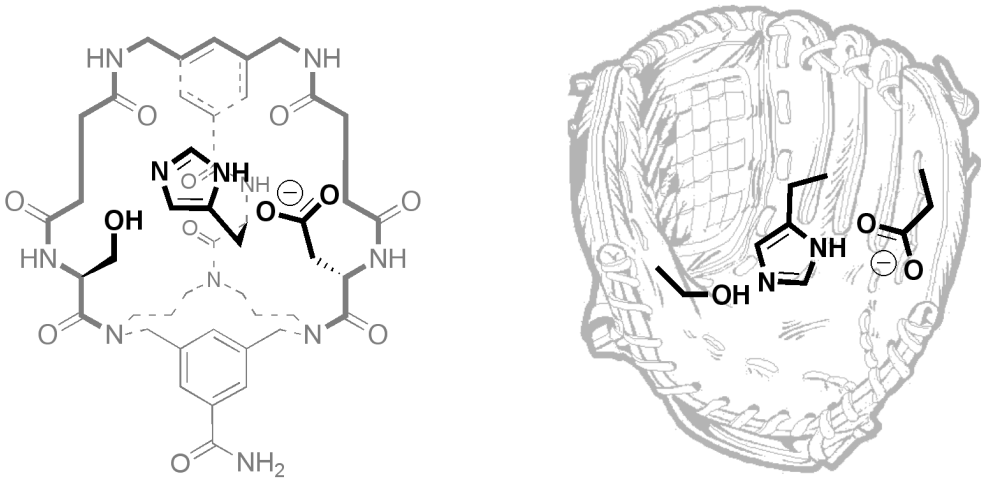

Figure 3. Illustration of a baseball glove[29] (right) resembling a TAC-based serine hydrolase mimicking cryptand molecules (left).

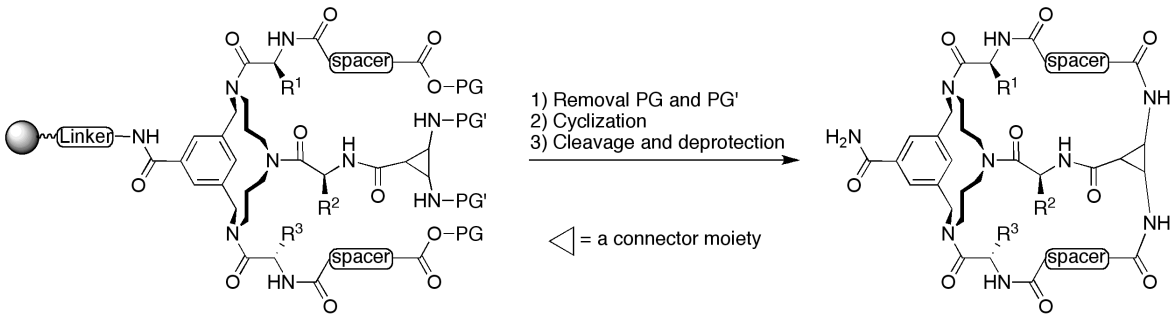

Scheme 1. Schematic outline of the synthetic approach towards the construction of amide-cyclized TAC-based peptidic cryptand molecules.

1.3. Outline of the project

The synthesis of flexible TAC-based peptidic receptors, described in detail previously,[30,31,33] also provided an ideal platform for the construction of pre-organized TAC-based molecules. By modifying the *N*-terminal groups, covalent linkage of the three 'arms' could be envisioned (*scheme 1*).

Obviously, the protecting groups of the carboxylic acid and amine functionalities had to be stable under Fmoc-, *o*-NBS- and Alloc-deprotection conditions, which include piperidine treatment, exposure to a thiolate nucleophile and palladium(0). For this reason we used a mono 2-(trimethylsilyl)-ethanol (Te) ester for the bis-acid, which is stable under these conditions and can be removed by fluoride.[34] For the bis-amine we initially used 3,5-bis(azidomethyl)benzoic acid in which the azide functionalities are masked amine groups. The conversion of azide to amine can be achieved by reduction.[35] In a later stage, the azide moieties were replaced by 2-(trimethylsilyl)-ethyloxycarbonyl (Teoc) protected amine groups.

2. Cryptand synthesis using terminal azide and Te protection

2.1 Synthesis of the resin-bound cryptand precursor

An initial attempt to construct double cyclized TAC-based peptidic cryptand was

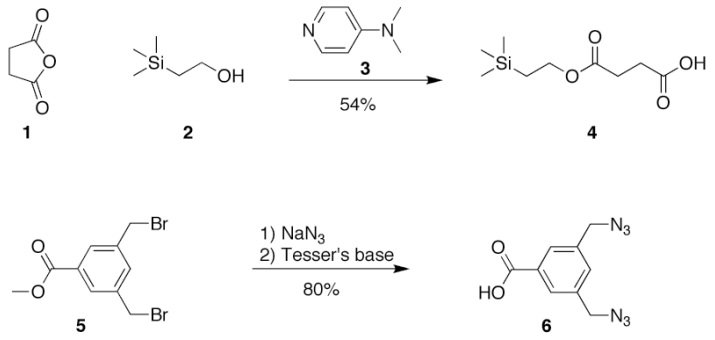

Scheme 2. Synthesis of protected succinic acid 4 and bis-azide 6.

based on a mono Te-protected bis-acid and 3,5-bis(azidomethyl)benzoic acid. Mono-protected acid **4** was prepared by mixing succinic anhydride **1** with a small excess of 2-(trimethylsilyl)-ethanol **2** in the presence of a catalytic amount of DMAP **3**. In addition, bis-azide **6** could be synthesized from bis-bromide **5** using NaN_3, followed by saponification of the methyl ester (*scheme 2*). Using acid **4** and bis-azide **6**, precursor **11** was prepared using Fmoc-based solid-phase peptide chemistry (*scheme 3*). This precursor was used to assess the feasibility of the construction of a TAC-based peptidic cryptand containing the serine hydrolase catalytic triad.

Loading of the resin with the HO-TAC(Fmoc/Alloc/*o*-NBS) scaffold resulted in a loading of 0.53 mmol/g. After Fmoc-deprotection of **8**, precursor **9** was obtained using Fmoc-Ser(*t*Bu)-OH and acid **4** in standard BOP/D*i*PEA based peptide chemistry. Removal of the *o*-NBS group in **9** was achieved using thiolate and after coupling of Fmoc-Asp(O*t*Bu)-OH and acid **4**, precursor **10** was obtained. The introduction of the middle arm started with removal of the Alloc group using Pd^0. After this, subsequent coupling of Fmoc-His(Trt)-OH and bis-azide **6** resulted in the formation of precursor **11**. HPLC and ESI-MS analysis of cleaved intermediates **9**, **10**, Alloc deprotected **10** and **11**, were satisfactory, indicating the applicability of this chemistry for the construction of precursor **11**. The thus obtained precursor **11** was subjected to several backbone deprotection (*scheme 4*) and double cyclization experiments (*scheme 5*).

First, Te-protected acids were deprotected using an excess of TBAF in DMF.[36] This deprotection could be visualized by standard ^{1}H-NMR of resin-bound constructs: diminishing of the TMS signals around zero ppm showed complete deprotection. After this, several conditions were applied to study the reduction of the azide groups to the corresponding amine functionalities (*table 1*). Initially, using D*i*PEA as a base did not result in the formation of the desired product (entries 1-4). An improvement of the reduction was observed upon addition of a catalytic amount of the strong base DBU (entry 5). By using only DBU and by prolonging the reaction time to overnight reaction, complete reduction of the azide-groups was achieved yielding precursor **12** (entry 6). During this reduction, HPLC analysis of intermediate products showed a rapid initial reduction of the azide-groups followed by slow completion of the reaction. In addition, several minor side-products were formed, which prompted us to explore an alternative synthetic route (*vide infra*). Nevertheless, the batch used for this test-reaction was suitable to test some double cyclization conditions.

2.2. Double cyclization experiments using precursor 12

Since only a limited number of precedents for the synthesis of double cyclized peptides are known,[38] some test-reactions were performed in order to gain insight in the best conditions for such a double cyclization (*scheme 5*). In these experiments the main focus was on temperature and coupling reagent. The results were evaluated using ESI-MS analysis of cleaved products.

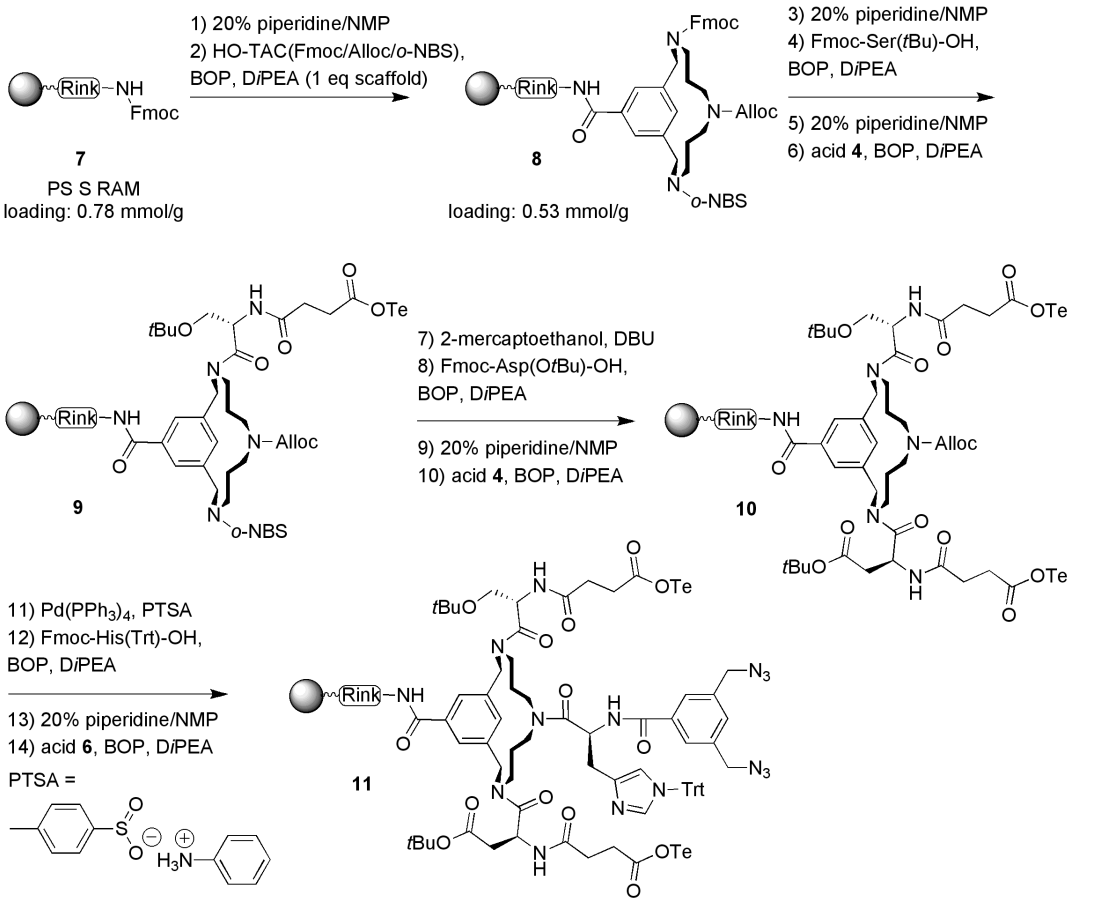

Scheme 3. Synthesis of solid-phase bound precursor **11**.

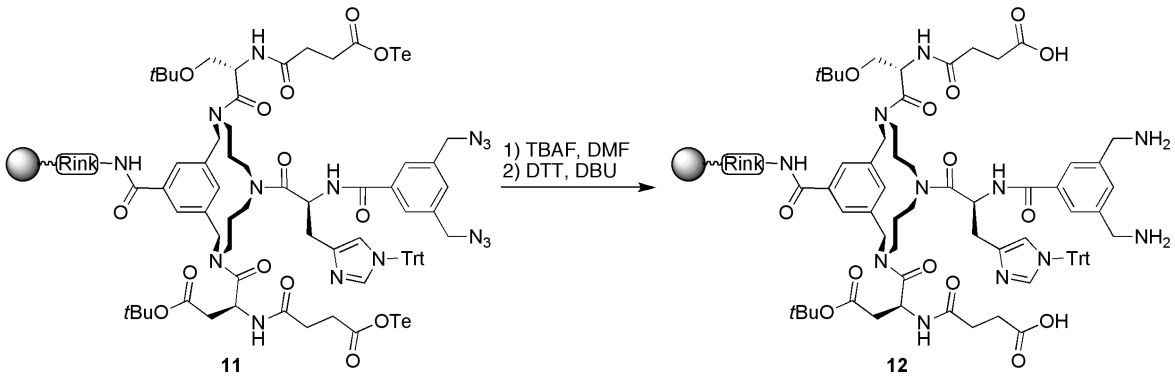

Scheme 4. Conditions for the conversion of **11** to **12**.

Table 1. Conditions used to study on-resin azide reduction of **11**.[37]

Entry	Thiol/Solvent	Base	Time	Results (ESI-MS)
1	0.2 M DTT/DMF	0.1 mM D*i*PEA	1 h	Bis-azide
2	0.2 M DTT/DMF	0.2 mM D*i*PEA	16 h	Bis-azide
3	20 equiv DTT/DCM	8 equiv D*i*PEA	1 h	Some mono-amine
4	20 equiv DTT/DMF	8 equiv D*i*PEA	1 h	Some mono-amine
5	20 equiv DTT/DMF	8 equiv D*i*PEA, cat DBU	1 h	Bis- and mono-amine
6	20 equiv DTT/DCM	10 equiv DBU	16 h	Bis-amine

Initially, the effect of the temperature on the double cyclization was studied by performing the reaction at room temperature, 50 °C (oil bath), 60 °C, 100 °C and 140 °C (all three using microwave heating). BOP and D*i*PEA were used as coupling reagents (*figure 4*).[39] Unfortunately, none of these conditions resulted in any observable cyclization. In addition, heating to 100 and 140 °C resulted in dark coloration of both resin and solution, indicating the occurrence of side-reactions of which none could be identified. As a result of this, we switched to the more reactive coupling combination HATU/HOAt (*figure 4*).[40] For this, two reactions were carried out: one at room temperature and one at 50 °C. For the reaction at room temperature some mono- and bi-cyclic product was detected and for the reaction performed at 50 °C even more bi-cyclic product was observed. Apparently, more active coupling reagents and slightly elevated temperatures are beneficial for the formation of **13**.

Although HATU/HOAt resulted in desired compound **13**, a significant amount of uronium adduct was also formed (*figure 5*).[41] Therefore, two other coupling reagents were also tested: a combination of EDC and HOAt, and PyBOP. Although EDC suffers from a similar disadvantage as HATU, *i.e.* the formation of EDC-adducts (*figure 5*), it can also give higher yields of the desired compound. From LC-MS analyses it was apparent that indeed EDC adducts were formed – although in smaller quantities than the uronium adduct – and that improvement of purity and yield of desired compound were insignificant. When PyBOP was used, much less side-product was observed but HPLC-profiles of the reaction did not show significant improvements of the formation

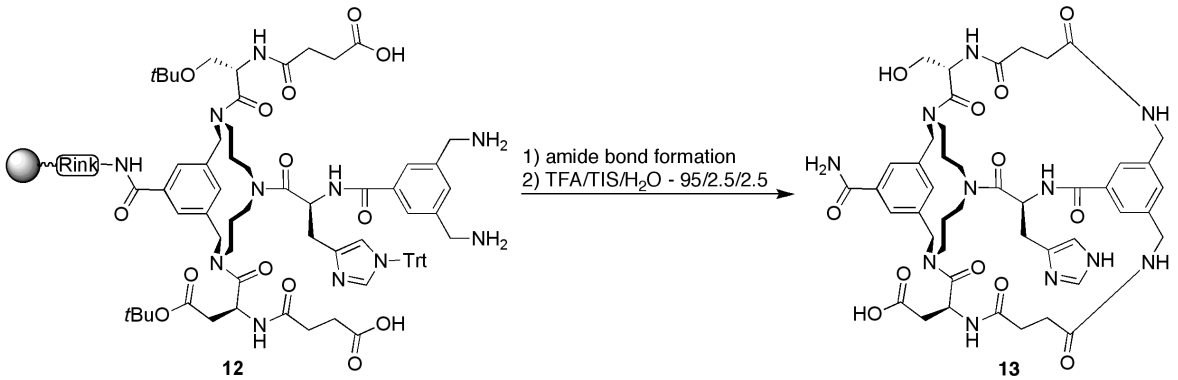

Scheme 5. Double cyclization of precursor **12** to afford cryptand **13**.

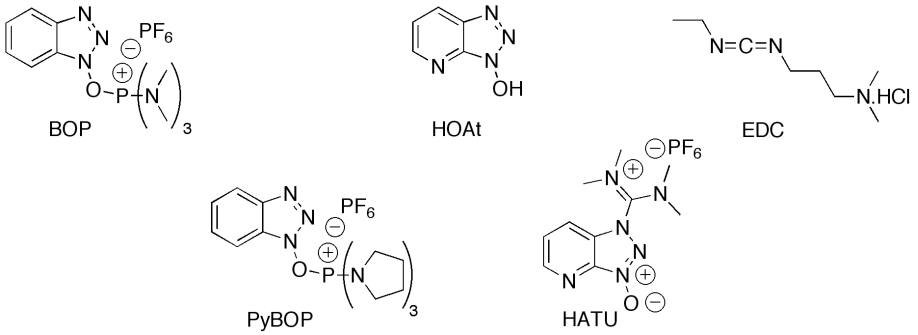

Figure 4. Coupling reagents used for the double cyclization of cryptand precursors.

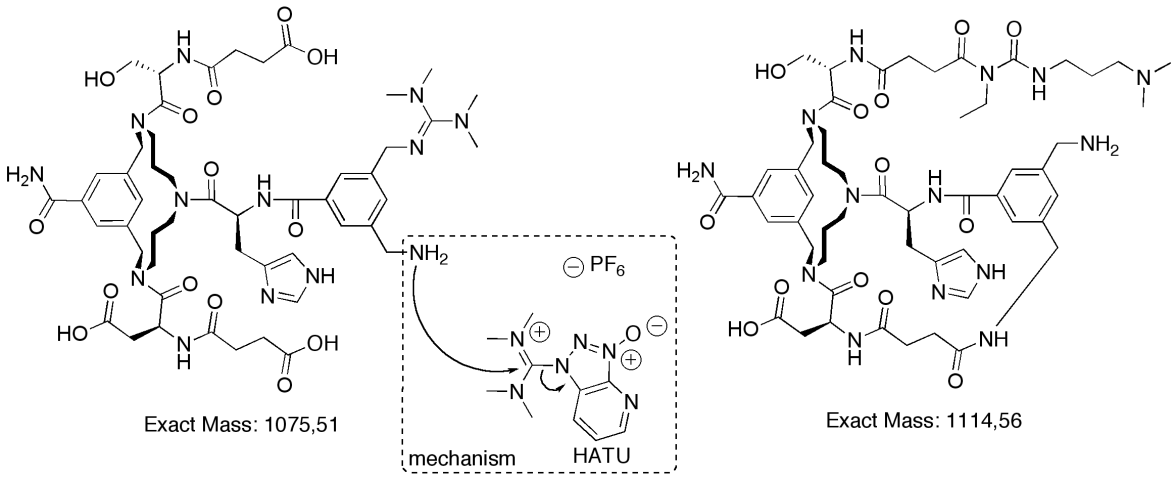

Figure 5. Side-products formed during the double cyclization. *Left*: structure corresponding to the mass observed when HATU was used; mechanism of formation is shown in the dotted box. *Right*: structure of the *N*-acyl urea compound corresponding to the mass observed when EDC was used.

of **13**. Apparently, the double cyclization reaction itself was so difficult that it could only marginally be optimized. Nevertheless, the batch of precursor **11** was used to attempt the preparation of larger quantities of cryptand **13**.

After very cumbersome HPLC-purifications, 1.1 mg of cryptand **13** was obtained, albeit in low purity. During the analysis of the purity of the obtained product it was observed that HPLC-analysis at elevated temperature gave better separations than when performed at room temperature. Also, compounds with identical *m*/*z*-values and different retention times were detected. This indicated that it was likely that similar compounds with different conformations were obtained. Unfortunately, the small amount and low purity of the products prevented us from performing reliable NMR and hydrolysis studies. Therefore, the effect of the double cyclization on the properties of the system could not be assessed. It was anticipated that by using an improved synthetic procedure involving cleaner cyclization precursors the double cyclization reaction should be facilitated and a larger quantity of more pure target molecule might be obtained.

3. Cryptand synthesis using similarly protected backbone functionalities

Using a Teoc-protected amine functionality instead of an azide moiety avoids the use of harsh azide reduction conditions and limits backbone deprotection to one step. This should result in a precursor of higher purity than **12**.

For the preparation of the Teoc-protected bis-amine, bis-bromide **5** was first converted into bis-diformylamide **14** (*scheme 6*). Subsequent acidic hydrolysis of the formyl groups, Teoc-protection of the amine functionalities using Teoc-OSu in the presence of Et_3N and saponification of the methyl ester with Tesser's resulted in Teoc-protected bis-amine **15**.

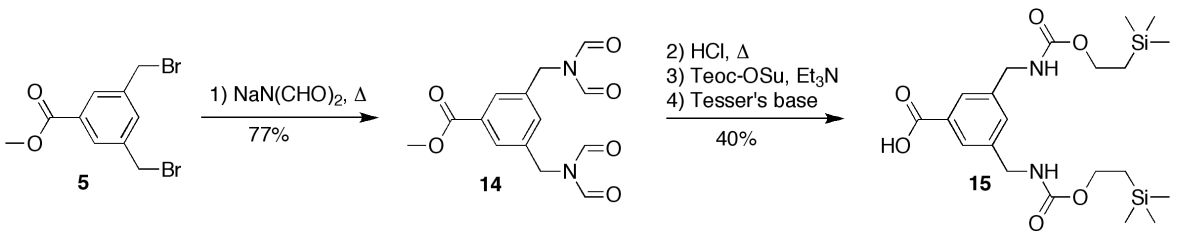

Scheme 6. Synthesis of Teoc-protected bis-amine **15**.

The synthesis of precursor **16** (*scheme 7*) was similar to the preparation of precursor **11** (*scheme 3*). The silyl-based protecting groups of precursor **16**, *i.e.* Te and Teoc, were simultaneous removed by TBAF. HPLC-analysis of a small amount of cleaved non-cyclized product indicated that the precursor obtained from **16** was of higher purity than that of precursor **12** (*scheme 4*).

Double cyclization was attempted at elevated temperature using both EDC/HOAt and PyBOP as coupling reagents. Initially, the effect of the temperature on the cyclization reactions was studied and earlier results were confirmed. For this, both heating by means of an oil-bath and a microwave was used. Although LC-MS analyses were cumbersome, it appeared that microwave heating to 80 or 100 °C resulted in similar product formation without significant differences in side-product formation. Although reactions performed at temperatures below 80 °C resulted in some product formation, the best results were obtained at 80 or 100 °C. This seemed to contradict the results obtained for the cyclization of precursor **12**, which was obtained from bis-azide containing precursor **11**. However, those results were possibly obscured by multiple by-products, formed by the harsh conditions that were needed for the azide-reduction, present on the precursor containing resin.

Even though a more advanced synthetic route for the synthesis of the precursor was taken, purification of cryptand **17** still proved to be extremely difficult and time-consuming. From the 3.5 g of resin loaded with 0.41 mmol/g TAC-scaffold, only 0.8 mg of the desired compound could be obtained with 89% purity. Important reasons

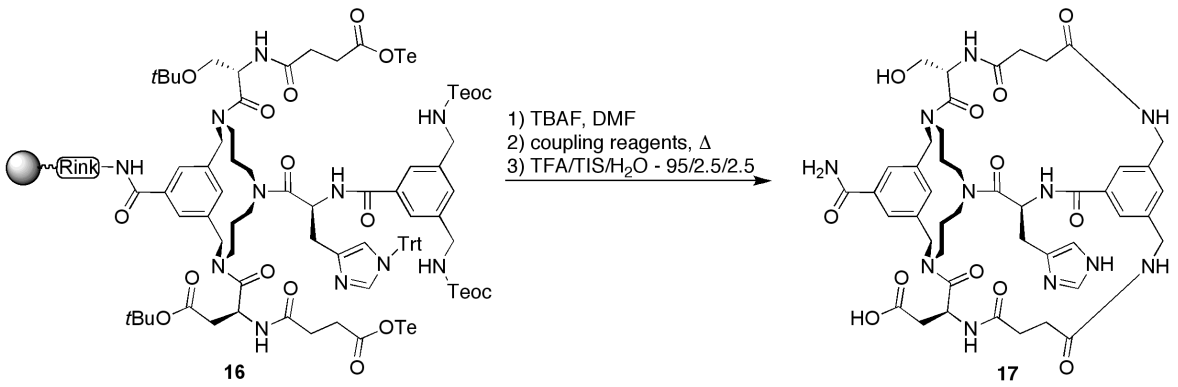

Scheme 7. Synthesis of cryptand **17** from precursor **16**.

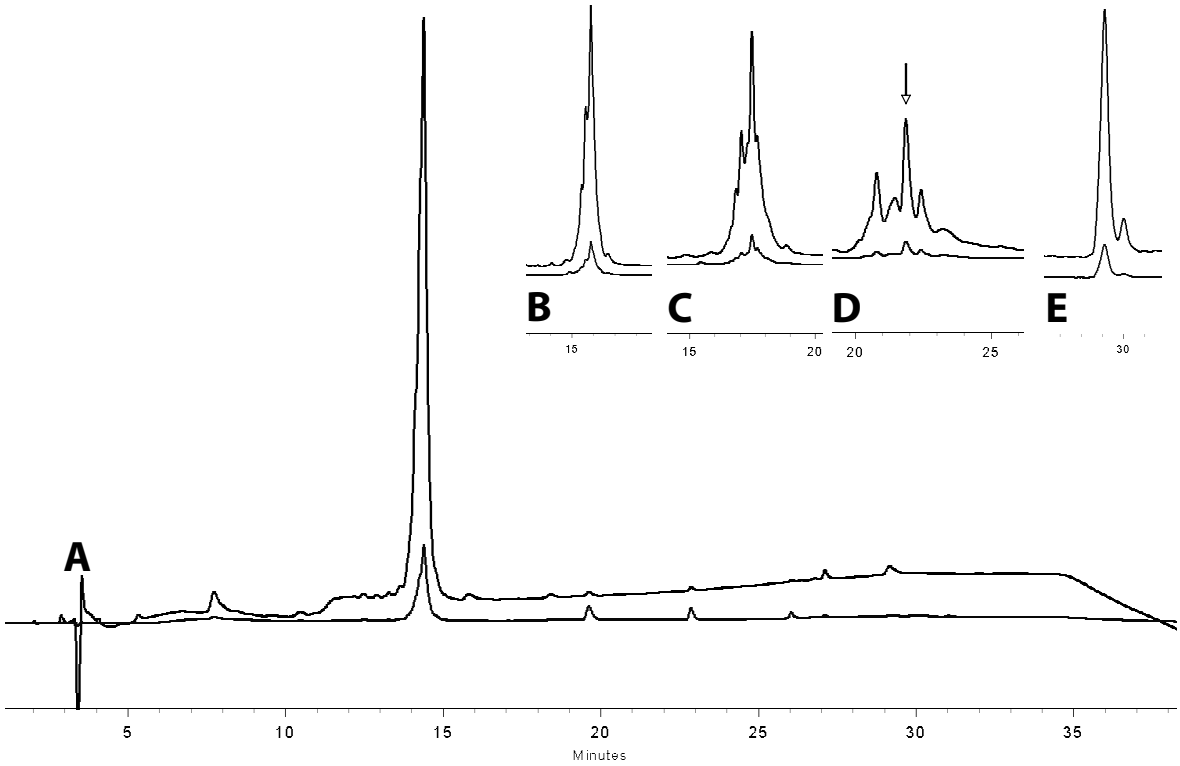

Figure 6. HPLC-profiles of the semi-purified cryptand **17** (on a C_{18} column). The use of a standard gradient indicated high purity (trace A), whereas less steep gradients showed that at least seven compounds were present (traces B-D). The vertical arrow in trace D marks the peak of the desired compound (as determined by LC-MS). From this mixture, cryptand **17** could be obtained with 89% purity (trace E). Gradients used: from 0-100% B in 25 min (trace A), from 0-30% B in 25 min (trace B), from 0-20% B in 25 min (trace C), and from 0-20% B in 45 min (traces D and E) (% in (v/v)).

for this low yield were the difficult double cyclization reactions and significant loss of product during subsequent HPLC-purification steps.

The difficult separation is illustrated by the HPLC-traces below (*figure 6*, traces A-D). Even though the standard gradient indicated a compound of high purity (*figure 6*, trace A), different gradients revealed that the product was far from pure (*figure 6*, traces B-D). Even a subsequent semi-preparative HPLC did not afford a pure product (*figure 6*, trace E).

4. NMR-analysis of cryptand 17

An NMR spectrum of the small amount of relatively pure cryptand **17** that was obtained was measured (*figure 7*).[42] The complicated nature of the spectrum indicated that the effect of the double cyclization reaction on the structure of the compound was difficult to establish using NMR techniques. Unfortunately, obtained two-dimensional NMR spectra could not be used for detailed structural analysis and determination of the three dimensional structure. The small amount also prevented studying the effect of this double cyclization on the hydrolytic activity of the construct **17**.

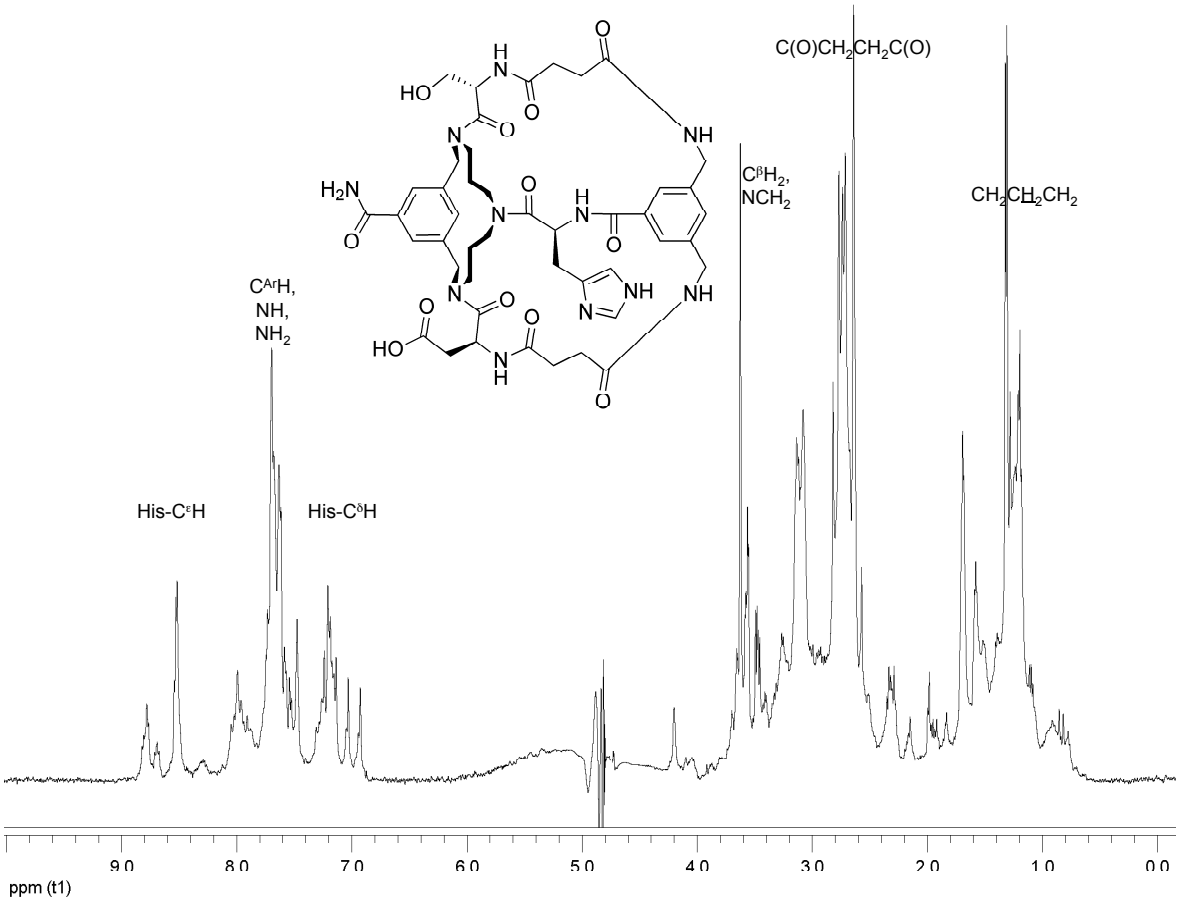

Figure 7. 500 MHz ^{1}H NMR spectrum of cryptand **17** (10% D_2O in H_2O). Global assignments are given; C^{α}-protons (typically at 4.5-5.0 ppm) are not visible due to suppression of the water peak.

5. Discussion and Conclusions

In this chapter two approaches toward the construction of TAC-based peptidic cryptands are described. One approach was based on the introduction of a bis-azide containing acid, for connecting the arms of the cryptand precursor, in which the azide-functionalities served as masked amine groups. Conversion of the azide-functionalities to the corresponding amine groups was achieved using DTT and DBU. Since by-products were formed, in the second approach the azide-functionalities were

replaced with suitably protected amine-functionalities. Simultaneous acid and amine deprotection became possible with formation of fewer by-products, therefore resulting in cyclization precursors of high purity.

With respect to double cyclization attempts, it was shown that reactions using BOP as a coupling reagent did not result in the formation of desired cryptand, even not at elevated temperature. However, the more reactive HATU/HOAt combination showed formation of desired compound and some undesired uronium adducts both at room temperature and at 50 °C. The ratio of mono- versus bi-cycle was more in favor of the bi-cycle at elevated temperature indicating that increased temperatures facilitate the formation of the bi-cycle. Using two other powerful coupling reagents, PyBOP or EDC/HOAt, did not result in more desired compound. Although the amount of product formation was similar to HATU/HOAt mediated couplings, the amount of by-products formed was less. Therefore, PyBOP and EDC/HOAt at 80 or 100 °C – using microwave heating – gave the best results with respect to the formation of more desired compound and less undesired by-products. These conditions were then used to prepare the cryptand on a larger scale.

However, purification of the obtained constructs was very cumbersome and time-consuming requiring several subsequent preparative HPLC runs. This may have been mainly caused by the formation of by-products during the difficult cyclization reaction.

Finally, although MS-analysis unambiguously showed that the desired bi-cyclic compound had been prepared, NMR-analysis of a small amount of semi-pure target compound resulted in a very complicated spectrum, which could not be assigned in detail.

Although the results described in this chapter indicate that the construction of these constructs is possible, their purification was cumbersome preventing an unambiguous characterization and evaluation. Significant improvements might be achieved using an adapted cryptand precursor, *i.e.* one with slightly elongated arms. This may lead to a higher yield of TAC-based peptidic cryptands and allow the assessment of the effect of rigidification on the structure and activity.

6. Experimental Section

Chemicals were obtained from commercial sources and used without further purification. Reactions were performed at room temperature. Solution phase reactions were monitored by TLC analysis and R_f-values were determined on Merck pre-coated silica gel 60 F-254 (0.25 mm) plates. Spots were visualized with UV-light. Solid-phase synthesis was carried out in plastic syringes with PE frit (20 mm), Applied Separations Inc., distributed by Alltech Applied Science Group (Hoogeveen, The Netherlands). Column chromatography was carried out using Silica-P Flash silica gel (60 Å; particle size 40-63 mm; Silicycle). Electrospray Ionisation mass spectrometry (ESI-MS) was performed on a Finnigan LCQ Deca XP MAX LC/MS system. HPLC was performed on a Shimadzu Class-VP automated high performance liquid system, using an analytical reverse-phase column (Alltima, C8 or C18, 300 Å, 5 μm, 250 × 4.6 mm) and a UV-detector (operating at 220 and 254 nm) as well as an ELSD-detector. Elution was realized using a gradient from water:MeCN:TFA – 95:5:0.1 % (v/v) to MeCN:water:TFA – 95:5:0.1 % (v/v) in 20 min and at a flow rate of 1 mL/min. NMR spectra were recorded on aVarian Gemini-300 (300 MHz) or on an INOVA-500 (500 MHz). ^{1}H NMR chemical shift values are given in ppm relative to TMS.

Mono Te-protected succinic acid 4

Succinic anhydride (2.0 g, 20 mmol), 2-(trimethyl)silyl-ethanol (3.5 mL, 25 mmol) and DMAP (244 mg, 2 mmol) were mixed in DCM (50 mL) and stirred untill completion of the reaction according to TLC. The mixture was washed with 1N $KHSO_4$ (50 mL) and after concentration the desired product was obtained as colorless liquid. Yield: 2.4 g (11 mmol, 54%). R_f = 0.66 (10% MeOH/DCM, trace AcOH). ^{1}H NMR (300 MHz, $CDCl_3$, TMS): δ 0.00 (9H, s, Si(CH_3)$_3$), 0.92-0.98 (2H, t ^3J 8.8 Hz, CH_2Si), 2.56-2.64 (4H, q ^3J 4.4 and 11.0 Hz, C(O)CH_2CH_2C(O)), 4.13-4.18 (2H, t ^3J 8.8 Hz, OCH_2), 10.8 (1H, s, COO*H*). ^{13}C NMR (75 MHz, $CDCl_3$, APT): δ -1.6, 17.2, 29.0, 63.1, 172.3, 178.2.

3,5-bis(azidomethyl)benzoic acid 6

Methyl 3,5-bis(bromomethyl)benzoate **5** (9.66 g, 30 mmol) and NaN_3 (5.86 g, 90 mmol) were allowed to react in acetonitril (250 mL) under reflux conditions for 2 h. After cooling to room temperature, the precipitate was removed by filtration and the filtrate was concentrated under reduced pressure. Purification by column chromatography (eluent: 10% EtOAc in hexanes) afforded methyl 3,5-bis(azidomethyl)benzoate as a colorless oil. Yield: 6 g (24 mmol, 81%). R_f = 0.28 (20% Et_2O/hexanes (v/v)). ^{1}H NMR (300 MHz, $CDCl_3$, TMS): δ 3.94 (3H, s, OCH_3), 4.44 (4H, s, CH_2N$_3$), 7.48 (1H, s, C^4*H*), 7.97 (2H, s, C^{2,6}*H*). ^{13}C NMR (75 MHz, $CDCl_3$, APT): δ 52.3 (O*C*H$_3$), 54.0 (N$_3$*C*H$_2$), 129-137 (Ar-C), 166 (*C*(O)OMe).

Saponification of the methyl ester was achieved by dissolving the methyl 3,5-bis(diformyl-amidomethyl)benzoate ester in Tesser's base (124 mL).[43] After overnight reaction, an

additional equivalent of NaOH was needed in order to ensure completion of the reaction. The mixture was concentrated under reduced pressure, acidified by the addition of 1N HCl and the product was extracted using EtOAc. The organic phase was dried over Na_2SO_4, followed by removal of the solvent *in vacuo*. The desired product was obtained as a white solid. Yield: 5.5 g (23.8 mmol, 99%). R_f = 0.54 (eluent: 10% MeOH in DCM). ^{1}H NMR (300 MHz, $CDCl_3$, TMS): δ 4.47 (4H, s, CH_2N_3), 7.56 (1H, s, C^4H), 8.04 (2H, s, C$^{2,6}H$), 12.2 (1H, s, COO*H*). ^{13}C NMR (75 MHz, $CDCl_3$, APT): δ 54.0 (N_3CH_2), 129-137 (C^{Ar}), 171 (*C*OOH).

Standard procedures used for solid-phase chemistry described below

Generally, ca 6 mL of solvent was used for each gram of resin.

- Fmoc-deprotection was performed using a 20% piperidine in NMP solution (2×8 min).
- Coupling (18 h) was performed using 4 equiv Fmoc-AA(PG)-OH, 4 equiv BOP, and 8 equiv D*i*PEA in NMP. The syringes were placed on a shaker.
- Capping of amines was carried out using a capping solution containing 0.5 M acetic anhydride, 0.125 M D*i*PEA and 0.015 M HOBt in NMP (2×10 min).
- Standard washing consists of treatment with NMP (3×2 min) and DCM (3×2 min).
- Coupling, deprotection and capping was monitored using the Kaiser test[44] (for primary amines) or chloranil[45] test (for secondary amines).

Solid-phase synthesis of precursor 11 (for test cyclization)

After each reaction-step the resin was washed using the standard washing protocol.

For the synthesis of precursor **11**, 1 g of PS S RAM resin (loading: 0.78 mmol/g) was used. The Fmoc groups were removed and to the librated amine functionality HO-TAC(Fmoc/Alloc/*o*-NBS) was coupled using 1 equiv of the scaffold (600 mg) in the presence of BOP (1 equiv, 345 mg) and D*i*PEA (2 equiv, 272 μL) in NMP (overnight coupling). After this, remaining amine functionalities were permanently protected with acetyl groups using the capping reagent. A Kaiser test indicated the absence of free amine groups and the loading of the resin was 0.53 mmol scaffold per gram of resin.

After deprotection of the Fmoc-protected amine of the scaffold, the first amino acid was coupled using Fmoc-Ser(*t*Bu)-OH (4 equiv, 813 mg), together with BOP (4 equiv, 937 mg) and D*i*PEA (8 equiv, 739 μL). A chloranil test indicated that resin bound secondary amine functionalities of the scaffold were successfully acylated. The *N*-terminal Fmoc-group was removed and replaced by mono Te-protected succinic acid **4** using acid (4 equiv, 506 mg), BOP (4 equiv) and D*i*PEA (8 equiv). A Kaiser test confirmed coupling and ESI-MS analysis of a small amount of cleaved product showed that precursor **9** was obtained: *m/z* 733.00 (calculated: 733.25 for $[(M\text{-}Te)+H]^+$); 754.85 (calculated: 755.23 for $[(M\text{-}Te)+Na]^+$).

Prior to *o*-NBS deprotection, the resin was thoroughly washed with DMF. Removal of

the *o*-NBS-protecting groups was performed using a solution of 2-mercaptoethanol in DMF (0.5 M, 6 mL) and DBU (225 μL) (2 × 30 min). Fmoc-Asp(O*t*Bu)-OH (4 equiv, 872 mg) was coupled using BOP (4 equiv) and D*i*PEA (8 equiv) in NMP. Deprotection and acylation were shown to be successful by means of a chloranil test. The *N*-terminal amine Fmoc-group was removed and the amine was acylated using acid **4**. ESI-MS analysis of a small amount of the cleaved product showed that precursor **10** was obtained: *m/z* 785.35 (calculated: 785.30 for $[(M\text{-}2Te)+Na]^+$); 763.30 (calculated: 763.32 for $[(M\text{-}2Te)+H]^+$).

Removal of the Alloc-protecting group was affected by 50% of $Pd(PPh_3)_4$ in the presence of *p*-toluenesulfinate anilinium salt (PTSA, 20 equiv, 2.04 g) in NMP (under Ar, overnight). ESI-MS analysis of the resulting compound indicated that all Alloc groups were successfully removed and that alkylation of the secondary amine[46] had not occurred (observed *m/z* 679.20 (calculated: 679.29 for $[(M\text{-}2Te)+H]^+$)). To the amine, Fmoc-His(Trt)-OH (4 equiv, 1.3 g) was coupled using BOP (4 equiv) and D*i*PEA (8 equiv) in NMP. After removal of the Fmoc-group, the resin was split into two equal protions. To one protion, 3,5-bis(azidomethyl) benzoic acid **6** (4 equiv, 246 mg) was coupled using BOP (4 equiv, 469 mg) and D*i*PEA (8 equiv, 544 μL). Purity and identity of cryptand precursor **11** was assessed by HPLC and ESI-MS analysis. HPLC (C_8): t_R = 16.95 min (purity: 70% (220 nm); 100% (254 nm); 100% (ELSD)). ESI-MS: *m/z* 1030.87 (calculated: 1031.02 for $[(M\text{-}2Te)+H]^+$).

Backbone deprotection of 11

Te-protecting groups were removed using TBAF (5 equiv, 836 mg) in DMF (4 mL) for 3 h. ^{1}H-NMR analysis of resin bound compounds indicated that deprotection was successful and no side-products were observed in ESI-MS and HPLC analyses. After performing several test reactions for reduction of the azide to the amine functionalities (*table 1*), overnight treatment of the resin with a pre-incubated mixture of DTT (20 equiv) and DBU (10 equiv) gave the best results. Only traces of a mono-azide could be observed (ESI-MS: *m/z* 1004.45 (calculated: 1004.42 for $[M_{mono\text{-}azide}+H]^+$)), but the major peak consisted of bis-amine cryptand precursor **12** (ESI-MS: *m/z* 978.25 (calculated: 978.43 for $[M_{bis\text{-}amine}+H]^+$)).

Cyclization experiments using precursor 12

The effect of the temperature on the cyclization reaction was first evaluated. The samples used for these studies typically consisted of approximately 50 mg of resin-bound precursor **12**. Firstly, two samples were subjected to amide-bond formation conditions using BOP (4 equiv), D*i*PEA (8 equiv) in NMP (1 mL), one at room temperature and one at 50 °C (heating by oil-bath). In addition, three samples were subjected to microwave heating at three temperatures: 60, 100 and 140 °C. After each test, resin-bound material was cleaved by TFA treatment and analyzed by ESI-MS. Unfortunately, none of these conditions afforded the desired product and only cleaved starting material was observed. Even more, the reactions

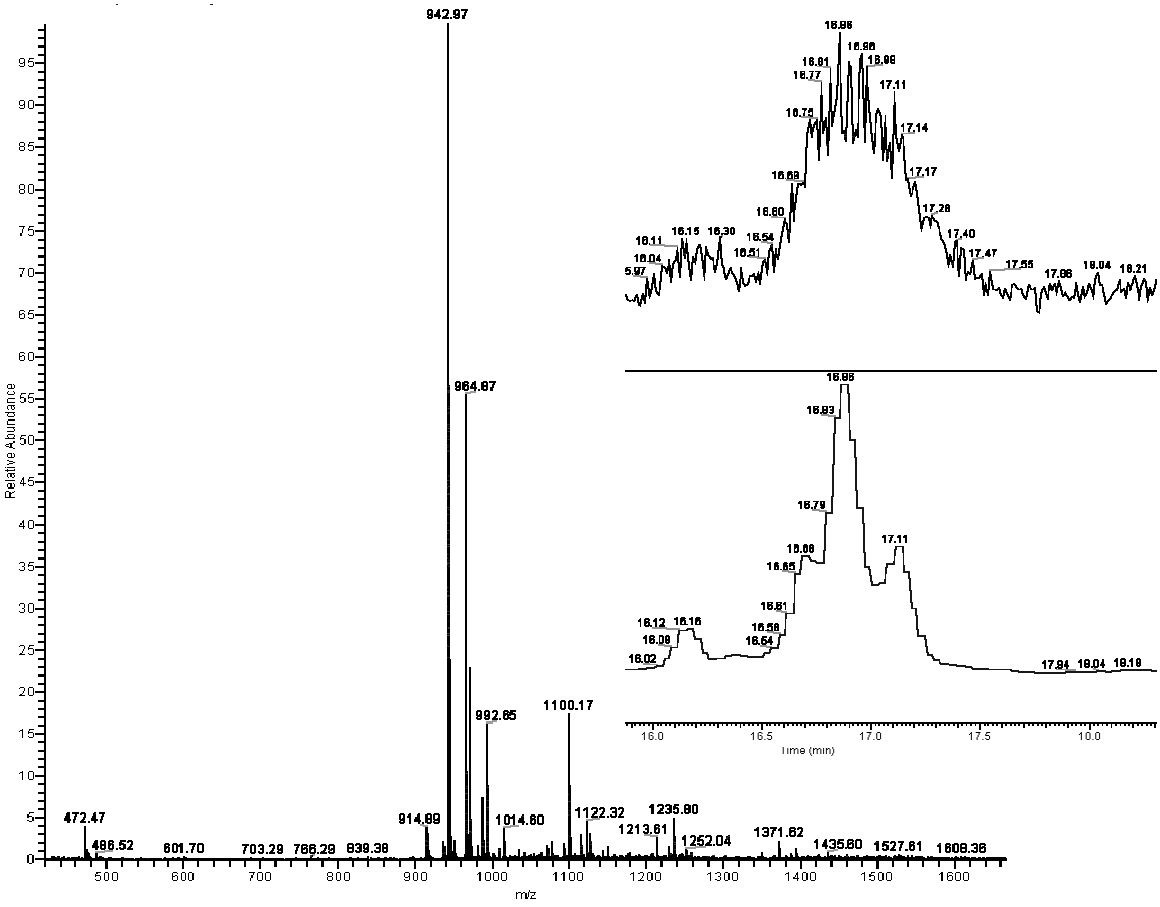

Figure 8. Mass spectrum of the peak at t_R 16.86 min, which was identified as compound **13**. Insert shows the total ion count (*top*) and UV absorption trace (*bottom*).

performed at 100 and 140 °C resulted in dark brown solution and resin and neither starting material nor desired product could be detected.

Two other test reactions using HATU/HOAt (10 equiv of each) and D*i*PEA (20 equiv) were performed. Since microwave heating resulted in a strong coloration of the solution and resin, we performed the following test-reactions using room temperature and conventional heating at 50 °C. After overnight stirring, the reaction carried out at 50 °C was less positive in a Kaiser test than the one carried out at room temperature. Also, the reaction mixture that was heated had a darker color than the mixture stirred at room temperature. HPLC and LC-MS analysis of cleaved product showed that the reaction performed at 50 °C gave more of the desired compound than the one performed at room temperature. HPLC-analysis also showed the presence of several side-products. In addition to the desired cryptand **13**, a dimeric species was identified: MALDI-TOF analysis: *m/z* 942.49 (calculated: 942.41 for $[M+H]^+$) and 1884.01 (calculated: 1883.81 for $[M_{dimer}+H]^+$).

After performing the reactions at a larger scale using 580 mg of loaded resin and heating at 50 °C, followed by a very tedious purification by preparative HPLC runs, 1.1 mg of the desired compound could be obtained, although far from pure. LC-MS analysis of this

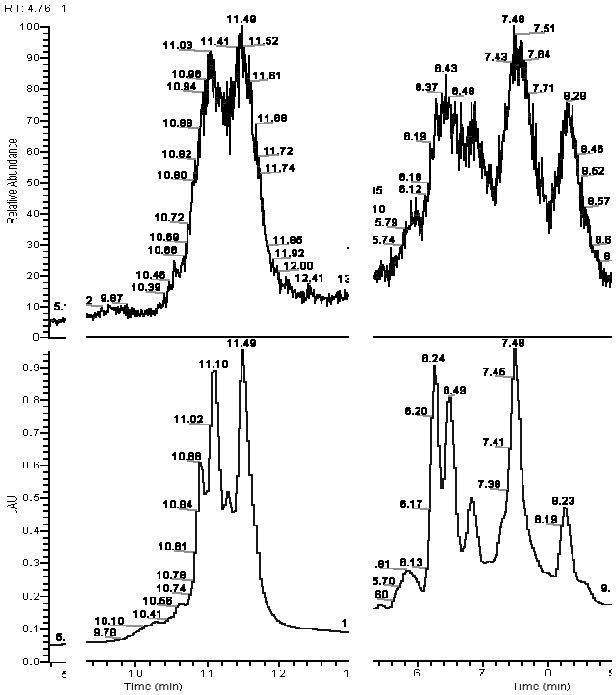

Figure 9. HPLC-analysis of a fraction of cleaved products containing several compounds was performed at room temperature (*left*) and at 80 °C (*right*). The following *m/z*-values were detected at the mentioned retention times, values of the desired compound are depicted in bold: *Left*: 758.81 (100), **942.53** (85), 688.80 (80), **964.54** (45) for t_R = 11.10 min; 771.81 (100), **942.53** (65), **964.53** (25), 643.73 (20) for t_R = 11.49 min. *Right*: 516.56 (100), **964.54** (80), **942.51** (70), 900.59 (55) for t_R = 6.24 min; 758.59 (100), 770.54 (70), **942.46** (35), **964.49** (30) for t_R = 6.85 min; 688.61 (100), **942.41** (90), 710.54 (75), **964.47** (60) for t_R = 7.48 min.

product revealed the presence of at least three species (*figure 8*, insert). The major peak was identified as being cryptand **13** ESI-MS: *m/z* 942.97 (calculated: 942.41 for $[M+H]^+$) and 964.87 (calculated: 964.39 for $[M+Na]^+$) (*figure 8*). HPLC: t_R (C_{18}): 16.9 min. Significant impurities with *m/z* 733.49 and 914.84, both unidentifiable, were detected.

Analysis of semi-purified product by HPLC at elevated temperature

The effect of the temperature on HPLC performance was also determined using a Prosphere C_{18}-column. A gradient of buffer A to buffer B was used: from 0% B to 100% B in 30 minutes. The used buffers were: buffer A: water/MeCN/TFA – 95/5/0.1 (%, v/v) and buffer B: water/MeCN/TFA – 5/95/0.1 (%, v/v). For this, a sample containing several compounds was analyzed by LC-MS: once at room temperature and once at 80 °C. It was found that at 80 °C a better separation of the compounds was obtained (*figure 9*). For instance, four poorly separated peaks were observed at room temperature, whereas at 80 °C six compounds could be detected, some of which were good separated. MS-analysis of the separated compounds indicated that several products were formed, some with similar *m/z* values at different retention times. This illustrated that separation could be improved by performing the HPLC at higher temperatures.

Observed side-products

By-products were detected after attempting the double cyclization using the following conditions: 50 mg of precursor containing resin, coupling reagent (10 equiv), D*i*PEA (20 equiv), 3 mL NMP, 30 min, 80 °C, microwave-heating. Products were cleaved from the resin using TFA/TIS/water – 95/2.5/2.5 (%, v/v) and analyzed by LC-MS. Coupling reagents used and by-products identified are listed below.

HATU/HOAt: uronium adduct of precursor at *m/z* 1076.35 (calculated: 1076.52 for $[M+C(NMe_2)_2+H]^+$) (t_R : 17.7-18.3 min, C_8).

EDC/HOAt: EDC-adduct of precursor at *m/z* 1097.69 (calculated: 1097.55 for $[M+EDC+H]^+$) (t_R: 12.4 min, C_8).

PyBOP: no adducts were observed.

Other identifiable side-products often found were: *m/z* 644.00 (calculated: 643.27 for $[M-(His-BAMB)-(H_2O)_2+H]^+$) and 798.70 (calculated: 798.34 for $[M-BAMB-(H_2O)+H]^+$).

Methyl 3,5-bis(diformylamidomethyl)benzoate 14

Methyl 3,5-bis(bromomethyl)benzoate (6.4 g, 20 mmol) was dissolved in MeCN (3Å, 100 mL) and $NaN(CHO)_2$ (4.8 g, 50 mmol) was added. After refluxing for 3 h, one additional equiv of $NaN(CHO)_2$ (1.9 g, 20 mmol) was added and the mixture was refluxed overnight. Column chromatography (eluent: EtOAc/hexanes – 3/1) and concentration afforded the pure product as a white solid. Yield: 3.9 g (15.3 mmol, 77%). R_f = 0.52 (eluent: EtOAc:hexanes – 3:1). ^{1}H NMR (300 MHz, DMSO-d_6, TMS): δ 3.84 (s, 3H, OCH_3), 4.70 (s, 4H, ArCH_2N), 7.44 (s, 1H, C^4*H*), 7.72 (s, 2H,C^{2,6}*H*), 9.09 (s, 4H, NC*H*O).

3,5-bis(Teoc-aminomethyl)benzoate 15

Methyl 3,5-bis(diformylamidomethyl)benzoate **14** (3.9 g, 15.3 mmol) was dissolved in MeOH (75 mL). To this solution, concentrated HCl (36%, 7.5 mL; ~ 90 mmol) was added and the mixture was refluxed for 2 h. The mixture was then concentrated under reduced pressure and product **14** was obtained as white solid. Yield: 3.4 g (12.9 mmol, 84%). Subsequently, product **14** (1.8 g, 6.8 mmol) and Et_3N (3.1 mL, 30 mmol) were mixed in DCM (30 mL). To this, a solution of commercially available Teoc-OSu (3.9 g, 15 mmol) in DCM (20 mL) was added slowly. After completion, the reaction mixture was filtered and washed with 1N $KHSO_4$ (2×50 mL), water (2×50 mL) and brine (50 mL). The organic phase was dried over Na_2SO_4, filtered and concentrated *in vacuo*. This afforded the desired product as a white solid. Yield: 3.1 g (6.4 mmol, 93%). R_f = 0.42 (eluent: 2% MeOH in DCM). ^{1}H NMR (300 MHz, $CDCl_3$): δ -0.13 (18H, s, Si(CH_3)$_3$), 0.80-0.86 (4H, m, SiCH_2), 3.74 (3H, s, OCH_3), 4.00-4.05 (m, 4H, OCH_2), 4.21-4.23 (4H, d, ArCH_2N), 4.88 (2H, br s, N*H*), 7.24 (1H, s, C^4*H*), 7.69 (2H, s, C^{2,6}*H*). ^{13}C NMR (75 MHz, $CDCl_3$, APT): δ -1.5 (Si(*C*H$_3$)$_3$), 17.7 (Si*C*H$_2$), 44.4, 52.2 (O*C*H$_3$), 63.4, 127.5, 139.7, 156.7 (*C*OOMe).

The methyl 3,5-bis(Teoc-aminomethyl)benzoate ester (1.88 g, 3.9 mmol) was dissolved in Tesser's base[43] (70 mL) and reacted overnight at room temperature. The basic aqueous phase was washed with DCM, acidified with $KHSO_4$ and the product was extracted with DCM (2×50 mL). Concentration of the organic phase afforded the product as a pure white solid. Yield: 1.8 g (3.9 mmol, quant). R_f = 0.45 (eluent: 10% MeOH in DCM). ^{1}H NMR ($CDCl_3$, 300 MHz): δ -0.09 (s, 18H, 2 × Si(CH_3)$_3$), 0.84-0.90 (t, 4H, 2 × SiCH_2, ^3J 8.8 Hz), 4.02-4.08 (t, 4H, 2 × OCH_2, ^3J 8.5 Hz), 4.23-4.25 (d, 4H, 2 × Ar-CH_2, ^3J 5.8 Hz), 5.61-5.98 (2 s, 0.3 H and 1.6 H, 2 × N*H*), 7.29 (s, 1H, ArC^4*H*), 7.73 (s, 2H, ArC^{2,6}*H*), 10.80 (br s, 1H, COO*H*). ^{13}C NMR (APT, $CDCl_3$, 75 MHz): δ -1.6 (Si(*C*H_3)), 17.6 (Si*C*H_2), 40.2 (Ar-*C*H_2N), 63.1 (O*C*H_2), 106.3, 108.0 (*C*^{Ar}H), 132.0 (*C*^{Ar}), 156.7 (NH*C*(O)O), 166.4 (*C*OOH). ESI-MS: *m*/*z* 793.30 (calculated: 793.36 for [2M-Teoc+2H]$^+$).

Resin-bound cryptand precursor 16

As a solid support PS S RAM resin (3.5 g) loaded with 0.41 mmol/g TAC(Fmoc/Alloc/*o*-NBS) scaffold was used. The synthesis was similar to that described for cryptand precursor **11** until the Fmoc-deprotection step prior to coupling of bis-azide **6**. 3,5-bis(Teoc-aminomethyl) benzoic acid **15** (3 equiv, 576 mg, 1.23 mmol) was coupled using BOP (3 equiv, 544 mg) and D*i*PEA (6 equiv, 429 μL) (over the weekend) in NMP (6 mL). A negative Kaiser test showed that acylation of amine groups was complete. HPLC and LC-MS analyses results of cleaved intermediate and final compounds (entries 1-8) are summarized in *table 2*.

Table 2. Detected intermediates during synthesis of cryptand precursor **16**. HPLC-analysis (C_8) was performed using standard buffers. SA = succinic acid (-C(O)CH_2CH_2COOH); BAMB = 3,5-bis(aminomethyl)benzoic acid.

Entry	t_R (min)	*m*/*z* found [proposed assignment]	*m*/*z* calculated
1	23.35	769.55 [TAC(Fmoc/Alloc/*o*-NBS)]	768.27
2	22.40	855.87 [TAC(Ser-Fmoc/Alloc/*o*-NBS)]	855.30
3	14.28	no *m*/*z* detection	
4	19.40	885.75 [TAC(Ser-SA/Alloc/Asp-Fmoc)]	885.37
5	14.98	763.73 [TAC(Ser-SA/Alloc/Asp-SA)]	763.32
6	12.17	679.44 [TAC(Ser-SA/H/Asp-SA)]	679.29
7	17.87	1039.07 [TAC(Ser-SA/His-Fmoc/Asp-SA)]	1038.42
8	12.95	978.66 [TAC(Ser-SA/His-BAMB/Asp-SA)]	978.43

Backbone deprotection of resin bound precursor 16

The Teoc- and Te-protecting groups were removed using 1.5 equiv of TBAF per protecting group (2.73 g dissolved in 20 mL DMF, overnight). Upon addition the color of the resin changed from yellow to pale brown. Removal of the protecting groups was monitored by ^{1}H-NMR which indicated incomplete deprotection. After repeating the deprotection procedure with 5 equiv of TBAF per protecting group the deprotection was complete 1 h.

Double cyclization of backbone unprotected precursor 16

For this, several conditions were used on different batches of resin-bound backbone unprotected cryptand precursor. After each reaction, a Kaiser test was performed to detect the presence of remaining amine groups. The best results were obtained when the reaction was performed at 80 or 100 °C. Although the combination of EDC/HOAt resulted in the formation of EDC-adducts, the HPLC-trace of the cleaved formed products was similar to that when PyBOP was used.

HPLC analysis of cryptand 17

This was performed on a Prosphere C_{18} column using different gradients of buffer A to buffer B. Buffer A: water/MeCN/TFA – 95/5/0.1 (%, v/v). Buffer B: water/MeCN/TFA – 5/95/0.1 (%, v/v). A 500 MHz spectrum was obtained with 0.8 mg of 89% pure cryptand was dissolved in H_2O containing 10% of D_2O.

7. References

1 See *Handbook of Proteolytic Enzymes*, eds. A.J. Barrett, N.D. Rawling, J.F. Woessner, New York, Elsevier Academic Press, **2004**, vol. 1; A. Fehrst, *Enzyme Structure and Mechanism in Protein Science: a Guide to Enzyme Catalysis and Protein Folding*, New York, W.H. Freeman and Company, **1999**; J.M. Berg, J.L. Tymoczko and L. Stryer, *Biochemistry*, 5th edition, New York, W.H. Freeman and company, **2006**. H. Dugas, *Bioorganic Chemistry: A Chemical Approach to Enzyme Action*, Springer, New York, 3rd edn., **1996**.

2 Characteristic features of this optimized environment include: distortion of the substrate (D.L. Pompliano, A. Peyman, J.R. Knowles, *Biochemistry* **1990**, *29*, 3186), the contribution of quantum mechanical tunneling to the rates of enzyme-catalyzed reactions whose mechanisms involve the transfer of hydrogen ions (Z.D. Nagel, J.P. Klinman, *Chem. Rev.* **2006**, *106*, 3095), precise matching of pK_a values of the donor and acceptor atoms in hydrogen bonds that stabilize the transition state, which can lead to short and symmetrical hydrogen bonds of greater-than-normal-strength (W.W. Cleland, P.A. Frey, J.A. Gerlt, *J. Biol. Chem.* **1998**, *273*, 25529; D.A. Kraut, P.A. Sigala, B. Pybus, C.W. Liu, D. Ringe, G.A. Petsko, D. Herschlag, *PLoS Biology* **2006**, *4*, e99, 0501), the role of protein dynamics in aiding the reacting species in crossing the transition-state barrier of the reaction (K.A. Henzler-Wildman, V. Thai, M. Lei, M. Ott, M. Wolf-Watz, T. Fenn, E. Pozharski, M.A. Wilson, G.A. Petsko, M. Karplus, C.G. Hübner, D. Kern, *Nature* **2007**, *450*, 838).

3 M. Paetzel, R.E. Dalbey, *Trends Biochem. Sci.* **1997**, *22*, 29; G. Dodson, A. Wlodawer, *Trends Biochem. Sci.* **1998**, *23*, 347; L. Hedstrom, *Chem. Rev.* **2002**, *102*, 4501; A.J.T. Smith, R. Müller, M.D. Toscano, P. Kast, H.W. Hellinga, D. Hilvert, K. N. Houk, *J. Am. Chem. Soc.* **2008**, *130*, 15361 and references cited therein.

4 D.L. Ollis, E. Cheah, M. Cygler, B. Dijkstra, F. Frolow, S.M. Franken, M. Harel, S.J. Remington, I. Silman, J. Schrag, J.L. Sussman, K.H.G. Verschueren, A. Goldman, *Protein Eng.* **1992**, *5*, 197; J.D. Hooper, J.A. Clements, J.P. Quigley, T.M. Antalis, *J. Biol. Chem.* **2001**, *276*, 857; M.J. Page, E. Di Cera, *Cell. Mol. Life Sci.* **2008**, *65*, 1220.

5 This has been shown by: crystal structure comparison in A. Gutteridge, J. Thornton, *J. Mol. Biol.* **2005**, *346*, 21; and temperature factors in Z. Yuan, J. Zhao, Z.X. Wang, *Protein Eng.* **2003**, *16*, 109. Indications

for this have also been found using computer models: L.W. Yang, X. Liu, C.J. Jursa, M. Holliman, A.J. Rader, H.A. Karimi, I. Bahar, *Bioinformatics* **2005**, *21*, 2978; S. Sacquin-Mora, R. Lavery, *Biophys. J.* **2006**, *90*, 2706.

6 See the family of hydrolases: E.C. 3.-.-.-.

7 L. Brady, A.M. Brzozowski, Z.S. Derewenda, E.J. Dodson, G.G. Dodson, S.P. Tolley, J.P. Turkenburg, L. Christiansen, B. Huge-Jensen, L. Norskov, L. Thim, *Acta Crystallogr., Sect. B.* **1992**, *48*, 307. PDB-code: 3TGL.

8 M.L. Raves, M. Harel, Y.-P. Pang, I. Silman, A.P. Kozikowski, J.L. Sussman, *Nature Structural Biology* **1997**, *4*, 57. PDB-code: 2ACE.

9 C. Betzel, S. Klupsch, G. Papendorf, S. Hastrup, S. Branner, K.S. Wilson, *J. Mol. Biol.* **1992**, *223*, 427. PDB-code: 1SVN.

10 R.J. Read, M.N. James, *J. Mol. Biol.* **1988**, *200*, 523. PDB-code: 1SGT.

11 A. Kashima, Y. Inoue, S. Sugio, I. Maeda, T. Nose, Y. Shimohigashi, *Eur. J. Biochem.* **1998**, *255*, 12. PDB-code: 1AB9.

12 M.J. Corey, E. Corey, *Proc. Natl. Acad. Sci., USA* **1996**, *93*, 11428.

13 F.M. Menger, M. Ladika, *J. Am. Chem. Soc.* **1987**, *109*, 3145; R. Breslow, S. Singh, *Bioorg. Chem.* **1988**, *16*, 408.

14 J. Suh, S.S. Hah, *J. Am. Chem. Soc.* **1998**, *120*, 10088.

15 D.J. Cram, J.M. Cram, *Science* **1974**, *183*, 803; D.J. Cram, J.M. Cram, *Acc. Chem. Res.* **1978**, *11*, 8.

16 J. Rebek, Jr., *Acc. Chem. Res.* **1984**, *17*, 258; J. Rebek, Jr., *Acc. Chem. Res.* **1990**, *23*, 399.

17 C.J. Pedersen, *J. Am. Chem. Soc.* **1967**, *89*, 2495; C.J. Pedersen, *J. Am. Chem. Soc.* **1967**, *89*, 7017.

18 D.J. Cram, *Science* **1988**, *240*, 760; J.-M. Lehn and D.J. Cram, both from *Nobel Lectures*, *Chemistry 1981-1990*, eds. T. Frängsmyr and B.G. Malmström, World Scientific Publishing Co., Singapore, **1992**.

19 E.J. Ruiz, D.N. Sears, A. Pines, C.J. Jameson, *J. Am. Chem. Soc.* **2006**, *128*, 16980.

20 H. Takemura, T. Shinmyozu, T. Iuazu, *Coord. Chem. Rev.* **1996**, *156*, 183.

21 D.M. Rudkevich, *Eur. J. Org. Chem.* **2007**, 3255.

22 K.A. Nielsen, J.O. Jeppesen, E. Levillain, N. Thorup, J. Becher, *Org. Lett.* **2002**, *4*, 4189.

23 Y. Murakami, O. Hayashida, *Proc. Natl. Acad. Sci., USA* **1993**, *90*, 1140; A. Tanaka, S. Fujiyoshi, K. Motomura, O. Hayashida, Y. Hisaeda, Y. Murakami, *Tetrahedron* **1998**, *54*, 5187.

24 M.M. Conn, J. Rebek, Jr., *Chem. Rev.* **1997**, *97*, 1647. See the 2,4,6-tri-3-pyridyl-1,3,5-triazine-Pt complexes for binding of small Trp-containing peptides (S. Tashiro, M. Fujita, *Bull. Chem. Soc. Jpn.* **2006**, *79*, 833).

25 N. Branda, R. Wyler, J. Rebek, Jr., *Science* **1994**, *263*, 1222; J. Rebek, Jr., *Acc. Chem. Res.* **1999**, *32*, 278; J. Santamaría, T. Martín, G. Hilmersson, S.L. Craig, J. Rekeb, Jr., *Proc. Natl. Acad. Sci., USA* **1999**, *96*, 8344; F. Hof, J. Rebek, Jr., *Proc. Natl. Acad. Sci., USA* **2002**, *99*, 4775; C.A. Schalley, R.K. Castellano, M.S. Brody, D.M. Rudkevich, G. Siuzdak, J. Rebek, Jr., *J. Am. Chem. Soc.* **1999**, *121*, 4568; O. Hayashida, L. Sebo, J. Rebek, Jr., *J. Org. Chem.* **2002**, *67*, 8291; A. Shivanyuk, A. Scarso, J. Rebek, Jr., *Chem. Commun.* **2003**, 1230; L.C. Palmer, Y.-L. Zhao, K.N. Houk, J. Rebek, Jr., *Chem Commun.* **2005**, 3667; U. Lücking, J. Chen, D.M. Rudkevich, J. Rebek, Jr., *J. Am. Chem. Soc.* **2001**, *123*, 9929.

26 J. Kang, G. Hilmersson, J. Santamaría, J. Rebek, Jr., *J. Am. Chem. Soc.* **1998**, *120*, 3650; J. Kang, G. Hilmersson, J. Santamaría, J. Rebek, Jr., *J. Am. Chem. Soc.* **1998**, *120*, 7389; F.H. Zelder, J. Rebek, Jr., *Chem. Commun.* **2006**, 753; B. W. Purse, P. Ballester, J. Reber, Jr., *J. Am. Chem. Soc.* **2003**, *125*, 14682; S. Richeter, J. Rebek, Jr., *J. Am. Chem. Soc.* **2004**, *126*, 16280; A. Gissot, J. Rebek, Jr., *J. Am. Chem. Soc.* **2004**, *126*, 7424; B.W. Purse, J. Rebek, Jr., *Proc. Natl. Acad. Sci., USA* **2005**, *102*, 10777; B.W. Purse, A. Gissot, J. Rebek, Jr., *J. Am. Chem. Soc.* **2005**, *127*, 11222; J. Chen, J. Rebek, Jr., *Org. Lett.* **2002**, *4*, 327.

27 J.B. Huff, B. Askew, R.J. Duff, J. Rebek, Jr., *J. Am. Chem. Soc.* **1988**, *110*, 5908; J. Wolfe, A. Muehldorf,

J. Rebek, Jr., *J. Am. Chem. Soc.* **1991**, *113*, 1453; K.D. Shimizu, T.M. Dewey, J. Rebek, Jr., *J. Am. Chem. Soc.* **1994**, *116*, 5145; I. Huc, R.J. Pieters, J. Rebek, Jr., *J. Am. Chem. Soc.* **1994**, *116*, 10296; I. Huc, R.J. Pieters, J. Rebek, Jr., *J. Am. Chem. Soc.* **1994**, *116*, 11592; B.L. Tsao, R.J. Pieters, J. Rebek, Jr., *J. Am. Chem. Soc.* **1995**, *117*, 2210; R.J. Pieters, I. Huc and J. Rebek, Jr., *Angew. Chem., Int. Ed. Engl.* **1994**, *33*, 1579; R.J. Pieters, I. Huc, J. Rebek, Jr., *Tetrahedron* **1995**, *51*, 485.

28 Peptoid-based cryptand molecules obtained by Ugi multicomponent reactions: D.G. Rivera, L.A. Wessjohann, *J. Am. Chem. Soc.* **2006**, *128*, 7122. Bi-cyclic peptides (cryptand): T. Marskela, P. Heinonen, P. Virta, H. Lönnberg, *Eur. J. Org. Chem.* **2003**, 1687. Spiropeptides: P. Virta, J. Rosenberg, T. Karskela, P. Heinonen, H. Lönnberg, *Eur. J. Org. Chem.* **2001**, 3467; P. Virta, J. Sinkkonen, H. Lönnberg, *Eur. J. Org. Chem.* **2002**, 3616. A recent example of a simple synthetic cryptand molecule: M. Arunachalam, E. Suresh, P. Grosh, *Tetrahedron Lett.* **2007**, *48*, 2909.

29 Illustration taken from http://thegloveman.com in December 2008.

30 M.C.F. Monnee, A.J. Brouwer, L.M. Verbeek, A.M.A. van Wageningen, R.M.J. Liskamp, *Bioorg. Med. Chem. Lett.* **2001**, *11*, 1521; C. Chamorro, J.-W. Hofman, R.M.J. Liskamp, *Tetrahedron* **2004**, *60*, 8691; T. Opatz, R.M.J. Liskamp, *J. Comb. Chem.* **2002**, *4*, 275; D.J. van Zoelen, M.R. Egmond, R.J. Pieters, R.M.J. Liskamp, *ChemBioChem* **2007**, *8*, 1950; M. Hijnen, D.J. van Zoelen, C. Chamorro, P. Van Gageldonk, F.R. Mooi, G. Berbers, R.M.J. Liskamp, *Vaccine* **2007**, *25*, 6807.

31 M.C.F. Monnee, *Bio-Inspired Artificial Receptors*, **2002**, thesis, pp. 127-131. See also: J. Bernard, H. Wennemers, *Org. Lett.* **2007**, *9*, 4283.

32 For a review on the concept: J. Rebek, Jr., *Science* **1987**, *235*, 1478. See for a bi-cyclic calcium-binding nonapeptide: R. Oliva, L. Falcigno, G. D'Auria, G. Zanotti, L. Paolillo, *Biopolymers* **2001**, *56*, 27.

33 C. Chamorro, J.-W. Hofman, R.M.J. Liskamp, *Tetrahedron* **2004**, *60*, 8691.

34 See *Protective groups in organic synthesis*, T.W. Greene, P.G.M. Wuts, 3rd edn, **1999**, John Wiley & Sons, Inc., New York, USA; C.K. Marlowe, *Bioorg. Med. Chem. Lett.* **1993**, *3*, 437.

35 Staudinger reduction: H. Staudinger, J. Meyer, *Helv. Chim. Acta* **1919**, *2*, 635; W.G. Tian, Y.A. Wang, *J. Org. Chem.* **2004**, *69*, 4299; F.L. Lin, H.M. Hoyt, H. Van Halbeek, R.G. Bergman, C.R. Bertozzi, *J. Am. Chem. Soc.* **2005**, *127*, 2686; S. Carrington, J. Renault, S. Tomasi, J.-C. Corbel, P. Uriac, I.S. Blagbrough, *Chem. Commun.* **1999**, 1341. Thiolate mediated reduction: J.V. Staros, H. Bayley, D.N. Standring, J.R. Knowles, *Biochem. Biophys. Res. Commun.* **1978**, *80*, 568; I.L. Cartwright, D.W. Hutchinsin, V.W. Armstrong, *Nucleic Acids Res.* **1976**, *3*, 2331. See also: J.W. Back, O. David, G. Kramer, G. Masson, P.T. Kasper, L.J. de Koning, L. de Jong, J.H. van Maarseveen, C.G. de Koster, *Angew. Chem. Int. Ed.* **2005**, *44*, 7946.

36 M. Wagner, H, Kunz, *Synlett* **2000**, 400; M. Wagner, H. Kunz, *Angew. Chem. Int. Ed.* **2002**, *41*, 317. Aspartimide formation was not possible due to the absence of a *C*-terminal NH-group: W.D.F. Meutermans, P.F. Alewood, G.T. Bourne, B. Hawkins, M.L. Smyth, *Lett. Pept. Sci.* **1997**, *4*, 79; M. Mergler, F. Dick, B. Sax, C. Stähelin, T. Vorherr, *J. Peptide Sci.* **2003**, *9*, 36 and 518.

37 References that were used to obtain conditions used. For **entries 1-5:** E. Meinjohanns, M. Meldal, T. Jensen, O. Werdelin, L. Gali-Stampino, S. Mouritsen, K. Bock, *J. Chem. Soc., Perkin Trans. 1* **1997**, 871; M. Meldal, M.A. Juliano, *Tetrahedron Lett.* **1997**, *38*, 2531; C.W. Tornøe, P. Davis, F. Porreca, M. Meldal, *J. Peptide Sci.* **2000**, *6*, 594; **entry 6:** P.M. St. Hilaire, L. Cipolla, A. Franco, U. Tedebark, D.A. Tilly, M. Meldal, *J. Chem. Soc., Perkin Trans. 1* **1999**, 3559; C.W. Tornøe, H. Sengeløv, M. Meldal, *J. Peptide Sci.* **2000**, *6*, 314; K.M. Halkes, P.M. St. Hilaire, A.M. Jansson, C.H. Gotfresden, M. Meldal, *J. Chem. Soc., Perkin Trans. 1* **2000**, 2127.

38 Solid-phase step-wise double cyclization: W. Zhang, J.W. Taylor, *Tetrahedron Lett.* **1996**, *37*, 2173; C. Yu, J.W. Taylor, *Tetrahedron Lett.* **1996**, *37*, 1731. Solution-phase step-wise double cyclization: K. Akaji, S. Aimoto, *Tetrahedron* **2001**, *57*, 1749; R. Oliva, L. Falcigno, G. D'Auria, M. Saviano, L. Paolillo, G.

Ansanelli, G. Zanotti, *Biopolymers* **2000**, *53*, 581. A combination of solid- and solution-phase cyclization: J.N. Lambert, J.P. Mitchell, K.D. Roberts, *J. Chem. Soc., Perkin Trans. 1* **2001**, 471; L. Quartara, V. Pavone, C. Pedone, A. Lombardi, A.R. Renzetti, C.A. Maggi, *Regul. Pept.* **1996**, *65*, 55; V. Pavone, A. Lombardi, F. Nastri, M. Saviano, O. Maglio, G. D'Auria, L. Quartara, C.A. Maggi, C. Pedone, *J. Chem. Soc., Perkin Trans. 2* **1995**, 987; A. Lombardi, G. D'Auria, M. Saviano, O. Maglio, F. Nastri, L. Quartara, C. Pedone, V. Pavone, *Biopolymers* **1996**, *40*, 505.

39 P. Rovero, L. Quartara, G. Fabbri, *Tetrahedron Lett.* **1991**, *32*, 2639.

40 L.A. Carpino, H. Imazumi, A. El-Faham, F.J. Ferrer, C. Zhang, Y. Lee, B.M. Foxman, P.nklein, C. Hanay, C. Mügge, H. Wenschuh, J. Klose, M. Beyermann, M. Bienert, *Angew. Chem. Int. Ed.* **2002**, *41*, 442; A. Ehrlich, H.-U. Heyne, R. Winter, M. Beyermann, H. Haber, L. A. Carpino, M. Bienert, *J. Org. Chem.* **1996**, *61*, 8831.

41 F. Albericio, J.M. Bofill, A. El-Faham, S.A. Kates, *J. Org. Chem.* **1998**, *63*, 9678. W.C. Chan and P.D. White, *Fmoc Solid Phase Peptide Synthesis: a practical approach*, Oxford University Press, New York, **2000**, p. 57.

42 For host-guest chemistry, X-ray crystallography is not always informative, see G. Ranghino, S. Romano, J.-M. Lehn, G. Wipff, *J. Am. Chem. Soc.* **1985**, *107*, 7873.

43 G.I. Tesser, I.C. Balvert-Geers, *Int. J. Pept. Protein Res.* **1975**, *7*, 295.

44 E. Kaiser, R.L. Colescott, C. D. Bossinger, P. I. Cook, *Anal. Biochem.* **1970**, *34*, 595.

45 T. Vojkovsky, *Pept. Res.* **1995**, *8*, 236.

46 F. Guibé, *Tetrahedron* **1998**, *54*, 2967; D. Fernández-Forner, G. Casals, E. Navarro, H. Ryder, F. Albericio, *Tetrahedron Lett.* **2001**, *42*, 4471; S. Komjya, *Synthesis of Organometallic Compounds*, **1997**, John Wiley & Sons Ltd, Chichester, England, pp. 265-285.

Chapter 5

1,2,3-Triazole Cyclized TAC-Based Cryptand Molecules Containing all Relevant Components of Serine Hydrolase Active Sites

Abstract

In this chapter our attempts are described towards the synthesis of TAC-based cryptand molecules that containing all relevant components of serine hydrolase active sites using copper-catalyzed alkyne-azide cycloaddition chemistry. First, some test-reactions were carried out using a resin-bound bis-azide molecule. Conditions that gave the desired bis-triazole containing product were then successfully applied on a resin-bound cryptand precursor. Several products were formed and one product could be purified. MS-MS fragmentation studies on this product showed that the desired cryptand molecule was most likely formed. In addition to the desired compound, a tert-butylated adduct was also observed. Infrared and NMR analysis and assessment of the catalytic properties of the construct should provide insight in the effects of the double cycloaddition cyclization on structure and function of this potential serine hydrolase mimic.

1. Introduction

A general method for the reduction of flexibility in peptides is cyclization. Cyclization of peptidic constructs using the popular copper-catalyzed cycloaddition reaction to yield 1,2,3-triazole moieties from terminal alkynes and azide groups offers an important alternative for cyclizations based on amide bond formation reactions.[1,2] For instance, for the construction of an amide bond, it is crucial to protect all possible interfering functionalities like carboxylic acids, amines, hydroxyl groups, and imidazole moieties.[3] This necessity to use protecting groups is absent when alkyne and azide moieties are used in a so-called "click" reaction since this chemistry is usually compatible with the functional groups present in peptides and proteins. Also, it has been shown that the cyclization of small peptides can be performed using Copper-catalyzed Alkyne-Azide Cycloaddition (CuAAC).[4] Therefore, this CuAAC could offer an important alternative for the synthesis of TAC-scaffolded peptidic cryptand molecules which have been obtained by amide-bond cyclization (chapter 4).

Although it has been postulated that secondary amide-bonds and the 1,2,3-triazole moiety share some properties,[5] a main advantage of the 1,2,3-triazole ring is that it is present in two not interconvertible isomers: the 1,4- or 1,5-regioisomer (*figure 1*). This is not the case with amide-bonds. Secondary and tertiary amide-bonds can be present in both *cisoid* or *transoid* conformation, of which the latter is preferred in linear peptides and of which the former can be found, for example, in small cyclic peptides. This presence of two isomeric structures of one functional group could hamper structural elucidation of peptidic cryptand molecules.

Figure 1. Comparison of amide bonds with 1,2,3-triazole moieties. Distances are between the two methyl-groups separated by the linkage.

1.1. An amide *versus* a 1,2,3-triazole cyclized TAC-based peptidic cryptand

A synthetic route towards the construction of a TAC-based serine protease active site mimicking cryptand molecule was described in chapter 4. Improved (catalytic) properties of the double cyclized compound when compared to those of the non-cyclized compound were anticipated. These attempts involved the formation of two amide-bonds between *N*-terminally installed carboxylic acid and amine functionalities (*figure 2*). Despite successful formation of the target compound, the cumbersome synthesis and extremely tedious purification of the constructs urged us to explore other methods for the construction of these cryptand molecules.

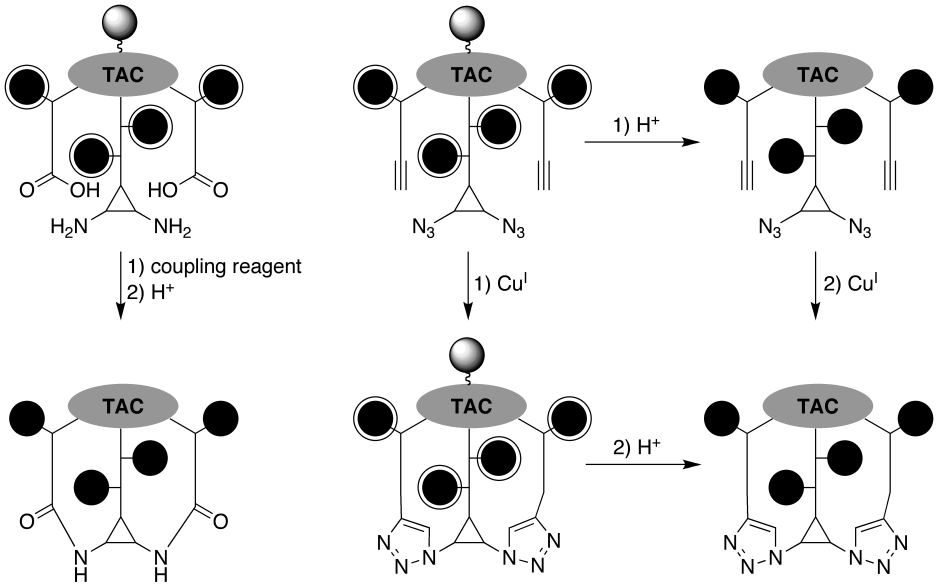

Figure 2. Schematic outline of the differences between amide-bond cyclized (*left*) and CuAAC cyclized (*right*) TAC-based peptidic cryptand molecules. Side chains of the amino acid residues are depicted by the black spheres, the circles around the spheres indicate protecting groups needed for functional amino acid residues.

In view of the successful application of CuAAC reactions in the formation of small cyclic peptides and the high functional group tolerance of this reaction, we decided to explore this chemistry in the construction of TAC-based cryptand molecules. The use of CuAAC chemistry would extend our synthetic arsenal beyond solid-phase methods for the double cyclization (*figure 2*). In addition, with respect to future catalytic studies, the large degree of similarity between open and closed form of the catalyst should allow a reliable assessment of the effect of cyclization on the catalytic properties.

2. Copper-catalyzed azide-alkyne click chemistry on a resin-bound bis-azide

The advantages of performing intramolecular chemistry on-resin are not so much related to the pseudo-dilution effect, but mainly to ease of purification, that is the simple removal of copper-salts, additives and solvents by filtration. However, the main disadvantage is that solid-phase chemistry turns more into black-box chemistry as the number of synthetic steps that are performed on the resin increases and, especially, when relatively undeveloped procedures for solid-phase chemistry have to be used. Whereas solid-phase peptide bond formation is well established as a synthetic tool, solid-phase click-chemistry is still relatively unknown. Apart from the paper by Meldal *et al*., that co-initiated CuAAC chemistry, only a few reports have appeared in which CuAAC has been performed on the resin.[6] Therefore, solid-phase CuAAC chemistry was first tested on resin-bound bis-azide containing modelsystem.

For this, both a TG- and a PS-Rink-His(Trt)-BAzMB construct was prepared by standard solid-phase peptide synthesis procedures (*scheme 2*, BAzMB = 3,5-bis-

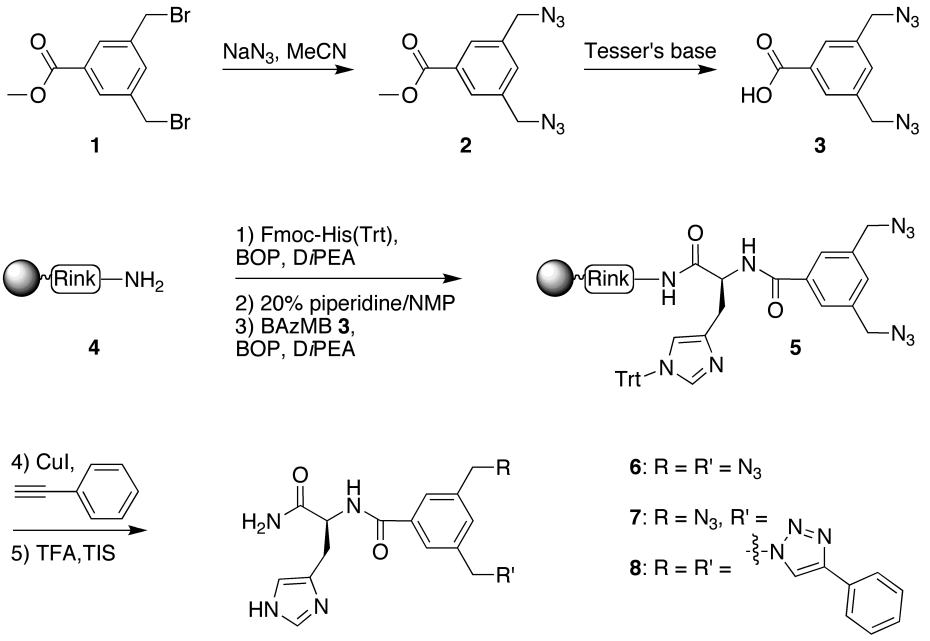

Scheme 1. Synthesis of the bis-azide **3** and construct **6** that was used for the test-reaction for solid-phase CuAAC chemistry. The resin was either of polystyrene (PS) or Tentagel (TG) origin.

(azidomethyl)benzoic acid **3** or amide). Two types of resin were used in order to determine to what extent the CuAAC reaction was influenced by the resin. For the synthesis of bis-azide **3**, the bromide atoms of the bis-bromide that was also used in the synthesis of the TAC-scaffold was substituted by azide groups followed by saponification of the methyl ester.

Initially, we applied three different in literature described conditions for the CuAAC reaction between resin-bound bis-azide **5** and phenylacetylene (*table 1*). From the results obtained it became clear that CuAAC chemistry using CuI was suitable for resin-bound constructs. Interestingly, the conditions for CuAAC similar to those reported by Finn *et al.* (entry 3) revealed a difference in behavior of polystyrene versus Tentagel resin. Besides CuAAC, we also attempted RuAAC on **5**, which would result in the formation of the 1,5-regioisomer of the 1,2,3-triazole ring instead of the 1,4-regioisomer.[7] Unfortunately, ruthenium-catalyzed azide-alkyne cycloaddition using bis-azide **5** and Cp*Ru(PPh_3)$_2$Cl did not result in the formation of desired products and mostly starting material was observed.

Table 1. CuAAC reaction of resin-bound bis-azide **5** and phenylacetylene.

Entry	Equiv CuI	Additive	Solvent	PS	TG
1[8]	0.5	--	20% piperidine/NMP	**8**	**8**
2[9]	2	50 equiv DiPEA	THF	**8**	**8**
3[10]	0.5	2 equiv NaAsc, 2 equiv 2,4,6-collidine	MeCH/DMSO/water - 8/2/1 (v/v)	**6, 7, 8**	**8**

Conditions: Reactions were performed with 10 mg of PS-Rink-resin or 30 mg of TG-Rink-resin and 2 equivalents of phenylacetylene at room temperature for 16 h.

3. Synthesis of 1,2,3-triazole cyclized TAC-based peptidic cryptands

Although initially designed for the synthesis of TAC-based phosphine-peptide constructs, an Fmoc/Teoc/*o*-NBS protected TAC-scaffold was used for the construction of the cryptands described in this chapter. Traces of Pd, which is used for the removal of the Alloc group of the scaffold that was used in chapter 4, are extremely difficult to remove, which might lead to alkyne-alkyne cross-coupling reactions in a later stage of the synthesis, for instance.[11] Therefore, a Teoc-protecting group, which is removed by fluoride, might be an attractive alternative for the Alloc-group.

3.1. Synthesis of a Teoc-protected TAC-scaffold

The synthesis of this scaffold (*scheme 2*) is similar to the described synthesis of the Alloc-protected TAC-scaffold (chapter 2). In this case, the *o*-NBS/Teoc/TFAc-protected triamine **10** – which was obtained by Teoc-protection on the secondary amine of triamine **9** – was reacted with bis-bromide **1**. This afforded cyclized monomer **11a** and dimer **11b** in 48% and 17% yield, respectively. The thus obtained

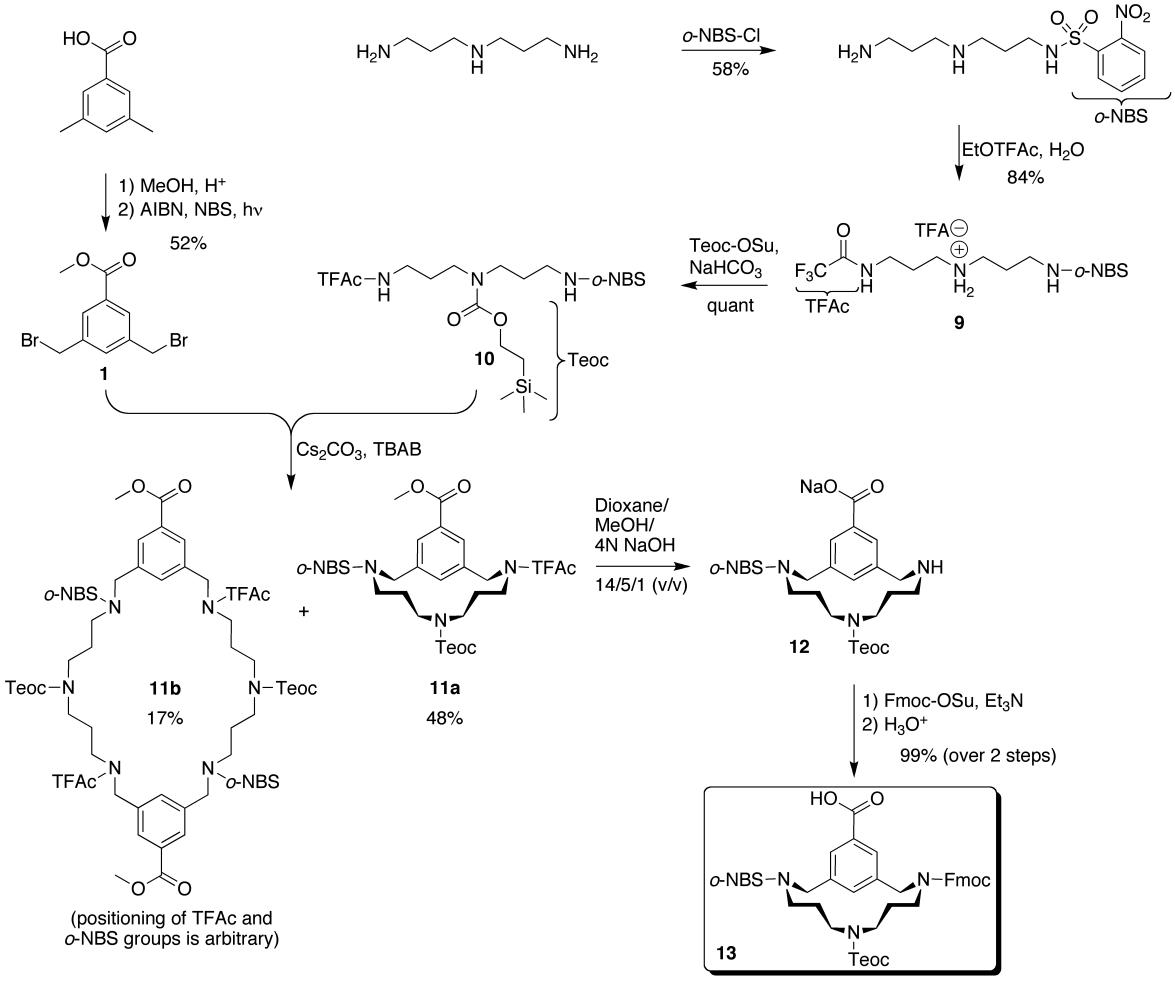

Scheme 2. Synthesis of the Teoc-protected TAC-scaffold.

protected TAC-scaffold **11a** was subjected to basic hydrolysis of the methyl ester and trifluoroacetyl-amide. The resulting carboxylate **12** was used without purification in the Fmoc-protection reaction, which afforded the desired scaffold **13** in near quantitative yields.

3.2. Solid-phase synthesis of the cryptand precursor to be used for mimicry of the serine hydrolase active site

In view of the difficult cyclization of the cryptand precursor described in chapter 4, we decided to introduce a glycine residue as an extra amino acid in the middle arm. We anticipated that this would introduce extra flexibility that was supposedly needed for the double cyclization reaction.

For the synthesis of the cryptand the Rink-linker containing polystyrene (PS) resin and the Rink-linker containing Tentagel (TG) resin was used (*scheme 3*). This was done in order to determine the extent to which the CuAAC cyclization of the resin-bound precursor depended on the resin. Protected TAC-scaffold **13** was coupled to the Rink-linker containing resins using one equivalent of **13** in the presence of HATU, HOAt and D*i*PEA as coupling reagents. Any remaining amine functionalities were permanently protected using a capping reagent. After this, the loading of resin **14** was determined to be 0.49 mmol/g for PS-resin **15a** and 0.18 mmol/g for TG-resin **15b**. On the Fmoc-position of the TAC-scaffold, Fmoc-Ser(*t*Bu)-OH and pentynoic acid were subsequently coupled, resulting in intermediates **16a** and **16b**. Then the *o*-NBS group was removed after which Fmoc-Asp(O*t*Bu)-OH and pentynoic acid were installed on this position, resulting in intermediates **17a** and **17b**.

Before removal of the Teoc-group the presence of aliphatic hydrocarbon groups next to the silyl atom of the Teoc-group was visualized by a broad peak around 0 ppm in the ^{1}H-NMR spectrum. This could be used in order to analyze the Teoc-deprotection conditions. For the removal of the Teoc-group, the resin was treated with 10 equivalents of TBAF in DMF for 30 min. ^{1}H-NMR analysis showed the absence of a peak around 0 ppm, indicating removal of the Teoc group. Since the Teoc-group is also cleaved by TFA its removal could not be monitored by ESI-MS analysis of the cleaved products. However, after coupling of Fmoc-His(Trt)-OH using BOP and D*i*PEA, mass spectrometry revealed the presence of the desired Fmoc-His acylated TAC-scaffold. After this, the histidine residue was extended using Fmoc-Gly-OH and 3,5-bis(azidomethyl)benzoic acid **5**. This resulted in resin-bound cryptand precursor **18** which was used in on-resin CuAAC reactions.

Both PS- and TG- bound precursors (**18a** and **18b**) were cleaved from the resin and analyzed using LC-MS (*figure 3* for the results for PS-bound precursor). MS-MS-analysis of this compound showed several fragments originated from cleaved precursor **18a** and **18b** (*figure 4*). These analyses showed that the resin-bound precursors were the desired compounds and were suitable for CuAAC double cyclization towards the

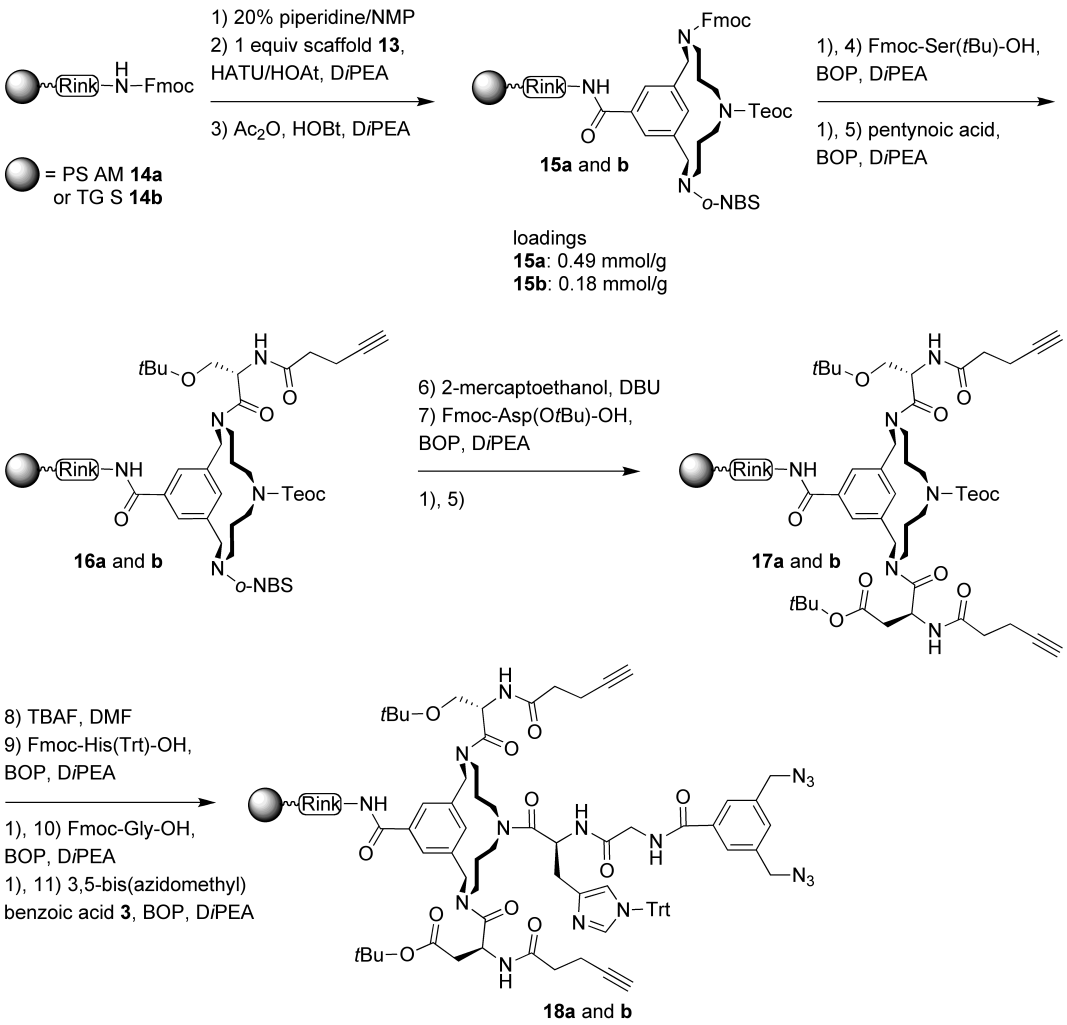

Scheme 3. Solid-phase synthesis of resin-bound precursor **18**.

construction of the target compound, *i.e.* a TAC-based serine hydrolase mimicking cryptand molecule of which the arms were connected by 1,2,3-triazole rings.

3.4. The CuAAC reaction towards double cyclization of resin-bound precursors 18a and 18b

For the CuAAC reaction on precursor, **18a** and **18b** (*scheme 4*) initially the conditions were tested that were also used for test-compound **5** (*table 2*, entries 1-3). After that, also the same reaction conditions were attempted at higher temperature using microwave heating (**table 2**, entries 4-6). In addition to double cyclized TAC-based molecule **19**, remaining starting material, two mono-cyclic and several possible dimeric products were obtained, all with the same or similar *m/z*-values as the desired product.[12] For instance, MALDI-TOF analysis of the crude products that were obtained from the PS-bound precursor also revealed the presence of dimeric species.[14]

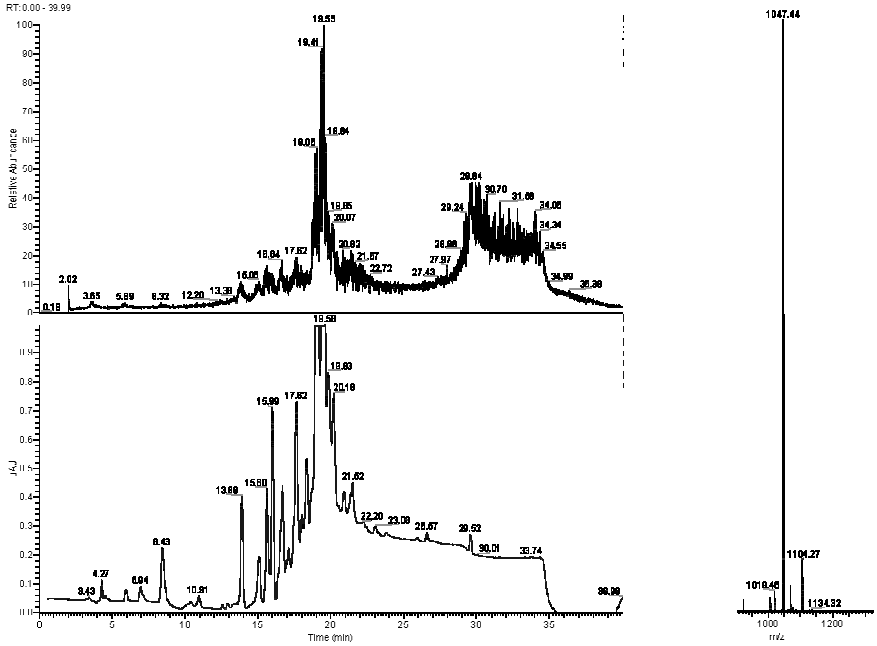

Figure 3. LC-MS analysis of cleaved cryptand precursor **18a** (left) with total ion current pattern (top), UV-trace (lower) and mass spectrum of **18a** $[M+H]^+$ in the main peak at t_R = 19.6 min (right).

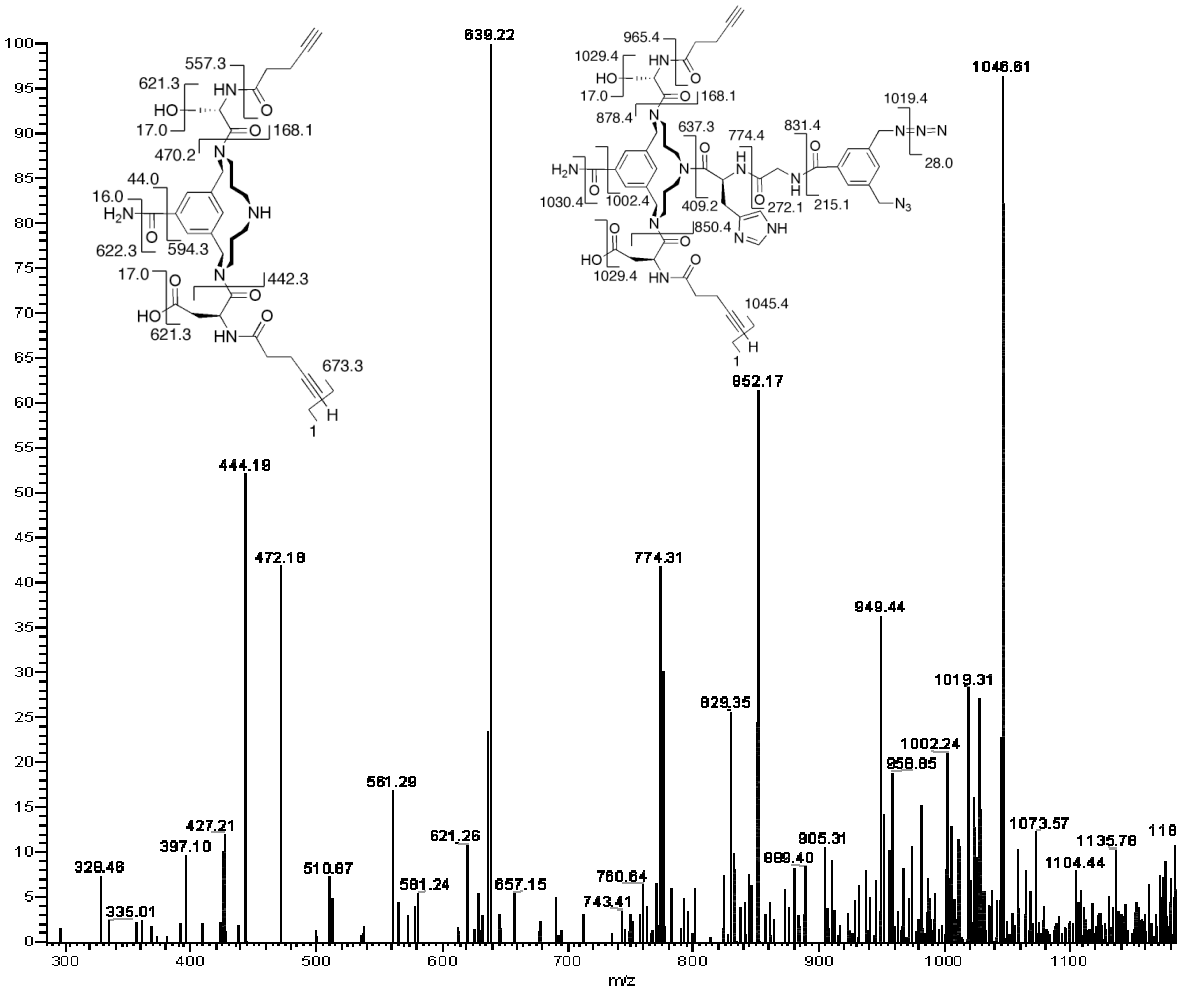

Figure 4. MS-MS-fragments of the cleaved starting material from PS-bound precursor **18a**. Fragmentation patterns of starting material are shown, loss of a hydrogen radical at the terminal position of the alkyne is arbitrary.

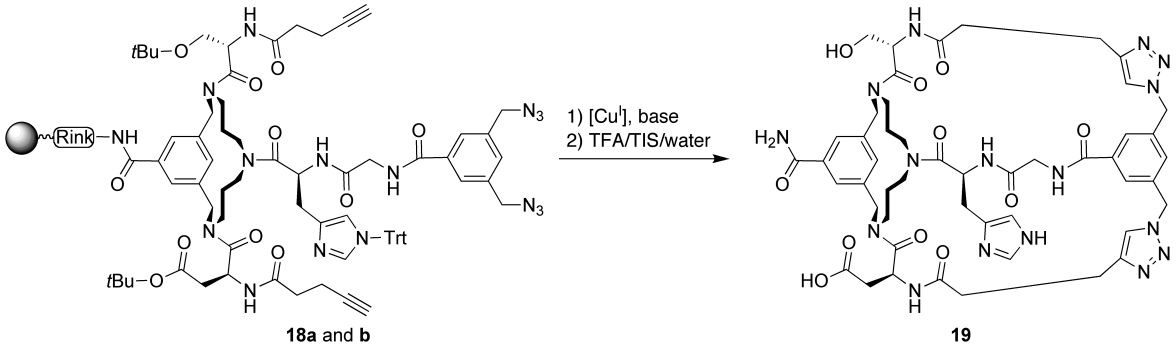

Scheme 4. Desired CuAAC reaction on resin-bound precursor **18**.

LC-MS analysis of the obtained products showed the presence of several compounds with different retention times and identical *m/z*-value, *i.e*. *m/z* 1047 (*figure 5*). In the absence of base, HPLC traces of cleaved products were similar to those of untreated cleaved products, indicating that the presence of base was shown to be necessary for the CuAAC reaction, as was also mentioned by Meldal *et al*.[15]

Table 2. Conditions for the CuAAC reaction using resin-bound precursor **18**.

Entry	Equiv CuI	Additive (eq)	t[a]	T (°C)[b]	Solvent	Results[c]
1	0.5	piperidine (7)	o.n.	r.t.	NMP	**s.m.**
2	0.5	D*i*PEA (50)	o.n.	r.t.	THF	**s.m.**
3	0.5	NaAsc (2), 2,6-DMP[c] (2)	o.n.	r.t.	MeCN/DMSO/H_2O - 8/2/1	**s.m.**
4	0.5	piperidine (7)	30 min	100	NMP	**s.m. + products**
5	0.5	D*i*PEA (50)	30 min	100	THF[e]	**s.m. + products**
6	0.5	NaAsc (2), 2,6-DMP[c] (2)	30 min	100	MeCN/DMSO/H_2O - 8/2/1	**s.m. + products**

Conditions: reactions were typically performed using 15 mg of **18a** or 45 mg of **18b**.
Notes: [a] o.n. means over night reaction; [b] r.t. room temperature; [c] products refer to compounds with different retention times on HPLC and identical *m/z*-values, s.m. starting material as it is obtained after cleavage from the resin; [d] 2,6-DMP: 2,6-dimethylpyridine (or 2,6-lutidine); [e] 100 μL of NMP was added to facilitate microwave heating of the microwave transparent THF.[13]

It was found that peaks with different retention times contained several compounds with an *m/z* value of 1047 (*figure 5*, *table 3*). Fortunately, we were able to purify the compound with a retention time of 17.65 min in the chromatogram (*figure 5*). However, at least two compounds were detected by MS-analysis of the collected fractions: one with *m/z* value of 1047.49 and one with *m/z* value of 1104.54.[16] Both of these compounds were subjected to MS-MS-analysis in order to determine if it was starting material or a cyclized product (*figure 6* and *figure 7*). These analyses showed that fragmentation of the arms that were attached to the TAC-scaffold did not occur, only loss of side-chain functionalities and nitrogen was observed.[17,18]

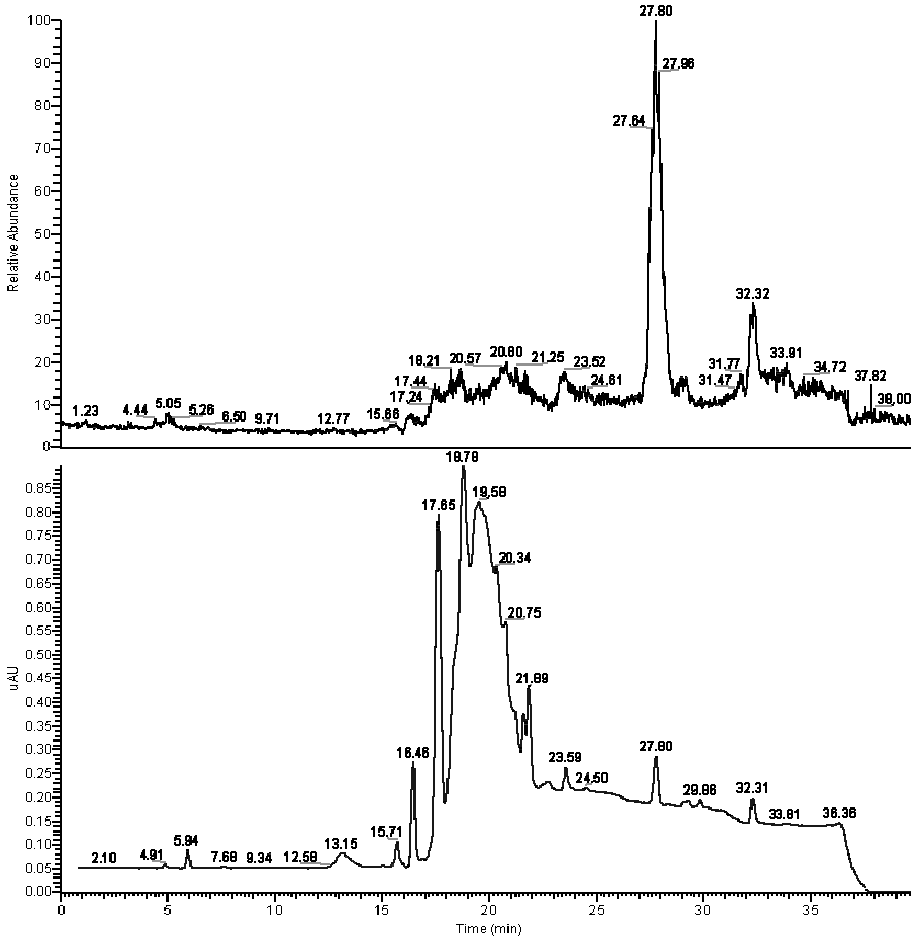

Figure 5. LC-MS analysis of cleaved products obtained after the CuAAC reaction on TG-bound precursor **18b** with total ion current pattern (top left) and UV-trace (lower left). Asterisks indicate compounds having an *m*/*z*-value of 1047. The peak at 21.89 min is due to starting material.

Table 3. Selection of the most important *m*/*z*-values detected at the different retention times. Bold values correspond to the desired material, italic values correspond to undesired *tert*-butylated side-product (*vide infra*).

t_R (min)	*m*/*z* (intensity in %)
16.46	639.22 (100), 661.15 (40), 796.63 (26), 818.96 (12)
17.65	552.90 (100), *1104.42* (44), 1126.45 (32), 524.37 (24), **1047.45** (18)
18.78	*1104.67* (100), 1076.13 (72), 872.24 (60), 681.06 (34), **1047.51** (32)
19.58[a]	715.08 (100), *1104.37* (80), 893.54 (75), 1076.64 (70)
21.89	475.46 (100), 750.18 (80), 453.31 (78), *1104.28* (60), **1047.24** (30)
27.80[b]	659.94 (100), 615.87 (80)

Notes: [a] poor quality of mass spectrum; [b] corresponding to cleaved PEG-derivatives.

This low tendency of the collected semi-pure fraction to produce fragment ions under the same conditions that resulted in fragmentation of the uncyclized starting material, indicated that a double cyclized product was formed. Also, the similarity between the two fragmentation patterns (*cf. figure 6* and *7*) indicated that both compounds were probably similar. Unfortunately, the compounds present in this fraction were not

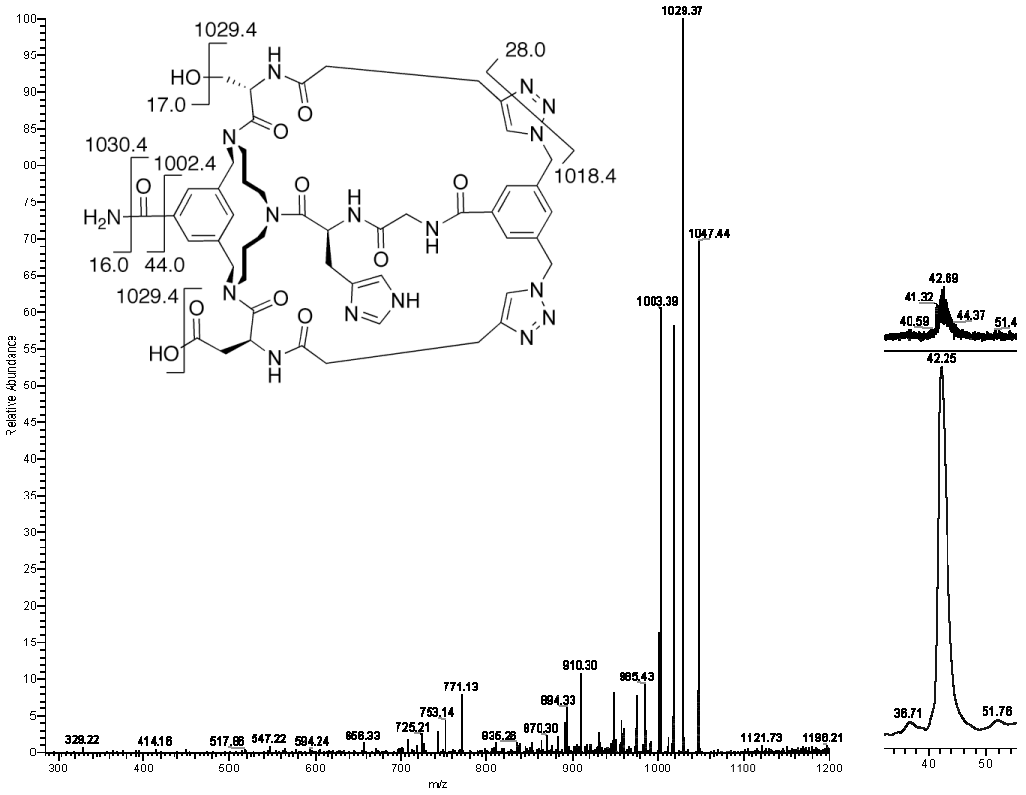

Figure 6. MS-MS-analysis of the 1047-peak in a collected fraction containing the desired compound (left). Also shown are the LC-MS analysis of the fraction (right: total ion current (top) and UV-trace (bottom)) on a different system as that which was used for *figure 5*. The peak between 1003.39 and 1029.37 had an *m*/*z* value of 1019.36.

separable by HPLC, which prevented determination of the ratios in which the products were formed. In addition, loss of *m*/*z* 56, corresponding to the loss of the *tert*-butyl group, was not observed, which indicated that the *tert*-butyl group remained attached to the molecule.

Although the peak at 1104.5 was also observed in the mass spectrum of the cleaved starting material (see *figure 3*), the intensity of this peak was much higher after the CuAAC reaction. Apparently, more of this product was formed in the sequence of reactions for the target compound than for the starting material. A likely explanation for the identity of this species is a *tert*-butylated product, which originated from the electrophilic addition of a *tert*-butyl cation to electron-rich parts of the molecule. Even though scavengers were used, this undesired side-reaction could not be prevented.

To determine whether this had occurred during the acidic cleavage of the compounds from the resin or during the microwave assisted CuAAC reaction, which could involve the electrophilic addition of a *tert*-butyl group to the nucleophilic metallated triazole intermediate that is formed during the click-reaction, a few control experiments were carried out. First, the temperature and reaction time were varied using 60, 80 and 100 °C during 2, 15, 30 and 60 min, respectively. Analysis of the cleaved products showed that formation of the product with an *m*/*z*-value of 1104 was independent of

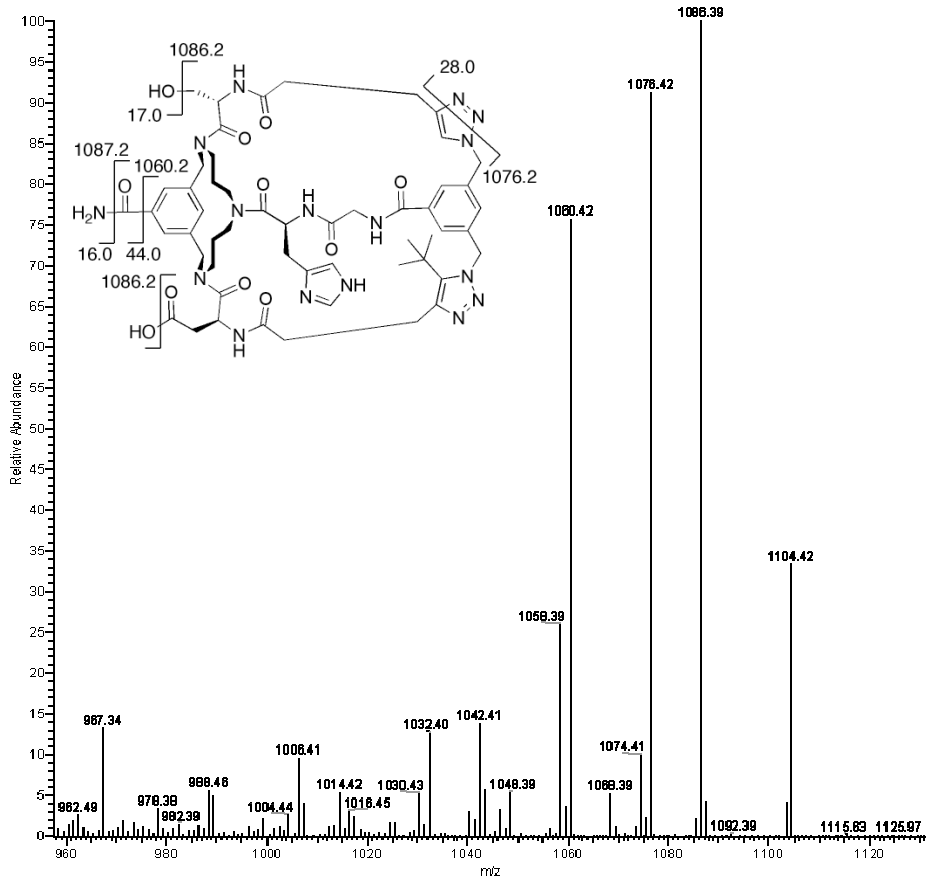

Figure 7. MS-MS-analysis of the 1104.31-peak in a collected fraction containing the desired compound (right). Smaller fragments were not detected, positioning of the *tert*-butyl group is arbitrary.

temperature and reaction time. This is in line with literature since thermolysis of *tert*-butyl esters usually only occurs at much higher temperatures (> 220 °C).[19] Another source for the formation of this *tert*-butylated product could be precipitation of the cleaved products, that were dissolved in TFA, in cold MTBE:*n*-hexanes.[20] However, precipitation of the product in cold Et_2O:*n*-hexanes instead of MTBE:*n*-hexanes did not reduce formation of this species. It was therefore concluded that this species was probably formed during the acidic cleavage of the products from the resin. It is known that electron-rich functionalities like aromatic rings can be alkylated during the acidic cleavage and deprotection of resin-bound peptides.[21] This important side-reaction, however, can usually be avoided using extra scavengers in the cleavage cocktail. Therefore, thioanisole was added to the acidic cleavage mixture.

Although the low tendency of the obtained molecule to produce fragments in MS-MS analysis indicates that the target compound was obtained, detailed structural analysis using infrared and NMR spectroscopy had to be performed. Unfortunately, the small amount of product and lack of time prevented us from performing these analyses.

4. Discussion, Conclusions and Future Prospects

In this chapter the solid-phase synthesis of TAC-based peptidic cryptand molecules that contain all the relevant components of serine hydrolase active sites was described. Since application of the copper-catalyzed alkyne-azide cycloaddition (CuAAC) reaction on these molecules was relatively new, first the applicability of this chemistry was tested using a resin-bound model compound. It was confirmed that CuAAC of an alkyne to a resin-bound bis-azide was feasible using CuI in 20% piperidine in NMP. Next, the same conditions were used for the construction of the target cryptand molecule. It was found that elevated temperatures were required for the reaction to occur, which indicated that the desired double cyclization reaction took place with difficulty. This was already apparent from cryptand molecules that were obtained by cyclization using amide-bond formation. Using LC-MS and MS-MS techniques we were able to show that the target molecule was most likely formed. Unfortunately, the small amount of product obtained, the presence of both desired cryptand and *tert*-butylated cryptand as well as the lack of time, prevented us from performing a detailed structural analysis of the obtained compound, let alone determination of its possible catalytic performance.

Nevertheless, the results described in this chapter offer an interesting alternative for the construction of TAC-based peptidic enzyme models in which pre-organized molecules with unparalleled functional-group density had to be obtained. Future work in this area should first be focused on the isolation, structural and functional analysis of the properties of these TAC-based cryptand molecules. Improvements on the synthetic route are also feasible, considering both solid-phase and solution-phase routes. As far as solution-phase CuAAC is concerned, especially heterogeneous systems like Cu/C,[22] resin-immobilized Cu [23] and solid Cu [24] are interesting in view of the ease of purification. Also, the construction of TAC-based ligand-systems for transition metal catalyzed reactions using this method is very interesting. In addition, the method described for the CuAAC of three scaffolded peptides can offer an important route for the construction of discontinuous epitope mimics that can be used to modulate protein-protein interactions.[25] Finally, the test-reaction on the resin-bound bis-azide could be used in the construction of tweezer-like receptors for host-guest chemistry[26] or catalysis.[27]

5. Experimental Section

For general information on used equipment see chapter 2.
HPLC eluents: mostly MeOH eluents were used: A_{MeOH}: MeOH/water/TFA – 20/80/0.1 (%, v/v) and B_{MeOH}: MeOH/water/TFA – 5/95/0.1 (%, v/v/). MeCN: A_{MeCN} (water/MeCN/TFA – 95/5/0.1 (%, v/v) to B_{MeCN} (MeCN/water/TFA – 95/5/0.1 (%, v/v) in 25 min.

Calculations of amide and 1,2,3-triazole

For calculation of the geometrical properties of amide bonds and 1,2,3-triazole linkages between two methyl-groups, YASARA (version 8.3.3) was used. Structures as shown in **figure 1** were drawn in ChemDraw (version 11.0) and saved as connection table (.ct) files. These were loaded in YASARA, the simulation cell was defined automatically, and the YASARA2 force field was selected with all force field terms activated. The energy of structures was minimized separately using identical settings. Energies found: for the 1,4-triazole -140.32 kJ/mol; for the 1,5-triazole -4.62 kJ/mol; for the *trans*-amide bond -115.01 kJ/mol; for the *cis*-amide bond -81.93 kJ/mol.

3,5-bis(azidomethyl)benzoic acid 3

3,5-bis(bromomethyl)benzoic acid **1** (3.51 g, 10.9 mmol) was dissolved in dry acetonitril and sodium azide (4 equiv, 43.6 mmol, 2.84 g) was added to the mixture. This was stirred overnight under reflux conditions, after which the solution was cooled and filtered in order to remove the precipitated NaBr. Concentration under reduced pressure was followed by purification using column chromatography (eluent: EtOAc:hexanes – 10:1 (v/v)) and afforded bis-azide ester **2**. Yield: 2.2 g (8.9 mmol, 82%). ^{1}H NMR ($CDCl_3$, 300 MHz): δ 3.94 (s, 3H, OC*H*$_3$), 4.44 (s, 4H, Ar-C*H*$_2$), 7.48 (s, 1H, C^{Ar}-*H*), 7.97 (s, 2H, C^{Ar}-*H*). APT ($CDCl_3$, 75 MHz): δ 52.3 (Ar-*C*H$_2$), 54.0 (O*C*H$_3$), 128.8, 131.3, 131.7, 136.7, 166.1 (*C*(O)OMe).
Ester **2** was dissolved in Tesser's base (50 mL) and stirred overnight. After this, the solution was acidified to pH 1 using 2N HCl and concentrated under reduced pressure. The resulting solid was dissolved in EtOAc and the organic phase was washed with water (50 mL) and brine (50 mL). The separated organic phase was dried over Na_2SO_4, filtered and concentrated to yield the desired bis-azide carboxylic acid as a white solid. Yield: 1.96 g (8.4 mmol; 95%). ^{1}H NMR ($CDCl_3$, 300 MHz): δ 4.43 (s, 4H, Ar-C*H*$_2$), 7.52 (s, 1H, C^{Ar}-*H*), 8.01 (s, 2H, C^{Ar}-*H*), 12.65 (s, 1H, COO*H*). APT ($CDCl_3$, 75 MHz): δ 53.6, 129.0, 130.2, 132.4, 136.7, 171.2 (*C*(O)OH).

Resin-bound bis-azide 5

The Fmoc-group of PS-Rink-Fmoc (100 mg; loading = 0.7 mmol/g) and TG-Rink-Fmoc (300 mg; loading = 0.2 mmol/g) was removed using 20% piperidine in NMP. After this, the resin was washed using standard washing procedures. To the free amine-functionality, Fmoc-

His(Trt)-OH (4 equiv, 174 mg) was coupled using BOP (4 equiv, 124 mg) and D*i*PEA (8 equiv, 97 μL) in NMP for 3 h. After coupling, the resin was washed and the *N*-terminal Fmoc-group was removed as mentioned above. To the liberated amine group, 3,5-bis(azidomethyl) benzoic acid **3** (4 equiv, 70 mg) was coupled using BOP (4 equiv, 124 mg) and D*i*PEA (8 equiv, 97 μL) (overnight coupling). After this, the resin was washed and a small fraction of each of the two batches was cleaved for analysis. R_f = 0.86 (eluens: $CHCl_3$/MeOH/25% NH_4OH (aq) – 8/3/2 (v/v/)). ESI-MS: *m*/*z* 368.95 (calculated 369.15 for $[M+H]^+$). HPLC: t_R = 24.74 min (C_8, MeOH-buffers).

Experimental procedure for the RuAAC test-reaction of phenylacetylene on resin-bound construct 1

Eight batches were tested in which the two different resins (10 mg of PS- or 30 mg of TG-resin) were used together with phenylacetylene (2 equiv, 1.5 μL) and 20% Cp*RuCl(PPh_3)$_2$ in four different deoxygenated solvents, *i.e.* toluene, DMF and freshly distilled THF or DCM (1 mL) (Cp* = pentamethylcyclopentadienyl). The reaction was performed overnight at room temperature. After this, the resin was placed into a syringe equipped with a filtering frit, and washed with sodium *N*,*N*-diethyldithiocarbamate in order to remove the Ru-catalyst. After extensive washing with NMP (3 × 2 min × 1 mL) and DCM (3 × 2 min × 1 mL), the products were cleaved from the resin using TFA containing 5% TIS (3 h). Precipitation of the cleaved products in cold MTBE:*n*-hexane – 1:1 (v/v) and centrifugation resulted in the formation of a white pellet which was suitable for analysis. Except for the reaction on TG-based construct **1** in toluene – which gave a mono-click product – only starting material was found.

Experimental procedure for the CuAAC test-reaction of phenylacetylene on resin-bound construct 5

Three batches of 10 mg of PS- and three batches of 30 mg of TG-resin **5** were placed in six ependorf vials. To one batch of each of the two types of resin was added CuI (0.5 equiv, 1.3 mg) and 20% piperidine in NMP (1 mL). To another batch of each of the two types of resin were added CuI (2 equiv, 5.3 mg), DiPEA (50 equiv, 122 μL) and THF (878 μL). To the last batch of each of the two types of resin were added CuI (0.5 equiv, 1.3 mg), NaAsc (2 equiv, 9.9 mg), 2,4,6-collidine (2 equiv, 3.7 μL) and MeCN/DMSO/water – 8/2/1 (v/v) was added. All six batches were gently shaken overnight. After this, the resin of all six batches were placed in six small syringes equipped with a filtering frit at the bottom and the resin was extensively washed with 0.2 M solution of sodium *N*,*N*-diethyldithiocarbamate in order to remove remaining copper. Subsequently, the resin was washed with NMP (3 × 2 min × 1 mL) and DCM (3 × 2 min × 1 mL). Products were cleaved from the resin using TFA containing 5% TIS (3 h). Precipitation in cold MTBE:*n*-hexane – 1:1 (v/v) followed by centrifugation of the samples afforded the cleaved products as white pellets at the bottom of the Falcon tubes.

HPLC and ESI-MS analysis was used to analyze the formed products.
Di-clicked product **8**: ESI-MS: *m/z* 573.25 (calculated: 573.25 for $[M+H]^+$). HPLC: t_R = 27.90 min (C_8, MeOH-buffers).
Mono-clicked product **7**: ESI-MS: *m/z* 471.00 (calculated: 471.20 for $[M+H]^+$). HPLC: t_R = 26.78 min (C_8, MeOH-buffers).
Starting material **6**: ESI-MS: *m/z* 368.95 (calculated: 369.15 for $[M+H]^+$). HPLC: t_R = 24.74 min (C_8, MeOH-buffers).

TAC-scaffold 13

Synthesis of the TAC-scaffold used in this chapter is similar to our earlier described procedure.[28] Deviations from this procedure concerned the last step in the synthesis of the fully protected triamine, and subsequent synthetic steps in the construction of the scaffold. These modified procedures are described below.

***o*-NBS/Teoc/TFAc-protected triamine 6**

Triamine **4** (13.2 g, 25 mmol) was dissolved in a mixture of MeCN (100 mL) and water (100 mL). To this solution, Et_3N was added in order adjust the pH to approximately 9. A solution of Teoc-OSu (7.8 g, 30 mmol) in MeCN (70 mL) was added in one portion and the pH was maintained at 9 using Et_3N. The reaction mixture was allowed to stir overnight. After completion of the reaction, the mixture was concentrated under reduced pressure and the resulting residue dissolved in EtOAc (200 mL). The organic phase was subsequently washed with water (2×100 mL), 1N $KHSO_4$ (2×100 mL), 5% $NaHCO_3$ (2×100 mL) and brine (100 mL), dried (Na_2SO_4) and concentrated *in vacuo* affording a yellow oil.
Yield: 14.28 g (25 mmol; quant). R_f = 0.67 (EtOAc:hexanes – 2:1). ^{1}H-NMR (300 MHz, $CDCl_3$): δ -0.02 (s, 9H, Si(C*H*$_3$)$_3$), 0.92-0.97 (t, ^3J 8.8 Hz, 2H, SiC*H*$_2$), 1.69-1.71 (br m, 4H, CH$_2$C*H*$_2$CH$_2$), 3.03-3.10 (q, ^3J 6.6 and 6.3 Hz, 2H, *o*-NBS-NHC*H*$_2$), 3.22-3.29 (br m, 6H, NC*H*$_2$CH$_2$), 4.09-4.14 (t, ^3J 8.8 Hz, 2H, OC*H*$_2$), 5.57 and 6.18 (2 s, 1H, *o*-NBS-N*H*), 7.07 and 8.04-8.07 (2 s, 1H, TFAc-N*H*), 7.69-8.07 (m, 4H, C^{Ar}-*H*). ^{13}C-NMR (75 MHz, $CDCl_3$, APT): δ -1.7 (Si(*C*H$_3$)$_3$), 17.7 (Si*C*H$_2$), 26.9, 28.4, 36.0, 36.7, 40.9 43.6 (*C*H$_2$ in triamine), 64.3 (O*C*H$_2$), 110.1-121.6 (q, $J_{C\text{-}F}$ 288 Hz, *C*F$_3$), 125.2, 130.7, 132.7, 133.7 (*C*^{Ar}H), 133.4, 147.9 (*C*^{Ar}), 156.4-157.9 (q, $J_{C\text{-}C\text{-}F}$ *C*(O)CF$_3$ and N*C*(O)O). ^{19}F-NMR (282 MHz, $CDCl_3$): δ -76.5 (NHC(O)C*F*$_3$). ESI-MS: *m/z* 579.80 (calculated: 579.16 for $[M+Na]^+$).

MeOC(O)-TAC(*o*-NBS/Teoc/TFAc) 8a

Triamine **6** (6.7 g, 12 mmol) was dissolved in MeCN (1L dried over molsieves 3Å). To this solution were added TBAB (3.9 g, 12 mmol), bis-bromide **1** (3.9 g, 12 mmol) and Cs_2CO_3 (15.6 g, 48 mmol). The resulting mixture was refluxed for 1 h after which TLC analyses indicated complete conversion of the starting materials. After this ca half of the solvent was

removed by evaporation under reduced pressure. A solution of $KHSO_4$ (9.8 g, 72 mmol) in water (350 mL) was added to this concentrated mixture. From this acidic mixture the products were extracted using DCM (200 mL). The organic phase was washed with brine (100 mL), dried over Na_2SO_4 and concentrated *in vacuo*.

Yield: 4.16 g (5.8 mmol, 48%). R_f = 0.54 (eluent: EtOAc/hexanes/DCM – 1/1/1 (v/v)). ^{1}H-NMR (300 MHz, $CDCl_3$): δ -0.04 (s, 9H, Si(CH_3)$_3$), 0.85-0.90 (d t, ^3J 8.8 Hz, 2H, SiCH_2), 1.22-1.56 (d quint, 4H, $CH_2CH_2CH_2$), 2.84-3.41 (m, 8H, NCH_2), 3.88-3.90 (d, $\delta_{T=25}$ 6.6 Hz, 3H, OCH_3), 3.98-4.05 (d t, ^3J 8.5 Hz, 2H, OCH_2), 4.41-4.73 (4 s, 4H, ArCH_2N), 7.63-8.02 (m, 7H, C^{Ar}-*H*). ^{13}C-NMR (75 MHz, $CDCl_3$, APT): δ -1.6 (Si(*C*H_3)$_3$), 17.7 (Si*C*H_2), 28.0, 28.4, 29.1, 29.6, 44.9, 46.4, 48.3, 51.3, 52.6, 53.7, 54.0 (8 × *C*H_2 in triazacyclophane ring), 52.4 (OCH_3), 63.5 (O*C*H_2), 110.8-122.2 (J_{C-F} 288 Hz, *C*F_3), 124.3, 129.4, 129.9, 130.1, 130.3, 130.8, 131.8, 133.6, 134.0 (*C*^{Ar}H), 131.8, 136.2, 137.8, 138.5 (*C*^{Ar}), 148.3 (*C*^{Ar,2}), 156.2-157.4 (*C*(O)CF_3 and N*C*(O)O), 165.7-165.9 (d, $\delta_{T=25}$ 12 Hz, *C*(O)OMe). ^{19}F-NMR (282 MHz, $CDCl_3$): δ -67.7, -68.8 ($\delta_{T=25}$ 308 Hz, TFAc). ESI-MS: *m*/*z* 739.35 (calculated: for 739.22 [M+Na]$^+$).

Dimer **8b** eluted after monomer **8a**. Yield: 1.43 g (1.0 mmol, 17%). R_f = 0.39 (eluent: EtOAc/hexanes/DCM – 1/1/1 (v/v)). ^{1}H-NMR (300 MHz, $CDCl_3$): δ -0.02 (d, 18H, Si(CH_3)$_3$), 0.83-0.92 (m, 4H, SiCH_2), 1.60-1.79 (br d, 8H, $CH_2CH_2CH_2$), 3.03-3.28 (m, 16H, NCH_2), 3.85-3.89 (m, 6H, OCH_3), 3.96-4.08 (m, 4H, OCH_2), 4.46-4.68 (m, 8H, ArCH_2N), 7.28-7.92 (m, 7H, C^{Ar}-*H*). ^{13}C-NMR (75 MHz, $CDCl_3$, APT): δ -1.6 (Si(*C*H_3)$_3$), 17.7 (Si*C*H_2), 25.5, 27.4, 44.5, 46.2, 49.0, 50.4, 51.6 (8 × *C*H_2 of azacyclophane ring), 52.3 (OCH_3), 63.6, 63.7 (d, δ 8.5 Hz, O*C*H_2), 110.8-122.1 (J_{C-F} 283 Hz, *C*F_3), 124.4, 127.6, 128.6, 130.5, 131.8, 132.1, 133.9, 135.6 (*C*^{Ar}H), 131.1, 132.7, 136.1, 136.7, 137.1, 137.5 (*C*^{Ar}), 148.0 (*C*^{Ar,2}), 156.3-158.0 (*C*(O)CF_3 and N*C*(O)O), 166.0 (*C*(O)OMe). ^{19}F-NMR (282 MHz, $CDCl_3$): δ -68.60, -68.67, -69.17, -69.25 (NC(O)C*F*$_3$). ESI-MS: *m*/*z* 1455.30 (calculated: 1455.43 for [M+Na]$^+$).

HOC(O)-TAC(*o*-NBS/Teoc/Fmoc) 10

Fully protected TAC-scaffold **8a** (2.4 g, 3.67 mmol) was dissolved in Tesser's base (128 mL; dioxane:methanol:4N NaOH – 14:5:1 (v/v)) and allowed to react overnight at room temperature. The resulting solution was neutralized using 1N HCl and concentrated under reduced pressure. The crude product was dissolved in 100 mL acetonitril:water – 1:1 (v/v) and the pH of the solution was adjusted to 9.5 using Et_3N. A solution of Fmoc-OSu (1.4 g, 4.0 mmol) in acetonitril (10 mL) was added and the pH of the mixture was maintained between 8.5-9.0 using Et_3N. After ca 90 min, the reaction was complete and acidified using 1N HCl. Water (350 mL) was added and the product was extracted with EtOAc. The collected organic layers were dried over Na_2SO_4, concentrated *in vacuo* and the product was purified by column chromatography (eluent: gradient from DCM to 2.5% MeOH in DCM). After concentration of the fractions, the product was obtained as off-white foam.

Yield: 3.0 g (3.64 mmol, 99%). R_f = 0.41 (10% MeOH in DCM). ^{1}H-NMR (300 MHz, $CDCl_3$): δ -0.02 (s, 9H, Si(CH_3)$_3$), 0.87-1.24 (br m, 6H, SiCH_2 and $CH_2CH_2CH_2$), 2.4-3.25 (br m, 8H, NCH_2), 4.03-4.70 (br m, 9H, OCH_2CH and ArCH_2N), 7.22-8.05 (m, 15H, C^{Ar}-*H*), 10.49 (br s, 1H, COO*H*). ^{13}C-NMR (75 MHz, $CDCl_3$, APT): δ -1.6 (Si(CH_3)$_3$), 17.7 (SiCH_2), 27.9, 45.1, 48.2, 52.8, 53.6 (8 × CH_2 in triazacyclophane ring), 47.1 (OCH_2CH), 63.4 (OCH_2-Teoc), 67.2, 67.6 (OCH_2-Fmoc), 119.8, 124.2, 124.5, 127.0, 127.5, 129.3, 130.9, 131.7, 133.4, 133.8 ($C^{Ar}H$), 130.7, 132.0, 138.0, 140.1, 141.2, 143.8 (C^{Ar}), 148.1 ($C^{Ar,2}$), 156.3-156.9 (N*C*(O)O), 169,4 (*C*(O)OH). ESI-MS: *m*/*z* 829.50 (calculated: 829.29 for $[M+H]^+$). Elemental analysis calculated (%) for $C_{42}H_{48}N_4O_{10}SSi$ (828.29): C 60.85, H 5.84, N 6.76, S 3.87, Si 3.39; found: C 59.59, H 5.99, N 6.57, S 3.75, Si 3.49.

General procedures for solid-phase peptide synthesis towards precursors 18a and 18b

The below described general procedures were applied in the standard solid-phase peptide synthesis used to construct the click-precursors.

- *Fmoc-removal*: 20% piperidine in NMP (2 × 8 min × 6 mL/g_{resin}).
- *N-terminal acetylation*: 0.5 M acetic anhydride, 0.125 M D*i*PEA and 0.015 M HOBt in NMP (2 × 30 min × 6 mL/g_{resin}).
- *Washing of resin*: washing subsequently with NMP (3 × 2 min × 6 mL/g_{resin}) and DCM (3 × 2 min × 6 mL/g_{resin}).
- *Amine functionality tests*: primary amine groups were detected using a Kaiser-test, secondary amine functionalities were detected using a chloranil or bromophenol blue test.

After each coupling or deprotection step, the resin was washed according to the washing procedure.

Solid-phase synthesis of precursor 18

For this, 1 g of PS AM RAM (loading: 0.73 mmol/g) and 3 g of TG S RAM (loading: 0.24 mmol/g) were used separately. Since 1g of PS- and 3 g of TG-resin had roughly the same total loading, *i.e.* 0.73 *vs*. 0.72 mmol/g, the procedure for the synthesis of the precursor is applicable for each of the batches, and the used quantities of reagents are similar.

First, the Fmoc-groups of the resin were removed. After this, the resin was loaded with the orthogonally protected TAC-scaffold **13** (1.5 equiv, 907 mg) using HATU (1.5 equiv, 416 mg), HOAt (1.5 equiv, 149 mg) and D*i*PEA (4 equiv, 509 μL) in NMP (overnight). After coupling, remaining amine functionalities were capped using the capping solution. The loading, corrected for the added mass, of the resin was determined to be 0.49 mmol/g for the PS-batch and 0.18 mmol/g for the TG-batch. The Fmoc-group of the scaffold was removed after which Fmoc-Ser(*t*Bu)-OH (4 equiv, PS: 752 mg and TG: 828 mg) was coupled using BOP (4 equiv, PS: 866 mg and TG: 955 mg) and D*i*PEA (8 equiv, PS: 683 μL and TG: 753

μL) in NMP (1 time overnight). To ensure complete coupling, this coupling of the amino acid building block to the scaffold was repeated once for (2 h). After removal of the Fmoc-group, 4-pentynoic acid (4 equiv, PS: 192 mg and TG: 212 mg) was coupled to the terminal amine functionality using BOP (4 equiv, PS: 866 mg and TG: 955 mg) and D*i*PEA (8 equiv, PS: 683 μL and TG: 753 μL) in NMP (overnight).

After washing with DMF deprotection of the *o*-NBS protected amine functionality of the scaffold was achieved by treatment with a mixture of 2-mercaptoethanol (6 equiv, 6 mL of 0.5 M in DMF) and DBU (3 equiv, 224 μL) (2 × 30 min). To the unprotected secondary amine, Fmoc-Asp(O*t*Bu)-OH (4 equiv, PS: 806 mg and TG: 889 mg) was coupled using BOP (4 equiv, PS: 866 mg and TG: 955 mg) and D*i*PEA (8 equiv, PS: 683 μL and TG: 753 μL) in NMP (1 time overnight). Again, this coupling of the amino acid to the scaffold was repeated once for (2 h). After removal of the Fmoc-group, 4-pentynoic acid (4 equiv, PS: 192 mg and TG: 212 mg) was coupled to the terminal amine functionality using BOP (4 equiv, PS: 866 mg and TG: 955 mg) and D*i*PEA (8 equiv, PS: 683 μL and TG: 753 μL) in NMP (overnight).

Before removal of the Teoc-group, a ^{1}H NMR spectrum was measured and a bromophenol blue test was performed. From both the ^{1}H NMR spectrum, which showed a broad peak around 0 ppm, and the bromophenol blue test, which remained yellow, it was clear that the Teoc-group was still in place. Treatment of the resin with TBAF (10 equiv, 1.58 g) in DMF for 30 minutes affected complete removal of the Teoc-groups, as was inferred from ^{1}H NMR spectroscopy. After this, Fmoc-His(Trt)-OH (4 equiv, PS: 1.21 g and TG: 1.34 g) was coupled using BOP (4 equiv, PS: 866 mg and TG: 955 mg) and D*i*PEA (8 equiv, PS: 683 μL and TG: 753 μL) in NMP (overnight). Also this coupling was repeated twice: one time overnight and one additional time for 2 h. After coupling of the Fmoc-His(Trt)-OH building block, a small fraction of each of the two batches of resin-bound product was cleaved for MS-analysis. The presence of any remaining Teoc-group during coupling of the Fmoc-His(Trt)-OH building block would result in two peaks in the MS-spectrum: one corresponding to the presence of Fmoc-His-residue (with a FW 998.44) and one without this residue (with a FW 639.31). Fortunately, only the mass of the Fmoc-His-adduct was found (with an *m*/*z*-value of 998.15). This Fmoc-group was removed and Fmoc-Gly-OH (4 equiv, PS: 582 mg and TG: 642 mg) was coupled using BOP (4 equiv, PS: 866 mg and TG: 955 mg) and D*i*PEA (8 equiv, PS: 683 μL and TG: 753 μL) in NMP (overnight). Removal of the *N*-terminal Fmoc-group was followed by coupling of 3,5-bis(azidomethyl)benzoic acid **3** (4 equiv, PS: 455 mg and TG: 502 mg) using BOP (4 equiv, PS: 866 mg and TG: 955 mg) and D*i*PEA (8 equiv, PS: 683 μL and TG: 753 μL) in NMP (overnight).

A small portion of the products of each of the two batches was cleaved and analyzed. TLC: R_f = 0.52 (eluent: $CHCl_3$/MeOH/25% NH_4OH (aq) – 8/3/2 (v/v/)). ESI-MS: *m*/*z* 1047.17 (calculated: 1047.45 for $[M+H]^+$). HPLC: t_R = 19.58 min (C_{18}, MeOH containing eluents).

Copper catalyzed click reaction: see **table 2** for conditions.

Typical procedure: a microwave reaction vessel was charged with PS- or TG-bound precursor 18 and add the appropriate amount of CuI was added. After this, 1 mL of 20% piperidine in NMP was added, the vessel was sealed with and microwave heating was applied. After completion of the reaction, the resin was transferred into a solid-phase reaction syringe that was equipped with a filtering frit. The reagents, which were used in the reaction, were filtered and the resin was washed, alternatively with a 20 mM solution of sodium *N*,*N*-diethyldithiocarbamate (DEDTC) in NMP and NMP until the color of the added solution did not change. Occasionally, precipitates of salts that obstructed the filter had to be removed by a quick rinse with water. After completion of the above-mentioned washings, the resin was washed with NMP (3 × 2 min × 1 mL) and DCM (3 × 2 min × 1 mL) and quickly rinsed with Et_2O. After this, nitrogen gas was blown through the syringe in order to dry the resin, and the products were cleaved from the resin using a cleavage cocktail containing TFA/TIS/water – 92.5/2.5/5 (%, v/v). The cleaved products were precipitated in an Eppendorf vial using cold Et_2O/*n*-hexanes (1 mL), the precipitate was collected as a pellet after filtration and used directly in the analysis of the products.

For large-scale CuAAC using **18a** and **18b** a similar procedure was used with the exception of the cleavage cocktail (TFA/PhSMe/TIS/H_2O – 87.5/5/2.5/5 (%, v/v)). Some dimeric product was observed in MALDI-TOF analysis of the cleaved products obtained from **18a**: *m*/*z* 2093.58 (calculated: 2093.90 for $[M+H]^+$).

6. References and Notes

1 C.W. Tornøe, C. Christensen, M. Meldal, *J. Org. Chem.* **2002**, *67*, 3057; V.V. Rostovtsev, L.G. Green, V.V. Fokin, B.K. Sharpless, *Angew. Chem. Int. Ed.* **2002**, *41*, 2596; M. Meldal, C.W. Tornøe, *Chem. Rev.* **2008**, *108*, 2952.

2 V.D. Bock, D. Speijer, H. Hiemstra, J.H. van Maarseveen, *Org. Biomol. Chem.* **2007**, *5*, 971; Y.L. Angell, K. Burgess, *Chem. Soc. Rev.* **2007,** *36*, 1674.

3 A. Isidro-Llobet, M. Alvarez, F. Albericio, *Chem. Rev.* **2009**, *109*, 2455.

4 V.D. Bock, R. Perciaccante, T.P. Jansen, H. Hiemstra, J.H. van Maarseveen, *Org. Lett.* **2006**, 8, 919.

5 V.D. Bock, H. Hiemstra, J.H. van Maarseveen, *Eur. J. Org. Chem.* **2006**, 51; A. Tam, U. Arnold, M.B. Soellner, R.T. Raines, *J. Am. Chem. Soc.* **2007**, *129*, 12670; see also: G. Appendino, S. Bacchiega, A. Minassi, M.G. Cascio, L. De Petrocellis, V. Di Marzo, *Angew. Chem. Int. Ed.* **2007**, *119*, 9472.

6 C.W. Tornøe, C. Christensen, M. Meldal, *J. Org. Chem.* **2002**, *67*, 3057; C.W. Tornøe, S.J. Sanderson, J.C. Mottram, G.H. Coombs, M. Meldal, *J. Comb. Chem.* **2004**, *6*, 312; Z. Zhang, E. Fan, *Tetrahedron Lett.* **2006**, *47*, 665; N.G. Angelo, P.S. Arora, *J. Org. Chem.* **2007**, *72*, 7963; N.G. Angelo, P.S. Arora, *J. Am. Chem. Soc.* **2005**, *72*, 17134; W.M. Xu, X. Huang, E. Tang, *J. Comb. Chem.* **2005**, *7*, 726; A.K. Oyelere, P.C. Chen, L.P. Yao, N. Boguslavsky, *J. Org. Chem.* **2006**, *71*, 3227; S. Löber, P. Gmeiner, *Tetrahedron* **2004**, *60*, 8699; S. Su, J.R. Giguere, S.E. Schaus, J. Porco, *Tetrahedron* **2004**, *60*, 8645; S. Löber, P. Rodriguez-Loaiza, P. Gmeiner, *Org. Lett.* **2003**, *5*, 1735; P.R. Loaiza, S. Löber, H. Hübner, P. Gmeiner, *J. Comb. Chem.* **2006**, *8*, 252; C.D. Smith, I.R. Baxendale, S. Lanners, J.J. Hayward, S.C. Smith, S.V. Ley, *Org. Biomol. Chem.* **2007**, *5*, 1559; M. Kümin, L.S. Sonntag, H. Wennemers, *J. Am. Chem. Soc.* **2007**, *129*,

466; .M. Holub, H. Jung, K. Kirschenbaum, *Org. Biomol. Chem.* **2006**, *4*, 1497.
7 B.C. Boren, S. Narayan, L.K. Rasmussen, L. Zhang, H. Zhao, Z. Lin, G. Jia, V.V. Fokin, *J. Am. Chem. Soc.* **2008**, *130*, 8923.
8 Z. Zhang, E. Fan, *Tetrahedron Lett.* **2006**, *47*, 665.
9 C.W. Tornøe, C. Christensen, M. Meldal, *J. Org. Chem.* **2002**, *67*, 3057.
10 S. Punna, J. Kuzelka, Q. Wang, M.G. Finn, *Angew. Chem. Int. Ed.* **2005**, *44*, 2215.
11 I.J.S. Fairlamb, P.S. Bäuerlein, L.R. Marrison, J.M. Dickinson, *Chem. Commun.* **2003**, 632.
12 Obviously, dimeric species would have *m*/*z*-values that would be twice as high as that of monomeric species. However, the detection-limit of the ESI-MS machine was an *m*/*z*-value <2000, which means that only doubly charged dimeric species can be observed resulting in the same *m*/*z*-value of a monomeric species, albeit with a different isotope pattern.
13 See *Practical Microwave Synthesis for Organic Chemists: Strategies, Instruments, Strategies and Protocols*, C.O. Kappe, D. Dallinger, S.S. Murphee, 1st edn., **2009**, Wiley-VCH Verlag, Weinheim, Germany, p. 112.
14 The sample that was obtained from the TG-resin was not suitable for MALDI-TOF analysis.
15 M. Meldal, C.W. Tornøe, *Chem. Rev.* **2008**, *108*, 2952 (see p 2958).
16 R.M. Silverstein and F.X. Webster, *Spectrometric Identification of Organic Compounds*, 6th edition, **1998**, Wiley, USA, chapter 1.
17 S. Hsieh, J.H.D. Eland, *J. Mass Spectrom.* **1996**, *31*, 1054. See also: *Heteroaromatic nitrogen componist: the azoles*, by K. Schofield, M.R. Grimmett, B.R.T. Keene, Cambridge University Press, **1976**, p. 173.
18 R.M. Silverstein and F.X. Webster, *Spectrometric Identification of Organic Compounds*, 6th edition, **1998**, Wiley, USA, chapter 1.
19 R. Tayler, In *The Chemistry of Functional Groups: Supplement B.*, Wiley, New York, **1979**, ch. 15.
20 B.G. de la Torre, D. Andreu, *J. Pept. Sci.* **2007**, *14*, 360.
21 See for example: W.C. Chan, P.D. White, *Fmoc Solid Phase Peptide Synthesis: A Practical Approach*; Oxford University Press: New York, **2000**.
22 B.H. Lipshutz, B.R. Taft, *Angew. Chem. Int. Ed.* **2006**, *45*, 8235.
23 C.D. Smith, I.R. Baxendale, S. Lanners, J.J. Hayward, S.C. Smith, S.V. Ley, *Org. Biomol. Chem.* **2007**, *5*, 1559.
24 A. Deiters, P.G. Schultz, *Bioorg. Med. Chem. Lett.* **2005**, *15*, 1521.
25 C. Chamorro, J.A.W. Kruijtzer, M. Farsaraki, J. Balzarini, R.M.J. Liskamp, *Chem. Commun.* **2009**, 821.
26 M.C.F. Monnee, A.J. Brouwer, R.M.J. Liskamp, *QSAR & Combinatorial Science* **2004**, *23*, 546; A.J. Brouwer, H.J. van der Linden, R.M.J. Liskamp, *Eur. J. Org. Chem.* **2000**, *65*, 1750.
27 T. Kehat, M. Portnoy, *Chem. Commun.* **2007**, 2823.
28 T. Opatz, R.M.J. Liskamp, *Org. Lett.* **2001**, *3*, 3499.

Chapter 6

Metalloenzyme Active Site Mimics Based on Aspartate and Histidine Residues Containing TAC-Scaffolds

Abstract

A triazacyclophane (TAC) scaffold was decorated with *N*-terminally acetylated histidine and/or aspartate amino acid residues in order to mimic several metal binding triads found in proteins and enzymes. Complexation of the mimics with copper(II) was visualized by UV-vis spectroscopy showing *N* and *O* coordination. ESI-MS spectrometry revealed the presence of 1:1 complexes. Infrared and Raman spectroscopic analysis of the complexes revealed predominantly binding by N^{τ}-nitrogen atoms of the imidazole ring and monodentate binding of the carboxylate residues. These results showed that close structural mimics of metalloenzyme active sites by TAC-based amino acid containing metalloreceptors are possible.

Parts of this chapter have been published: H.B. Albada, F. Soulimani, B.M. Weckhuysen, R.M.J. Liskamp, *Chem. Commun*. **2007**, 4895.

1. Introduction

1.1. From *functional group* enzymes to *metallo*enzymes

In general, enzymatic activity can be the result of either cooperativity of functional groups or to a metal-ion bound to functional groups present in the active site of an enzyme. It has been estimated that approximately 30% of all enzymes have a catalytically crucial transition metal ion bound to their structure.[1] For hydrolytic reactions, functional group enzymes as well as metalloenzymes are used by Nature.[2] In addition to hydrolytic reactions, metalloenzymes also catalyze other reactions including electron transfer, redox catalysis, and group transfer (*e.g.* CH_3, S, O) reactions.[3] Whereas mimics of hydrolytic enzymes can be used to study the hydrolysis of only a few substrates, like amides, esters and phosphate-esters, mimics of metalloenzymes also find applications in other reactions, like electron transfer reactions, small molecule activation and the oxidation of olefins, phenols and catechols.[4]

One of the functions of the protein scaffold surrounding the active site of an enzyme is to pre-position the catalytically crucial functionalities, thereby enabling catalysis (*figure 1*). This pre-positioning leads to activation of an otherwise unreactive functional group, as in functional group enzymes, or results in a simultaneous presentation of metal-chelating functionalities of amino acid residues, as in certain metalloenzymes.[5] Common metal-donor atoms found in proteins are sulfur (Cys and Met), nitrogen (His), and oxygen (Asp, Glu, and Tyr). In addition, some coordination to the metal ion can originate from the peptidic backbone, the oxygen atom in serine and threonine and nitrogen atom in lysine. Also, tetrapyrroles (like heme, chlorophylls and corrins) and iron-sulfur clusters are common non-amino acid based metal-ion chelating functionalities.[6]

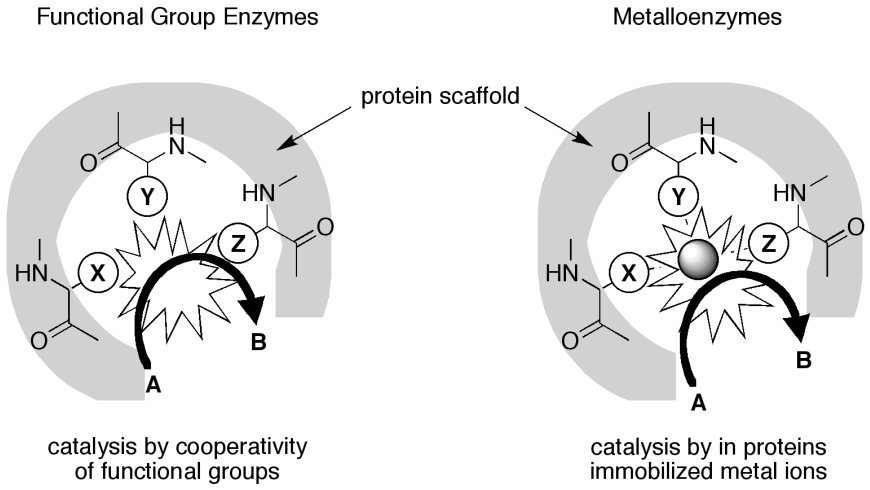

Figure 1. Schematic representation of the active sites of functional group enzymes (*left*) and metalloenzymes (*right*). **X**, **Y**, and **Z** represent amino acid side-chain functionalities, **A** and **B** are substrate and product, respectively. Gray sphere in the metalloenzyme represents the metal-ion.

1.2. Metalloenzyme active sites based on imidazole and carboxylate ligands

Many metalloenzymes use histidine and aspartate or glutamate amino acid residues for the construction of their active site. Active sites based on these residues are found in numerous metallohydrolases based on Zn^{2+} (in Carboxypeptidase A), Mn^{2+} (in Arginase) Ni^{2+} (in Urease),[7] in carbonic anhydrase, in non-heme iron enzymes and in copper enzymes like tyrosinase and catechol oxidase,[8] in the oxygen transporting enzymes hemocyanin and hemerythrin,[9] and in superoxide dismutase and reductase (see *figure 2*).[10] Interestingly, the histidinyl imidazole ring can coordinate by one of the two slightly different nitrogen atoms and, as can be seen in the active site of Arginase, the carboxylate moiety can display even more modes of coordination.

In view of the many types of reactions catalyzed by metalloenzymes and the apparently high similarity between the ligands used to construct their active sites, it is not surprising that many attempts have been undertaken to mimic their structure and function.

1.3. Mimics of metalloenzyme active sites

Although the large number of factors that determine the activity of the enzyme might prevent mimicry of all crucial components of enzyme active sites by synthetic constructs,[11] mimics can lead to novel catalytic systems[12] and may even find applications in industry.[13] In addition, studying these mimics can help to elucidate crucial reaction

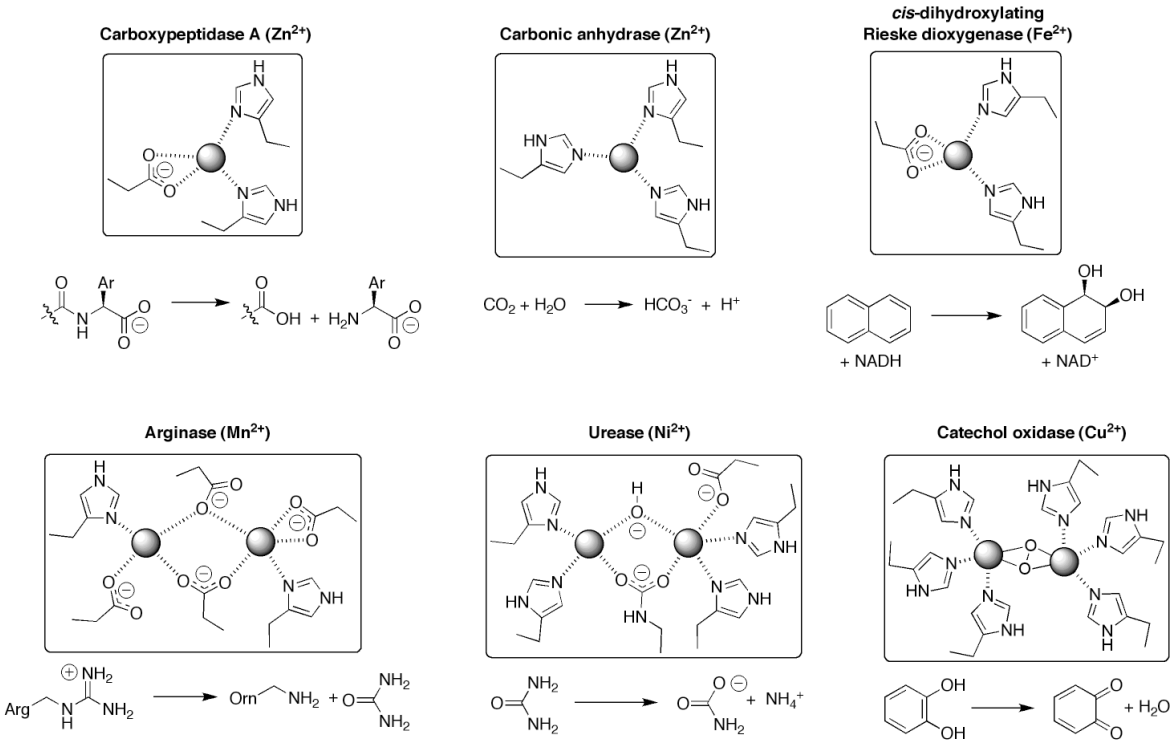

Figure 2. Overview of some metalloenzyme active sites based on histidine and carboxylate amino acid residues. The gray spheres represent metal-ions, which are identified after the name of the enzyme given above the active site. The catalyzed reaction is shown below the active site.

intermediates.[14] Especially mimics of metalloenzymes containing manganese, iron, copper and zinc have been successful in yielding active catalytic species and elucidating crucial steps in the enzymatic reaction.[15] Apart from the mimics based on tetrapyrrole ligands, functional groups like a pyridine moiety,[16] an aliphatic amine,[17] an azole moiety,[18] or combinations thereof have been particularly useful as nitrogen donor atoms for metal ions.[19] In addition, mimics based on biologically relevant molecules like amino acids,[20] (pseudo)peptides,[21] (synthetic) proteins[22] and even peptide bond mimetics[23] have emerged. However, involvement of carboxylate and amine functionalities at the *C*- and *N*-termini as well as the nitrogen and oxygen atoms of the peptide bond can lead to poorly defined coordination complexes. This has prevented these mimics based on amino acid residues from becoming as successful as their small organic counterparts. Therefore, the application of natural ligand systems in the construction of metalloenzyme active sites has been lagging behind. Therefore, in this chapter a new class of small mimics containing biologically inspired relevant ligands is presented.

1.4. Outline

In addition to the synthesis of serine hydrolase active sites, successful mimicry of a metalloenzyme active site would illustrate and lead to a more general applicability of the TAC-scaffold as a platform for the construction of enzyme active site mimics. In the past, we have already shown that TAC-based receptors containing 2-Asp/Glu-1-His triads were able to bind Fe(III).[24] As an extension of this research, we whished to gain detailed insight in the interaction between the mimic and the metal ions and determine their metalloenzyme active site mimicking capability. Therefore, we have prepared and studied three mimics, which together cover a significant spectrum of metalloenzyme active sites found in nature. These active sites were based on the tris-histidine triad, which are for example found in carbonic anhydrase, tyrosinase, catechol oxidase and hemocyanine, for instance. In addition, they were based on the 2-His-1-Asp triad, which is for example found in carboxypeptidase A, Rieske dioxygenases and urease, as well as the triad based on 2-Asp-1-His, which is found in Arginase and methane monooxygenase, among others. Several spectroscopic techniques were used in order to determine the structures of coordination complexes of these mimics with Cu(II).

2. Synthesis of the metalloenzyme active site mimics

For the synthesis of TAC-based mimics of metalloenzyme active sites, we first prepared two suitably protected TAC-scaffolds: HOC(O)-TAC(*o*-NBS)$_3$ **5** and HO-TAC(Fmoc/Alloc/Fmoc) **7**. These could then be used in the syntheses of the mimics.

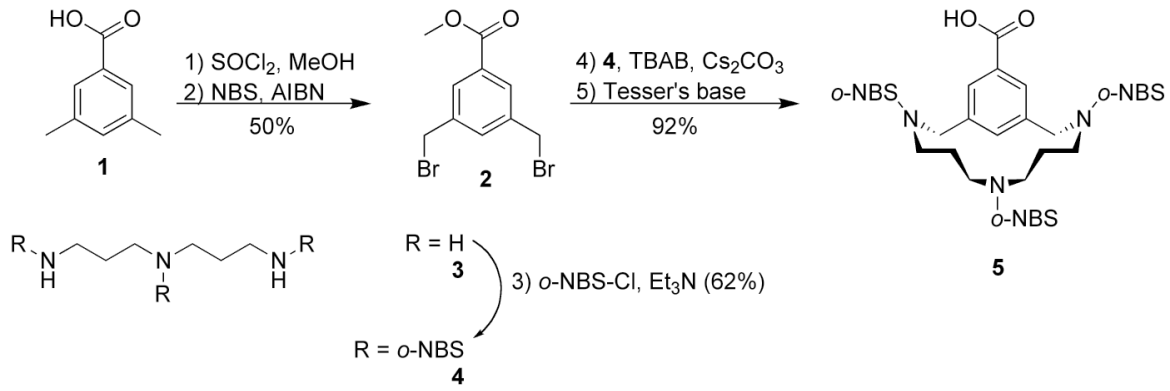

Scheme 1. Synthesis of scaffold **5**.

2.1.1. Synthesis of the HOC(O)-TAC(*o*-NBS)$_3$ scaffold

For the synthesis of HOC(O)-TAC(*o*-NBS)$_3$ **5**, bis-bromide **2** was used together with fully *o*-NBS protected triamine **4** (*scheme 1*). This tri-amine was prepared using *o*-NBS-Cl and bis-(3-aminopropyl)amine **3** in the presence of Et_3N as a base. The acidic sulfonamide functionalities could be deprotonated using Cs_2CO_3, followed by condensation of the amine-fragment to bis-bromide **2** in the presence of TBAB as a phase-transfer catalyst. Column chromatography afforded pure fully protected compound of which the methyl ester was saponified using Tesser's base.[25] Pure scaffold **5** was obtained by crystallization from DMF in which water was allowed to diffuse.[26]

2.1.2. Synthesis of the HOC(O)-TAC(Fmoc/Alloc/Fmoc) scaffold

For the synthesis of HOC(O)-TAC(Fmoc/Alloc/Fmoc) **7** scaffold, the two primary amine functionalities of **3** were selectively protected with trifluoroacetyl-groups using ethyl trifluoroacetate in refluxing acetonitril. Introduction of the Alloc-group on the secondary amine afforded protected triamine **6** (*scheme 2*). This protected triamine was cyclized with bis-bromide **2** in the presence of Cs_2CO_3 and TBAB. After cyclization, the methyl ester and TFAc-amides of the product were hydrolyzed using Tesser's base.[25] The resulting two benzylic amine-groups were protected with a Fmoc-groups and scaffold **7** was obtained in an overall yield of 10%.

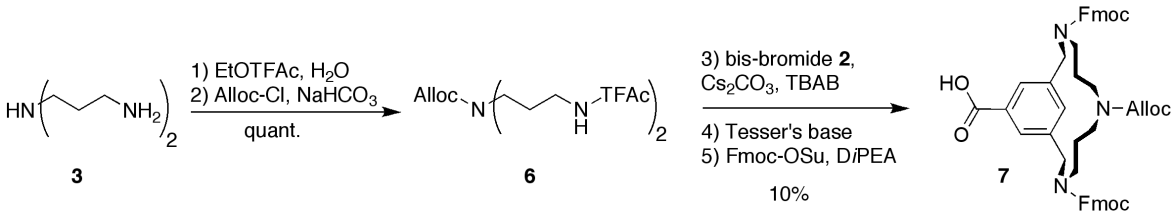

Scheme 2. Synthesis of scaffold **7**.

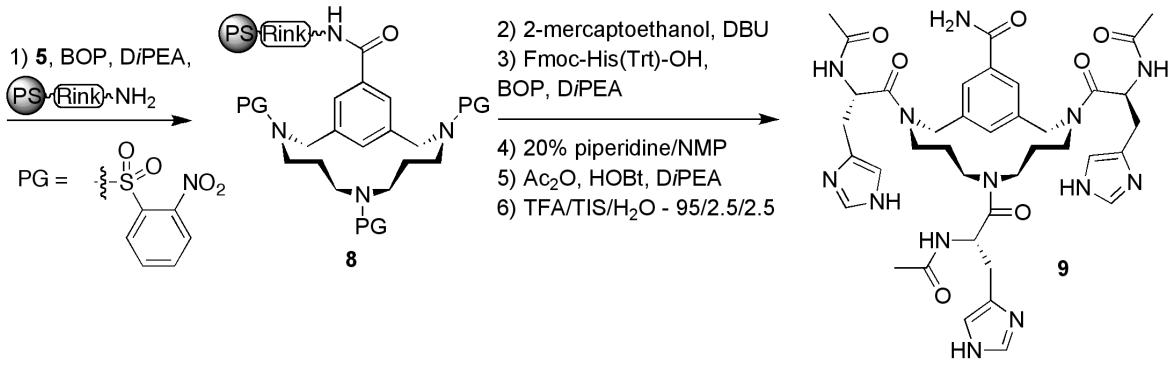

Scheme 3. Synthesis of TAC-based 3-His triad mimic **9**.

2.2.1. Synthesis of the 3-His triad mimic

For the synthesis of the tris-histidine triad mimic, HOC(O)-TAC(*o*-NBS)$_3$ **5** was used as a scaffold for three acetylated histidine residues (*scheme 3*). To this end, scaffold **5** was coupled to a polystyrene resin containing the Rink amide linker using BOP and D*i*PEA as coupling reagents. Any remaining amine functional groups were capped with acetyl-groups. The *o*-NBS protecting groups were removed from **8** using a thiolate nucleophile generated *in situ* from a mixture of 2-mercaptoethanol and DBU. Fmoc-His(Trt)-OH was attached to the liberated amines using BOP and D*i*PEA as coupling reagents. From this fully protected resin bound mimic, *N*-terminal amine Fmoc-protecting groups were removed and replaced with the acetyl group using a capping solution. Target compound **9** was obtained after cleavage from the resin by

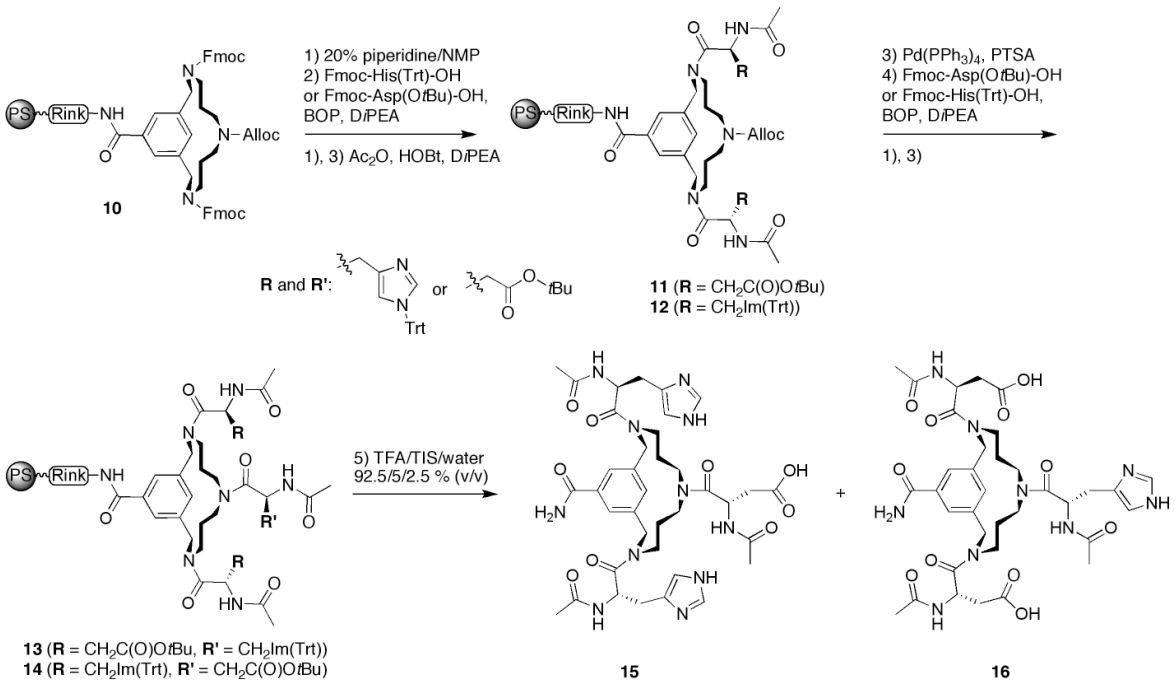

Scheme 4. Synthesis of the TAC-based 2-His-1-Asp (**15**) and 2-Asp-1-His triads (**16**).

acidic treatment. The cleaved product was precipitated in a mixture of MTBE and hexane, and purified by column chromatography. This mimic was suitable to be used in the spectroscopic analysis of the copper complex.

2.2.2. Synthesis of the 2-His-1-Asp and 2-Asp-1-His triad mimics

For the synthesis of the mimics based on both histidine and aspartate, a slightly different procedure was followed based on scaffold **7** (*scheme 4*). This scaffold was attached to PS-Rink amide resin using BOP and D*i*PEA. After piperidine affected Fmoc-removal, Fmoc-His(Trt)-OH or Fmoc-Asp(O*t*Bu)-OH were introduced using BOP and D*i*PEA. The protecting group of the *N*-terminal amine groups was then changed from Fmoc into the acetyl-group affording **11** and **12**. Subsequently, the position was functionalized. For this, the Alloc-group was removed using Pd^0 and to the liberated secondary amine, Fmoc-Asp(O*t*Bu)-OH or Fmoc-His(Trt)-OH were coupled, respectively. Again, the Fmoc-group was replaced by the acetyl-group, thereby mimicking the peptide-backbone and preventing the *N*-terminal amine to interfere with coordination of metal-ions. Lastly, the two resin-bound mimics **13** and **14** were simultaneously deprotected and cleaved from the resin by acidic treatment with TFA. After precipitation of the cleaved product in MTBE-hexane, mimics **15** and **16** were purified by column chromatography.

3. Analysis of the complexation properties of the mimics with Cu(II)

To analyze the feasibility of these mimics to function as structural metalloenzyme active site mimics, we studied the coordination complexes of these mimics with Cu(II).[27] Detailed assessment of the complexes was needed since each of these three mimics has several potential coordinating atoms: seven carbonyl oxygen atoms, two

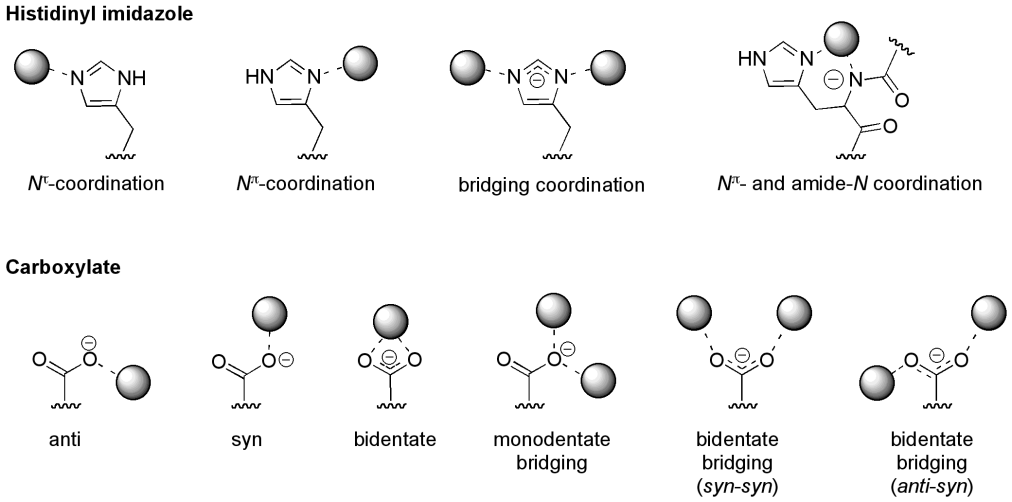

Figure 3. Overview of the main coordination modes of the amino acid side chains present in the mimics.

distinct imidazole ring nitrogen atoms, two carboxylate oxygen atoms and four primary or secondary amide-bond nitrogen atoms.[28] Concerning the imidazole ring, this can coordinate via its N^{π}- or N^{τ}-nitrogen atom, or by both resulting in an imidazole ring that bridges two metal ions (*figure 3*). Similarly, the carboxylate group can coordinate by one oxygen atom to one or two metal ions, or by two oxygen atoms to one or two metal ions.

To gain insight in the interaction between the mimics and Cu(II), several spectroscopic techniques were used.[29] UV-vis spectroscopy is used to determine the coordinating atoms and the geometry of the complexes.[30a,31] ESI-MS spectroscopy is used to determine the ratio in which the complexes were present in solution. Infrared and Raman spectroscopy has been applied to determine the changes in the vibrational properties of the functional groups as result of coordination.

3.1. UV-vis analysis: coordinating atoms and geometry[32]

Initially, the coordinating properties of these mimics to copper(II) was studied using UV-vis absorption spectroscopy. From these studies, information on the coordinating atoms and the geometry of the complexes was obtained.

For this, a stoichiometric mixture of both the mimic and $CuSO_4$ was prepared for each of the mimics. Using diluted HCl, the pH of the solution was lowered to approximately 1 and UV-vis spectra were measured at this pH-value. Using $NaHCO_3$ the pH was slowly raised and absorption spectra were measured (*figure 4*). For each of the samples, addition of $NaHCO_3$ resulted in an increase in intensity of the blue color, indicating a hange in coordination around Cu(II).

As the pH of the solution increased, carboxylate and imidazole functionalities

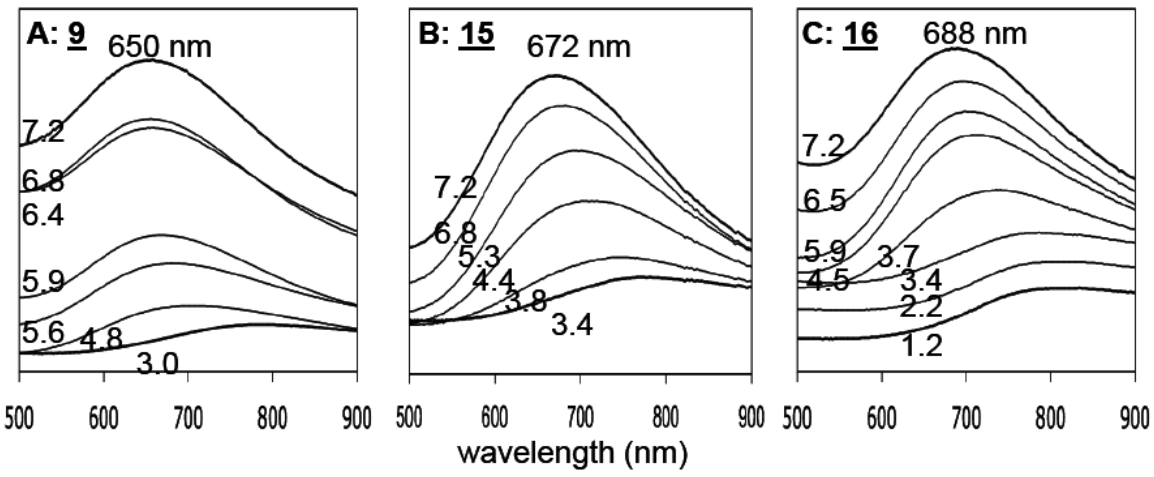

Figure 4. Absorption spectra of the d-d transitions in the three Cu(II)-complex with mimics **9**, **15** and **16** as function of pH (given in the graph). The absorption maximum at pH 7.2 is given at the top of the graphs. **A**: 3-His (mimic **9**); **B**: 2-His-1-Asp (mimic **15**); **C**: 1-His-2-Asp (mimic **16**).

became available for coordination. Since these functionalities have a stronger affinity for Cu(II) than water molecules, they replaced any coordinating water molecules. As a result of the coordination of stronger coordinating atoms like the nitrogen atoms of imidazole or the oxygen atom of the carboxylate, a change in absorption maximum was likely to occur. Also, as a result of that stronger coordination, a change in geometry of the coordination complex is also like to take place. Cu(II)-ions are known for their strong tendency to suffer from Jahn-Teller distortion and prefer square-planar based geometries and derivatives thereof.[33]

From literature it is known that Cu(II)-complexes with three imidazole ring nitrogen atoms and one oxygen atom, originating from water or a carbonyl functionality, coordinating in a square-planar fashion, have an absorption maximum at 634 ± 1.5 nm.[34] For square-planar complexes with two imidazole ring atoms, one carboxylate oxygen atom and one oxygen atom from either water or a carbonyl functionality the absorption maximum is found at 665 ± 2 nm.[34] Concerning the square-planar complex with one imidazole ring nitrogen atom, two carboxylate oxygen atoms and one oxygen atom originating from water or a carbonyl group, the absorption maximum should be found at 700 ± 1.5 nm.[34] Deviations from a square-planar geometry to a more tetrahedral geometry will result shift of the absorption maximum to longer wavelengths.[32,35] In addition, the concomitant decrease in symmetry in the coordination complex should result in an increase in intensity, which is seen in all three complexes. It is therefore likely that the geometry of the coordination complex became distorted as the number stronger coordinating atoms originating from the mimics increased.

Based on these results it can be concluded that at pH ~ 7, all three amino acid side chain functionalities of the three mimics coordinate to the Cu(II)-ion. The maxima correspond nicely with values known for similar complexes. Although a crystal-structure could not be obtained to confirm the geometry of the complex, the positioning and the increase in intensity of the d-d absorption band revealed that the complexes between the mimics and Cu(II) in an aqueous environment at pH 7.2 were most likely distorted square-planar. Lastly, coordination of the imidazole ring nitrogen atoms was clear from an increase in absorption originating from the charge-transfer band of the imidazole ring.[36] As coordination of the imidazole ring to Cu(II) occurred, an absorption found around 285 nm increased significantly.

3.2. ESI-MS spectra of the Cu(II)-complexes with the three mimics to determine the mimic:Cu(II)-ratio[37]

In order to determine the preferred ratio of coordination, we measured ESI-MS spectra of the stoichiometric complexes (*figure 5*). From the isotope pattern of copper, a 1:1 complex can be distinguished from a 2:2 complex (see inserts in *figure 5*).

Dilution of the samples, from 100 mM to 20 mM using both water and methanol did not result in significant changes in the spectra. From these spectra can be concluded

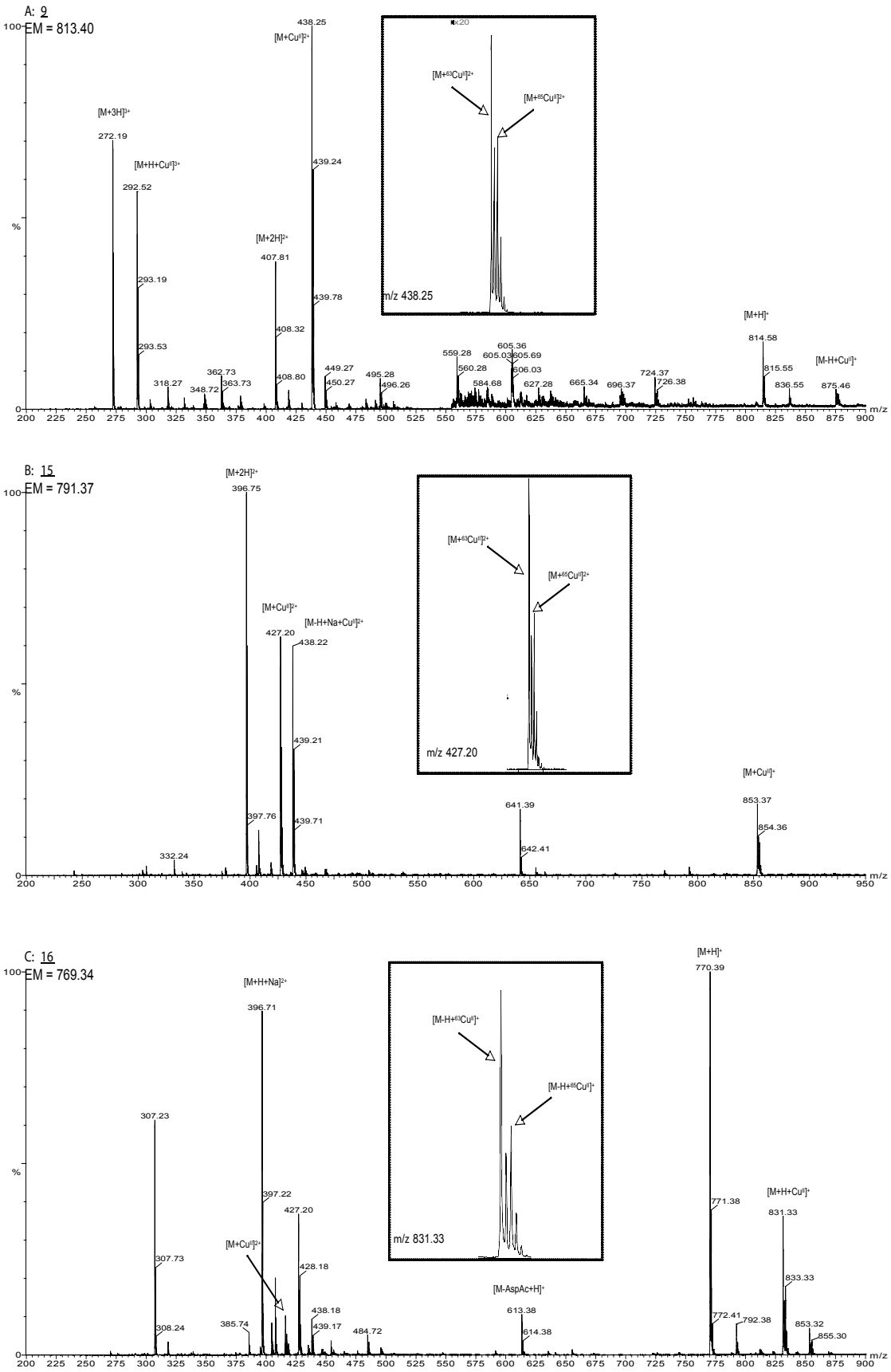

Figure 5. ESI-MS spectra of the Cu(II)-complexes of TAC-based 3-His **9** (**A**, note 20× enlargement at *m/z* > 550), 2-His-1-Asp **15** (**B**), and 2-Asp-1-His **16** (**C**) mimics. *Conditions*: 100 μM solutions of the complexes in water (pH 7.2); ratio mimic:copper(II) – 1:1.

that the complexes formed were 1:1 complexes and not 2:2 complexes. Although the 2:2 complexes would have resulted in similar *m/z* values, the isotope pattern would be different. For a 1:1 complex the intensity of the peaks should be 100% for ^{63}Cu and 45% for ^{65}Cu, for a 2:2 complex this would be 100% for $^{63}Cu^{63}Cu$, 89% $^{63}Cu^{65}Cu$ and 20% $^{65}Cu^{65}Cu$. In addition, whereas the non-coordinated 1-His-2-Asp mimic was still observed as the major species, the 3-His mimic predominantly present as its coordination complex with copper(II). Therefore, it seems that the stability of the coordination complexes decreases in the series 3-His > 2-His-1Asp > 1-His-2-Asp. It should be noted however, that the concentration of the ESI-MS samples was lower than those used in the UV-vis measurements. Nevertheless, at this stage there is no indication that these mimics prefer to form 2:2 complexes instead of 1:1 complexes.

3.3. Infrared and Raman spectroscopic analysis: coordinating functional groups[38]

Infrared spectra were obtained using KBr pellets of lyophilized samples of the three mimics and their Cu(II)-complexs (*figure 6*, see also *table 1* for a complete assignment). In the full width spectra, features corresponding to amide N-H stretching and methylene and methyl C-H stretching vibrations were found displaying only small differences between mimics and their Cu(II)-complexes. For the interpretation of the complexes, the range from 1800-600 cm^{-1} is most useful.

For the assignments of the bands originating from functional groups, each functional group present in the mimics will be treated separately. The traces for which the considerations apply are given between the brackets.

Imidazole rings that were present in all three mimics (**A**, **B** and **C**). Several stretching vibrations of the histidinyl imidazole ring were found between 1205 and 1130 cm^{-1}. In each of the mimics, three distinct bands were observed: a C-H bending vibration just above 1200 cm^{-1}, coupled =C-NH stretching and N-H bending vibrations around 1180 cm^{-1} and =C-N= stretching and N-H bending vibrations around 1135 cm^{-1}. Whereas the C-H bending vibration just above 1200 cm^{-1} did not change upon coordination, the imidazole ring stretching vibrations significantly increased in intensity, especially in trace **A** of the complex of **9**. In addition, in each of the complexes a shoulder became apparent at 1115 cm^{-1}, corresponding to an isolated =C-N= stretching vibration.[39] It became clear that coordination of the imidazole ring to the Cu(II)-ion had significant effect on the properties of the imidazole ring. This might be expected since electron density is donated to the positively charged ion. Just below 1600 cm^{-1}, a C=N stretching vibration was found, but differences between mimic and complex are less clear, especially in trace **B** and **C** of **15** and **16**, respectively (arrow (a)). Lastly, in trace **A**, mimic **9** showed a small broad peak just below 1000 cm^{-1} and a small sharp peak at the same wavenumber (arrow (b)). This is indicative of the N^{π}-tautomeric

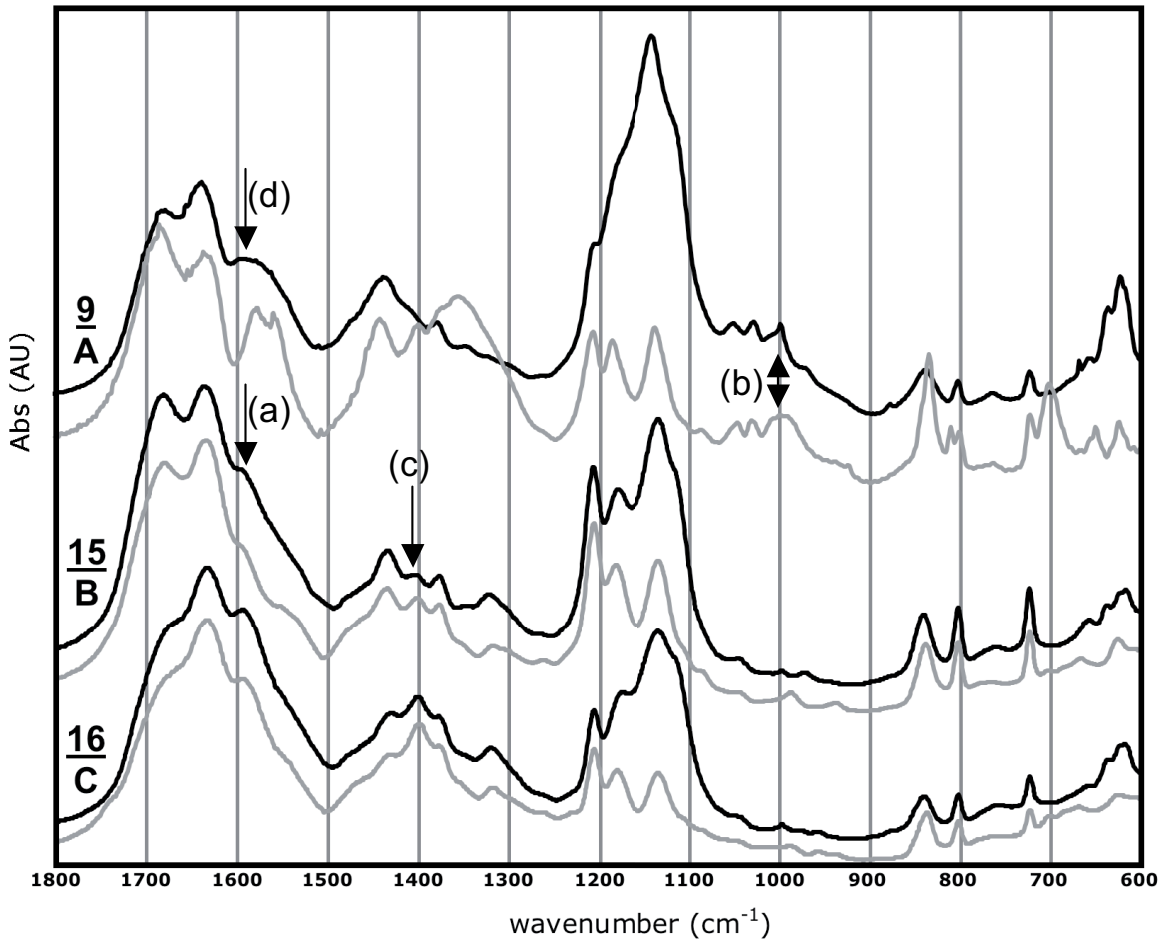

Figure 6. Infrared spectra of the three mimics (gray) and their complexes with Cu(II) (black). **A**: "3-His" **9**; **B**: "2-His-1-Asp" **15**; **C**: "1-His-2-Asp" **16**. Arrows indicate less prominent but important features, the small letters by the arrows refer to peaks mentioned in the text.

form of imidazole where the N^{π}-nitrogen atom is protonated and the N^{τ}-nitrogen atom coordinates to Cu(II). More conclusive information on the tautomeric forms of the histidinyl imidazole ring was obtained from the Raman spectra.

Carboxylate groups that were present in mimic **15** and **16** showed small changes as result of coordination to copper(II) (**B** and **C**). As was shown in *figure 3*, the carboxylate functionality can have several modes of coordination to a metal ion: monodentate (*anti* or *syn*), bidentate chelate and bridging (with one or with both oxygen atoms of which the last can be *syn-syn* or *syn-anti*). Fortunately, most of these modes have a specific vibrational pattern, allowing assessment of the type of carboxylate-ion interaction. A fingerprint for the type of carboxylate coordination is found in the difference between the frequency of symmetric (ν_s) and anti-symmetric (ν_{as}) carboxylate vibrations: $\Delta = \nu_{as} - \nu_s$. It should be noted that the spectra of the mimics are those of the sodium salts. For the sodium-salt of aspartate, the frequencies of the carboxylate functionality are 1597 (ν_{as}) and 1400 cm^{-1} (ν_s).[40] These were also observed in the spectra of the "2-His-1-Asp" **15** and "1-His-2-Asp" **16** containing

mimics (**B** and **C**, gray trace, arrows (a) and (c)) and absent in the spectrum of the 3-His mimic (trace **A**). The Δ-values of these bands are 1592 – 1398 = 194 cm^{-1} (**B**) and 1590 – 1395 = 195 cm^{-1} (**C**). For the Cu(II)-complexes of the mimics, the bands were found at almost identical frequencies: 1593 (ν_{as}) and 1397 (ν_s) for **15** (**B**) and 1594 (ν_{as}) and 1398 (ν_s) for **16** (**C**), resulting in Δ-values of 196 cm^{-1}. These values revealed that coordination of the aspartate carboxylate functionalities in **15** and **16** was via a mono-dentate fashion.[41]

Both primary, secondary and tertiary amide bonds were present in all three mimics (**A**, **B** and **C**). Especially C=O stretching vibrations, seen by two overlapping absorptions in the region 1700-1600 cm^{-1}, are useful. In cases where electron density of the carbonyl oxygen atom is donated to an interacting cation, a significant shift towards lower frequencies should be observed.[42] Such a shift was not apparent from comparison of the spectra of the mimic and complex, indicating that coordination of carbonyl oxygen atoms to the Cu(II)-ion was unlikely.

A coordinating water molecule could be present in all three complexes (**A**, **B** and **C**). Rocking vibrations of coordinating water could be observed as a broad absorption of medium intensity at 1595 cm^{-1} in complex of **9** (**A**) (*figure 6*, black trace **A**, arrow (d)). Such an absorption was less clear from the spectra of the other two mimics since the ν_{as} of carboxylate groups were also found there (traces **B** and **C**).

Since infrared and Raman spectroscopy can yield complementary information, also Raman spectra of these samples were measured (*figure 7*). Analysis of the Raman spectra should provide information on the tautomeric form of the coordinating histidinyl imidazole ring,[43] illustrate the type of interaction between the carboxylate residues and Cu(II) and visualize the Cu-N and/or Cu-O bons.

Again, the assignments of the bands originating from the functional groups will be treated separately. Traces for which the considerations apply are given between the brackets.

Imidazole rings were present in all three mimics and significant differences were observed as result of coordintion to copper(II) (**A**, **B** and **C**). The histidinyl imidazole

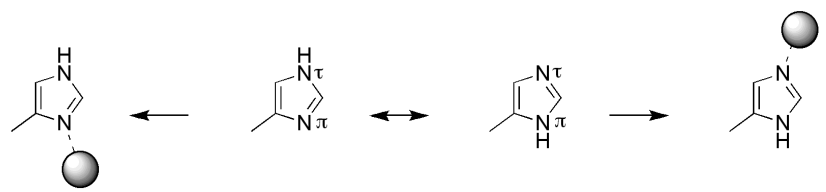

Figure 8. Structures of the two tautomeric forms of the imidazole ring. Typical frequencies correlated to two important vibrations are given below the structures.

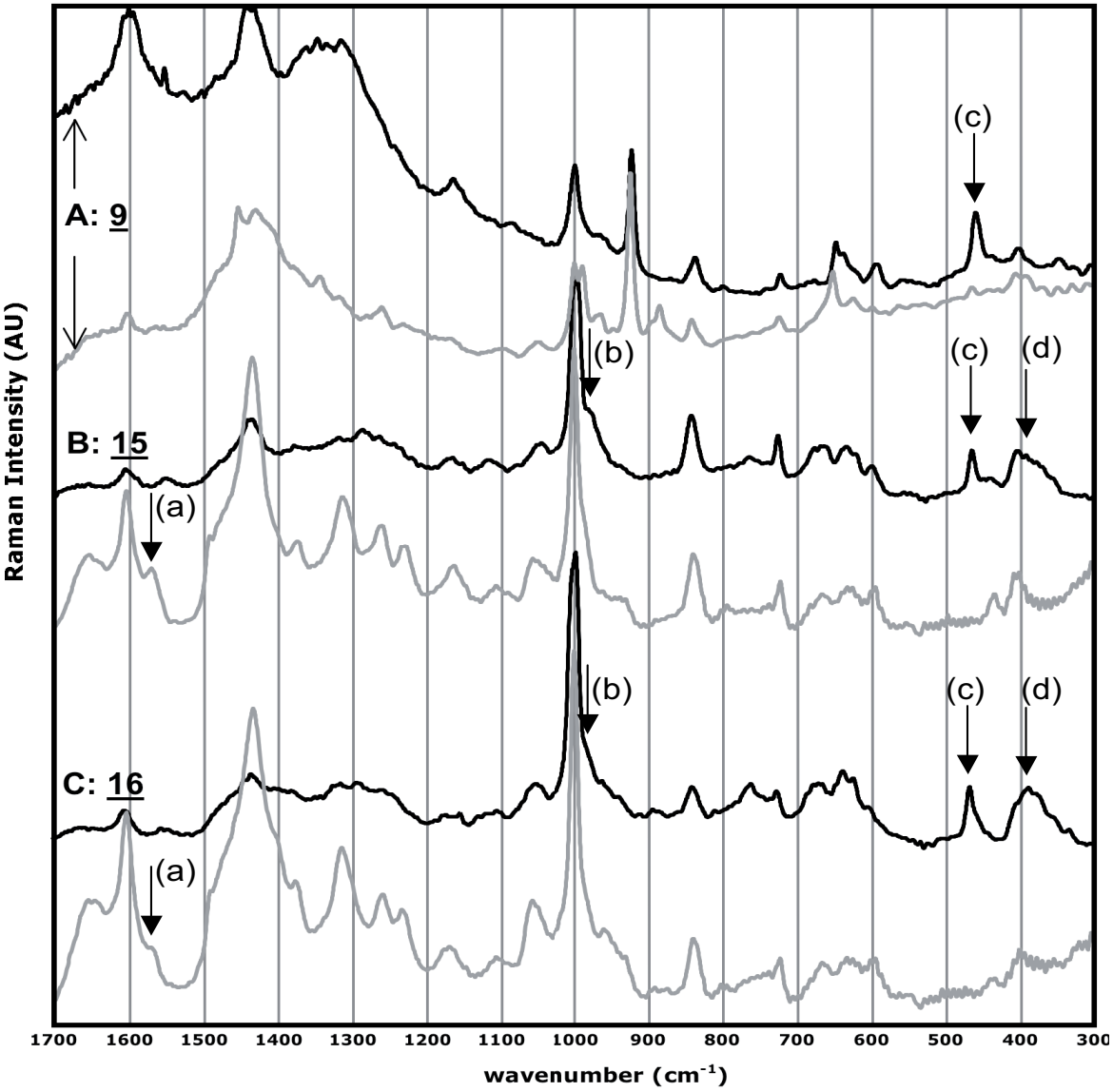

Figure 7. Raman spectra of the three mimics (*gray*) and their stoichiometric complexes with Cu(II) (*black*). **A**: "3-His" **9**; **B**: "2-His-1-Asp" **15**; **C**: "1-His-2-Asp" **16**. The small letters by the arrows refer to peaks mentioned in the text.

ring can be present in two distinct tautomeric forms (*figure 8*). Coordination to a metal-ion by imidazole occurs by the pyridine like nitrogen atom, the other nitrogen atom bears the proton. Which tautomeric form is present can be determined by the frequencies characteristic of these tautomeric forms. From literature it is known that coupled stretching vibrations of the C=C and C=N bond of the N^{π}-tautomer are found at 1580 cm^{-1} and those of the N^{τ}-tautomer at 1565 cm^{-1}.[44] These signals shift to higher wavenumbers upon coordination of the imidazole ring to metal-ions, usually to 1606-1594 cm^{-1} and 1588-1573 cm^{-1}, respectively.[44] In each of the spectra of the mimics a broad intensity around 1645 cm^{-1}, weak in **A** but stronger in **B** and **C**, correspond to not coordinating imidazole rings.[39] In addition, in the spectra of mimics **15** and **16** (*figure 7*, **B** and **C**, gray traces), a peak was observed at 1565 cm^{-1} (arrows (a)) indicating

the presence of the N^{τ}-tautomer; a signal at 1580 cm^{-1} could have been obscured by an intensity at 1600 cm^{-1}. In the complexes of these mimics (**B** and **C**, black traces), however, only a signal at 1606 cm^{-1} was observed, indicating the presence of the N^{π}-tautomer. A small shoulder at 1590 cm^{-1} in **B** of **15** (black trace) indicated that some N^{τ}-tautomer might also have been present. This implies that coordination of the imidazole ring of the 2-His-1-Asp (**15**) and 1-His-2-Asp (**16**) mimics to the Cu(II)-centre was predominantly by its N^{τ}-nitrogen atom. Concerning the 3-His mimic **9**, the spectrum of the mimic was inconclusive concerning these coupled C=C and C=N vibrations although a weak intensity was observed around 1650 cm^{-1} (**A**, gray trace). For the complex, however, the intensity around 1600 cm^{-1} indicates that in the complex the N^{π}-tautomer is abundant (**A**, black trace). The presence of multiple peaks might originate from decoupled C=C and C=N vibrations or different orientations of the histidinyl imidazole rings to the Cu ion.[45] The spike at 1548 cm^{-1} can not be related to imidazole ring vibrations. In addition to the coupled vibrations of the C=C and C=N bonds, a =C–NH stretching vibration can usually be observed in the region just below 1000 cm^{-1}.[44] Depending on the tautomer present a signal can be observed at 997 (N^{π}-tautomer) or 986 cm^{-1} (N^{τ}-tautomer) (*figure 8*). Concerning the 3-His mimic, a doublet in trace **A** – at 997 and 986 cm^{-1} – illustrated the presence of the two tautomeric forms. This confirmed our finding based on the IR-spectra (arrow (c) at trace **A** of **9** in *figure 5*). For the other two mimics, the presence of both tautomeric forms could be inferred from a shoulder around 980 cm^{-1} (*figure 7*, **B** and **C**, black traces), but this was more conclusively shown by the intensities between 1580-1610 cm^{-1}. For the complexes, a shoulder at the same position, clear in trace **B** and less clear in trace **C**, indicated the presence of N^{π}-coordination, next to predominantly N^{τ}-coordination. Although the 3-His mimic **9** seemed to coordinate only by the N^{τ}-nitrogen atoms, the 2-His-1-Asp **15** and 1-His-2-Asp **16** mimics coordinated also by the N^{π}-nitrogen atom, although predominantly by the N^{τ}-nitrogen atom. It should be noted that aromatic ring vibrations of the benzamide core of the TAC-scaffold are located at 1000 cm^{-1} and can obscure this assignment.[46]

Information on carboxylate coordination in the complexes of mimics **15** and **16** was less clear (traces **B** and **C**). Monodentate carboxylate vibrations are usually weak in Raman spectra. However, bidentate chelation and bidentate bridging usually display medium to strong signals between 1610 and 1515 cm^{-1}. These are completely absent, indicating that this type of coordination is not present.

Cu-N and Cu-O bonds were observed in all three complexes (**A**, **B** and **C**, black traces). In the spectra of the complexes, intensities corresponding to the stretching vibrations of a dative Cu-N bond were observed at 458 cm^{-1} (**A**) and 466 cm^{-1} (**B** and **C**). The Cu-O bonds were less clear but intensities just below 400 cm^{-1} (trace **B** and **C**) might indicate the presence of these Cu-O bonds in which the coordinating oxygen atom originated from the carboxylate.[47] For the 3-His complex, an intensity at 588

cm^{-1} could be assigned to a Cu-O bond in the equatorial plane of the coordination complex of which the oxygen atom originated from a coordinating water molecule. Similar bands were also observed in the complexes of the "2-His-1-Asp" and "1-His-2-Asp" mimics **15** and **16**, respectively, suggesting the presence of a coordinating water molecule.

The results obtained from these studies strongly indicate that in each of the mimics, coordination of the histidinyl imidazole ring occurs. Although coordination was mostly by its N^{τ}-nitrogen atom, some N^{π}-coordination was observed for the 2-His-1-Asp (**15**) and 1-His-2-Asp (**16**) mimics. In these last two mimics, coordination of the carboxylate was shown to be monodentate. Coordination of amide-bond carbonyl oxygen atoms was not confirmed by these studies whereas the presence of a coordinating water molecule was suggested by Raman.

4. Discussion and Conclusions

In this chapter we have described the synthesis and spectroscopic evaluation of three TAC-based mimics of the three most prominent non-heme metalloenzyme active sites.

Synthesis of the mimics was straightforward using two TAC scaffolds of which the amine functionalities were protected with three *o*-NBS-groups or with two Fmoc- and one Alloc-group. These scaffolds were used in the solid-phase synthesis of the mimics, resulting in mimics of high quality.

For the coordination properties of the mimics to divalent metal ions, we studied the mixtures of the mimics with $CuSO_4$. UV-vis spectroscopy of a copper(II)-complex of the mimics at increasing pH-values showed coordination by amino acid residues originating from the mimics. Analysis of the spectra at pH 7.2 showed the presence of distorted square-planar complexes. ESI-MS analysis revealed that the complexes were present in 1:1 ratio of mimic to Cu(II). It was also concluded that the stability of the complex decreased as the number of histidine residues present in the mimics also decreased. Infrared and Raman spectroscopy showed that coordination of the histidinyl imidazole rings occurred predominantly via the N^{τ}-nitrogen. Coordination of the carboxylate functionalities present in the 2-His-1-Asp and 1-His-2-Asp mimics occurred mostly in a monodentate fashion.

The results presented in this chapter showed that close structural mimics of three different non-heme metalloenzyme active sites can be obtained using a TAC-scaffold. Analysis of some catalytic properties of these mimics will be presented in the next chapter.

5. Experimental Section

General Information

Chemicals were obtained from commercial sources and used without further purification. Reactions were performed at room temperature. Solution phase reactions were monitored by TLC analysis and R_f-values were determined on Merck pre-coated silica gel 60 F-254 (0.25 mm) plates. Spots were visualized with UV-light. Solid-phase synthesis was carried out in plastic syringes with PE frit (20 μm), Applied Separations Inc., distributed by Alltech Applied Science Group (Hoogeveen, The Netherlands). Column chromatography was carried out using Silica-P Flash silica gel (60 Å; particle size 40-63 μm; Silicycle). Electrospray Ionisation mass spectrometry (ESI–MS) was performed on a Finnigan LCQ Deca XP MAX LC/MS system. HPLC was performed on a Shimadzu Class-VP automated high performance liquid system, using an analytical reverse-phase column (Alltima, C8, 300 Å, 5 μm, 250 × 4.6 mm) and a UV-detector (operating at 220 and 254 nm) and an ELSD-detector. Elution was realized using a gradient from water/MeCN/TFA – 95/5/0.1 % (v/v) to MeCN/water/TFA – 95/5/0.1 % (v/v) in 20 min and at a flow rate of 1 mL/min.

A PHM120 standard pH-meter from Meterlab was used in the titration experiment. Microtiterplate reader was from BioTek mQuant (Beun De Ronde, Abcoude, The Netherlands). The UV-vis microtiterplate was from Greiner bio-one (Alphen aan de Rijn, The Netherlands). Software used for data analysis was the Full Mode-KC4 (Version 3.4 (Rev 21)) software (BioTek instruments) and data point resolution was set at 2 nm. ESI-MS spectra were recorded on a Micromass LCT mass spectrometer calibrated with CsI using nano-ESI at 1200V capillairy voltage and 50V at the sample cone. IR spectra were recorded on a Bruker Tensor 37 FT-IR spectrometer with a DTGS detector using KBr pellets, at a point resolution of 4 cm^{-1}. Raman spectra of the complexes were recorded on a Kaiser RXN spectrometer equipped with a 785 nm diode laser was used in combination with a Hololab 5000 Raman microscope. A 10× objective was used for beam focusing and collection of scattered radiation. The laser output power was 70 mW for **9** and 18 mW for **15** and **16**. Mimics **15** and **16** were measured on a spectrometer equipped with a 1064 nm diode laser using 30 mW laser output. The data point resolution was about 2 cm^{-1} and 10 scans were accumulated with an exposure time of 30 s for each spectrum. The setup for diffuse reflection measurements is based on an Olympus BX41 upright research microscope with a 50× 0.5 NA high working distance microscope objective. A 75 W Xenon lamp is used for illumination. The microscope was equipped with a 50/50 double viewport tube, which accommodates a CCD video camera (ColorViewIIIu, Soft Imaging System GmbH) and an optical fiber mount. A 200 micrometer-core fiber connects the microscope to a CCD UV/vis spectrometer (AvaSpec-2048TEC, Avantes BV). 10 scans were collected with an integration time of 50 ms per scan.

Table 1. Proposed assignment for both Infrared and Raman spectra of the mimics and their Cu(II)-complexes.

3-His (**A** traces)				**2-His-1-Asp** (**B** traces)				**1-His-2-Asp** (**C** traces)				
Infrared		Raman		Infrared		Raman		Infrared		Raman		
Mimic	Complex	Mimic	Complex	Mimic	Complex	Mimic	Complex	Mimic	Complex	Mimic	Complex	
3400 (m br)				3400 (m br)				3400 (m br)				ν N-H (1º and 2º) [a]
3280 (m br)				3280 (m br)				3280 (m br)				ν N-H (1º and 2º) [a]
3070 (w br)				3070 (w br)		3110 (w)		3070 (w br)		3110 (w)		ν N-H (2º) [a]
2983 (w)				2983 (w)				2979 (w)				ν_a CH_3 [a]
2931 (w)		2925 (vs)		2928 (w)		2932 (vs)	2945 (vs)	2916 (w)		2932 (vs)	2941 (vs)	ν_a CH_2 [a]
2845 (w)				2847 (w)				2847 (w)				ν_s CH_2 + CH_3 [a]
2600 (w br)				2600 (w br)				2600 (w br)				ν Im^+-H [a]
1680 (s)	1674 (s)			1676 (s)	1675 (s)			1670 (s)	1670 (s)			ν C=O (A-I: 1º, 2º and 3º) [a]
1631 (s)	1632 (s)			1630 (s)	1629 (s)			1627 (s)	1627 (s)			δ N-H + ν C-N (A-II: 1º) [a]
		1650 (brw)				1645 (w)				1645 (*m*)		ν C=C* + ν C=N* [d]
		1600 (w)	1598 (s)			1601 (m)	1606 (w)			1601 (m)	1606 (w)	ν C=C* + ν C=N* (N^{π}) [d]
				1591 (*m*)	1593 (*m*)		1591 (*w*)	1587 (m)	1588 (m)			ν C=O (carboxylate) [b,d]
	1595 (m)											δ H_2O [c]
1574 (m)												δ N-H ν C-N (A-II 2º) [a]
						1564 (w)				1565 (*w*)		ν C=C* + ν C=N* (N^{π}) [d]
1557 (m)			1550 (w)	1547 (*w*)			1552 (vw)	1544 (*w*)				
						1485 (*w*)				1485 (*w*)		
1437 (m)	1435 (m)	1452 (s)	1439 (s)	1430 (w)	1430 (w)	1431 (s)	1437 (m)	1426 (w)	1426 (w)	1430 (s)	1435 (m)	ν ring* [d] / δ CH_2 [d]
		1427 (s)	1429 (s)									ν ring* [d]
				1397 (*w*)	1398 (*w*)			1396 (m)	1396 (m)	1400 (*m*)		ν C-O (carboxylate) [b,d]
1398 (m)	~1400 (*w*)											ν ring* [d]
1369 (*m*)	1373 (w)			1374 (w)	1371 (w)	1369 (w)		1373 (w)	1374 (w)	1372 (w)		ν C-N (A-III: 1º) [a]
1348 (s)	1342 (w)		1355 (m)									ν C(O)-N [a] / ν ring*
	1320 (*w*)	1340 (w)	1345 (m)									ν C(O)-N [a] / ν ring*
			1329 (m)									ν C(O)-N [a] / ν ring*
			1313 (m)	1312 (w)	1316 (w)	1308 (m)		1312 (w)	1317 (w)	1310 (m)	1312 (w)	δ CH_2 [d] / δ =C-H [d]
		1273 (w)	1267 (*w*)				1290 (brw)				1290 (brw)	ν ring* (N^{π}) [d] / A-III: 2º [a]
		1260 (w)				1256 (w)				1255 (w)		ν ring* (N^{π}) [d] / A-III: 2º [a]
1205 (m)	1203 (*m*)		1239 (w)	1205 (s)	1205 (s)	1225 (w)		1202 (m)	1205 (m)	1227 (w)		ν ring* (N^{π}) [d] / τ CH_2 [a]
1182 (m)	1166 (*s*)			1179 (s)	1176 (s)		1167 (w)	1176 (w)	1172 (m)	1165 (w)	1153 (w)	ν N-C=N + δ_{ip} N-H* [d]
1135 (m)	1137 (vs)		1162 (w)	1132 (m)	1130 (s)	1157 (w)		1129 (m)	1129 (s)			ν =C-N* + δ N-H* [d]
	1115 (*s*)				1114 (*s*)		1120 (w)		1116 (*s*)			ν =C-N=* + δ N-H* [d]
1084 (w)				1084 (w)		1099 (vw)				1099 (w)	1104 (vw)	ν =C-N=* / δ =C-N (N^{π}) [d]

1043 (w)	1048 (w)			1041 (vw)	1041 (vw)	1050 (w)	1049 (w)	1042 (vw)	1043 (vw)	1050 (m)	1052 (m)	ν C(O)-N [a]
1025 (w)	1026 (w)											δ C-H* / δ_{ip} C^{Ar}-H
995 (br)	997 (w)	997 (m)	997 (s)		994 (vw)	998 (s)	998 (s)		993 (vw)	998 (s)	998 (s)	ν =C-NH* (N^{π}) / δ_{ip} C^{BA}-H [d]
		986 (m)		983 (vw)			984 (*m*)	980 (vw)			980 (*m*)	ν =C-NH* (N^{t}) [d]
		960 (w)	960 (w)		968 (vw)			955 (vw)		954 (w)		ν =C-N* + δ ring [d]
		921 (s)	920 (s)									δ_{ip} C^3-H* [d]
	875 (vw)	881 (w)										δ ring* [a]
834 (m)	834 (w)	838 (w)	834 (w)	836 (m)	837 (m)	836 (m)	843 (m)	834 (m)	836 (m)	836 (m)	839 (w)	δ_{oop} =C-H* [d]
800 (w)	800 (w)			801 (m)	801 (m)			801 (m)	801 (m)			δ_{oop} C^{Ar}-H [a]
763 (vw)	764 (vw)										761 (w)	δ_{oop} C-H*
722 (w)	723 (w)		719 (w)	722 (m)	722 (m)	720 (w)	727 (m)	722 (w)	722 (w)	720 (w)	726 (w)	δ_{oop} N-H [a] / ρ_{ip} CH_2 [a]
700 (m)												ω N-H (2^o) [a]
	668 (w)				663 (w)		668 (w)	667(w)			673 (w)	δ ring* [d]
650 (w)	655 (w)	649 (m)	645 (m)		654 (w)	658 (w)				658 (w)		δ ring* [d]
	636 (w)		636 (w)		635 (w)	628 (w)	638 (w)	631 (w)			638 (m)	δ ring* [d]
625 (w)	622 (m)			622 (w)	615 (w)		624 (w)	622 (w)	615 (w)	625 (w)	623 (w)	δ ring* [d]
			588 (w)									ν Cu-OH_2^{eq} [d], [e]
						593 (w)	601 (w)			592 (w)	604 (w)	δ_{oop} CO_2 [d]
			458 (m)				467 (m)				466 (m)	ν Cu-N [d]
						430 (w)						
							406 (m)				404 (*w*)	ν Cu-O
						399 (w)	394 (*w*)			394 (w)	389 (w)	ν Cu-O
							355 (*w*)				359 (*w*)	ν Cu-O
											334 (*w*)	ν Cu-O

Used abbreviations In the peak section (*italic* refers to a shoulder): s = strong, m = medium, w = weak, v = very, br = broad. In the assignment section: ν = stretching, δ = bending, ρ = rocking, τ = twisting, ω = wagging; subscript s = symmetric; subscript a = anti-symmetric; * = imidazole ring vibrations; N^{π} = tautomer; N^{t} = tautomer; ip = in-plane; oop = out-of-plane; C^{BA} = aromatic ring (from the benzamide-core of the TAC-scaffold); 1^o, 2^o or 3^o refer to the type of amide involved (primary, secondary or tertiary, respectively); + = coupled vibrations; / = isolated vibrations; Im = imidazole; A-I = Amide I; A-II = Amide II; A-III = Amide III.

Specified references: a) R.M. Silverstein and F.X. Webster, *Spectrometric Identification of Organic Compounds*, 6th edition, **1998**, Wiley, USA, ch. 3, pp. 71-143; b) G.B. Deacon, R.J. Philips, *Coord. Chem. Rev.* **1980**, *33*, 227-250; V. Zelenák, Z. Vargová, K. Györyová, *Spectrochimica Acta Part A* **2007**, *66*, 262-272; c) K. Nakamoto, *Infrared and Raman Spectra of Inorganic and Coordination Compounds*, 5th edition, **1997**, Wiley, USA, pp. 227-230; P.A. Thiel, T.E. Madey, *Surface Sceince Reports* **1987**, *7*, 211; d) J.G. Mesu, T. Visser, F. Soulimani, E.E. van Faassen, P. de Peinder, A.M. Baele, B.M. Weckhuysen, *Inorg. Chem.* **2006**, *45*, 1960 and J.G. Mesu, T. Visser, F. Soulimani, B.M. Weckhuysen, *Vibr. Spectrosc.* **2005**, *39*, 114; e) C.R. Andrew, J. Han, T. Den Blaauwen, G. Van Pouderoyen, E. Vijgenboom, G.W. Canters, T.M. Loehr, J. Sanders-Loehr, *J. Biol. Inorg. Chem.* **1997**, *2*, 98.

Scaffold 5 and 7: Syntheses of these have been described in chapter 2.

Solid-phase synthesis of the TAC-based mimics

For the solid-phase synthesis of the mimics, several standard procedures were applied. These are described below. In general, for each gram of resin roughly 6 mL of solvent/solution (stored on 4 Å molsieves) was used. The reactions were carried out in special solid-phase reaction syringes equipped with filtering frit above the outlet.

- Fmoc-removal: 20% piperidine/NMP was used (2×6 mL each 8 min), after which the resin was washed with NMP (3×6 mL each 2 min) and DCM (3×6 mL each 2 min). Fmoc removal was monitored using a Kaisertest[48].
- *o*-NBS-removal[49]: prior to deprotection, the resin was washed with DMF (3×6 mL each 2 min). After this, a solution of 2-mercaptoethanol (0.5 M in DMF: 6 mL, 3 mmol) and DBU (224 μL, 1.5 mmol) was added (3×30 min). Subsequently, the resin was washed with DMF (3×6 mL each 2 min) and DCM (3×6 mL each 2 min) and the liberated amines were detected using the Chloranil test.[50]
- Alloc-removal: to the resin were subsequently added anilinium *p*-toluenesulfinate (PTSA) (20 eq) and $Pd(PPh_3)_4$ (0.25 eq). The reaction was allowed to proceed for 16 h, after which the reaction mixture was removed by filtration. Remaining Pd was removed by extensive washing with a 20 mM solution of sodium *N*,*N*-diethyldithiocarbamate (3×6 mL each 5 min). After this, the resin was washed with NMP (3×6 mL each 2 min) and DCM (3×6 mL each 2 min) and the liberated amines were detected using the Chloranil test.
- Coupling of acids: 3 eq of scaffold or 4 eq Fmoc-AA(PG)-OH was used together with 3 or 4 eq BOP and 6 or 8 eq D*i*PEA, respectively, in NMP. Coupling was performed overnight in case of the scaffolds and for 3 h in case of Fmoc-AA(PG)-OH and. The resin was washed with NMP (3×6 mL each 2 min) and DCM (3×6 mL each 2 min). Coupling was monitored using the Kaisertest in case of coupling to primary amines and the Chloranil test in case of coupling to secondary amines.
- Acetylation: A freshly prepared solution was applied in order to acetylate the *N*-terminal amine. This solution consists of Ac_2O (14.2 mL), D*i*PEA (6.5 mL) and HOBt (608 mg). After acetylation the resin was washed with NMP (3×6 mL each 2 min) and DCM (3×6 mL each 2 min).
- Deprotection and cleavage: The ligand was deprotected on the histidine side-chains and simultaneously removed from the resin using 3 mL TFA/TIS/H_2O – 92.5/5/2.5 (v/v).

TAC-based 3-His mimic 9

For the synthesis, 1 g of PS-S RAM-Fmoc resin (loading: 0.78 mmol/g) was used. Firstly, the Fmoc-group was removed and the scaffold was attached overnight. Remaining amines on the resin were capped by acetylation, followed by removal of the *o*-NBS-groups. After this,

conditions used for coupling of Fmoc-His(Trt)-OH were applied twice, in order to ensure complete acylation of the scaffold. The Fmoc-group was removed and the *N*-terminal amine was acetylated. The mimic was deprotected and cleaved from the resin, precipitated in MTBE and hexanes (1:1) and purified by column chromatography ($CHCl_3$/MeOH/25% NH_4OH – 8/4/1.5 (v/v)). The pure fractions were concentrated and lyophilized from water with pH 7. Purity of mimic **9** was assessed by TLC and HPLC and the identity was confirmed by ESI-MS. Yield: 572 mg (702 μmol, 90 %). R_f = 0.67 ($CHCl_3$/MeOH/25% NH_4OH – 60/45/20 (v/v)). ESI-MS: *m/z* = 814.58 (calculated: 814.40 for $[M+H]^+$).

TAC-based 2-His-1-Asp (15) and 1-His-2-Asp (16) mimics

For the synthesis of these two mimics, scaffold **7** was coupled to 500 mg of PS-S RAM-Fmoc resin (loading: 0.78 mmol/g) using 1 equiv of the scaffold. After overnight coupling, remaining amine functionalities were protected with the acetyl-group using the capping reagent. For coupling of the amino acids, 8 equiv were used compared to the initial loading of the resin. After removal of the Fmoc-groups, the scaffold containing resin was divided in two equal portions: one to construct mimic **15** and one for mimic **16**. For mimic **15** Fmoc-His(Trt)-OH and for mimic **16** Fmoc-Asp(O*t*Bu)-OH were coupled. After coupling, the *N*-terminal Fmoc-protecting group was removed and replaced by an acetyl-group. For the functionalization of the middle position, the Alloc-group was removed using Pd^0 and a scavenger. To the liberated amine, Fmoc-Asp(O*t*Bu)-OH (for mimic **15**) and Fmoc-His(Trt)-OH (for mimic **16**) were coupled. Acetylation of the *N*-terminal amine functionality was performed after Fmoc-removal. The resin-bound protected mimics were cleaved and deprotected using the cleavage cocktail and the released mimics were precipitated in cold MTBE and hexanes (1:1, at -20 °C). Lastly, the mimics were purified by column chromatography ($CHCl_3$/MeOH/25% NH_4OH – 8/4/1.5 (v/v)). Pure fractions were concentrated and lyophilized from water with pH 7. Purity of mimic **15** and **16** was assessed by TLC and HPLC and the identity confirmed by ESI-MS. Yields: 185 mg for **15** (234 μmol, 63 %) and 174 mg for **16** (226 μmol, 58 %). R_f = 0.58 for **15** and 0.33 for **16** ($CHCl_3$/MeOH/25% NH_4OH - 60/45/20 (v/v)). ESI-MS: mimic **15**: *m/z* 792.42 (calculated: 792.38 for $[M+H]^+$), mimic **16**: *m/z* 770.39 (calculated: 770.34 for $[M+H]^+$).

pH-titration and UV-vis spectroscopy

For each of the three ligands, stoichiometric mixtures of both ligand and copper-salt were prepared and the pH was adjusted to ~ 1.5 using 1N HCl. Using 0.5-5% solutions of $NaHCO_3$ the pH of the mimic-copper containing solutions was slowly raised and at each significant difference in pH-value an absorption spectrum was measured. For the d-d transition absorptions, 25 mM solutions of the complexes were prepared by mixing equal amounts of 50 mM solutions of both mimic and $CuSO_4$. For the charge-transfer spectra this was done

with 5 mM solutions of the complexes. These measurements were performed until pH 7.5 was reached.

Spectra were recorded on a 96-well microtiterplate suitable for UV-measurements using a microtiterplate reader measuring from 200-998 nm. Ligand-to-metal charge transfer absorptions (LMCT) were observed in the spectra of the mimics: 230, 242, 248 and 282 nm. In the spectra of the complexes, as the pH-value of the solution increased, an increase in intensity was observed for the band at 280 nm.

ESI-MS

For this, the end-stages of the samples used in the UV-vis analysis were used. After completion of the titration, the samples, having pH-value of ~ 7.5 were lyophilized. Before MS-analysis, these samples were dissolved in water and diluted with either water or methanol to a final concentration of 100 μM. For the analysis, the cone voltage was 20 V.

Infrared and Raman spectroscopy of the ligand and complex

Lyophilized samples were used for measuring infrared and Raman spectra. Infrared spectra of the mimics were obtained from freshly lyophilized samples (pH ~ 7.5), for the complexes lyophilized samples obtained in the UV-vis study were used. These were mixed with KBr and pressed into a pellet that could be measured on the infrared spectrophotometer. Raman spectra of both ligand and complex were obtained from lyophilized samples (pH ~ 7.5). Unfortunately, high (background) fluorescence of concentrated solutions and incineration of dry samples prevented Raman measurements of these samples. However, by applying a drop of water to the powder, a gel-like substance was formed in which the heat of the incoming radiation could be dispersed over present water molecules. The spectra shown in *figure 7* were obtained in this way.

6. References and Notes

1 D.F. Shriver, P.W. Atkins, *Inorganic Chemistry*, Oxford university press, 3rd edition, **1999**, Ghent, Belgium, p. 646.

2 L. Stryer, *Biochemistry*, Freeman and Company, 4th edition, **1995**, New York, USA, ch 9, pp. 207-236.

3 See *Biological Inorganic Chemistry*, edited by I. Bertini, H.B. Gray, E.I. Stiefel, J.S. Valentine, 1st edition, University Science Books, Sausalito, **2007**.

4 H.-B. Kraatz, N. Metzler-Nolte, *Concepts and Models in Bioinorganic Chemistry*, Wiley-VCH, Weinheim, Germany, 1st edition, **2006**.

5 D.E. Fenton, *Biocoordination Chemistry*, Oxford University Press, 1st edition, **1995**; C.D. Garner, D. Collison, E. Pidcock, *Philosophical Transactions: Mathematical, Physical and Engineering Sciences* **1996**, *354*, 325.

6 I. Bertini, P. Turano, in *Biological Inorganic Chemistry*, edited by I. Bertini, H.B. Gray, E.I. Stiefel, J.S. Valentine, 1st edition, University Science Books, Sausalito, **2007**, ch III and IV, pp. 31-56.

7 J.A. Cowan, in *Biological Inorganic Chemistry*, edited by I. Bertini, H.B. Gray, E.I. Stiefel, J.S. Valentine,

1st edition, University Science Books, Sausalito, **2007**, ch IX, pp. 175-208.

8 L. Que, Jr., in *Biological Inorganic Chemistry*, edited by I. Bertini, H.B. Gray, E.I. Stiefel, J.S. Valentine, 1st edition, University Science Books, Sausalito, **2007**, ch XI.5, pp. 388-413.

9 G.B. Jameson, J.A. Ibers, in *Biological Inorganic Chemistry*, edited by I. Bertini, H.B. Gray, E.I. Stiefel, J.S. Valentine, 1st edition, University Science Books, Sausalito, **2007**, ch XI.4, pp. 366-370.

10 J.S. Selverston, in *Biological Inorganic Chemistry*, edited by I. Bertini, H.B. Gray, E.I. Stiefel, J.S. Valentine, 1st edition, University Science Books, Sausalito, **2007**, ch XI.2, pp. 331-342.

11 H. Dugas, *Bioorganic Chemistry*: *A Chemical Approach to Enzyme Action*, 3rd edition; Springer: New York, **1996**; M.J. Corey, E. Corey, *Proc. Natl. Acad. Sci. U.S.A.* **1996**, *93*, 11428.

12 T.B. Rauchfuss, *Science* **2007**, *316*, 553; S. Ogo, R. Kabe, K. Uehara, B. Kure, T. Nishimura, S.C. Menon, R. Harada, S. Fukuzumi, Y. Higuchi, T. Ohhara, T. Tamada, R. Kuroki, *Science* **2007**, *316*, 585.

13 F.H. Arnold, *Nature* **2001**, *409*, 253; A. Schmid, J.S. Dordick, B. Hauer, A. Kieners, M. Wubbolts, B. Witholt, *Nature* **2001**, *409*, 258.

14 J.A. Ibers, R.H. Holm, *Science* **1980**, *209*, 223.

15 H.-B. Kraatz, N. Metzler-Nolte, *Concepts and Models in Bioinorganic Chemistry*, Wiley-VCH, Weinheim, Germany, 1st edition, **2006**, especially K.D. Karlin, *Model Complexes for Copper-Containing Enzymes*, ch 16, pp. 363-395; K.D. Karlin, A.D. Zuberbühler, *Formation, Structure and Reactivity of Copper Dioxygen Complexes*, ed. J. Reedijk and E. Bouwman, Marcel Dekker, New York, **1999**, ch 14, pp. 469-534; M.-A. Kopf, K.D. Karlin, in *Models of Copper Enzymes and Heme–Copper Oxidases*, ed. B. Meunier, Imperial College Press, London, **2000**, ch 7, pp. 309-362.

16 Usually, one amine is available for coordination. See for instance F. Chioccara, G. Chiodini, F. Farina, M. Orlando, B. Rindone, R. Sebastiano, *J. Mol. Catalysis A: Chemical*, **1995**, *97*, 183; H. Hayashi, S. Fujinami, S. Nagatomo, S. Ogo, M. Suzuki, A. Uehara, Y. Watanabe, T. Kitagawa, *J. Am. Chem. Soc.* **2000**, *122*, 2124; K.D. Karlin, Q. Gan, Z. Tyeklár, *Chem. Commun.* **1999**, 2295; R.J.M. Klein Gebbink, C.F. Martens, M.C. Feiters, K.D. Karlin, R.J.M. Nolte, *Chem. Commun.* **1997**, 389.

17 V. Fusi, A. Llobet, J. Mahía, M. Micheloni, P. Paoli, X. Ribas, P. Rossi, *Eur. J. Inorg. Chem.* **2002**, 987; K. Komiyama, H. Furutachi, S. Nagatomo, A. Hashimoto, H. Hayashi, S. Fujinami, M. Suzuki, T. Kitagawa, *Bull. Chem. Soc. Jpn.* **2004**, *77*, 59; M.T. Burger, W.C. Still, *J. Org. Chem.* **1995**, *60*, 7382; W.B. Tolman, *Acc. Chem. Res.* **1997**, *30*, 227; L.M. Mirica, D. Jackson Rudd, M.A. Vance, E.I. Solomon, K.O. Hodgson, B. Hedman, T.D.P. Stack, *J. Am. Chem. Soc.* **2006**, *128*, 2654; G. Izzet, B. Douziech, T. Prangé, A. Tomas, I. Jabin, Y. Le Mest, O. Reinaud, *Proc. Natl. Acad. Sci., USA* **2005**, *102*, 6831.

18 M.J. Baldwin, D.E. Root, J.E. Pate, K. Fujisawa, N. Kitajima, E.I. Solomon, *J. Am. Chem. Soc.* **1992**, *114*, 10421; N. Kitajima, K. Fujisawa, C. Fujimoto, Y. Moro-oka, S. Hashimoto, T. Kitagawa, K. Toriumi, K. Tatsumi, A. Nakamura, *J. Am. Chem. Soc.* **1992**, *114*, 1277; P. Gamez, C. Simons, G. Aromí, W.L. Driessen, G. Challa, J. Reedijk, *Applied Catalysis A: General* **2001**, *214*, 187; Y. Moro-oka, K. Fujisawa, N. Kitajima, *Pure & Appl. Chem.* **1995**, *67*, 241; P. Molenveld, J.F.J. Engbergen, D.N. Reinhoudt, *J. Org. Chem.* **1999**, *64*, 6337.

19 See for example P.L. Holland, W.B. Tolman, *Coord. Chem. Rev.* **1999**, *190-192*, 855; Z. Tyeklár, K.D. Karlin, *Acc. Chem. Res.* **1989**, *22*, 241.

20 M. Pasenkiewicz-Gierula, W. Froncisz, R. Basosi, W.E. Antholine, J.S. Hyde, *Inorg. Chem.* **1987**, *26*, 801; A. Bonamartini Corradi, *Coord. Chem. Rev.* **1992**, *117*, 45.

21 J.-P. Laussac, A. Robert, R. Haran, B. Sarkar, *Inorg. Chem.* **1986**, *25*, 2760; J. Ueda, N. Ikota, A. Hanaki, K. Koga, *Inorg. Chim. Acta* **1987**, *135*, 43; C.E. Livera, L.D. Pettit, M. Bataille, B. Perly, H. Kozlowski, B. Radomska, *J. Chem. Soc. Dalton Trans.* **1987**, 661; P.G. Daniele, O. Zerbinati, V. Zelano, G. Ostacoli, *J. Chem. Soc. Dalton Trans.* **1991**, 2711; F. Ryvkin, F.T. Greenaway, *J. Inorg. Biochem.* **2004**, *98*, 1427; J. Brasun, C. Gabbiani, M. Ginanneschi, L. Messori, M. Orfei, J. Swiatek-Kozlowska, *J. Inorg. Biochem.*

2004, *98*, 2016; H. Miyake, Y. Kojima, *Coord. Chem. Rev.* **1996**, *148*, 301; O. Szilágyi, K.Ösz, K. Várnagy, D. Sanna, H. Süli-Vargha, I. Sóvágó, G. Micera, *Polyhedron* **2006**, *25*, 3173; H. Kozlowski, T. Kowalik-Jankowska, M. Jezowska-Bojczuk, *Coord. Chem. Rev.* **2005**, *249*, 2323; G.F. Bryce, F.R.N. Gurd, *J. Biol. Chem.* **1966**, *241*, 122; A.P. Tofteng, T.H. Hansen, J. Brask, J. Nielsen, P.W. Thulstrup, K.J. Jensen, *Org. Biomol. Chem.* **2007**, *5*, 2225; F. Namuswe, D.P. Goldberg, *Chem. Commun.* **2006**, 2326.

22 R. Schnepf, W. Haehnel, K. Wieghardt, P. Hildebrandt, *J. Am. Chem. Soc.* **2004**, *126*, 14389; L. Regan, *Annu. Rev. Biophys. Biomol. Struct.* **1993**, *22*, 257; A. Lombardi, C.M. Summa, S. Geremia, L. Randaccio, V. Pavone, W.F. DeGrado, *Proc. Natl. Acad. Sci. USA* **2000**, *97*, 6298; C.M. Summa, M.M. Rosenbladtt, J.-K. Hong, J.D. Lear, W.F. DeGRado, *J. Mol. Biol.* **2002**, *321*, 923; M.A. Wells, C. Jelinska, L.L.P. Hosszu, C.J. Craven, A.R. Clarke, J. Collinge, J.P. Waltho, G.S. Jackson, *Biochem. J.* **2006**, *400*, 501.

23 A.S. Borovik, *Acc. Chem. Res.* **2005**, *38*, 54.

24 T. Opatz, R. M. J. Liskamp, *J. Comb. Chem.* **2002**, *4*, 275.

25 G.I. Tesser, I.C. Balvert-Geers, *Int. J. Pept. Protein Res.* **1975**, *7*, 295-305.

26 Unfortunately, the obtained crystals were too small for X-ray crystallographic analysis. All kinds of techniques were attempted in order to obtain larger crystals, including crystallization in a gel (H. Arend, J.J. Connelly, *J. Cryst. Growth* **1982**, *56*, 642), sublimation, crystallization from DMSO and co-crystallization with $Ph_3P{=}O$ (M.C. Etter, P.W. Baures, *J. Am. Chem. Soc.* **1988**, *110*, 639). None of the applied techniques gave crystals that were big enough for X-ray crystalographic analysis.

27 B.N. Figgis, M.A. Hitchman, *Ligand and Field Theory and Its Applications*, Wiley-VCH, **2000**, USA, especially ch. 8; M. Gerloch, E.C. Constable, *Transition Metal Chemistry – The Valence Shell in d-Block Chemistry*, **1994**, Weinheim, Germany; D.F. Shriver, P.W. Atkins, *Inorganic Chemistry*, Oxford university press, 3rd edition, **1999**, Ghent, Belgium.

28 I. Bertini, P. Turano, in *Biological Inorganic Chemistry*, edited by I. Bertini, H.B. Gray, E.I. Stiefel, J.S. Valentine, 1st edition, University Science Books, Sausalito, **2007**, ch. III, p. 34.

29 D.A. Skoog, J.J. Leary, *Principles of Instrumental Analysis*, Saunders College Publishing, **1992**, USA; E.I. Solomon, *Inorg. Chem.* **2006**, *45*, 8012; L.M. Mirica, X. Ottenwaelder, T.D.P. Stack, *Chem. Rev.* **2004**, *104*, 1013; S. Itoh, *Curr. Opin. Chem. Biol.* **2006**, *10*, 115; Y. Nishida, S. Kida, *Coord. Chem. Rev.* **1979**, *27*, 275; E.I. Solomon, *Inorg. Chem.* **2005**, *44*, 723

30 D.F. Shriver, P.W. Atkins, *Inorganic Chemistry*, Oxford University Press, 3rd edition, **1999**, ch. 7.

31 W.L. Jolly, *Modern Inorganic Chemistry*, 2nd edition, McGraw-Hill Book Co., New York, **1991**; E.T. Adman, *Curr. Opin. Struct. Biol.* **1991**, *1*, 895; E.I. Solomon, M.D. Lowery, *Science* **1993**, *259*, 1575.

32 B.N. Figgis, M.A. Hitchman, *Ligand and Field Theory and Its Applications*, Wiley-VCH, **2000**, USA, especially ch. 8; M. Gerloch, E.C. Constable, *Transition Metal Chemistry – The Valence Shell in d-Block Chemistry*, **1994**, Weinheim, Germany; D.F. Shriver, P.W. Atkins, *Inorganic Chemistry*, Oxford university press, 3rd edition, **1999**, Ghent, Belgium.

33 D.F. Shriver, P.W. Atkins, *Inorganic Chemistry*, Oxford University Press, 3rd edition, **1999**. See also: B.J. Hathaway, D.E. Billing, *Coord. Chem. Rev.* **1970**, *5*, 143.

34 E. Prenesti, P.G. Daniele, M. Prencipe, G. Ostacoli, *Polyhedron* **1999**, *18*, 3233; E. Prenesti, P.G. Daniele, S. Toso, *Analytica Chimica Acta* **2002**, *459*, 323; E. Prenesti, P.G. Daniele, S. Berto, S. Toso, *Polyhedron* **2006**, *25*, 2815; E.J. Billo, *Inorg. Nucl .Chem. Lett.* **1974**, *10*, 613.

35 B.J. Hathaway, P.G. Hodgson, *J. Inorg. Nucl. Chem.* **1973**, *35*, 4071.

36 See also T.G. Fawcett, E.E. Bernarducci, K. Krogh-Jespersen, H.J. Schugar, *J. Am. Chem. Soc.* **1980**, *102*, 2598.

37 W. Henderson and J.S. McIndoe, *Mass Spectrometry of Inorganic, Coordination and Organometallic Compounds: Tools – Techniques – Tips*, **2005**, John Wiley & Sons, West Sussex, England, ch 4 (pp. 106-125), ch 5 (pp. 126-173).

38 References used throughout this section are in addition to those mentioned under **table 1**: P. Patnaik, *Dean's Analytical Chemistry Handbook*, 2nd edition, **2004**, McGraw-Hill, section VII; B. Stuart, *Infrared Spectroscopy: fundamentals and applications*, 1st edition, **2004**, John Wiley and Sons; J.B. Hodgson, G.C. Percy, D.A. Thornton, *J. Mol. Struct.* **1980**, *66*, 81; A. Torreggiani, M. Tamba, G. Fini, *Biopolymers (Biospectroscopy)* **2000**, *57*, 149; A. Torreggiani, M. Tamba, S. Bonora, G. Fini, *Biopolymers (Biospectroscopy)* **2003**, *72*, 290; T. Miura, T. Satoh, A. Hori-i, H. Takeuchi, *J. Raman Spectr.* **1998**, *29*, 41; T. Miura, A. Hori-i, H. Mototani, H. Takeuchi, *Biochemistry* **1999**, *38*, 11560; T. Miura, T. Satoh, H. Takeuchi, *Biochim. Biophys. Acta* **1998**, *1384*, 171; M. Jackson, H.H. Mantsch, *Crit. Rev. Biochem. Mol Biol.* **1995**, *30*, 95; G. Socrates, *Infrared and Raman Characteristic Group Frequencies*, 3rd edition, **2004**, John Wiley and Sons.

39 J.G. Mesu, T. Visser, F. Soulimani, E.E. van Faassen, P. de Peinder, A.M. Baele, B.M. Weckhuysen, *Inorg. Chem.* **2006**, *45*, 1960

40 Y. Soeda, K.Toshima, S. Matsumura, *Biomacromolecules* **2003**, *4*, 196-203.

41 G.B. Deacon, R.J. Philips, *Coord. Chem. Rev.* **1980**, *33*, 227-250; V. Zelenák, Z. Vargová, K. Györyová, *Spectrochimica Acta Part A* **2007**, *66*, 262-272.

42 Shifts up to 100 cm^{-1} have been observed, see for instance: R.C. Paul, S.L. Chadha, *J. Inorg. Nucl. Chem.* **1969**, *31*, 2753.

43 A. Torreggiani, G. Fini, G. Bottura, *J. Mol. Struct.* **2001**, *565-566*, 341.

44 T. Miura, A. Hori-i, H. Mototani, H. Takeuchi, *Biochemistry* **1999**, *38*, 11560.

45 Ref. 39, see page 1970.

46 H.G. Brittain, *Crystal Growth & Design* **2009**, *9*, 2492; B. Schrader, W. Meier, *Z. Anal. Chem.* **1972**, *260*, 248.

47 J.A. Faniran, K.S. Patel, *J. Inorg. Nucl. Chem.* **1974**, *36*, 2261; Y. Mathey, D.R. Greig, D.F. Shriver, *Inorg. Chem.* **1982**, *21*, 3409.

48 E. Kaiser, R.L. Colescott, C.D. Bossinger, P.I. Cook, *Anal. Biochem.* **1970**, *34*, 595; V.K. Sarin, S.B.H. Kent, J.P. Tam, R.B. Merrifield, *Anal. Biochem.* **1981**, *117*, 147.

49 S.C. Miller, T.S. Scanlan, *J. Am. Chem. Soc.* **1997**, *119*, 2301; J.F. Reichwein, R.M.J. Liskamp, *Tetrahedron Lett.* **1998**, *39*, 1243; T. Fukuyama, C.-H. Jow, M. Cheung, *Tetrahedron Lett.* **1995**, *36*, 6373.

50 T. Voijkovsky, *Pept. Res.* **1995**, *8*, 236.

Chapter 7

Biomimetic Chemistry of Metalloenzyme Active Site Mimics Based on a TAC-Scaffold Decorated with Aspartic Acid and Histidine Residues

Abstract

The TAC-based metalloenzyme active site mimics presented in the previous chapter were used as ligands in two biologically relevant metal-ion catalyzed reactions. Firstly, the reaction between molecular oxygen and copper(I) complexes of the mimics was studied. This reaction resulted in the formation of dimerc bis(μ-hydroxo) dicopper(II) complexes for all three ligands. Additional information on the coordination behavior of the metalloenzyme active site mimics was obtained and their structural similarity to biological systems was apparent. Secondly, the mimics were used as ligands in iron(II) catalyzed oxidation of olefins, in an attempt to mimic oxygenation by non-heme iron enzymes. Unfortunately, very low turnovers were observed. Nevertheless, the results show that TAC-based metalloenzyme active site mimics can be used in Cu(I)-O_2 and Fe(II)-H_2O_2 chemistry and are an interesting addition to existing biomimetic and bioinspired approaches.

Parts of this chapter have been published: H.B. Albada, F. Soulimani, B.M. Weckhuysen, R.M.J. Liskamp, *Chem. Commun.* **2007**, 4895.

1. Introduction

Many metal-ion binding sites in proteins originate from the amino acid side chains of histidine, aspartate acid and/or glutamic acid.[1] These binding sites of metal-ions by proteins are used for both structural and functional purposes.[1] Examples of the latter include redox reactions, electron transfer reactions and Lewis-acid catalyzed reactions. In this broad spectrum for which metal-ions have been sequestered by nature, the application of metal-ions to generate reactive metal-oxygen species that can be used in catalytic transformations of organic substrates is especially interesting.[2] In order to increase our understanding of the reaction that is catalyzed, detailed knowledge of intermediate structures of an enzyme active site along a reaction pathway is needed.[3] As a result of this, our growing understanding of the mechanism by which an enzyme performs a reaction can be used for the construction of novel catalytic species.[4]

Structure elucidation of enzymes in the presence of their substrate by means of X-ray crystallography has provided detailed information on certain resting states of the enzyme-substrate complexes.[5] However, due to the high activity of the enzyme and the complex nature of the enzyme active sites in which these reactions occur,[6] small organic models of active sites are often needed to elucidate specific steps in their mode of action.[7,8] Approaches that have been employed can be classified as biomimetic or bioinspired,[9] although combinations of both have emerged more recently.[10] A biomimetic ligand system refers to a construct that mimics the coordinating atoms and structure found in nature whereas a bioinspired ligand system refers to a ligand in which achieving the function under ambient conditions is the prime target.[9] For Cu(I)-O_2 and Fe(II)-H_2O_2 chemistry, especially bioinspired approaches have been used to understand the mechanisms of the metalloenzymes having copper and iron in the catalytic cycle. For example, analysis of a non-natural model-system for type-3 copper binding sites suggested the presence of a certain reactive active site

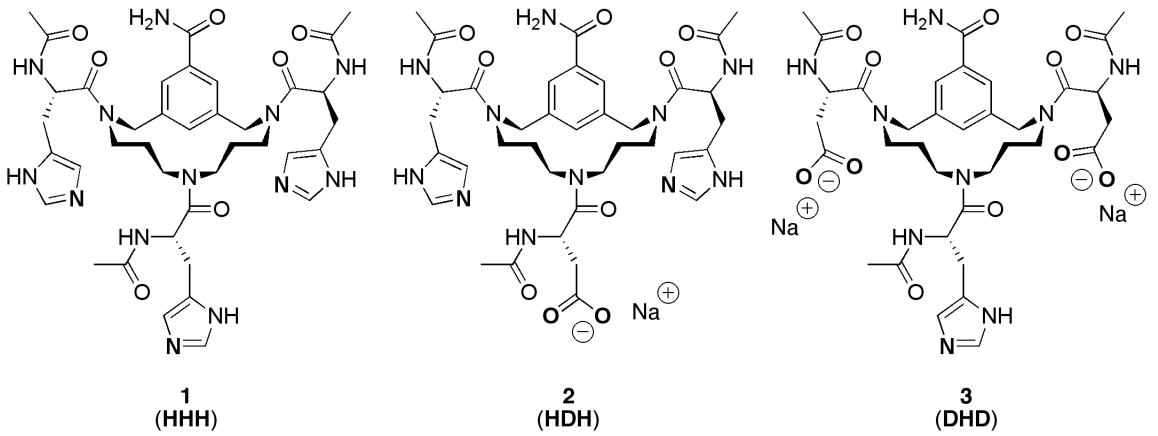

Figure 1. Three TAC-based mimics of TACzymes of three distinct metalloenzyme active sites. The one-letter codes of the amino acid residues attached to the TAC-scaffold are given between brackets.

structure even before its presence was confirmed by the X-ray crystal structure of the enzyme.[11]

In the previous chapter, three biomimetic ligands were presented that showed close structural mimicry of three different metalloenzyme active sites. These mimics, or TACzymes, contained a TAC-scaffold decorated with histidine and aspartate amino acid residues (*figure 1*). These three mimics will be referred to by the one-letter code of the amino acid residues that are attached to the scaffold, *i.e.* histidine or His by **H** and aspartic acid or Asp by **D**. In this chapter our initial work on the application of the three mimics as ligands in two biologically relevant reactions is described. First, the complexation behavior of the three mimics with copper(I) and their subsequent reaction with molecular oxygen from the air is described (section 2). After this, the three mimics are applied as ligands in iron-catalyzed olefin oxidation (section 3).

2. Complexation of copper(I) with three TACzymes and their reaction with molecular oxygen

After a brief introduction on copper binding sites in metalloenzymes, the reaction of molecular oxygen with three TACzyme-Cu(I)-complexes is described. This reaction was initially studied by UV-vis spectroscopy and the dried complexes were studied by infrared and Raman spectroscopy in order to gain insight in the final structure of the compounds. Similarities between natural counterparts are also discussed.

2.1.1 Introduction to biological Cu(I)-O_2 chemistry

Copper binding sites are prominent in metalloenzymes. The copper-ions are embedded in proteins most often by coordination to imidazole rings and less often to sulfur atoms (for example in azurin and plastocyanin) or phenoxo-groups (as in galactose oxidase). These functional groups originate from the side chains of histidine, cysteine or methionine, and tyrosine, respectively. In addition to these proteinogenic ligands, small molecules like water, O_2 or NO are often coordinating to and in some cases activated by the copper centre.[12] This activation of certain small molecules can lead

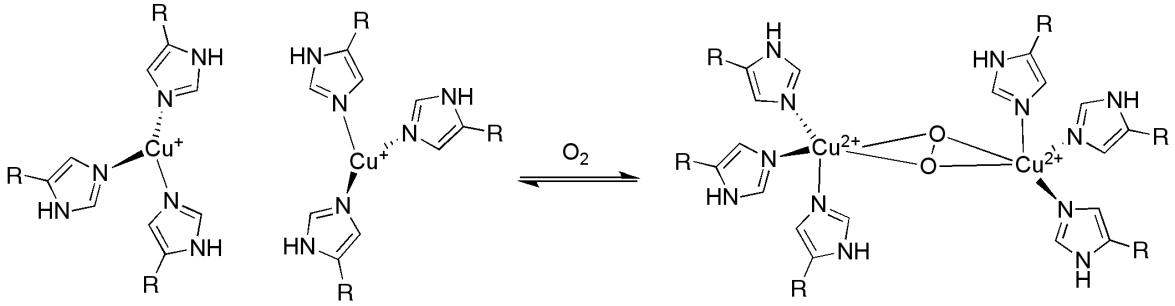

Figure 2. Deoxygenated (*left*) and oxygenated (*right*) type-3 copper binding site.[18] Note that coordination of the imidazole ring occurs by the N^{τ}-nitrogen atom of the imidazole ring.

to subsequent incorporation of single atoms into an organic substrate, a reaction that is mostly determined by the accessibility of the reactive species. For instance, a common oxygen-binding motive contains two copper(I)-ions each of which is surrounded by three histidine amino acid residues (*figure 2*). Upon binding of oxygen, Cu(I) is oxidized to Cu(II) and oxygen reduced to the corresponding peroxo-species. This so-called type-3 copper-binding site is found in tyrosinase[13], catechol oxidase[14] and hemocyanin[15], an oxygen carrying protein found in Arthropods and Mollusks.[16] Concerning this last class of proteins, limited proteolysis of tarantula hemocyanin resulted in tyrosinase activity in which oxygen was incorporated into tyrosine.[17]

2.1.2 Mimics of type-3 copper binding sites described in literature

This elegant mechanism of oxygen activation has attracted the attention of chemists and challenged them to construct mimics of these type-3 copper-binding sites. Small organic molecules containing three or four coordinating nitrogen atoms – originating from pyridine, azole or amine functionalities (see also the previous chapter) – have been extensively used as bioinspired mimics.[2,8] On the other hand, biomimetic ligand systems, *i.e.* compounds that use histidinyl imidazole rings for coordination to copper, are far more rare.[2,8] Some attempts have been undertaken using synthetic peptides, but undesired coordination by peptide-bond nitrogen atoms has proven to be difficult to prevent.[19] Also, the presence of strongly coordinating *N*-terminal amine and *C*-terminal carboxylate functionalities has hampered this line of research. In view of the small number of truly biomimetic ligand systems that have been used to mimic the Cu(I)-O_2 chemistry of type-3 copper binding sites, we were interested in the behavior of our TACzymes as mimics containing amino acid derived ligands.

Many complexes of copper(I)-ions readily react with oxygen under formation of CuO-species. Under the right circumstances this binding of oxygen is a dynamic process that depends on factors like bulkiness of the ligands, the type and number of coordinating atoms, the temperature and the solvent in which the experiment is conducted.[20] Identification of the CuO-species that is present is usually achieved by studying UV-vis,[21] infrared and Raman spectra of the complex.[22] Under ambient conditions, however, biologically most relevant CuO-species for type-3 copper binding sites – the μ-η^2:η^2-peroxodicopper(II) and bis(μ-oxo)dicopper(III) complexes[16] (*figure*

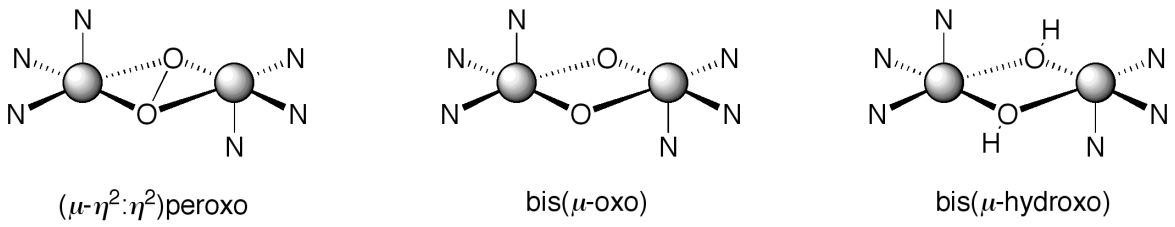

Figure 3. Three CuO-species often present in the reaction of Cu(I)-complexes with O_2.

3) – are usually unstable. Instead, these circumstance usually lead to the formation of bis(μ-hydroxo)dicopper(II) species (*figure 3*). This last species has also been observed in the presence of moisture and by reaction with a substrate or ligand cleavage.[23]

Although type-3 copper binding sites exclusively contain two tris-histidine triads for copper-coordination, we not only tested our 3-His containing TACzyme but also our other two mimics, *i.e.* the 2-His-1-Asp and 1-His-2-Asp containing TACzymes. In this way we would be able to generate a general picture of the behaviour of our three TACzymes in Cu(I)-O_2 chemistry.

2.2.1. UV-vis analysis of the oxygenation of Cu(I)-TACzyme complexes

The reaction between TACzyme-Cu(I) complexes and molecular oxygen was initially studied by UV-vis spectroscopy (*scheme 1*). For this, equimolar amounts of one of the three TACzymes – *i.e.* 3-His **1** (of **HHH**), 2-His-1-Asp **2** (or **HDH**) or 1-Asp-2-His **3** (or **DHD**) – and $[Cu(MeCN)_4]PF_6$ were mixed in DMSO, and air was bubbled through at regular intervals. The synthesis of the TACzymes has been described in chapter 6 of this thesis. It should be noted that the TACzymes were used as carboxylate sodium salts, obtained after lyophilization from aqueous solution of pH 7.5. As a result of the reaction with oxygen from the air the solution became blue indicating the formation of Cu(II) (*figure 4*). Under exclusion of air only a small change in color was observed, indicating that Cu(I) was not oxidized by DMSO.

As result of the reaction between molecular oxygen and the Cu(I)-complexes with the **HHH** and **HDH** TACzymes, the absorption maxima (λ_{max}) increased in intensity and showed a shift to *shorter* wavelengths. For the complex with mimic **DHD**, however, an increase in intensity and a shift to *longer* wavelengths was observed. The largest shifts in λ_{max} occurred during the first 15 minutes. After this, only small changes in the absorption maxima were observed resulting in the following λ_{max} values and molar extinction coefficients (ε) that were obtained after 2 h: at 722 nm (or 13 850 cm^{-1}) with ε = 64.6 $M^{-1} \cdot cm^{-1}$ for **HHH**, at 718 nm (or 13 928 cm^{-1}) with ε = 78.3 $M^{-1} \cdot cm^{-1}$ for **HDH**, and at 740 nm (or 13 514 cm^{-1}) with ε = 46.8 $M^{-1} \cdot cm^{-1}$ for **DHD**. For all three complexes, an intense charge transfer band was observed around 310 nm or (32 250 cm^{-1}). In addition, using UV-vis diffuse reflection an absorption band was observed at 423 nm (or 23 641 cm^{-1}) for the **HHH**-based complex, corresponding to hydroxo-to-copper charge transfer absorption.[24]

Visible absorption spectra of copper(II)-complexes with coordinating amide or imidazole nitrogen and carboxylate, hydroxide, water or carbonyl oxygen atoms in aqueous solutions have been extensively described.[25] Even though our complexes were prepared in DMSO, which usually results in a deviation from the value known for the same complex in aqueous solution due to solvatochromic effects,[26] the information was nevertheless useful for interpretation of the present complexes.

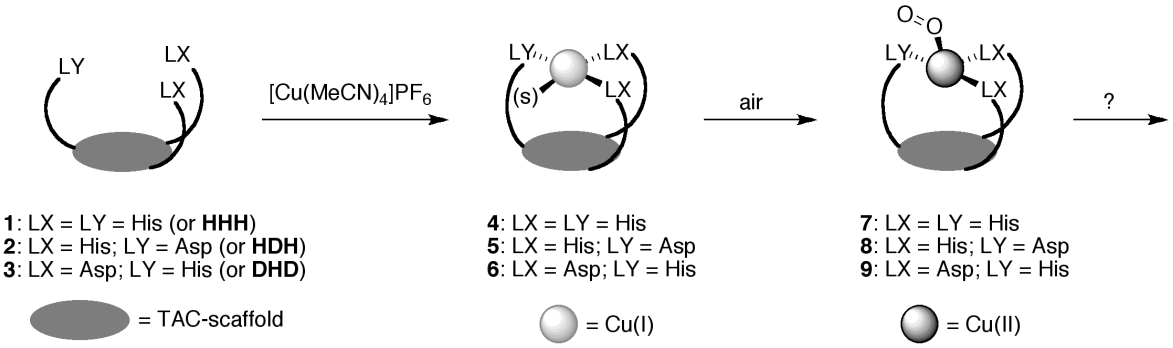

Scheme 1. Reaction between three TACzyme-Cu(I)-complexes and oxygen ((s) = optional solvent molecule).

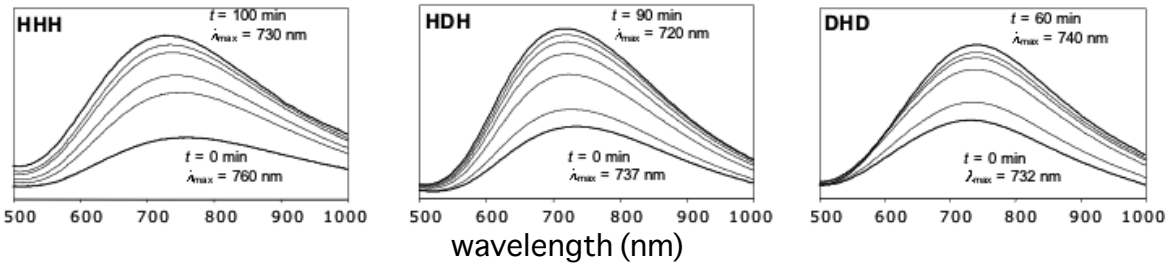

Figure 4. Changes in d-d absorption bands as result of the oxygen-binding by the Cu(I)-complexes (*top*, one letter-code of the amino acid residues that were attached to the scaffold are used throughout this section).

For the **HHH**-TACzyme formation of a bis(μ-hydroxo) dicopper(II) complex in which each copper(II)-ion was surrounded by three imidazole rings and two hydroxo groups was most likely. Concerning the average geometry around the Cu(II)-centra, the λ_{max} at 722 nm corresponds better with a distorted square pyramidal complex than with a trigonal bipyramidal complex[27], even though the latter geometry cannot be entirely excluded.[28] Distortion from a perfect square-pyramidal complex as result of the Jahn-Teller effect is a well-known phenomenon for strong coordinating functionalities like imidazole rings.[18] From literature it is known that an aqueous solution of a square pyramidal complex like complex **a** (*figure 5*) should have a λ_{max} at 674 ± 9 nm.[29] Even considering a solvatochromic shift of this absorption maximum caused by DMSO, some distortion of this square-pyramidal complex is required to obtain a λ_{max} of 722 nm. It is therefore most likely that the **HHH**-TACzyme formed a coordination complex in which the geometry was between square-pyramidal and trigonal bipyramidal (complex **b** in *figure 5*).

For the bis(μ-hydroxo) dicopper(II) complexes based on the **HDH**- and **DHD**-TACzymes similar analyses could be made. Concerning the **HDH**-TACzyme two square-pyramidal complexes were possible, one of which had a λ_{max} at 706 ± 8 nm (complex **c** in *figure 5*).[30] Complex **d** should have a λ_{max} of 672 ± 14 nm, which is well below the observed 718 nm, making this arrangement of the ligands around copper unlikely.[31] On the other hand, the difference of 12 nm between the calculated value of

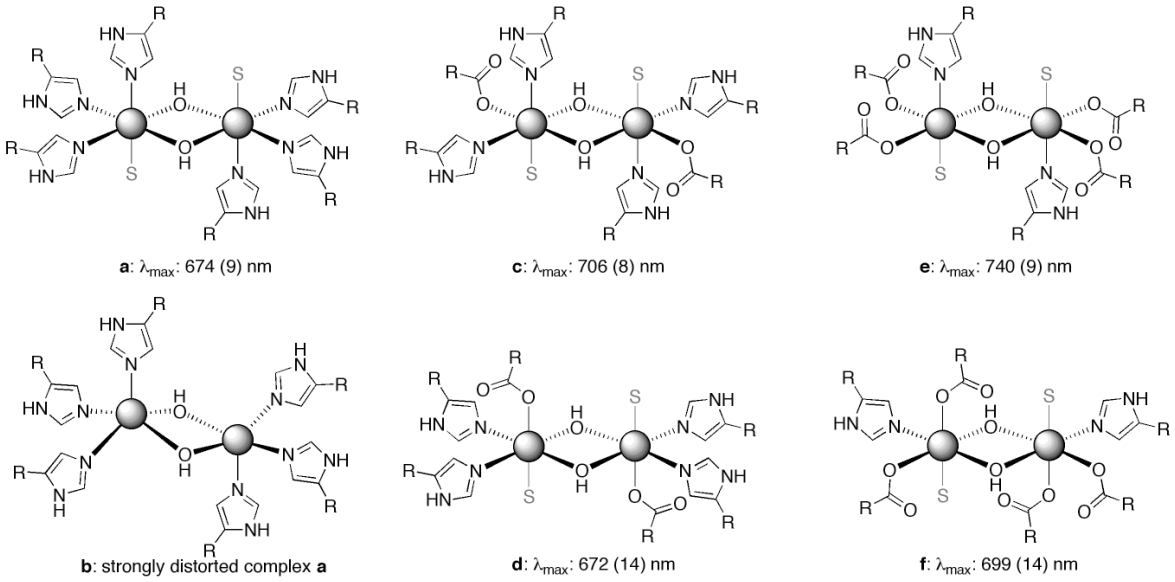

Figure 5. Overview of possible bis(μ-hydroxo) dicopper(II) structures based on TACzymes **1**, **2**, and **3** (*figure 1*). The corresponding λ_{max} values as calculated for aqueous solutions (S = water),[25] values in brackets give the error in λ_{max}. S = solvent molecule; R = remainder of the His or Asp residue connected to the TAC-scaffold.

706 nm and the observed λ_{max} of 718 nm is well in the range of known values for shifts caused by solvatochromic effects. Therefore, complex **c** in *figure 5* was likely present at the end of this experiment.

For the **DHD**-TACzyme, of the two possible square-pyramidal complexes that could be present, the one with a λ_{max} of 740 ± 9 nm (complex **e**) was more likely than the one with λ_{max} at 684 ± 7 nm (complex **f**). The observed absorption maximum at 740 nm corresponds nicely with the first geometry, making this complex **e** most likely.[32]

For each of the three ligand systems discussed, the presence of the corresponding bis(μ-hydroxo) dicopper(II) complexes could be envisioned. In generally, reaction of the Cu(I)-complexes of each of the TACzymes with O_2 resulted in the formation of square-pyramidal complexes. Decreasing distortion from this geometry towards trigonal bipyramidal geometry was observed going from **HHH** via **HDH** to **DHD**. It is known that strongly coordinating groups like imidazole rings can cause a significant Jahn-Teller distortion, more than weaker coordinating functionalities like carboxylate groups.[33] Also, solvatochromic effects seemed to be weaker going from **HHH** via **HDH** to **DHD**. This might be the result of the differences in overall charge of complexes, that is 2+ for **HHH**, 0 for **HDH** and 2- for **DHD**, and the concomitant accessibility of the copper-centre for the electron-rich oxygen atom of DMSO. Additional information on the properties of the formed [**HHH**-Cu^{II}-(μ-$OH)_2$-Cu^{II}-**HHH**]$^{2+}$, [**HDH**-Cu^{II}-(μ-$OH)_2$-Cu^{II}-**HDH**], and [**DHD**-Cu^{II}-(μ-$OH)_2$-Cu^{II}-**DHD**]$^{2-}$ complexes could be obtained from infrared and Raman spectroscopic analysis on the dried complexes.

2.2.2. Infrared and Raman analysis of complexes

Infrared and Raman vibrational spectra of dried samples of complexes obtained after reaction with oxygen were measured. These dried complexes were obtained by evaporating DMSO under *vacuo* (*figures 6* and *figure 7*, see also *table 1*).

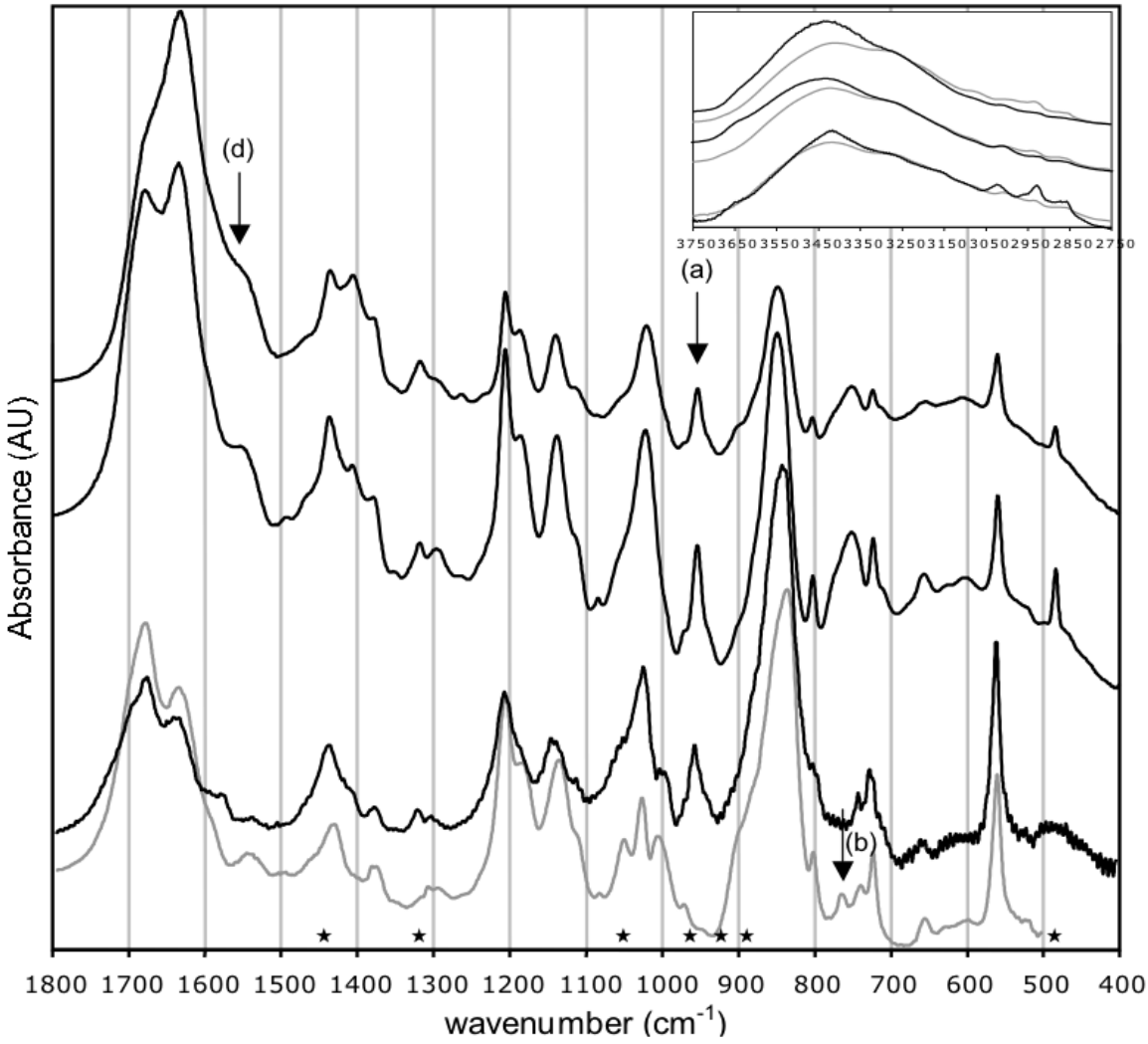

Figure 6. Infrared spectra of the dried complexes obtained after reaction of the Cu(I)-mimic complexes with oxygen. Insert shows the area in which O-H stretching vibrations can be observed, gray traces are from the Cu(II)-mimic complexes. Mimics corresponding to the traces: **DHD** (*top* trace), **HDH** (*middle* trace), **HHH** (*lower* trace), grey trace underlying the lower trace is from the species prepared in DMSO-d_6. Arrows indicate the most important peaks for the interpretation of complex, small letters refer to assignments mentioned in the text. Asterisks above the horizontal axis mark frequencies at which DMSO vibrations are positioned.

Hydroxo groups positioned between the two copper ions and which were present in all three complexes. A broad absorption around 3450 cm^{-1} is present in all three IR spectra originated from O-H stretching vibrations (*figure 6*, insert). Although H-O stretching vibrations of bridging hydroxo groups usually give a sharp peak around 3650 cm^{-1}, hydrogen bonding to the proton of the hydroxo groups broadens the peak

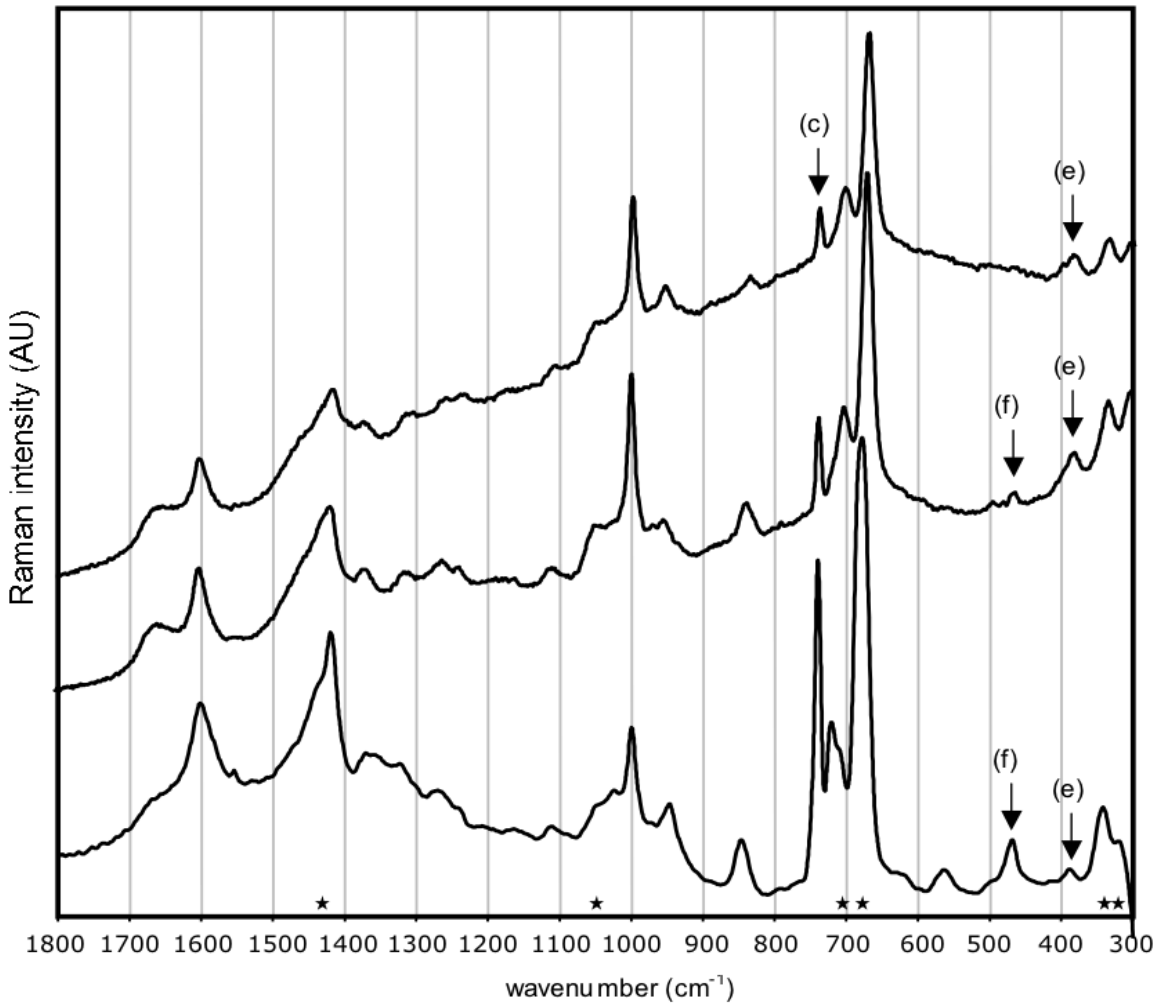

Figure 7. Raman spectra of the dried complexes obtained after reaction of the Cu(I)-mimic complexes with air. Mimics corresponding to the traces: **DHD** (top trace), **HDH** (middle trace), **HHH** (lower trace). Arrows indicate the most important peaks for the interpretation of complex, small letters refer to assignments mentioned in the text. Asterisks above the horizontal axis mark frequencies at which DMSO vibrations are positioned.

and shifts this peak to lower wavenumbers.[34] In addition to this O-H stretching vibration, in-plane bending vibrations of the hydrogen atoms that are part of the $Cu_2(OH)_2$-core of the complex resulted in an absorption at 957 cm^{-1} (*figure 6*, arrow (a)).[35] This assignment was supported by the observation that the IR-spectrum of a deuterated complex with the **HHH**-TACzyme as a ligand – which was prepared using DMSO-d_6 and an additional small amount of D_2O added after 2 h – lacked this absorption. Instead, a peak was observed at 761 cm^{-1}, corresponding to in-plane $(Cu)_2O$-D bending vibrations (arrow (b) in *figure 6*).[22] This indicates that hydroxo-bridged species were formed.

The $Cu_2(\mu\text{-}OH)_2$-core was detected in all three complexes. In the Raman spectra, intensities corresponding to symmetric Cu_2O_2-core vibrations of the $Cu_2(\mu\text{-}OH)_2$-species were also observed. For the **HHH**-TACzymes this was found at 740 cm^{-1} and for those with the **HDH**- or **DHD**-TACzymes at 739 cm^{-1} (*figure 7*, arrow (c)).[36] For

the related $Cu_2(\mu\text{-}O)_2$ core it is known that the frequency at which this vibration was found does not significantly depend on the nature of the ligands.[6] The decreasing intensity of this peak in the series **HHH**, **HDH**, **DHD** indicated that the change in polarizability as result of the vibration of the Cu_2O_2-core was largest for the **HHH**-TACzyme and smallest for the **DHD**-TACzyme based complexes.

Concerning the imidazole rings that were present in all three mimics, significant differences between complexes and free mimics were observed. For all three complexes, predominant coordination of N^{τ}-nitrogen atoms of the histidinyl imidazole rings could be derived from the Raman spectra based on intensities at 1600 cm^{-1} and at 1000 cm^{-1} (*figure 7*). This last vibration coincided with a vibration of the 1,3,5-trisubstituted aromatic core of the TAC-scaffold. The absence of a distinct shoulder at 986 cm^{-1} and a signal around 1570 cm^{-1} indicated that N^{π}-coordination did not occur. Apparently, binding to Cu(II) by the TACzymes was preferably mediated by the N^{τ}-nitrogen atoms of the imidazole rings. For the **HHH**-mimic, this binding mode closely mimics the binding modes found in type-3 copper binding sites (*cf. figure 2*).

For coordination of the carboxylate groups present in the **HDH** and **DHD** containing mimics, several possibilities were present. Whereas the mononuclear complexes with Cu(II) and these two mimics showed predominant monodentate coordination, as was apparent from vibrations around 1600 and 1400 cm^{-1}, the interpretation of the IR spectra of these dinuclear complexes is less straightforward. Besides possible shoulders around 1600 cm^{-1}, obscured by the intense absorptions at 1626 (**DHD**) or 1629 cm^{-1} (**HDH**) corresponding to vibrations of the amide bonds, absorptions at 1548 (**DHD**) and 1541 cm^{-1} (**HDH**) were also observed (*figure 6*, arrow (d)). Since the spectrum of the **HHH**-complex also showed an absorption around this frequency, it was not clear if the absorptions at 1548 and 1541 cm^{-1} originate from the carboxylate groups. Nevertheless, carboxylate vibrations found around 1550 cm^{-1} can correspond to anti symmetric vibrations of a coordinating carboxylate group and have been assigned to monodentate, bidentate or even bidentate bridging coordination.[37] On the other hand, symmetric vibrations of the carboxylate groups were found at 1402 and 1403 cm^{-1} for **HDH** and **DHD**, respectively. With this, the differences between the symmetric and anti symmetric vibrations (Δ) are 139 cm^{-1} (for **HDH**) and 145 cm^{-1} (for **DHD**), which is well below the value of 180 cm^{-1} that is typical for monodentate coordination.[38] To make matters more complicated, the presence of a hydrogen bond to the not coordinating oxygen atom of a carboxylate can also reduce the Δ-value.[46] Even though the spectra of the **DHD** and **DHD** TACzyme complexes displayed an absorption at 745 cm^{-1}, most likely originating from a COO deformation vibration[46], this has not been established as a marker band for carboxylate coordination. Therefore, which of the above-mentioned coordination possibilities for the carboxylate groups is predominant was not entirely clear at this stage. It is most likely that multiple modes of carboxylate coordination are present.

Lastly, ligand-metal bonds present in the complexes of all three mimics were observed in the Raman spectra.[39] Cu-O dative bonds could be found at 392, 386 or 390 cm^{-1}, for **HHH**, **HDH** or **DHD**, respectively (arrows (e) in *figure 7*). Cu-N bonds in **HHH** and **HDH** were observed at 472 or 470 cm^{-1} (arrows (f) in *figure 7*).[40] Surprisingly, in the complex of the **DHD** TACzyme a vibration of the Cu-N bond was not observed. This might have been due to a weaker axial coordination of the imidazole ring to the Cu(II)-ion.[41] It is possible that the small shoulder at 404 cm^{-1} originated from this vibration. In line with this, the low intensity of the Cu-N vibration in the **HDH**-TACzyme complex might indicate that only one of the two imidazole rings present in the mimic is coordinated in the equatorial plane. This was already inferred from the UV-vis experiment.

Analysis of the infrared and Raman spectra support the finding obtained from the UV-vis study that the three Cu(I)-TACzyme complexes reacted with molecular oxygen under formation of the corresponding bis(μ-hydroxo) dicopper(II) complexes. Coordination of histidinyl imidazole rings was almost exclusively by the N^{τ}-nitrogen atom of the ring. For the coordination of the carboxylate moieties a mixed picture was obtained in which multiple coordination modes were present. The presence of bridging hydroxo groups was inferred from the signals originating from O-H bending (IR) and $Cu_2(OH)_2$-core (Raman) vibrations. Metal-ligand bonds were also observed in Raman, indicating the formation of the anticipated coordination complex.

2.2.3. Reaction of type-3 copper binding site mimic with a catechol substrate

In view of the resemblance of the bis(μ-hydroxo) dicopper(II) complex based on the **HHH**-TACzyme with the active site of catechol oxidase, a reaction was performed with 3,5-di-*tert*-butylcatechol. This catechol can be oxidized to the corresponding quinone (*figure 8*, left). For this, a solution containing one equivalent of 3,5-di-*tert*-butylcatechol was added to a freshly prepared or aged bis(μ-hydroxo) complex. Before and after addition of the substrate UV-vis spectra were measured (*figure 8*, right).[42]

Upon addition of the substrate the colour of the solution immediately changed from mint-green to yellow, indicating rapid conversion of the catechol to the quinone. In the UV-vis spectrum the absorption band of the complex at ~ 722 nm shifted to about 780 nm and two new bands emerged, one at 400 nm and one at 574 nm (*figure 8*, right), corresponding to absorptions of 3,5-di-*tert*-butylbenzoquinone. This illustrated that the copper-ions in the compact bis(μ-hydroxo) dicopper(II) species[23] were still accessible for coordination and reaction.

Due to the poor solubility of these constructs in aprotic organic solvents – which is needed to perform the low-temperature (< -40 °C) Cu(I)-O_2-chemistry that generates highly reactive metal-oxygen species of which the oxygen atom(s) can be incorporated into organic substrates – the behaviour of this type-3 copper binding site mimic in Ar-H to Ar-OH oxidation reaction could not be tested. Therefore, true biomimetic

Table 1. Proposed assignment for the Infrared and Raman spectra of the bis(μ-hydroxo) dicopper(II) complexes based on the three mimics.

3-His		**2-His-1-Asp**		**1-His-2-Asp**		
Infrared	Raman	Infrared	Raman	Infrared	Raman	
3420 (br)		3420 (br)		3430 (br)		ν C(O)N-H (1° and 2°) / ν O-H (H-bonded) [a]
2931 (w)	2925 (vs)	2923 (*w*)		2915 (*w*)		ν_a CH_2
1680 (s)		1674 (s)	1660 (w br)	1669 (*s*)	1663 (w br)	ν C=O (A-I: 1°, 2° and 3°) [a]
1645 (s)		1629 (s)		1626 (vs)		δ N-H + ν C-N (A-II: 1°) [a]
	1600 (s)		1603 (w)		1604 (w)	ν C=C* + ν C=N* (N^{π}) [d]
		1541 (*m*)		1548 (*m*)		ν C=O (carboxylate) [b),d]
1443 (m)		1432 (m)		1431 (m)		δ N-H* / ν C=C* / δ_a CH_3
	1420 (s)		1421 (m)		1419 (m)	δ N-H* / ν C=C* / δ CH_2
		1402 (m)		1403 (m)		ν C-O (carboxylate) [b),d]
	1374 (w)	1376 (w)	1375 (w)	1375 (w)		ν C-N (A-III: 1°) [a]
	1330 (w)	1315 (w)	1316 (w)	1312 (w)	1314 (w)	δ =C-H [d] / ν C(O)-N [a] / ν ring*
		1289 (w)		1289 (*w*)		
			1265 (brw)		1263 (brw)	ν ring* (N^{π}) [d] / A-III: 2° [a]
1209 (m)		1203 (s)		1204 (m)		ν ring* (N^{π}) [d] / τ CH_2 [a]
1146 (m)		1182 (m)		1182 (m)		ν N-C=N + δ_{ip} N-H* [d]
		1136 (m)		1136 (s)		ν =C-N* + δ N-H* [d]
		1113 (*m*)	1112 (w)	1109 (*w*)		ν =C-N=* + δ N-H* [d]
1051 (w)	1050 (m)		1052 (w)		1053 (m)	ν C(O)-N [a]
1024 (m)		1020 (m)		1016 (m)		δ C-H* / δ_{ip} C^{Ar}-H
1003, 999 (w)	1000 (s)		999 (s)		999 (s)	ν =C-NH* (N^{π}) / δ_{ip} C^{BA}-H [d]
957 (m)	950 (w)	953 (m)	958 (w)	950 (w)	955 (w)	δ CuO-H (ip) / ν =C-N* + δ ring*
841 (s)		848 (s)		844 (s)		PF_6-ion
	834 (w)		843 (m)		838 (w)	δ_{oop} =C-H* [d]
		801 (w)		800 (w)		δ_{oop} C^{Ar}-H [a]
761 (w)						δ CuO-D (ip)
		745 (br m)		745 (br w)		
	741 (s)		739 (m)		739 (m)	$Cu_2(OH)_2$ core breathing
727 (w)	722 (w)	722 (m)		719 (w)		δ_{oop} N-H [a] / ρ_{ip} CH_2 [a]
			705 (m)		705 (m)	DMSO
			671 (vs)		672 (vs)	DMSO
		650 (w)		650 (vw)		
	568 (w)					ν Cu-OH_2^{eq} [d), e]
559 (s)		560 (m)		559 (m)		δ_{oop} CO_2 [d]
		483 (m)		482 (w)		
	472 (m)		470 (w)			ν Cu-N^{eq} [d]
			409 (*vw*)		404 (*w*)	ν Cu-N^{ax}
	392 (w)		386 (m)		390 (w)	ν Cu-O
			339 (m)		339 (m)	DMSO
			307 (m)		307 (m)	DMSO

Used abbreviations In the peak section (*italic* refers to a shoulder): s = strong, m = medium, w = weak, v = very, br = broad. In the assignment section: ν = stretching, δ = bending, τ = twisting; subscript s = symmetric; subscript a = anti symmetric; * = imidazole ring vibrations; N^{π} = tautomer; N^{τ} = tautomer; ip = in-plane; oop = out-of-plane; C^{BA} = aromatic ring (from the benzamide-core of the TAC-scaffold); 1°, 2° or 3° refer to the type of amide involved (primary, secondary or tertiary, respectively); + = coupled vibrations; / = isolated vibrations; A-I = Amide I; A-II = Amide II; A-III = Amide III; *deut* (at 761 cm^{-1}) means that this vibration was only observed in the deuterated complex.

Specified references: a) R.M. Silverstein and F.X. Webster, *Spectrometric Identification of Organic Compounds*, 6th edition, **1998**, Wiley, USA, ch. 3, pp. 71-143; b) G.B. Deacon, R.J. Philips, *Coord. Chem. Rev.* **1980**, *33*, 227-250; V. Zelenák, Z. Vargová, K. Györyová, *Spectrochimica Acta Part A* **2007**, *66*, 262-272; c) K. Nakamoto, *Infrared and Raman Spectra of Inorganic and Coordination Compounds*, 5th edition, **1997**, Wiley, USA, pp. 227-230; P.A. Thiel, T.E. Madey, *Surface Sceince Reports* **1987**, *7*, 211-385; d) J.G. Mesu, T. Visser, F. Soulimani, E.E. van Faassen, P. de Peinder, A.M. Baele, B.M. Weckhuysen, *Inorg. Chem.* **2006**, *45*, 1960 and J.G. Mesu, T. Visser, F. Soulimani, B.M. Weckhuysen, *Vibr. Spectrosc.* **2005**, *39*, 114; e) C.R. Andrew, J. Han, T. Den Blaauwen, G. Van Pouderoyen, E. Vijgenboom, G.W. Canters, T.M. Loehr, J. Sanders-Loehr, *J. Biol. Inorg. Chem.* **1997**, *2*, 98.

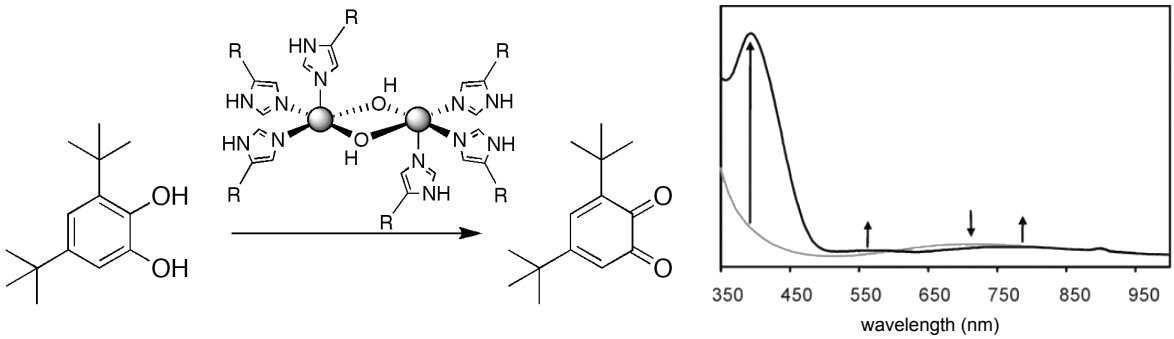

Figure 8. Oxidation of 3,5-di-*tert*-butylcatechol to the corresponding benzoquinone (left). The change in the UV-vis spectrum was clearly visible (right). Arrows indicate the changes in the absorption spectrum before (gray line) and after (black line) addition of 1 equiv of the catechol.

catalysis of, for instance, dopamine β-hydroxylase or tyrosinase oxidase remained elusive at this stage.[43] For the same reasons, generation of a highly reactive bis(μ-1,1-hydroxo)(μ-peroxo) dicopper(II) complex from a reaction of a bis(μ-hydroxo) dicopper(II) complex by reaction with H_2O_2 could not be investigated.[44]

2.3. Discussion and Conclusions on the application of the mimics Cu(I)-O_2 chemistry

In this first part, the complexation behaviour of three TACzymes, containing as well as the 3-His (**HHH**), 2-His-1-Asp (**HDH**), or 1-His-2-Asp (**DHD**) triad, with Cu(I) and the subsequent reaction of these complexes with molecular oxygen was described. The Cu(I)-complexes of the three TACzymes readily reacted with molecular oxygen under formation of Cu(II) as was monitored by UV-vis. The reaction with oxygen was complete after approximately 15 minutes, as was apparent from almost stationary position of the absorption maxima. From the position of the absorption maxima, formation of bis(μ-hydroxo) dicopper(II) complexes could be deduced. The absorption maxima of the final complexes were in agreement with square-pyramidal complexes containing imidazole, carboxylate and hydroxo groups described in literature. Deviations from literature values for similar complexes were most likely due to distortion of the square-pyramidal complex and solvatochromic effects.

Raman spectroscopy of dried samples of the final complexes unambiguously showed coordination of histidinyl imidazole N^{τ}-nitrogen atoms and thereby structural mimicry of many non-heme metal-binding sites found in proteins. In addition, infrared spectroscopy showed the presence of bridging hydroxo-groups, indicating that a dimeric bis(μ-hydroxo) dicopper(II) complex was formed. Even more, Raman spectroscopy revealed the presence of a $Cu_2(OH)_2$-core by its Cu_2O_2-diamond core vibration. Also, the Cu-N and Cu-O bonds that were visualized by Raman spectroscopy revealed different binding strengths of the ligands, thereby providing clues on the spatial rearrangement of the ligands.

The final complex of the **HHH**-TACzyme showed close structural resemblance with the peroxo dicopper(II) and bis(μ-oxo) dicopper(III) species found in nature, even though the chemistry of the two complexes is different. The **HDH**- and **DHD**-TACzyme based bis(μ-hydroxo) dicopper(II) complexes have not yet been encountered in nature. However, they could represent copper-versions of mimics of arginase, urease, hemerythrin and methane monooxygenase, which use manganese, nickel or iron in their active site, respectively.

Whether these three TACzymes can also act as true functional mimics of biological processes remains to be seen. Unfortunately, assessment of this was hampered by the poor solubility of our complexes in aprotic solvents. Fortunately, however, Fe(II)-H_2O_2 chemistry – that is often used for oxidation of olefins as mimics of, for instance, naphthalene dioxygenase[45] – can be performed at room temperature in mixtures of water an methanol, a solvent system that is compatible with our TACzymes. We therefore shifted our attention from Cu(I)-O_2-chemistry to Fe(II)-H_2O_2-chemistry in order to determine the performance of our TACzymes in biologically relevant iron catalyzed oxidation chemistry.

3. Mimicry of non-heme iron containing oxidation enzymes

Besides copper and other metals, metalloenzymes also use iron to catalyze controlled and selective oxidations of organic substrates and a wide variety of mono- or multinuclear iron metalloenzymes have been discovered. In general, iron metalloenzymes that are involved in oxygen activation can be divided into two groups: heme and non-heme enzymes. This last group can be either mononuclear of dinuclear and usually constitute of histidine and carboxylate ligands surrounding the iron centre(s) (*figure 9*). Important members of this class of non-heme iron enzymes are methane monooxygenase hydroxylase[46], ribonucleotide reductase[47] and fatty acid desaturase[48]. It has been suggested that the carboxylate rich ligand environment found in these enzymes may be important for the activation of molecular oxygen at non-heme diiron centres.[48]

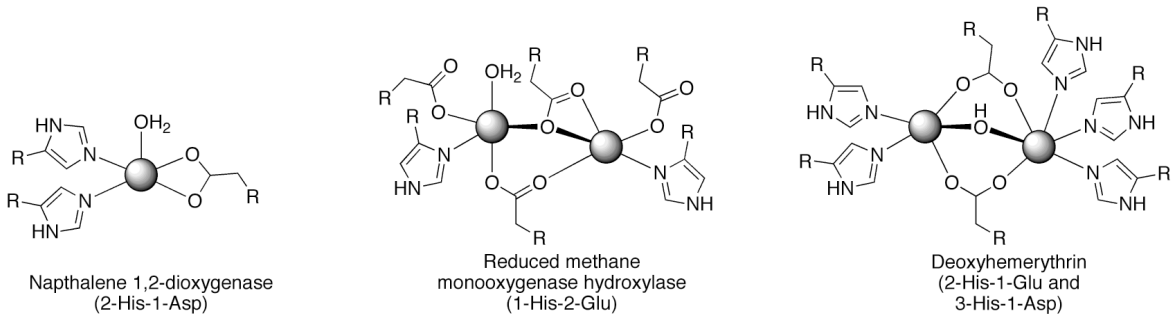

Figure 9. Three examples of mono- and dinuclear iron-containing metalloenzyme active sites that are based on imidazole and carboxylate coordination environment (iron is represented by the shaded spheres). R = remainder of the amino acid residues connected to the protein.

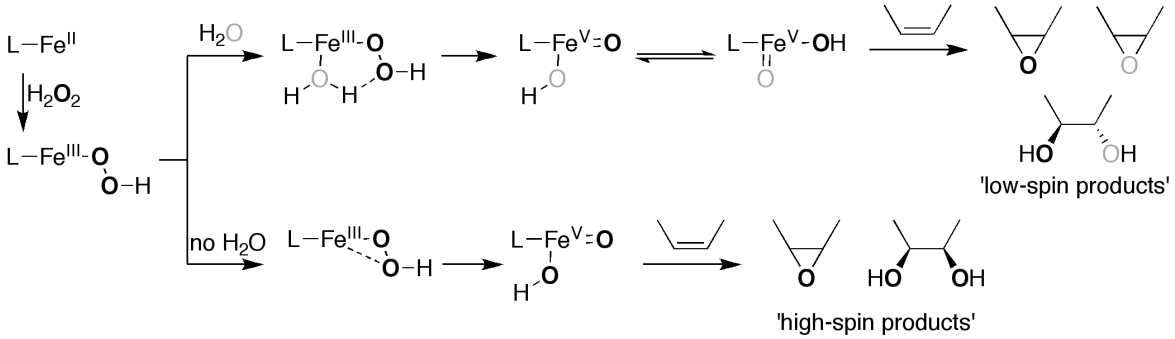

Figure 10. The two proposed pathways for the oxidation of olefins by non-heme iron catalysts.

In view of the diverse transformations that these enzymes can catalyze, it is not surprising that especially mononuclear non-heme iron oxygenases have received much attention recently and have been reviewed extensively.[1,49] Reaction mechanisms in both enzymes and model systems have been studied extensively.[50] As was the case for bio-inspired models of biological CuO-chemistry, models of non-heme iron enzymes are mostly based on pyridine, amine, *N*-methylimidazole and/or phenolate containing ligands. These studies have yielded detailed information on reaction intermediates and have produced effective catalysts for selective epoxidation or *cis*-1,2-dihydroxylation, for instance.[8] From these studies the formation of the two products by two distinct pathways was proposed (*figure 10*). Which of the two routes is followed is mostly determined by the spin-state of the iron(III)-OOH intermediate, which on its turn is greatly influenced by the type of ligand.[51]

Especially noteworthy are the recent contributions by the group of Klein Gebbink to the field of biomimetic chemistry. They described more biological relevant mimics based on 2-imidazole-1-carboxylate triads, thereby closing the gap between bioinspired and biomimetic systems.[52] Interestingly, Bruijnincx *et al*. reported that the ester-derivative of a 2-imidazole-1-carboxylate was active whereas the carboxylate counterpart was not.[53] Mimics that imitate biological systems even better, by using naturally occurring coordinating moieties like amino acid side chain functionalities, especially of histidine, aspartate and glutamate, are very rare.[54] In view of this we wanted to determine the applicability of our mimics in iron-catalyzed oxidations of olefins.

3.1. Olefin epoxidation and *cis*-dihydroxylation in Fe(II)-H_2O_2-chemistry using the HHH-, HDH-, and DHD-TACzymes

For the oxidation of olefins, Fe(II)-complexes of the three TACzymes – containing the biologically relevant 3-His (**HHH**), 2-His-1-Asp (**HDH**) or 1-His-2-Asp (**DHD**) triads – were prepared *in situ*.[55] This was done by mixing $Fe^{II}(OTf)_2 \cdot 2MeCN$ with 1.1 or 2.2 equiv of one of the TACzymes in MeOH or aceton. After incubation for 10 minutes, substrate was added followed by the dropwise addition of a solution of

hydrogen peroxide. The substrates used for the oxidation were cyclooctene, 1-octene and styrene. Of the latter two substrates, 1-octene was not oxidized and oxidation of styrene gave small amounts of epoxide (TON of 0.9 for Fe:**HHH** – 1:1 and 1.3 for Fe:**HHH** – 1:2) and benzaldehyde (TON of 6.5 for Fe:**HHH** – 1:1 and 6.9 for Fe:**HHH** – 1:2). The results for cyclooctene are shown in *table 2*.

As can be inferred from the results presented in this table, our TACzymes performed poor as ligands in the Fe(II)-H_2O_2 mediated oxidation of olefins. Turn-over numbers (TON) of the reactions in the presence of ligand were well below that of the oxidation by only Fe(II) (*cf.* entries 2-5 with entry 1). A significant drop in TON for the epoxide was observed when acetone was used instead of MeOH (*cf.* entry 2 or 4 with 6 or 7, respectively). This drop in formation of the epoxide was also found when the amount of H_2O_2 was reduced from 500 to 5-20 equivalents. The amount of epoxide slowly increased over time (entries 18-20), with most product being formed in the initial stages of the experiment. Lastly, the addition of *N*-methylimidazole or potassium acetate did not improve the reaction significantly (entries 13, 14, 16, 17, 19, and 20).

Table 2. Oxidation of cyclooctene by Fe(II)-H_2O_2 chemistry using **HHH**-, **HDH**- and **DHD**-TACzymes. Equivalents of ligand are compared to Fe(II).

	Eq. TACzyme	Eq H_2O_2	TON[c] epoxide (time in h)	TON[c] diol	Additive
1	-- [a]	500	9.99 (18)	trace	
2	1.1 **HHH** [a]	500	6.36 (18)	trace	
3	1.1 **HHH** [a]	500	5.05 (18)	trace	air
4	2.2 **HHH** [a]	500	4.69 (18)	trace	
5	2.2 **HHH** [a]	500	4.79 (18)	trace	air
6	1.1 **HHH** [b]	500	0.61 (3), 0.86 (18)	trace	
7	2.2 **HHH** [b]	500	0.46 (3), 0.73 (18)	trace	
8	1.1 **HDH** [b]	500	0.46 (3), 0.72 (18)	trace	
9	2.2 **HDH** [b]	500	0.39 (3), 0.61 (18)	trace	
10	1.1 **DHD** [b]	500	0.52 (3), 0.82 (18)	trace	
11	2.2 **DHD** [b]	500	0.38 (3), 0.64 (18)	trace	
12	1.1 **HHH** [a]	5	0.07 (18)	trace	
13	1.1 **HHH** [a]	5	0.07 (18)	trace	1 MeIm
14	1.1 **HHH** [a]	5	0.05 (18)	trace	1 KOAc
15	1.1 **HHH** [a]	10	0.11 (18)	trace	
16	1.1 **HHH** [a]	10	0.10 (18)	trace	1 MeIm
17	1.1 **HHH** [a]	10	0.28 (18)	trace	1 KOAc
18	1.1 **HHH** [a]	20	0.12 (1), 0.31 (4), 0.41 (18)	trace	
19	1.1 **HHH** [a]	20	0.17 (1), 0.29 (4), 0.42 (18)	trace	1 MeIm
20	1.1 **HHH** [a]	20	0.18 (1), 0.31 (4), 0.36 (18)	trace	1 KOAc

Notes: [a] in MeOH; [b] in acetone; [c] Yields expressed as turnover numbers (TON = mol product/mol metal).

3.3. Conclusions on the application of TACzymes in Fe(II)-H_2O_2-catalyzed olefin oxidation reactions

In general, the activity of Fe(II)-H_2O_2-mediated olefin oxidation became lower in the presence of TACzymes and the activity of TACzyme assisted oxidation of cyclooctene was low. More research has to be performed in order to establish the origin of the low activity and to come up with improvements of the system.

For instance, *in situ* spectroscopic techniques like UV-vis, infrared and Raman spectroscopy could provide detailed information on the coordination behavior of the TACzymes to iron. This could give important clues considering the extent in which the iron centre was coordinatively saturated or not. Although coordination to copper was shown to be mainly by the amino acid side chain functionalities, coordination of the TACzyme to the harder iron ion could have been different. On the other hand, rapid dissociation of the metal from the ligand might be a reason for the low activity. From the active catalysts described in literature, which all contain the coordinating atoms only separated by a few atoms (typically 2 or 3 atoms), it is likely that a larger degree of pre-organization of the ligating entities of the TACzymes will be beneficial for biomimetic catalysis.

4. Conclusions on the applicability of TACzymes in biomimetic reactions

In this chapter, the application of three TAC-based mimics of histidine and aspartate or glutamate containing metalloenzymes active sites, *i.e.* the 3-His, 2-His-1-Asp and 1-His-2-Asp triads, in two biologically relevant reactions is described. Firstly, Cu(I)-complexes of the so-called TACzymes reacted at ambient conditions readily with molecular oxygen under formation of bis(μ-hydroxo) dicopper(II) complexes. UV-vis spectroscopic analysis of this reaction showed that complexes with mostly square-pyramidal geometry were formed. Infrared and Raman spectroscopy showed coordination of N^{τ}-nitrogen atoms of the imidazole rings and predominant coordination of the carboxylate groups in a monodentate fashion. Secondly, the behavior of TACzymes in Fe(II)-H_2O_2 mediated oxidation of olefins was studied. It became clear that the effect of the TACzymes on the turnover numbers (TON) was detrimental when compared to the TON in the absence of a TACzyme.

The results presented in this chapter clearly illustrate that, although restricted by the limited solubility of the constructs, TACzymes can be close structural mimics of non-heme metalloenzyme active sites. Despite the fact that the activity is well below of many bioinspired mimics described in literature, these TAC-based mimics are truly biomimetic since they apply amino acid side chains as chelating groups for metal-ions.

5. Experimental Section

For general information, the experimental procedures as well as the synthesis of the TACzymes see the previous chapter. Methanol was dried over magnesium methoxide and distilled under N_2 prior to use. GC analyses were performed on a Perkin Elmer Autosystem XL GC (30m, PE-17 capillary column) or a Perkin Elmer Clarus 500 GC (30m) Econo-Cap EC-5) both with FID detector. $[Cu(MeCN)_4]PF_6$ was obtained from Aldrich; $Fe(OTf)_2 \cdot 2MeCN$ was prepared according to a published procedure.[56]

UV-vis analysis of the reaction between the Cu(I)-complexes and oxygen:
The HHH-TACzyme-Cu(I)-complex: A solution of the **HHH**-TACzyme in DMSO (40 mM, 200 μL) was added to a freshly prepared solution of $[Cu(MeCN)_4](PF_6)$ in DMSO (29.2 mM, 274 μL) in a cuvet. The resulting 17 mM solution of the Cu(I)-complex was analyzed immediately after preparation. The 17 mM solution was suitable for analysis of d-d transition absorptions, a 2.5 mM solution was used to measure changes in the charge-transfer bands.
The HDH-TACzyme-Cu(I)-complex: The above procedure was repeated with a solution of the **HDH**-TACzyme in DMSO (50 mM, 150 μL) and a solution of $[Cu(MeCN)_4](PF_6)$ in DMSO (50 mM, 150 μL). Addition of 300 μL resulted in a 12.5 mM solution.
The DHD-TACzyme-Cu(I)-complex: For this, a solution of the **DHD**-TACzyme in DMSO (50 mM, 150 μL) and a solution of $[Cu(MeCN)_4](PF_6)$ in DMSO (50 mM, 150 μL). Addition of 300 μL resulted in a 12.5 mM solution.

Infrared and Raman spectroscopic analysis of the final species
Both IR and Raman spectra were obtained using a dried sample of the final TACzyme bis(μ-hydroxo) dicopper(II) species. The IR-spectrum was obtained from a KBr pellet containing the dried sample; the Raman spectrum was obtained using a dried sample on a Petri-dish glass.

Oxidation of 3,5-di-*tert*-butyl-catechol by HHH-Cu^{II}-(μ-OH)$_2$-Cu^{II}-HHH
To two 2.5 mM solutions, one of a three week old and one of a freshly prepared [**HHH**-Cu^{II}-(μ-OH)$_2$-Cu^{II}-**HHH**] complex in DMSO, was added 1 equiv of 3,5-di-*tert*-butyl-catechol (11.1 mg/mL) dissolved in DMSO. An instantaneous change in color from mint-green to yellow was observed.

Oxidation of olefins using Fe(II)-H_2O_2 and the HHH-, HDH-, or DHD-TACzymes
The air-sensitive Fe(II)-TACzyme complexes were prepared *in situ* by the addition of 1 equiv of $Fe(OTf)_2 \cdot 2MeCN$ dissolved in MeOH to 1.1 or 2.2 equiv of the TACzymes in water:MeOH – 1:10 (v/v) under N_2 atmosphere. The total volume at this stage was 2 mL. After incubation for 10 minutes the substrate was added (1000 equiv) and subsequently, 0.5

mL of the hydrogenperoxide solution (5-500 equiv in MeOH diluted from 35% aqueous H_2O_2) was added dropwise over the course of 30 min. The reaction mixture was kept under N_2, after 1 h (from the start of the addition of the oxidant) 1,2-dibromobenzene (10 μL) was added as the internal standard and the first sample (0.5 mL) was collected. This sample was diluted with 0.5 mL of Et_2O and analyzed by GC.

6. Notes and References

1 See *Biological Inorganic Chemistry*, edited by I. Bertini, H.B. Gray, E.I. Stiefel, J.S. Valentine, 1st edition, University Science Books, Sausalito, **2007**.

2 See *Activation of Small Molecules: Organometallic and Bioinorganic Perspectives*, edited by W.B. Tolman, Wiley-VCH Verlag GmbH & Co. KGaA: Weinheim, Germany, **2006**; E.I. Solomon, R. Sarangi, J.S. Woertink, A.J. Augustine, J. Yoon, S. Ghosh, *Acc. Chem. Res.* **2007**, *40*, 581.

3 E.Z. Eisenmesser, O. Millet, W. Labeikovsky, D.M. Korzhnev, M. Wolf-Watz, D.A. Bosco, J.J. Skalicky, L.E. Kay, D. Kern, *Nature* **2005**, *438*, 1171; K.A. Henzler-Wildman, M Lei, V. Thai, S.J. Kerns, M. Karplus, D. Kern, *Nature* **2007**, *450*, 913; K.A. Henzler-Wildman, V. Thai, M Lei, M. Ott, M. Wolf-Watz, T. Fenn, E. Pozharski, M.A. Wilson, G.A. Petsko, M. Karplus, C.G. Hübner, D. Kern, *Nature* **2007**, *450*, 838; K.A. Henzler-Wildman, D. Kern, *Nature* **2007**, *450*, 964.

4 H. Dugas, *Bioorganic Chemistry: A Chemical Approach to Enzyme Action*, Springer, New York, 3rd edn., **1996**.

5 Peptidylglycine-alphahydroxylating monooxygenase (PHM): see S.T. Prigge, B.A. Eipper, R.E. Mains, L.M. Amzel, *Science* **2004**, *304*, 864. Nitrite reductase (NiR): see E.I. Tocheva, F.I. Rosell, A.G. Mauk, M.E.P. Murphy, *Science* **2004**, *304*, 867.

6 L. Que, Jr., W.B. Tolman, *Angew. Chem. Int. Ed.* **2002**, *41*, 1114.

7 R. Breslow, *Artificial Enzymes*, Wiley, Weinheim, 1st edn., **2005**, see also ref. 4.

8 H.-B. Kraatz, N. Metzler-Nolte, *Concepts and Models in Bioinorganic Chemistry*, Wiley-VCH, Weinheim, Germany, **2006**.

9 S.J. Lippard, *Nature Chemical Biology* **2006**, *2*, 504.

10 P.C.A. Bruijnincx, G. Van Koten, R.J.M. Klein Gebbink, *Chem. Soc. Rev.* **2008**, *37*, 2716.

11 N. Kitajima, K. Fujisawa, Y. Moro-oka, K. Toriumi, *J. Am. Chem. Soc.* **1989**, *111*, 8975. See also ref. 8.

12 N.W. Aboelella, A.M. Reynolds, W.B. Tolman, *Science* **2004**, *304*, 836.

13 H. Decker, T. Schweikardt, F. Tuczek, *Angew. Chem. Int. Ed.* **2006**, *45*, 4546.

14 C. Gerdemann, C. Eicken, B. Krebs, *Acc. Chem. Res.* **2002**, *35*, 183.

15 K.A. Magnus, B. Hazes, H. Ton-That, C. Bonaventura, J. Bonaventura, W.G.J. Hol, *Proteins: Structure, Function, and Genetics* **1994**, *19*, 302.

16 E.I. Solomon, R. Sarangi, J.S. Woertink, A.J. Augustine, J. Yoon, S. Ghosh, *Acc. Chem. Res.* **2007**, *40*, 581.

17 H. Decker, T. Rimke, *J. Biol. Chem.* **1998**, *273*, 25889.

18 D.F. Shriver, P.W. Atkins, *Inorganic Chemistry*, Oxford university press, 3rd edition, **1999**, Ghent, Belgium, see for instance p. 235-236 on coordination complexes of copper.

19 J.-P. Laussac, A. Robert, R. Haran, B. Sarkar, *Inorg. Chem.* **1986**, *25*, 2760.

20 J.A. Halfen, S. Mahapatra, E.C. Wilkinson, S. Kaderli, V.G. Young Jr., L. Que Jr., A.D. Zuberbühler, W.B. Tolman, *Science* **1996**, *271*, 1397; L. M. Mirica, X. Ottenwaelder and T. D. P. Stack, *Chem. Rev.* **2004**, *104*, 1013.

21 E.I. Solomon, R.K. Szilagyi, S. DeBeer George, L. Basumallick, *Chem. Rev.* **2004**, *104*, 419.

22 K. Nakamoto, *Infrared and Raman Spectra of Inorganic and Coordination Compounds: Applications in Coordination, Organometallic, and Bioinorganic Chemistry*; L. M. Mirica, X. Ottenwaelder and T. D. P. Stack, *Chem. Rev.* **2004**, *104*, 1013.

23 Ref. 6; L.Q. Hatcher, K.D. Karlin, *J. Biol. Inorg. Chem.* **2004**, *9*, 669; W.B. Tolman, *Acc. Chem. Res.* **1997**, *30*, 227; E.A. Lewis, W.B. Tolman, *Chem. Rev.* **2004**, *104*, 1047; A.P. Cole, V. Mahadevan, L.M. Mirica, X. Ottenwaelder, T.D.P. Stack, *Inorg. Chem.* **2005**, *44*, 7345.

24 Phenoxo-to-Cu(II) LMCT has been assigned to 420 nm: R.C. Holz, J.M. Brink, F.T. Gobena, C.J. O'Connor, *Inorg. Chem.* **1994**, *33*, 6086.

25 E. Prenesti, P.G. Daniele, M. Prencipe, G. Ostacoli, *Polyhedron* **1999**, *18*, 3233; E. Prenesti, P.G. Daniele, S. Toso, *Analytica Chimica Acta* **2002**, *459*, 323; E. Prenesti, P.G. Daniele, S. Berto, S. Toso, *Polyhedron* **2006**, *25*, 2815; E.J. Billo, *Inorg. Nucl .Chem. Lett.* **1974**, *10*, 613.

26 For instance, a simple complex like [Cu(acac)(deen)]ClO_4 (acac = acetylacetone; deen = *N*,*N*'-diethylethylenediamine) has an absorption maximum of ~ 614 nm in DMSO and ~ 600 nm in water. Differences up to 33 nm have been reported: J. Labuda, K. Mafune, Y. Fukuda, *Bull. Chem. Soc. Jpn.* **1990**, *63*, 2610; D.-T. Wu, T.-Y. Lee, C.-S. Chung, *J. Chem. Soc., Dalton Trans.* **1986**, 1995. See also *Inorganic Chromotropism, Basic Concepts and Applications of Colored Materials*, Y. Fukuda Ed., Berlin (Germany), Springer, **2007**.

27 Penta-coordinate square-planar complexes of Cu(II) display their d-d absorption at 580-670 nm approximately, whereas the maximum for trigonal bipyramidal complexes is found at higher wavelength, between 780 and 950 nm. A.G. Algarra, M.G. Basallote, C.E. Castillo, M.P. Clares, A. Ferrer, E. Gacia-Espana, J.M. Llinares, M.A. Manez, C. Soriano, *Inorg. Chem.* **2009**, *48*, 902; F. Thaler, C.D. Hubbard, F.W. Heinemann, R. van Eldik, S. Schindler, I. Fabian, A.M. Dittler-Klingemann, F.E. Hahn, C. Orvig, *Inorg. Chem.* **1998**, *37*, 4022. A square-pyramidal complex with imidazole and hydroxo groups in MeCN had a λ_{max} of 690 nm, indicating that values above 670 nm are also possible: K. Itoh, H. Hayashi, H. Furutachi, T. Matsumoto, S. Nagatomo, T. Tosha, S. Terada, S. Fujinami, M. Suzuki, T. Kitagawa, *J. Am. Chem. Soc.* **2005**, *127*, 5212.

28 Trigonal-bipyramidal Cu(II)-complexes based on the 2,2',2''-terpyridine ligands with two axial coordinating pyridinyl nitrogen atoms, one equatorial coordinating pyridinyl nitrogen atom and two equatorial coördinaten oxygen atoms from phenoxy residues have λ_{max} values of 700-720 nm in DMSO: W.L. Kwik, K.-P. Ang, *Transition Met. Chem.* **1987**, *12*, 58.

29 H. Aiba, A. Yokoyama, H. Tanaka, *Bull. Chem. Soc. Jpn.* **1974**, *47*, 1003. A similar square-pyramidal complex, with secondary amine functionalities instead of imidazole rings, in MeCN had a λ_{max} of 650 nm: S. Mahapatra, J.A. Halfsen, E.C. Wilkinson, G. Pan, X. Wang, V.G. Young Jr., C.J. Cramer, L. Que Jr. and W.B. Tolman, *J. Am. Chem. Soc.* **1996**, *118*, 11555.

30 See ref 25. A similar square-pyramidal complex with one equatorial amine and three equatorial carboxylate coordinating groups and with one axial coordinating amine group had a λ_{max} of 707 nm (Z.D. Matovic, A. Meetsma, V.D. Miletic, P.J. van Koningsbruggen, *Inorg. Chim. Acta* **2007**, *360*, 2420).

31 Using diffuse reflectance, a λ_{max} of 662 nm was observed for the square-planar complex [$Cu(pyr)_2^{eq}$(oxalato)$^{eq}(H_2O)^{ax}$]: G.A. van Albada, I. Mutikainen, U. Turpeinen, J. Reedijk, *Inorg. Chem. Commun.* **2006**, *9*, 1067.

32 Z.D. Matovíc, G. Pelosi, S. Ianelli, G. Ponticelli, D.D. Radanovic, D.J. Radanovic, *Inorg. Chimica Acta* **1998**, *268*, 221; U. Rychlewska, Z.D. Matovíc, D.D. Radanovic, M.Dj. Dimitrijevic, D.M. Ristanovic, M.M. Vasojevic, D.J. Radanovic, *Polyhedron* **2001**, *20*, 2523.

33 Ref 18, p. 235.

34 J.R. Ferraro, W.R. Walker *Inorg. Chem.* **1965**, *10*, 1382.

35 J. Gao, S.-h. Zhong, *J. Mol. Catal. A: Chem.* **1999**, *164*, 1.

36 M.J. Henson, M.A. Vance, C. Xin Zhang, H.-C. Liang, K.D. Karlin, E.I. Solomon, *J. Am. Chem. Soc.* **2003**, *125*, 5186.

37 G.B. Deacon, R.J. Philips, *Coord. Chem. Rev.* **1980**, *33*, 227. N.F. Curtis, *J. Chem. Soc. A*, **1968**, 1579.

38 V. Zelenák, Z. Vargová, K. Györyová, *Spectrochimica Acta Part A* **2007**, *66*, 262.
39 Differences in geometry can have significant effect on the observed frequencies, see for instance: B.C. Cornilsen, K. Nakamoto, *J. Inorg. Nucl. Chem.* **1974**, 36, 2467; J.A. Larrabee, T.G. Spiro, *J. Am. Chem. Soc.* **1980**, *102*, 4217.
40 W.R. McWhinnie, *J. Inorg. Nucl. Chem.* **1965**, *27*, 1063.
41 M.J. Baldwin, P.K. Ross, J.E. Pate, Z. Tyeklár, K.D. Karlin, E.I. Solomon, *J. Am. Chem. Soc.* **1991**, *113*, 8671.
42 R. Wegner, M. Gottschaldt, H. Görls, E.-G. Jäger, D. Klemm, *Chem. Eur. J.* **2001**, *7*, 2143; Y. Hitomi, A. Ando, H. Matsui, T. Ito, T. Tanaka, S. Ogo, T. Funabiki, *Inorg. Chem.* **2005**, *44*, 3473.
43 E.I. Solomon, P. Cheng, M. Metz, S.-K. Lee, A.E. Palmer, *Angew. Chem. Int. Ed.* **2001**, *40*, 4570.
44 K. Itoh, H. Hayashi, H. Furutachi, T. Matsumoto, S. Nagatomo, T. Tosha, S. Terada, S. Fujinami, M. Suzuki, T. Kitagawa, *J. Am. Chem. Soc.* **2005**, *127*, 5212.
45 A. Karlsson, J.V. Parales, R.E. Parales, D.T. Gibson, H. Eklund, S. Ramaswamy, *Science* **2003**, *299*, 1039.
46 L. Que, Jr., in *Bioinorganic Catalysis*, edited by J. Reedijk and E. Bouwman, Marcel Dekker, Inc., New York, USA, **1999**, 269-322; B.J. Waller, J.D. Lipscomb, *Chem. Rev.* **1996**, *96*, 2625; A.L. Feig, S.J. Lippard, *Chem. Rev.* **1994**, *94*, 759.
47 E. Mulliez, M. Fontecave, *Chem. Ber./Recueil* **1997**, *130*, 317.
48 L. Que, Jr., *Dioxygen Activating Enzymes*, in *Biological Inorganic Chemistry*, edited by I. Bertini, H.B. Gray, E.I. Stiefel, J.S. Valentine, 1st edition, University Science Books, Sausalito, **2007**, p. 398.
49 E.I. Solomon, T.C. Brunold, M.I. Davis, J.N. Kemsley, S.-K. Lee, N. Lehnert, F. Neese, A.J. Skulan, Y.-S. Yang, J. Zhou, *Chem. Rev.* **2000**, *100*, 235; T.D.H. Bugg, *Tetrahedron* **2003**, *59*, 7075; M. Costas, M.P. Mehn, M.P. Jensen, L. Que, Jr., *Chem. Rev.* **2004**, *104*, 939; K.D. Koehntop, J.O. Emerson, L. Que, Jr., *J. Biol. Inorg. Chem.* **2005**, *10*, 87; P.C.A. Bruijnincx, G. Van Koten, R.J.M. Klein Gebbink, *Chem. Soc. Rev.* **2008**, *37*, 2716.
50 Mechanism in oxygenases: M.M. Abu-Omar, A. Loaiza, N. Hontzeas, *Chem. Rev.* **2005**, *105*, 2227. For mechanisms in models: ref 1 and 8.
51 K. Chen, M. Costas, J. Kim, A.K. Tipton, L. Que, Jr., *J. Am. Chem. Soc.* **2002**, *124*, 3026; R. Mas-Ballesté, M. Costas, T. Van den Berg, L. Que, Jr., *Chem. Eur. J.* **2006**, *12*, 7489.
52 P.C.A. Bruijnincx, *Structural and Functional Models of Non-Heme Iron Enzymes: A Study of the 2-His-1-Carboxylate Facial Triad*, thesis, University of Utrecht, **2007**.
53 P.C.A. Bruijnincx, I.L.C. Buurmans, S. Gosiewska, M.A.H. Moelands, M. Lutz, A.L. Spek, G. van Koten, R.J.M. Klein Gebbink, *Chem. Eur. J.* **2008**, *14*, 1228. See also: P.C.A. Bruijnincx, *Structural and Functional Models of Non-Heme Iron Enzymes: A Study of the 2-His-1-Carboxylate Facial Triad*, thesis, University of Utrecht, **2007**, p. 114.
54 T.Opatz, R.M.J. Liskamp, *J. Comb. Chem.* **2002**, *4*, 275; H. Wade, S.E. Stayrook, W.F. DeGrado, *Angew. Chem. Int. Ed.* **2006**, *45*, 4951; A. Lombardi, C.M. Summa, S. Geremia, L. Randaccio, V. Pavone, W.F. DeGrado, *Proc. Natl. Acad. Sci., USA* **2000**, *97*, 6298.
55 Manganese(II), obtained from $Mn(OTf)_2 \cdot MeCN$, another metal that can be very effective in these oxydation experiments, did not show improved activity when compared to iron.
56 K.S. Hagen, *Inorg. Chem.* **2000**, *39*, 5867.

Chapter 8

Application of tris-Histidine Containing TACzymes in Asymmetric Copper(II)-Catalyzed Diels-Alder and Michael Addition Reactions

Abstract

In this chapter the results of our initial studies on the performance of the TAC(HisAc)$_3$ ligand in asymmetric copper(II)-catalyzed Diels-Alder and Michael addition reaction are described. Both for the Diels-Alder reaction and for the Michael addition reaction moderate enantioselectivity were obtained, with ee-values up to 55% for both reactions. The origin of the enantioselectivity was determined to be the chirality of the amino acid residues: the TACzyme with L-histidine amino acid residues gave excess of the opposite enantiomer with respect to the TACzyme with D-histidine residues. Surprisingly, bulky *N*-terminal extensions – *i.e.* a valine residue and isovaleric amide – completely removed the enantioselectivity. Extension on the *C*-terminus of the TAC-scaffold, *i.e.* on the C1-position of the aromatic ring, did not significantly affect the outcome. This last ligand is particularly interesting since it can be incorporated in larger systems like proteins and dendrimers.

1. Introduction

Despite the enormous diversity that is offered by TAC-based ligand systems, little or nothing is known about the properties of these ligands with respect to their performance in asymmetric reactions catalyzed by coordination complexes with metal ions. To illustrate the diversity of the ligands that can be prepared using an orthogonally protected TAC-scaffold, a TAC-scaffold decorated with the 20 proteinogenic amino acid residues directly attached to the scaffold can give rise to $20^3 = 8000$ different ligands. The chelating moieties of these potential ligands can consist of likely candidates like imidazole (His), amine (Lys or *N*-terminal amine), carboxylate (Asp or Glu), phenolate (Tyr), thiol (Cys or Met), but also less often occurring moieties like guanidine (Arg), amide (Asn or Gln), alkoxy (Ser or Thr).[1] Besides these functional amino acid residues, the incorporation of the other non-functional amino acid residues may help to tune the properties of a hit and thereby help to tune the outcome of the reaction. In view of this possible diversity, it is surprising that these constructs have not yet been used as tridentate ligands in transition metal catalyzed reactions,[2] so far we have only reported the screening of a library of TAC-based ligands for their ability to bind iron(III)[3]. So far no catalytic studies were performed on tripodal TAC-based ligand systems.[4] Recently, we have described a TAC-based mimic of tris-histidine based metalloenzyme active sites been described using copper(II) as transition metal ion.[5] In this chapter we describe our initial studies on tris-histidine containing TAC-scaffolds as ligands in asymmetric catalysis. We were especially interested to determine the effect of the chirality of the amino acid residues on the catalytic reaction and how this effect could be modulated.

1.1. Copper-catalyzed Diels-Alder and Michael addition reactions in water

The Diels-Alder (DA)[6] and Michael addition (MA)[7] reaction are among the most powerful C-C bond forming reactions known. In the past, these reactions were performed in organic solvents. More than a decade ago, the groups of Engberts and Feringa described Lewis-acid catalyzed DA and MA reactions in water.[8] Recently, the group of Roelfes has expanded on this concept using copper(II)-catalyzed Diels-Alder (DA), Michael addition (MA) and Friedel-Crafts (FC) reactions in which chirality was induced from a ligand that was embedded in DNA.[9] In this system, the most successful ligands were nitrogen atom donating aromatic di- or tridentate ligands.

With respect to the use of amino acids and peptides, a few examples have been described in the literature in which these were used for copper(II)-catalyzed DA and MA reactions in water.[10] One of the first examples was presented in 1998 by Engberts *et al*.[11] They reported that a Cu(II)-catalyzed DA reaction between cyclopentadiene and aza-chalcone in the presence of L-abrine (*N*-methyl-tryptophan) gave 74% enantiomeric excess (*ee*) (*figure 1*). Surprisingly, L-tryptophan gave only 25% *ee*, indicating that even a small *N*-terminal modification had a pronounced effect on the outcome of the reaction.

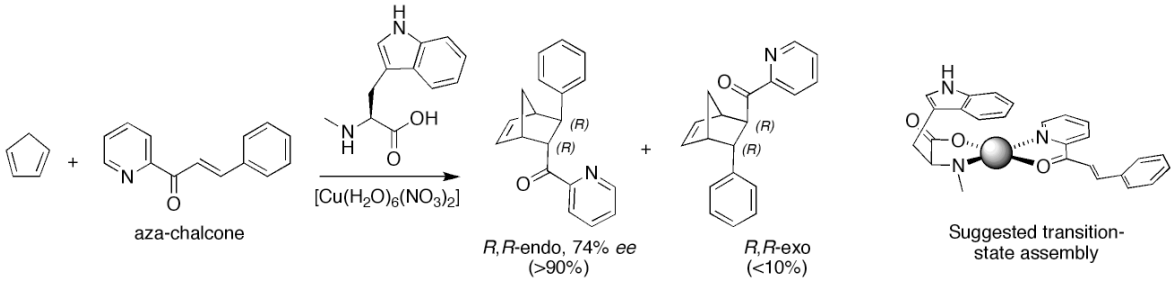

Figure 1. One of the first examples of Cu(II)-catalyzed Diels-Alder reaction in which the copper-centre formed a coordination complex with L-abrine (*right*).

Very recently, Roelfes *et al*. published a paper in which a bovine pancreatic polypeptide scaffold was used to induce enantioselectivity in Cu(II) catalyzed DA and MA reactions.[12] Although this peptide based catalyst was not as successful as their DNA-based catalysts – which gave *ee*-values >99% for the DA[13], >99% for the MA[14] and <93% for the FC[15] reaction – they still were able to obtain good *ee*-values of 80% for DA and 86% for MA reaction. It should be noted, however, that these high *ee*-values were obtained for constructs in which unnatural pyridylalanine residues were used to immobilize copper. In case of chelating histidine residues the *ee*-value dropped to just above background. A small Glu-3-pyridylalanine-Pro tripeptide gave no *ee*-value in both the DA and the MA reaction.[12] This indicates that the proximity of a structured molecular entity was needed for asymmetric catalysis, as was clearly shown for the DNA-based catalysis.

To our knowledge, only one other histidine-based ligand system has been described in the literature. Kudo *et al*. described the application of cyclo[His(Trt)-His(Trt)] in Cu(II)-catalyzed DA reactions in dichloromethane.[16] This gave only poor to moderate *ee*-values up to 40% and with an endo:exo ratio of 6.3:1. As a reference, Fmoc-His(Trt)-OMe gave no *ee* with an endo:exo ratio of 14:1. Unfortunately, unprotected histidine residues were not tested and since these values were determined in DCM they were not suitable for comparison with the values obtained with our TAC-based systems. For this comparison we used the results recently published by Roelfes *et al*.[14]

In view of the small number of histidine containing systems as catalysts and the absence of knowledge about the behavior of TAC-based tridentate ligands in asymmetric catalysis, we wanted to explore the performance of our tris-histidine based TACzyme ligand in copper(II)-catalyzed DA and MA reactions.

2. Synthesis and catalytic properties of tris-histidine containing TACzymes

Several tris-histidine containing TAC-scaffolded constructs were prepared and their performance in Cu(II)-catalyzed DA and MA was measured. We prepared five ligand systems containing the tris-histidine triad, each with a slightly different modification in order to determine the scope of these ligands.

To determine the effect of the chirality of the C^{α}-carbon atom on the outcome of the reaction, TAC(L-His-Ac)$_3$ (**8**) and TAC(D-His-Ac)$_3$ (**6**) were tested. The effect of *N*-terminal extension was assessed using the tris-L-histidine residue containing TAC-scaffold with three different *N*-terminal acyl groups: acetyl (**8**), valine-acetyl (**10**) and isovaleric amide (**9**). The effect of *C*-terminal extensions on the TAC-scaffold could be tested due to the presence of H_2N-Glu($NHCH_2CH_2CH_2N_3$)-TAC(L-His-Ac)$_3$ (**17**) in our laboratory.[17] This last ligand is particularly interesting since the *C*-terminally positioned azide functionality allows further derivatization of the ligand so that it can be incorporated into proteins,[18] on surfaces[19] or on dendrimers,[17] for instance.

2.1 Synthesis of the ligands

For synthesis of the ligands, tri-*o*-NBS protected TAC-scaffold **1** was used (*scheme 1*). This was prepared according to a literature procedure[20] from bis-bromide **2** and the fully protected triamine **3** using Cs_2CO_3 as a base. Saponification resulted in scaffold **1** which could directly be applied in the synthesis of the ligands using standard solid-phase peptide chemistry.

First, a polystyrene resin decorated with the Rink-linker was functionalized with scaffold **1** using BOP and D*i*PEA as coupling reagents. The *o*-NBS protecting groups of resin **4** were removed by treatment of the resin with a mixture of 2-mercaptoethanol and DBU (*scheme 1*). Subsequently, the TAC-loaded resin **5** was divided in two portions, one with approximately 75% of the original amount (arrow **B**) and one with approximately 25% of the original amount of resin (arrow **A**). To the free amines of the larger portion, Fmoc-L-His(Trt)-OH was attached using BOP/D*i*PEA (arrow **B**). The scaffold of the smaller portion was derivatized with Fmoc-D-His(Trt)-OH also using BOP and D*i*PEA (arrow **A**). Both portions were then subjected to Fmoc-removal conditions using piperidine after which the larger portion was divided in three equal portions (arrows **C**, **D**, and **E**). One portion containing the L-histidine derivative (arrow **C**) and the portion containing the D-histidine derivative (arrow **A**) were *N*-terminally protected with the acetyl-group. This prevented undesired coordination of *N*-terminally amine functionalities. Cleavage of these two resin bound TACzymes resulted in tridentate ligand systems with L-histidine (**8**) and D-histidine (**6**) amino acid derivatives in high purity and good yields.

The two remaining equal portions of **7** were acylated with two different acyl-groups. For one portion, the terminally amine was acylated with isovaleric acid using BOP and D*i*PEA (arrow **D**). The other portion was derivatized with Ac-Val by coupling first Fmoc-Val-OH using BOP/DiPEA and subsequent conversion of the Fmoc group to the Ac group (arrow **E**). After simultaneous side-chain deprotection and cleavage from the resin TACzymes **9** and **10** were obtained in high yields and of good purity. Purification by preparative HPLC afforded the pure products. All products were analyzed by HPLC and ESI-MS.

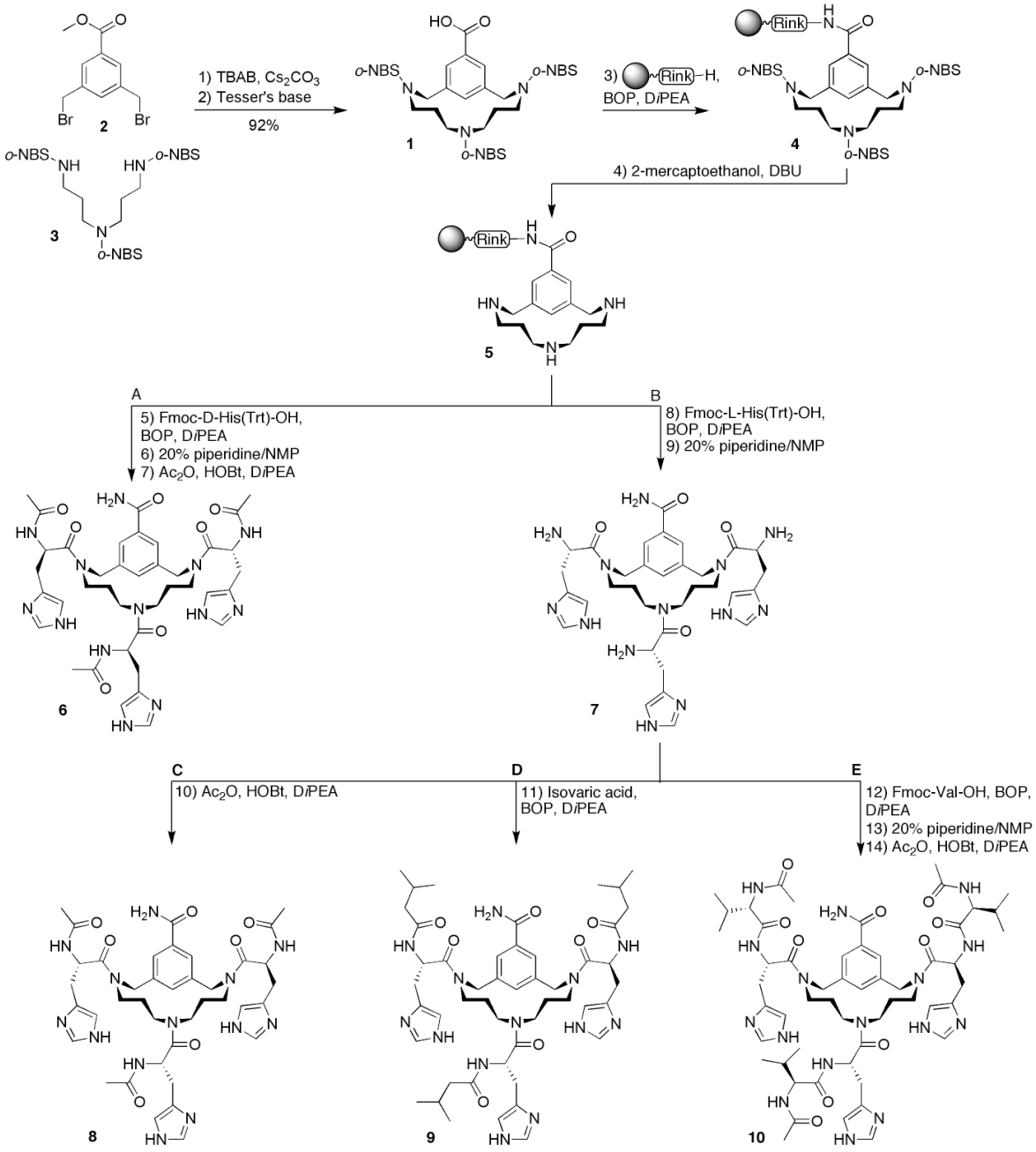

Scheme 1. Synthesis of four tris-histidine containing TACzymes used in this study.

These four tris-histidine containing TACzymes were now suitable to assess their properties in copper(II) catalyzed reactions. The synthesis of *C*-terminally modified tris-histidine containing TAC-scaffold **17** (*figure 2*) has been described elsewhere.[17]

2.2 Copper catalyzed Diels-Alder (DA) reaction

For the copper-catalyzed DA reaction, which is superior to the zinc(II) catalyzed DA reaction[21], cyclopentadiene **11** and two different dienophiles were used: α,β-unsaturated 2-acyl pyridine or aza-chalcone **12** and α,β-unsaturated 2-acyl 1-methylimidazole **13**

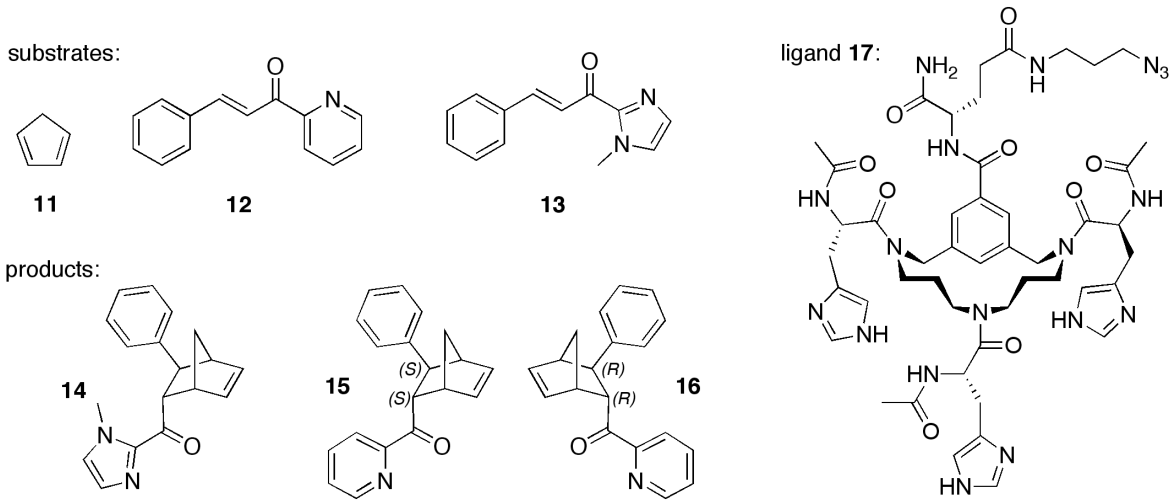

Figure 2. Structures of cyclopentadiene **11**, the two dienophiles **12** and **13**, *endo*-products **14** and two enantiomers of the *endo*-products **15** and **16** of the copper(II)-catalyzed Diels-Alder reaction. The structure of ligand **17** is also given.

(*figure 2*). The results of this reaction in the presence of $Cu(H_2O)_6(NO_3)_2$ and five tris-histidine based TACzyme ligands (**6**, **8**, **9**, **10**, and **17**) are given in *table 1.*

In the absence of a ligand a mixture of *endo*:*exo* of 93:7 with no *ee* was obtained (entry 0).[11,22] As in other systems,[9] the *endo* product was strongly favoured over the *exo* product[23], only in the case of ligand **17** and substrate **12** (Pyr) some *exo* product was formed, albeit with a low *ee*-value (entry 9). The necessity of copper(II) for this reaction was apparent from the reaction with ligand **17** in the absence of copper, which gave low conversion (< 5%) and a racemic mixture of the products. For the *N*-acetylated histidine residue containing TACzymes **6** and **8** good *ee*-values of 40-55% were observed (entries 1-4), which were similar to the ones described for the first generation of DNA-based catalysts.[24] Compared with a recently published Cu(II)-complex based on a bovine pancreatic polypeptide scaffold with histidine residues as chelating moieties, resulting in *ee* <3%, this *ee*-value is remarkable.[12]

Concerning the origin of the enantioselectivity, the results in entries 1-4 clearly indicate that the origin of the induced chirality if found at the chiral C^{α}-carbon atoms of the amino acids. Surprisingly, *N*-terminal extensions as present in ligands **9** and **10** completely suppressed the enantioselectivity of the complexes (entries 5-8). In the one case that some enantiomeric excess was observed (entry 5) it was the opposite enantiomer than was found for the acetylated ligand (entry 1). The same was observed for TACzyme **17**, a slightly lower *ee*-value of the opposite enantiomer as produced by **8** was observed (*cf.* entry 9 and 10 with 1 and 2). This was unexpected even though a recent study showed that even a small change in an ordered structure completely suppressed enantioselectivity.[25] Lastly, the stereoselectivity is temperature dependent, which would be expected for catalysis by a coordination complex (entry 9).

Table 1. Results of the Diels-Alder reaction between diene **11** and two dienophiles – α,β-unsaturated 2-acyl pyridine (Pyr, **12**) and α,β-unsaturated 2-acyl 1-methylimidazole (MeIm, **13**) – catalyzed by several Cu(II)-TACzyme complexes.

Entry	TACzyme	Dienophile	Conversion (%)	ee_{endo} (%)	ee_{exo} (%)[c]
0[11,12]	--	Pyr	full	0	nd
1	**8**	Pyr	full	55 (2*R*,3*R*)	nd
2	**8**	MeIm	full	54 (2*R*,3*R*)	nd
3	**6**	Pyr	full	50 (2*S*,3*S*)	nd
4	**6**	MeIm	> 80	40 (2*S*,3*S*)	nd
5	**10**	Pyr	full	9 (2*S*,3*S*)	nd
6	**10**	MeIm	full	< 5	nd
7	**9**	Pyr	full	< 5	nd
8	**9**	MeIm	full	< 5	nd
9	**17**[a]	Pyr	full	42 (25[b]) (2*R*,3*R*)	16 (6[b])
10	**17**[a]	MeIm	full	39 (2*R*,3*R*)	nd

Conditions: Ligand (30%/mol), $Cu(H_2O)_6(NO_3)_2$ (23%/mol), dienophile (1 mM), MOPS buffer (20 mM, pH 6.5, 300 μL), cyclopentadiene **11** (1.5 μL, 18 mmol), 5 °C, 3 days. HPLC: AD 99:1 (**12**); ODH 98:2 (**13**). *Notes*: [a] reaction stopped after 2 days; [b] reaction at room temperature; [c] nd means not determined and indicates that small amounts of racemic product was formed.

2.3 Copper catalyzed Michael addition (MA) reaction

The TAC-based tris-histidine amino acid residue containing ligands were also applied in copper-catalyzed MA reactions. For these, azachalcone **12** and Ph-imidazole **13** were used as substrates and nitromethane (NM) **18** or dimethyl malonate (DMM) **19** were used as nucleophiles (*figure 3*). The results of the reaction of these nucleophiles with Michael-acceptors **12** or **13** in the presence of $Cu(H_2O)_6(NO_3)_2$ and five tris-histidine TACzyme ligands (**6**, **8**, **9**, **10**, and **17**) are given in *table 2*.

As was the case for copper-catalyzed DA reactions, the MA reactions catalyzed by the coordination complexes of copper(II) and the tris-histidine TAC-based ligands also showed enantioselective catalysis. Firstly, as was the case for the DA reaction, the chirality of the attached histidine residues determined the outcome of the reaction (entries 11-14). The enantiomeric excess was not identical and was very different for the reaction of DMM with MeIm (entries 12 and 14), but the chirality of the product is opposite for each of the ligands. Secondly, for the L-histidine containing TACzymes **8**

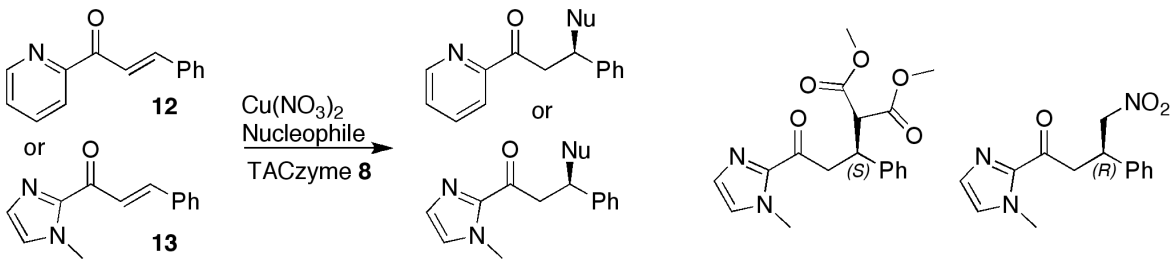

Figure 3. Michael-addition reaction of a nucleophile to α,β-unsaturated carbonyl compounds **12** or **13**. The major species for the reaction of **13** with the two nucleophiles (DMM, *left*; NM, *right*) in the presence of TACzyme **8** are shown on the right.

Table 2. Results of the Michael-addition of nitromethane (NM) **18** or dimethyl malonate (DMM) **19** to two electrophiles, α,β-unsaturated 2-acyl pyridine (Pyr) **12** and α,β-unsaturated 2-acyl 1-methylimidazole (MeIm) **13** catalyzed by several Cu(II)-TACzyme complexes.

Entry	TACzyme	Electrophile	Nucleophile	Conv. (%)	*ee* (%)
11	**8**	Pyr	DMM	full	14 (*S*)
12	**8**	MeIm	DMM	full	54 (*S*)
13	**6**	Pyr	DMM	full	25 (*R*)
14	**6**	MeIm	DMM	full	20 (*R*)
15	**9**	Pyr	DMM	full	< 5
16	**9**	MeIm	DMM	full	< 5
17	**10**	Pyr	DMM	full	< 5
18	**10**	MeIm	DMM	full	< 5
19	**17**	Pyr	NM	full	39 (*R*)
20	**17**	Pyr	DMM	full	6 (*S*)
21	**17**	MeIm	NM	full	43 (*R*)
22	**17**	MeIm	DMM	full	23 (*S*)

Conditions: Ligand (30%/mol), $Cu(H_2O)_6(NO_3)_2$ (23%/mol), substrate (1 mM), MOPS buffer (20 mmol, pH 6.5, 300 μL), nucleophile (100 eq), 3 days, 5 °C. HPLC: AD 99:1 (**12**); ODH 98:2 (**13**).

and **17**, the stereoselectivity for the Michael addition of DMM seemed to be substrate dependent with the highest *ee*-values obtained for MeIm (*cf.* entries 11, 12, 20 and 22). The opposite and to a much smaller extent was the case for the D-histidine containing TACzyme **6**. Thirdly, *N*-terminal extensions of the histidine residues leading to **9** and **10** completely reduced the enantioselectivity for all four reactions (entries 15-18), as was also the case for the DA reaction (entries 5-8, *table 1*). With respect to *C*-terminal extension of the TAC-scaffold, the enantioselective addition of DMM to the electrophiles was lower for ligand **17** (6 and 23%, entries 20 and 22, respectively) than for ligand **8** (14 and 54%, entries 11 and 12, respectively). Lastly, the addition of NM is more enantioselective than the addition of DMM (*cf.* entries 19 and 21 with entries 20 and 22).

3. Discussion and Conclusions

TAC-based tris-histidine triad containing ligand systems in which the *N*-termini are acetylated can be used in asymmetric copper(II)-catalyzed Diels-Alder (DA) and Michael addition (MA) reactions. Enantiomeric excess up to 55% for both the DA and MA reaction was observed. The enantioselectivity of the ligands was largely determined by the chirality of the histidine amino acid residues. However, the difference in *ee*-values for the MA of DMM to the α,β-unsaturated 2-acyl 1-methylimidazole, for instance, in the presence of the L- (**8**) or D-histidine (**6**) containing TACzyme, *i.e.* 54% *S* for **8** *vs.* 20% *R* for **6**, indicated that an additional effect might have been present. Also, bulky *N*-terminal substituents like isovaleric amide and valine completely suppressed the enantioselectivity. Expansion on the *C*-terminus of the TAC-scaffold does not affect the outcome of the reaction significantly.

4. Experimental section

General information: see chapter 5 for detailed general information. Reported retention times (t_R) were obtained on a Shimadzu HPLC system with a standard gradient of water/ MeCN/TFA – 95/5/0.1 (v/v) to MeCN/water/TFA – 95/5/0.1 (v/v) in 25 min.

TACzymes 8 and 17: Syntheses of these have been described elsewhere.[26]

Tris-D-histidine containing TACzymes 6

The synthesis of this construct was performed similarly to the synthesis of **8** with the exception that 2 equiv of the more expensive Fmoc-D-His(Trt)-OH (650 mg, 1 mmol) was used. Also, 0.25 g of resin with a loading of 0.7 mmol/g was used in order to reduce the required amount of this building block. This amino acid building block was coupled using BOP (442 mg, 1 mmol) and D*i*PEA (348 μL, 2 mmol) in NMP. A chloranil test indicated that the coupling was successful. After removal of the Fmoc-group and protection of the *N*-terminus with the acetyl-groups, the resin-bound construct was cleaved from the resin and simultaneously deprotected. Purification by column chromatography (eluent: $CHCl_3$/ MeOH/25% NH_4OH (aq) – 8/3/0.5 (v/v)) and lyophilization gave TACzyme **6** as white solid. Yield: 132.5 mg (163 μmol; 93%). ESI-MS: m/z = 837.25 (calculated: 836.89 for $[M+Na]^+$) and 815.40 (calculated: 814.91 for $[M+H]^+$). HPLC: t_R = 12.10 min (C_{18}).

Tris-histidine containing TACzymes 9 and 10

Synthesis of these constructs was identical to that for the synthesis of constructs **6** and **8** until the Fmoc-removal step. After this, the resin was split in two equal portions of 0.5 g each (loading = 0.7 mmol/g): one portion was used for the synthesis of **9** and the other portion was used for **10**. For the synthesis of **9**, the *N*-terminus was acylated with isovaleric acid (4 equiv, 4 mmol, 464 μL) using BOP (4 equiv, 4 mmol, 1.86 g) and D*i*PEA (8 equiv, 8 mmol, 1.46 mL) in NMP (3 mL). After coupling the resin was extensively washed with NMP (3×6 mL, each 2 min) and DCM (3×6 mL, each 2 min) and the coupling was verified with a Kaiser-test. For the synthesis of **10**, the *N*-terminus was acylated with Fmoc-Val-OH (4 equiv, 4 mmol, 1,43 g) using BOP (4 equiv, 4 mmol, 1.86 g) and D*i*PEA (8 equiv, 8 mmol, 1.46 mL) in NMP (3 mL). After coupling the resin was extensively washed with NMP (3×6 mL, each 2 min) and DCM (3×6 mL, each 2 min) and coupling was again verified with a Kaiser-test. In order to complete the synthesis of **10**, the Fmoc-group was removed using 20% piperidine/NMP and the resin washed with NMP (3×6 mL, each 2 min) and DCM (3×6 mL, each 2 min). Deprotection of the amine functionality was monitored with a Kaiser test and the liberated amine was acetylated using a capping solution that consisted of Ac_2O, HOBt and D*i*PEA in NMP.

After completion of the solid-phase synthesis, the constructs were cleaved from the resin

and 50 mg of the crude material of both **9** and **10** was purified with preparative HPLC. Pure fractions were pooled and lyophilized. After this, TACzymes **9** and **10** were dissolved in water, the pH of the solution was set at ~ 7 and the samples were again lyophilized. Yield of **9**: 68.7 mg (73 μmol, 22%). ESI-MS: m/z = 940.25 (calculated: 940.55 for $[M+H]^+$); HPLC: t_R = 15.14 min (C_{18}). Yield of **10**: 101.2 mg (91 μmol, 27%). ESI-MS: m/z = 1111.55 (calculated: 1111.62 for $[M+H]^+$); HPLC: t_R = 14.00 min (C_{18}).

Catalytic studies: these were performed according to literature procedures.[12] Conditions have been briefly indicated under *table 1* and *table 2*.

5. References and Notes

1 See *Biological Inorganic Chemistry*, edited by I. Bertini, H.B. Gray, E.I. Stiefel, J.S. Valentine, 1st edition, University Science Books, Sausalito, **2007**.

2 O. Lavastre, F. Bonnette, L. Gallard, *Current Opinion in Chemical Biology* **2004**, *8*, 311.

3 T. Opatz, R.M.J. Liskamp, *J. Comb. Chem.* **2002**, *4*, 275.

4 For an example of the application of tweezers in catalysis: A.J. Brouwer, H.J. van der Linden, R.M.J. Liskamp, *J. Org. Chem.* **2000**, *65*, 1750.

5 H.B. Albada, F. Soulimani, B.M. Weckhuysen, R.M.J. Liskamp, *Chem. Commun.* **2007**, 4895.

6 O. Diels, K. Alder, *Liebigs Annalen der Chemie* **1928**, *460*, 98.

7 A. Michael, *J. Prakt. Chem.* **1887**, *35*, 349.

8 DA reaction: S. Otto, J.B.F.N. Engberts, *Tetrahedron Lett.* **1995**, *36*, 2645; MA reaction: E. Keller, B.L. Feringa, *Tetrahedron Lett.* **1996**, *37*, 1879.

9 A.J. Boersma, *DNA-catalyzed Asymmetric Catalysis*, thesis, **2009**, Rijksuniversiteit Groningen. Available online at: http://dissertations.ub.rug.nl/FILES/faculties/science/2009/a.j.boersma/

10 J. Paradowska, M. Stodulski, J. Mlynarski, *Angew. Chem. Int. Ed.* **2009**, *48*, 4288 and references cited therein.

11 S. Otto, G. Boccaletti, J.B.F.N. Engberts, *J. Am. Chem. Soc.* **1998**, *120*, 4238.

12 D. Coquière, J. Bos, J. Beld, G. Roelfes, *Angew. Chem. Int. Ed.* **2009**, *48*, 5159.

13 G. Roelfes, A.J. Boersma, B.L. Feringa, *Chem. Commun.* **2006**, 635; A.J. Boersma, B.L. Feringa, G. Roelfes, *Org. Let.* **2007**, *9*, 3647.

14 D. Coquière, B.L. Feringa, G. Roelfes, *Angew. Chem. Int. Ed.* **2007**, *46*, 9308.

15 A.J. Boersma, B.L. Feringa, G. Roelfes, *Angew. Chem. Int. Ed.* **2009**, *48*, 3346.

16 M. Furutani, S. Sakamoto, K. Kudo, *Heterocycles* **2009**, *78*, 1171.

17 H.B. Albada, C.J. Arnusch, H.M. Branderhorst, A.-M. Verel, W.T.M. Jansen, E. Breukink, B. de Kruijff, R.J. Pieters, R.M.J. Liskamp, *Bioorg. Med. Chem. Lett.* **2009**, *19*, 3721.

18 T. Ueno, S. Abe, N. Yokoi, Y. Watanabe, *Coord. Chem. Rev.* **2007**, *251*, 2717.

19 G.D. Pirngruber, L Frunz, M. Lüchinger, *Phys. Chem. Chem. Phys.* **2009**, *11*, 2928.

20 M.C.F. Monnee, A.J. Brouwer, R.M.J. Liskamp, *QSAR & Combinatorial Science* **2004**, *23*, 546.

21 S. Otto, J.B.F.N. Engberts, *Tetrahedron Lett.* **1995**, *36*, 2645; E.J. Corey, T.W. Lee, *Tetrahedron Lett.* **1997**, *38*, 5755.

22 S. Otto, F. Bertoncin, J.B.F.N. Engberts, *J. Am. Chem. Soc.* **1996**, *118*, 7702.

23 G. Roelfes, B.L. Feringa, *Angew. Chem. Int. Ed.* **2005**, *44*, 3230.

24 See ref. 24: an *ee* up to 49% was reported (for *endo* product).

25 See ref. 12: substitution of one amino acid (L24A) that was positioned close to the active site resulted in a drop from 80% to 4%. Also consider the difference between L-tryptophan and L-abrine mentioned in the introduction.

26 TACzyme **8**: ref. 5; TACzyme **17**: ref. 17.

Chapter 9

Synthesis of Vancomycin-TACzyme Conjugates and Evaluation of their Applicability as Scorpionate Antibiotics

Abstract

In this chapter the synthesis and initial evaluations of vancomycin-TACzyme conjugates is described. These compounds might encompass an alternative approach for fighting pathogens. For this approach, a TAC-based enzyme active site mimic – a TAC-scaffold containing three histidine residues – was conjugated in a mono- and tetravalent fashion to vancomycin. A convenient synthesis of the construct was developed in which both parts of the conjugate were connected via copper-catalyzed acetylene-azide cycloaddition chemistry. Targeted hydrolysis was shown in a model system. Unfortunately, MIC-values showed that attachment of TACzymes to vancomycin reduced the activity of the latter. Nevertheless, the synthesis of these novel drugs is convenient and higher activity might be obtained using more active TACzymes and tuning the spacer properties.

Parts of this chapter have been published: H.B. Albada, C.J. Arnusch, H.M. Branderhorst, A.-M. Verel, W.T.M. Janssen, E. Breukink, B. de Kruijff, R.J. Pieters, R.M.J. Liskamp, *Bioorg. Med. Chem. Lett.* **2009**, *19*, 3721.

1. Introduction

One of the potential applications of artificial enzymes, enzyme mimics or synthetic hydrolases[1] can be found in the development of new drugs. The ever-increasing reports on multi drug resistant pathogens found in hospitals[2] urges the scientific community to find new drugs[3] and novel approaches to fight pathogens.[4] Specifically, conjugation of an active molecule to a molecule with different activity can lead to novel and more powerful drugs.[5] Examples of this approach can be found in molecular constructs used in the treatment of tumors,[6] targeted hydrolysis of DNA and proteins[7] and for hydrolysis bacterial cell-wall components.[8] In case of the development of an effective drug, the latter example can be regarded as a first step towards the development of a hydrolytic drug. In view of the challenge of constructing hydrolytic drugs and our interest in the construction of artificial hydrolase mimics, we performed some initial experiments to synthesize and evaluate a conjugate of a close structural mimic of an enzyme active site[9] and vancomycin.

The combination of vancomycin, an antibiotic that targets a specific part of a pathogen,[10] with a nonselective hydrolysis catalyst, may result in the emergence of hydrolytic drugs capable of targeting. Since the cell-wall targeting propensity of vancomycin resembles the head of a scorpion that tracks down its prey, and the hydrolytic part resembles the stinging action of the tail of a scorpion, delivering a deadly sting to the target, these constructs are denoted 'scorpionate antibiotics'. Moreover, as the enzyme active site mimic is based on the TAC-scaffold, this part of the conjugate is called TACzyme. For the synthesis of these scorpionate antibiotics we relied on the now established click-cycloaddition chemistry as a valuable synthetic linkage between the two structural moieties.[11]

1.1. Vancomycin

Vancomycin – often called the drug of last resort – targets specifically a *C*-terminal D-Ala-D-Ala-OH motive present in the cell-wall precursor of Gram-positive bacteria.[12] The affinity of vancomycin for an analogue of the cell-wall precursor, *i.e.* Ac-Lys(Ac)-D-Ala-D-Ala-OH is in the μM range.[13] This is mainly caused by strong hydrogen bonds between host and guest in the hydrophobic interior of the drug (*figure 1*).

Many derivatives of vancomycin have been described and it has been shown that the addition of a hydrophobic moiety generally leads to an increased activity.[15] This increase in activity is thought to be due to membrane anchoring of the drug, thereby enhancing the effective molarity of the drug at the bacterial cell-wall. Also, trimerization of vancomycin has been shown to increase the affinity towards trimeric D-Ala-D-Ala sequences.[16] Multimerization as result of hydrophobic interactions might therefore also play a role in the enhanced activity of hydrophobic constructs.

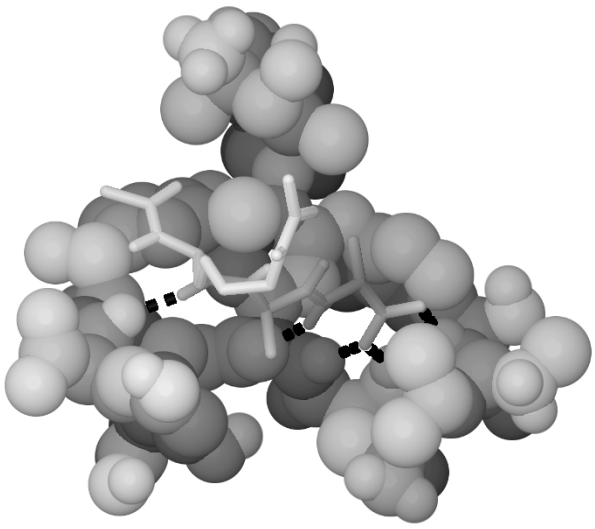

Figure 1. X-ray crystal structure of vancomycin (spacefilling model) bound to Ac-Lys(Ac)-D-Ala-D-Ala (stick model).[14] The five intermolecular hydrogen bonds are depicted in black.

Thus this drug used as a targeting devise, which is facilitated by the presence of several alkyne-functionalized vancomycin derivatives in our laboratory. By exploring the synthetic availability of these constructs, we might be able to gain insight into the possibilities of using even more powerful enzyme mimics in a latter stage.

1.2. TACzyme

Mimicry of enzyme active sites, especially those of hydrolytic enzymes,[17] has received considerable attention ever since the unraveling of the structures of enzyme active sites.[18] In the search towards hydrolase mimics it has been discovered that especially mimics containing histidine residues, or more generally imidazole rings, are most successful in the catalysis of hydrolytic reactions.[19] With respect to this, it is noteworthy that many enzyme active sites both of functional group enzymes (like serine and cysteine proteases) and of cofactor enzymes (like metalloproteases) involve at least one crucial histidine residue.[20]

Recently, we have described the synthesis and characterization of a TAC-based tridentate ligand as a mimic of tris-histidine triads often found in copper metalloenzymes (*figure 2*, left).[21] Although the binding mode of this TAC-based mimic with Zn(II) can be different from that which was earlier described for Cu(II), it still might resemble the active site of many Zn(II)-containing metalloproteases (*figure 2*, middle).[22] Interestingly, some very powerful snake venoms contain proteases having tris-histidine bound Zn(II) active sites to mediate hydrolytic reactions (*figure 2*, right).

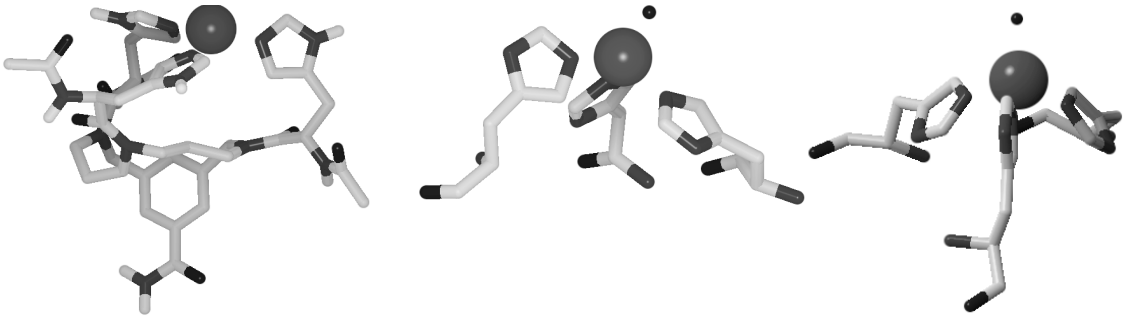

Figure 2. TAC-based mimic of tris-histidine metal binding sites (*left*). Possible similarity with: the active site of a tris-His-based Zinc metalloprotease (*middle*)[23], and with a Zinc metalloprotease active site found in sharp-nosed viper venom (*right*)[24]. Metal-ions are represented by the spheres, dots represent coordinated water.

2. Synthesis of vancomycin-TACzyme conjugates

The synthesis consisted of the preparation of two parts: that is the azide functionalized TACzyme and the alkyne functionalized vancomycin. These two parts were then conjugated using cycloaddition click-chemistry to give the potential scorpionate antibiotic.

2.1. Synthesis of the azide functionalized TACzyme

The azide functionalized TACzyme was prepared using solid-phase peptide chemistry similar to previously described procedures.[25] Since thiolate mediated deprotection of the *o*-NBS protected amines of the TAC-scaffold most likely to also reduce the azide functionality,[26] the azide had to be incorporated after *o*-NBS deprotection. Therefore, Fmoc-Glu(OAll)-OH was attached to the polystyrene-Rink resin, of which the allyl-ester protected carboxylic acid functionality could be accessed after completion of the tris-histidine triad.

First, the Fmoc protecting group of **1** was removed and the *o*-NBS protected TAC-scaffold was attached. The tris-histidine triad could be installed after 2-mercaptoethanol/DBU mediated *o*-NBS deprotection of **2** followed by coupling of Fmoc-His(Trt)-OH. The Fmoc protecting groups were replaced by acetyl groups, which allowed a more reliable mimicry of the protein backbone and prevented undesired coordination to the metal-ion by *N*-terminal amine functionalities. Lastly, the allyl-ester of the glutamate side-chain of **3** was removed using $Pd(PPh_3)_4$ and 3-aminopropylazide was coupled in order to introduce the azide moiety. Cleavage from the resin with TFA/TIS/water resulted in mimic **4**, which after preparative HPLC was used for conjugation to alkyne functionalized vancomycin.

2.2. Synthesis of alkyne-functionalized vancomycin

The vancomycin alkyne derivatives **7a** and **7b** were prepared from unprotected

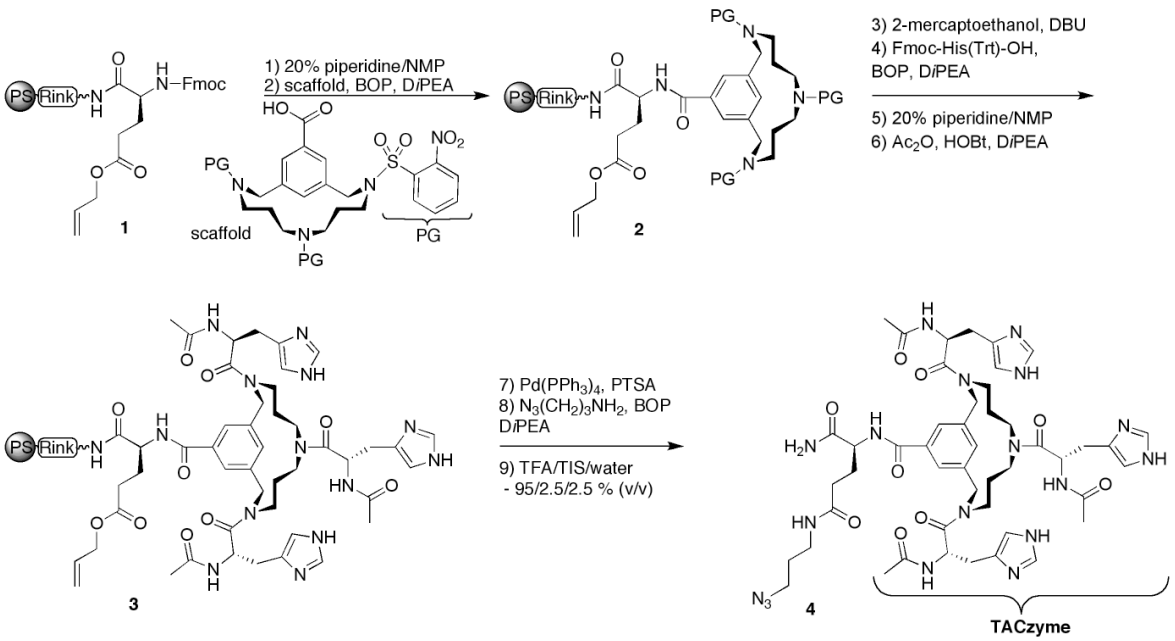

Scheme 1. Solid-phase synthesis of the *C*-terminally azide-functionalized tris-histidine triad mimic (**4**) (PTSA = anilinium *p*-toluenesulfinate).

vancomycin and mono-alkyne functionalized PEG-spacer **6a** and tetra-alkyne functionalized PEG-spacer **6b**, respectively. A tetravalent alkyne spacer was coupled since we anticipated a positive multivalency effect with respect to the hydrolytic activity of the construct.[27] Coupling of spacer **6a** or **6b** to vancomycin was achieved by EDC, HOAt and D*i*PEA (*scheme 2*). The resulting products **7a** and **7b** were purified by preparative HPLC.

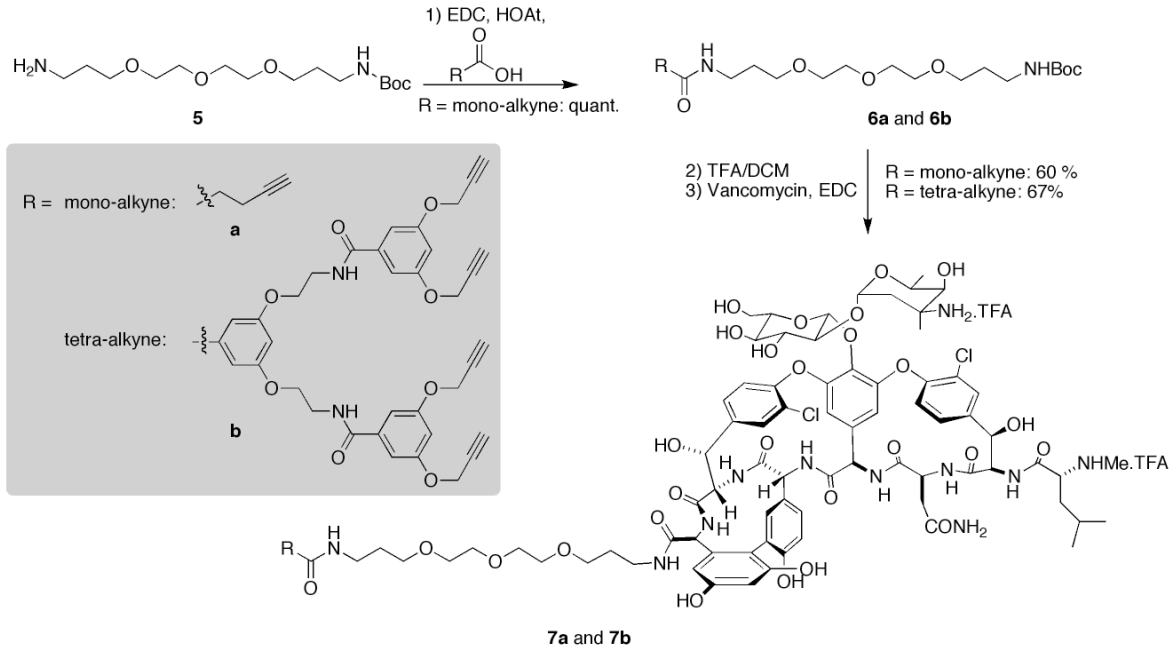

Scheme 2. Synthesis of alkyne-functionalized vancomycin **7a** and **7b**.

2.3. Synthesis of Vancomycin-TACzyme conjugates

Conjugation of the two parts of the scorpionate antibiotic was achieved by click-chemistry using $CuSO_4$ and sodium ascorbate in a microwave (*scheme 4*). For comparison, a tetravalent TACzyme without vancomycin was also prepared (*scheme 3*).

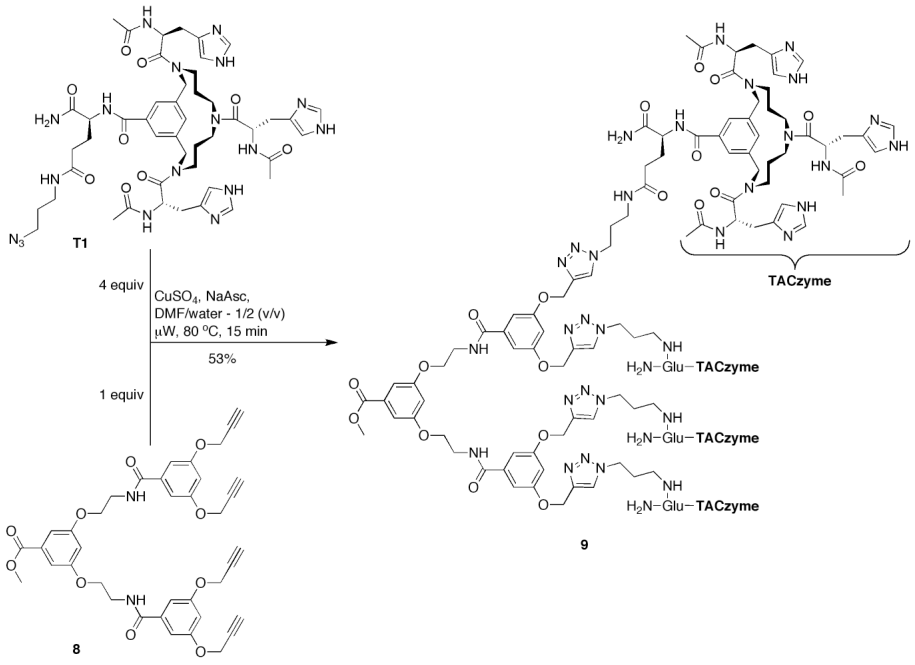

Scheme 3. Synthesis of tetravalent TACzyme dendrimer **9**.

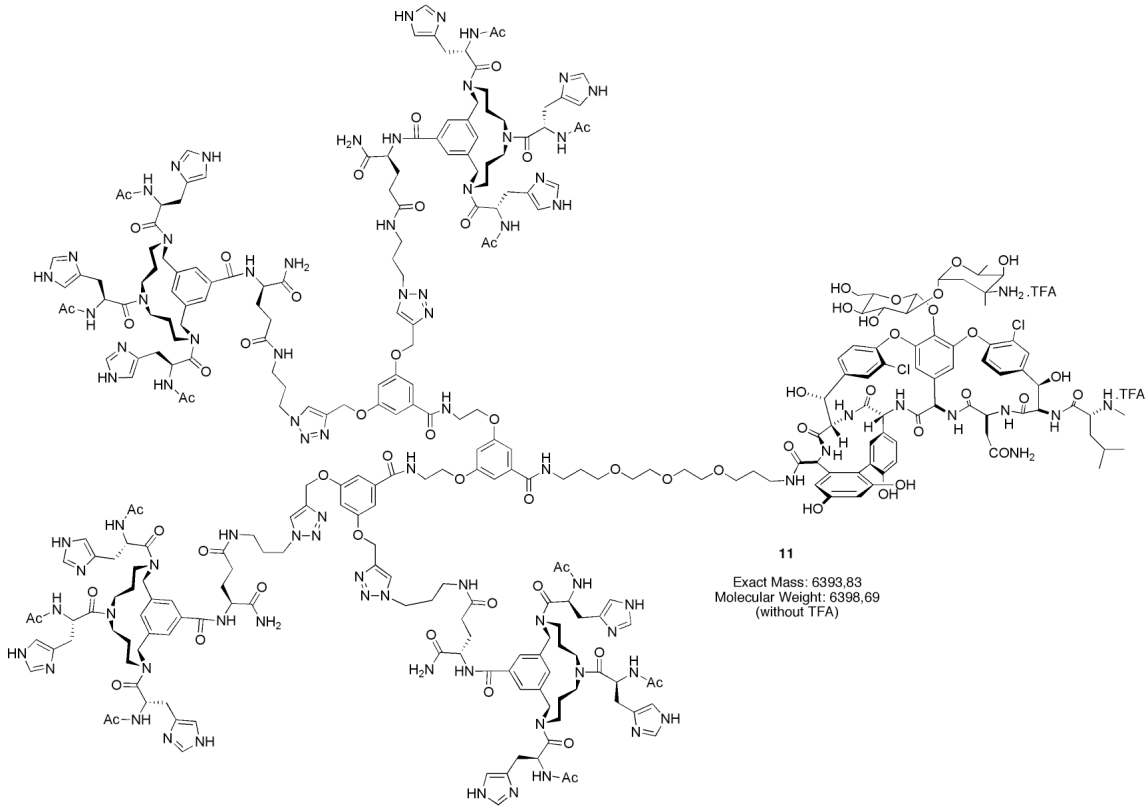

Figure 3. Synthesized scorpionate antibiotic **11**.

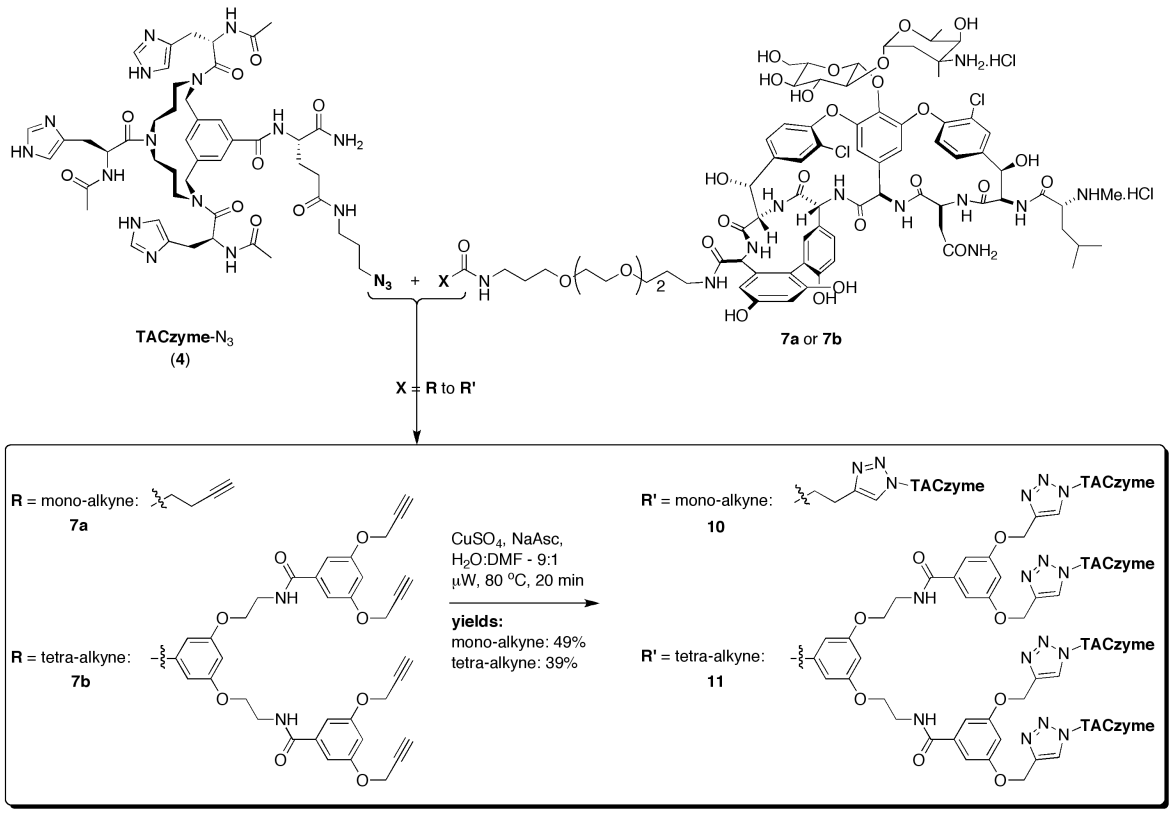

Scheme 4. Synthesis of mono- and tetravalent TACzyme-vancomycin conjugates **10** and **11**.

All click-products were purified by reversed-phase preparative HPLC, obtained in high purity (*figure 4*) and analyzed by ESI-MS or MALDI-TOF (*figure 5*). The structure of conjugate **11** is shown in *figure 3*. Lyophilization of the compounds afforded white fluffy compounds.

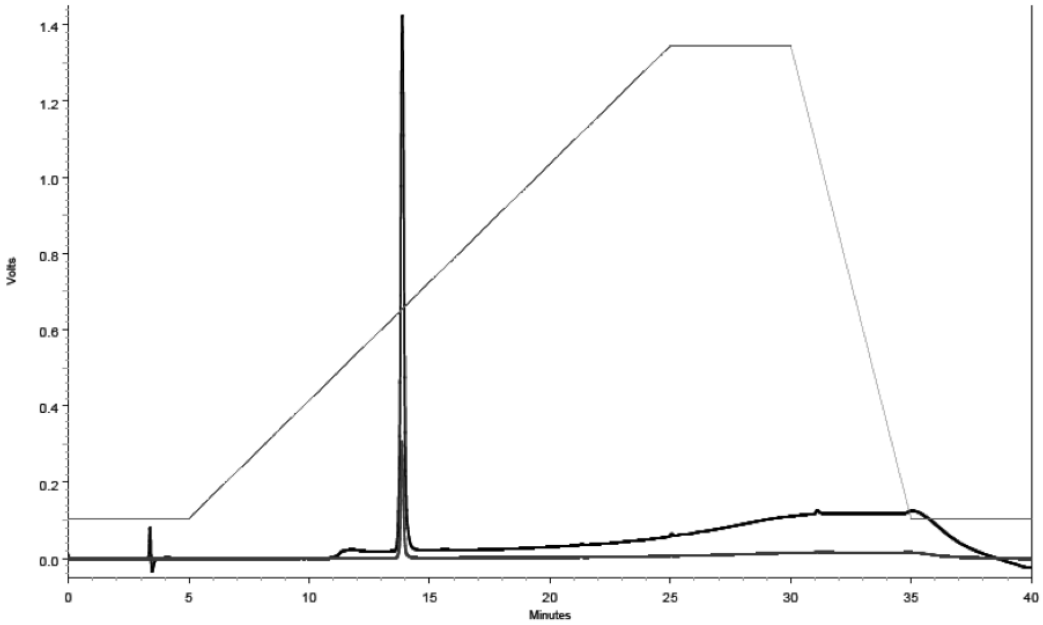

Figure 4. HPLC trace of purified **11** (t_R = 14.27 min). Upper trace: UV-detection at 220 nm, lower trace UV-detection at 254 nm.

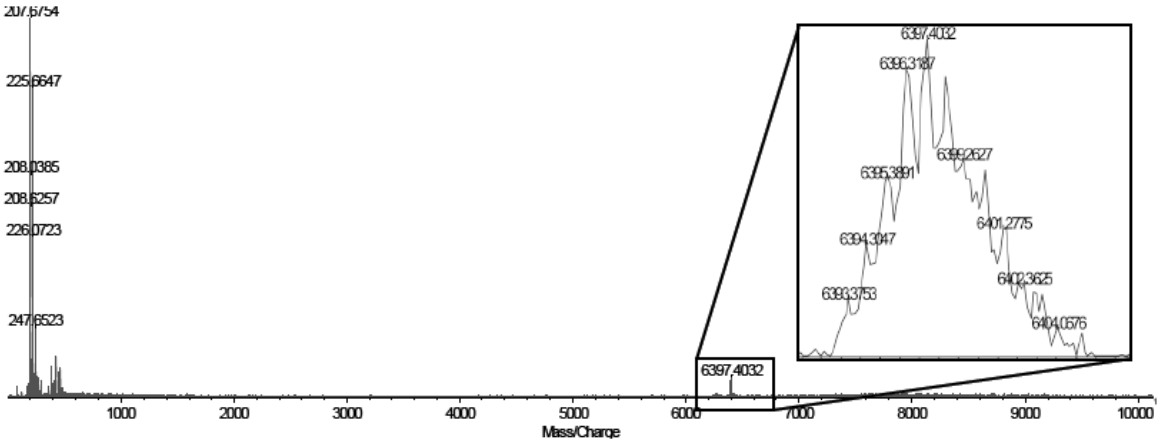

Figure 5. MALDI-TOF spectrum of purified **11**.

3. Targeted hydrolysis of vancomycin-TACzyme conjugates using vesicles equiped with acetylated carboxyfluorescein

Both non-conjugated compounds **4** and **9** and vancomycin-conjugated compounds **10** and **11** were tested in a model-system to determine the efficacy of targeted hydrolysis. For this the rate of hydrolysis of the acetyl-groups of di-acetylated carboxyfluorescein (DACF) present on the surface of lipid II containing DOPC/DOPE vesicles was measured (*figure 6*). In order to create these DOPC/DOPE vesicles, a chloroform-solution of DOPC (phosphatidylcholine) was mixed stoichiometrically with a chloroform-solution of DOPE (phosphatidylethylene-amine), to which di-acetylated carboxyfluorescein (DACF-DOPE) was covalently connected (*scheme 5*, also for

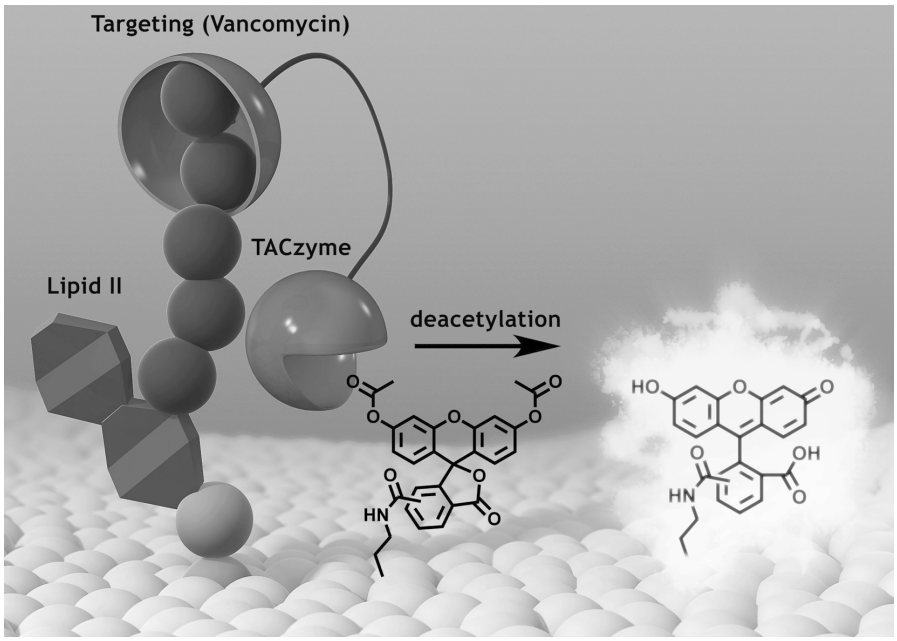

Figure 6. Cartoon of the anticipated mode of action of vancomycin-TACzyme conjugate **9** towards hydrolysis of membrane bound di-acetyl-carboxyfluorescein.

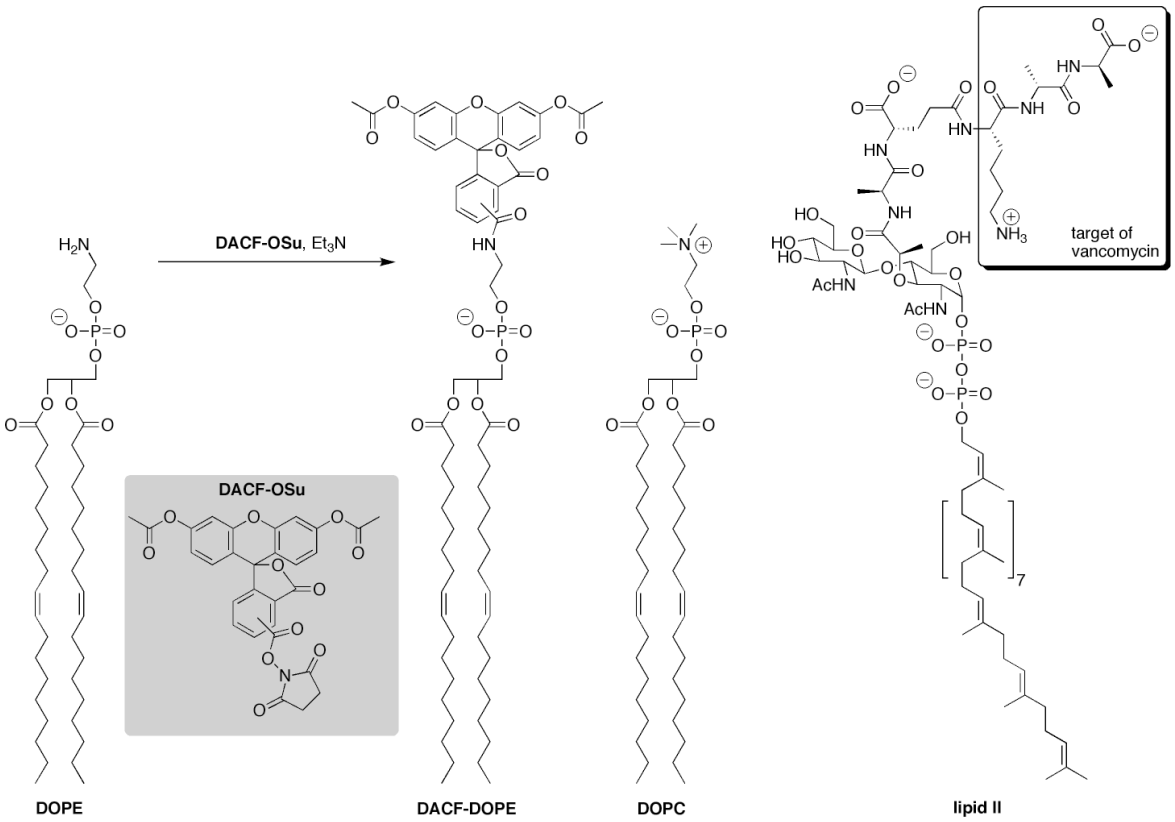

Scheme 5. Synthesis of DACF-decorated DOPE-lipids. Structures of DOPC and Lipid II are also given; the vancomycin targeting part of lipid II is highlighted.

structures of lipids that are mentioned in the text). This high 'loading' of the vesicles with carboxyfluorescein (CF) was anticipated to be necessary in order to measure even low hydrolytic rates. To this 50:50 mixture of DOPC/DACF-DOPE, 0.1% of Lipid II was added for binding to vancomycin in order to target the TACzymes to the vesicles, enabling analysis of targeted hydrolysis.

After evaporation of the chloroform, a concentrated solution of the mixture was prepared by dissolving them in 100 mM NaCl 20 mM Tris-buffer (pH 7.0). The resulting concentrated solution of vesicles was diluted in 20 mM HEPES (pH 7.5) buffer and vesicles were prepared according to a standard protocol. Increasing fluorescence as result of hydrolysis was measured on a fluorescent spectrophotometer. An additional control for TACzyme-dendrimer **9** was included by measuring the rate of hydrolysis of construct **11** using vesicles that contain no lipid II.

An increase in fluorescence as result of hydrolysis was measured upon addition of 20 μM TACzyme equivalents corresponding to 20 μM of **4** and **10**, and to 5 μM of **9** and **11** (*figure 7*). We observed that the rate of hydrolysis by tetra-TACzyme-vancomycin **11** using vesicles containing no lipid II, denoted by '**11** (no L-II)' in *figure 7*, was only marginally higher than the rate of tetravalent-TACzyme **9** using vesicles containing lipid II. In case of targeting to lipid II, the multivalency effect was

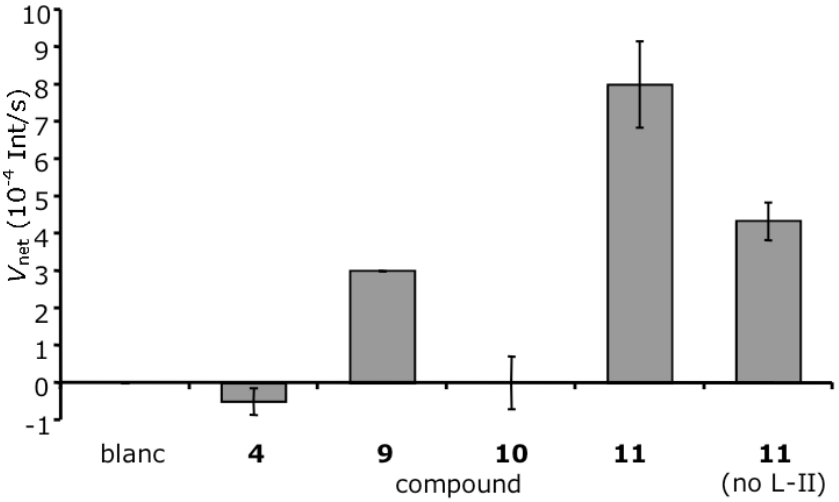

Figure 7. Rate of hydrolysis of on DOPE-'immobilized' di-acetyl-carboxyfluorescein by TACzyme containing compounds **4**, **9**, **10** and **11**. The bar-graph represents the differences in changes in intensity measured.

especially clear considering that mono-TACzyme–vancomycin **10** showed hydrolytic activity similar to that of TACzyme **4** and the blanc, whereas the activity of tetra-TACzyme–vancomycin **11** was significantly higher. Even though there was only 0.1% of lipid II present in the membranes, the enhanced hydrolytic activity of tetra-TACzyme–vancomycin **11** conclusively showed the concept of targeted hydrolysis.

4. Minimum inhibitory concentration for bacteria

The antibiotic activity of the molecules was assessed by determination of the MIC values towards one vancomycin sensitive enterococcus (VSE) and one vancomycin resistant enterococcus (VRE) bacterial strain (*table 1*).

Table 1. MIC-values (μM) of vancomycin (**V**), conjugates **4**, **9**, **10** and **11** and vancomycin derivatives **7a** and **7b** for vancomycin susceptible (VSE) and vancomycin resistant *Enterococci* (VRE).

	without $ZnSO_4$							with $ZnSO_4$ [c]			
Strain	**V**	**7a**	**7b**	**4**	**9**	**10**	**11**[d]	**10**	**11**[d]	**4**	**9**
VSE	0.3	1.0	1.6	*a*	*b*	5.8	40	2.9	5	*a*	*b*
VRE	86	*a*	3.2	*a*	*b*	*a*	*a*	92.8	*a*	*a*	*b*

Notes: *a* = > 92.8 μM. *b* = > 46.4 μM. [c] The presence of $ZnSO_4$ already inhibited the growth of the bacteria; [d] **11** containing wells, both with and without $ZnSO_4$, were turbid.

Compounds **4** and **9**, which lacked vancomycin, did not show any activity toward both VRE and VSE (MIC>256 mg/L), indicating that targeting is crucial for activity. In contrast, vancomycin conjugated constructs **10** and **11** showed interesting differences in activity toward VSE: monovalent TACzyme construct **10** was almost seven times more active than tetravalent TACzyme containing construct **11**. Thus, even though the hydrolytic activity of **11** was higher (*vide supra*) than that of **10**, the added steric

bulk may have a negative effect on the antibacterial activity. However, the presence of $ZnSO_4$ in the medium had a beneficial effect on the antibacterial activity of the constructs: the activity of monovalent TACzyme **10** doubled and tetravalent TACzyme **11** became even eight times more active. Whether this is due to increased hydrolytic activity as result of added $ZnSO_4$ remains unclear at this point.[28] Importantly, it was found that $ZnSO_4$ itself did not act as an inhibitor of bacterial growth when non-conjugated **4** and **8** were evaluated in the presence of $ZnSO_4$. Although the coupling of TACzyme **4** to vancomycin derivatives **7a** and **7b**, leading to **10** and **11**, had a negative effect on the antibacterial activity of the latter, the presence of $ZnSO_4$ in the medium partly restored the antibacterial activity. With respect to the effect of hydrophobic extensions on vancomycin it is interesting to note that vancomycin-tetra-alkyne **7b** showed higher activity toward VRE than vancomycin. The hydrophobic dendrimer increased the activity from 86 to 3.2 μM, whereas it even decreased activity toward VSE (*table 1*). This is another example that addition of hydrophobic extensions on vancomycin, in our case on the *C*-terminus, can increase its activity.[29]

4. Discussion

In general, hydrophobic extensions on vancomycin as in derivatives **7a** and **7b** resulted in an increase in activity towards VRE. The addition of TACzymes to vancomycin, as in **10** or **11**, did not result in any activity toward VRE and resulted in a lower activity toward VSE. Apparently, the attachment of TACzymes to vancomycin derivatives **7a** and **7b** had a negative impact on their activity, especially towards VRE.

Considering the activity of the TACzyme containing constructs, *i.e.* **10** and **11**, different activities were measured. It should be mentioned that this part only deals with VSE, since the constructs were inactive toward VRE. First of all, like **7a** and **7b**, the activity of the constructs was lower than that of vancomycin. Whereas vancomycin had an MIC of 0.17, vancomycin derivatives **10** or **11** were a factor of 34 or 235 less active. The addition on $ZnSO_4$ to the medium reduced these factors to 16 and 29. Secondly, TACzymes **4** and **9** were not active at all, indicating that the TACzyme constructs themselves do not have any anti-bacterial properties. Also, intermediates **7a** and **7b** were more active than **10** and **11**. This might indicate that the observed activity of **10** and **11** is solely due to the presence of vancomycin and that the observed reduction in activity was related to the attachments. Thirdly, considering the multivalency effect of the TACzyme part of the constructs, by comparing monovalent TACzyme construct **10** to the tetravalent construct **11**, the activity was reduced by a factor of 7. This might be the result of an increase in solubility of **11** over **10**, which can reduce the activity of vancomycin. It might also reflect a reduced availability of vancomycin for the target, due to increased bulk and unfavorable folding of the construct. Fourthly, concerning the presence of $ZnSO_4$ in the medium, when the activities of **10** and **11** in the $ZnSO_4$-containing medium are compared, the difference was only a factor of

1.7. The activity of both of the constructs was increased upon addition of $ZnSO_4$. The activity of **10** doubled and the activity of **11** increased 8-fold. Although the reasons for this unequal increase of activity remain unclear, the difference might be due to a higher hydrolytic activity of tetravalent **11** as compared to monovalent **10**. Another reason for the observed activities, next to the presence of vancomycin in the molecular constructs, might be that it binds Zn(II) that is also present in peptidases involved in bacterial cell-wall biosynthesis and lysis.[30]

Finally, vancomycin derivative **7b** showed an interesting difference in activity: attachment of a large hydrophobic tetra-alkyne dendrimer to vancomycin via a small hydrophilic EG-spacer reduced the activity of the construct toward VSE, even though it increased the activity toward VRE. It seems that a particular manipulation can reduce the activity of a good binder – vancomycin to D-Ala-D-Ala of VSE – or increase the activity of a poor binder – vancomycin to D-Ala-D-Lac of VRE. The increase in activity towards VRE might well be due to a mechanism similar to that of other hydrophobic vancomycin derivatives that are more active toward VRE than vancomycin itself.[29]

5. Conclusions

First of all, the activity of scorpionate antibiotics **10** and **11** is too low in order to consider these constructs as improvements on vancomycin, especially when compared to derivatives **7a** and **7b**. Apparently, the hydrolytic activity of the TACzymes is too low for improvement of the antibacterial properties of vancomycin. The fact that the hydrolytic activity of these constructs could be too low in order to make vancomycin an even more powerful drug was already inferred from the results of the targeted hydrolysis study. Targeted hydrolysis could be demonstrated and showed even slightly higher activity for the dendrimeric construct, but the activity was relatively low.

However, we have shown that scorpionate antibiotics can conveniently be prepared and that conjugation of TACzymes to vancomycin is straightforward. Preparation of these constructs involved three novel synthetic steps: (1) *C*-terminal modification of the TAC-scaffold, the resulting azide functionalized TACzyme can be used in other studies as well. (2) Alkyne-azide conjugation of TACzymes to a drug, in this case vancomycin, and (3) a first study toward the properties of multivalent TACzyme-containing constructs. Therefore, incorporation of more active hydrolase mimics might be envisioned.

Although the activity of the constructs presented in this chapter is slightly lower than that of vancomycin, the concept of combining two modes-of-action might lead to new and more powerful antibiotics that potentially can even challenge resistant bacterial strains. With respect to this, we anticipate an increased activity when more powerful enzyme mimics are attached and when spacer-lengths are tuned. Ultimately, with the construction of specific hydrolase mimics, specific targets might be addressed.

6. Experimental Section

General

Vancomycin was obtained from Sigma. Electrospray ionization (ESI) mass spectrometry was carried out using a Shimadzu LCMS QP-8000 single quadrupole bench top mass spectrometer (*m*/*z* range <2000), coupled with a QP-8000 data system. MALDI-TOF spectra were recorded using a Kratos Axima, CFR spectrometer. Analytical HPLC was performed on a Shimadzu Class-VP automated HPLC using an analytical reversed-phase column (Alltech Adsorbosphere C18, 300 Å, 5 μm, 250 × 4.6 nm) coupled to a UV detector operating at 220 nm and 254 nm. Preparative HPLC was performed on a Gilson automated HPLC using a preparative reversed-phase column (Alltech Adsorbosphere C18, 10 μm, 250 × 22 mm) and a UV detector operating at 220 nm and 254 nm. Elution of both HPLC systems was effected using an appropriate gradient from 0.1% TFA in MeCN/H_2O (5/95, v/v) to 0.1% TFA in MeCN/H_2O (95/5, v/v) using a flow rate of 1 mL/min (analytical) or 11.5 mL/min (preparative). Microwave reactions were performed in an Initiator reactor from Biotage.
Bacterial strains: Vancomycin susceptible *Enterococci* (VSE, strain 15A797), and vancomycin resistant *Enterococci* (VRE, strain 15A799) were clinical blood isolates obtained from the strain collection of the University Medical Center, a teaching hospital in Coimbra (Portugal), respectively. *Antibacterial activity*: MICs were determined by broth microdilution, utilizing CA-MHB as described by the CLSI guidelines [National Committee for Clinical Laboratory Standards 2002, 5th edn, M7-A5] (formerly the NCCLS guidelines).

H_2N-Glu($NHCH_2CH_2CH_2N_3$)-TAC-$(HisAc)_3$ 4 (or T1)

For this synthesis, the fully *o*-NBS-protected triazacyclophane (TAC)-scaffold was used.[31] Polystyrene AM RAM resin was used (550 mg, with a loading 0.7 mmol/g) to attach Fmoc-Glu(OAll)-OH (4 eq, 639 mg) using BOP (4 eq, 690 mg) and D*i*PEA (8 eq, 543 μL) as the coupling reagents and NMP (3 mL) as a solvent. Excess reagents were removed by washing with NMP (3×6 mL, each 2 min), DCM (3×6 mL, each 2 min) and the coupling was monitored using a Kaiser-test.[32] Potentially remaining amines were capped by a capping reagent, that is a solution of 0.5 M Ac_2O, 0.125 M D*i*PEA, 0.015 M HOBt in NMP. The Fmoc-group of **1** was removed using 20% piperidine in NMP, the presence of the resulting free amine was visualized using a Kaiser-test. To this amine the HO-TAC(*o*-NBS)$_3$ scaffold (2 eq, 583 mg) was attached using BOP (2 eq, 309 mg) and D*i*PEA (4 eq, 244 μL). After washing with NMP and DCM (each 3×6 mL, each for 2 min) a negative Kaisertest showed coupling of the scaffold. Again, remaining amines were capped using the capping reagent. Washing with DMF (3×6 mL, each for 5 min) was performed to ensure complete removal of DCM. After this, the *o*-NBS protecting group of **2** was removed in a S_NAr substitution reaction[33] by *in situ* generation of a thiolate using 2-mercaptoethanol (6 mL of a 0.5 M solution in DMF) and DBU (5 eq compared to the thiol, 224 μL). To the liberated secondary amines of the scaffold,

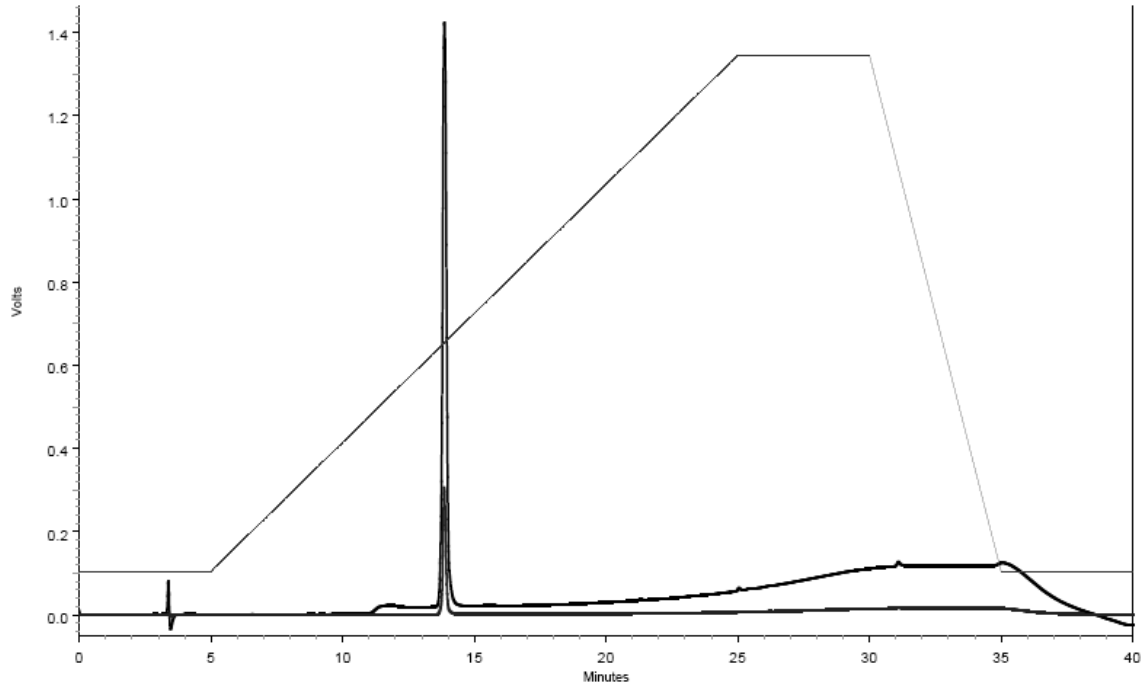

Figure 8. HPLC-trace of compound **10** (t_R = 13.85 min, C8). Upper trace: UV-detection at 220 nm; lower trace: UV-detection at 254 nm.

Fmoc-His(Trt)-OH (~3 eq per amine, 1.95 g) was attached using BOP (3 eq, 1.39 g) and D*i*PEA (6 eq, 1.1 mL). After this, the Fmoc-protecting group was replaced by the permanent acetyl-protecting group using a solution of Ac_2O, HOBt and D*i*PEA in NMP.

For introduction of the azide on the *C*-terminus of the scaffold, the allyl-ester of **3** was removed using $Pd(PPh_3)_4$ (0.5 eq, 222 mg) and anilinium *p*-toluenesulfinate (20 eq, 1.67 g). HPLC and ESI-MS were used to analyze the removal of the allyl-ester. To the liberated acid, 1-azido-3-aminopropane (4 eq, 140 mg) was coupled using BOP (4 eq, 619 mg) and D*i*PEA (4 eq, 488 μL). Finally, azide-containing TACzyme **4** was cleaved from the resin using TFA/TIS/water – 95/2.5/2.5 (%, v/v) yielding the crude product (66% product content by HPLC, UV and ELSD-detection). After purification by reversed phase preparative HPLC (C_8 column) the pure product was obtained as a white fluffy powder. HPLC: t_R = 13.55 min (C_8). ESI-MS: *m*/*z* 1026.30 (calculated: 1026.13 for $[M+H]^+$).

Vancomycin-spacer-alkyne 7a

4-Pentynoic acid (92 mg, 0.94 mmol), EDC (180 mg, 0.94 mmol) and HOAt (127 mg, 0.94 mmol) were dissolved in DCM (5 mL) and added to mono-*N*-Boc-tridecanediamine **5** (300 mg, 0.94 mmol)[34] and stirred overnight at room temperature. The solvent was evaporated *in vacuo* and product **6a** was purified using column chromatography (eluents: DCM/MeOH 95/5, % v/v) and obtained in quantitative yield. R_f = 0.29 (eluents: DCM/MeOH 95/5, % v/v). ^{1}H-NMR: ($CDCl_3$) δ = 1.39 (s, 9H), 1.7 (m, 4H), 1.93 (m, 1H), 2.33 (m, 2H), 2.46 (m, 2H), 3.16 (q, 2H), 3.33 (q, 2H), 3.4-3.62 (m, 12H), 4.94 (t, 1H), 6.44 (s, 1H).

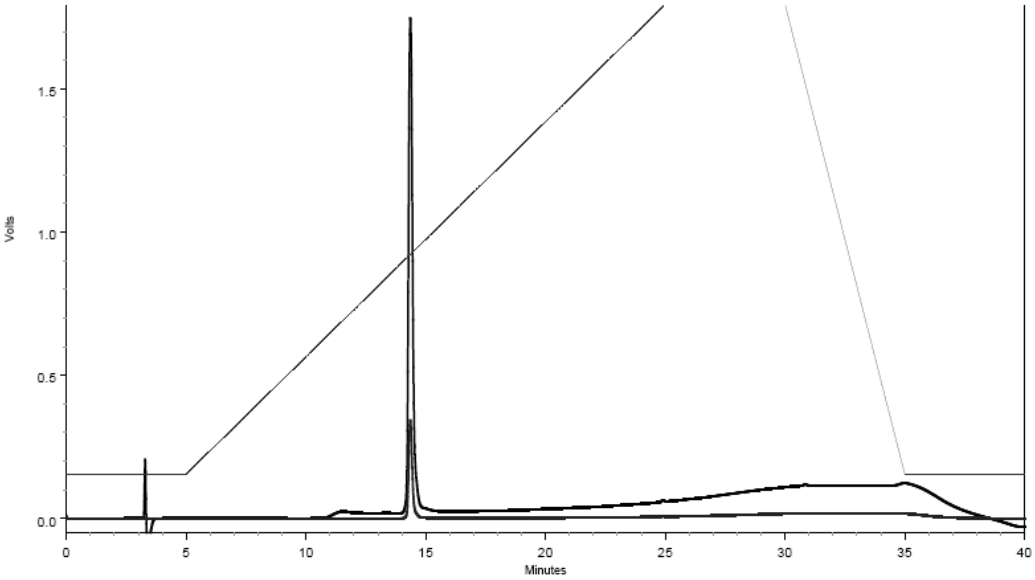

Figure 9. HPLC-trace of compound **9** (t_R = 14.33 min, C8). Upper trace: UV-detection at 220 nm; lower trace: UV-detection at 254 nm.

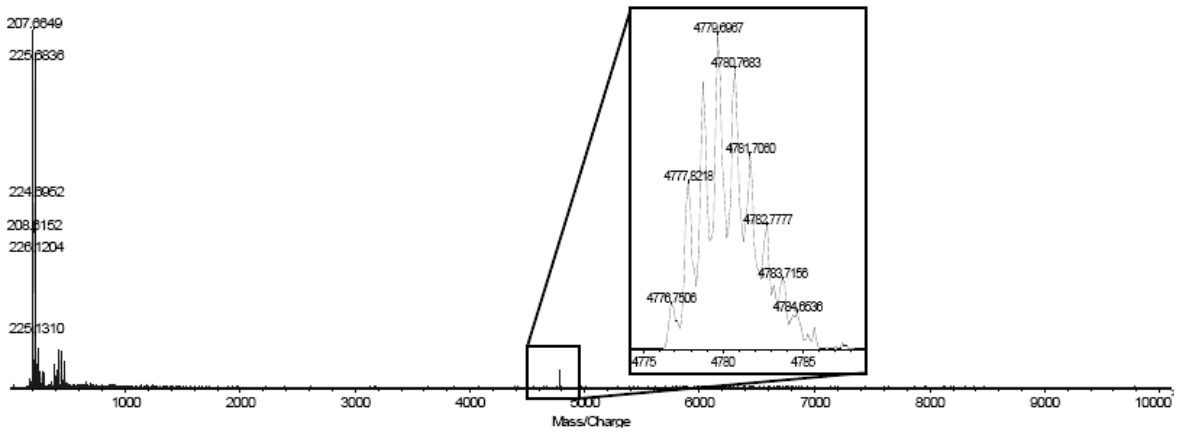

Figure 10. MALDI-TOF spectrum of compound **9**.

A portion of this product (36 mg, 0.09 mmol) was dissolved in DCM (15 mL) and TFA (15 mL) was added and the mixture stirred at room temperature for 1.5 h. The solvents were removed *in vacuo* and the residue dissolved in DMF. The pH was adjusted to 8 using Et_3N. DMF (6 mL) was added to a mixture of vancomycin.HCl (200 mg, 0.135 mmol), EDC (21 mg, 0.11 mmol) and HOAt (15 mg, 0.11 mmol). The resulting slurry was added to the solution of the above residue in DMF and the reaction was stirred at room temperature for 3 days. Then, the DMF was removed *in vacuo* and the residue was purified by preparative HPLC and lyophilized to yield 94 mg of compound **7a** as white power (60%). HPLC: t_R = 15.9 min (C_8, >95% pure). ESI-MS: *m/z* 866.1 (calculated: 867.3 for $[M+2H]^{2+}$), 1155.1 (calculated: 1155.7 for $[2M+3H]^{3+}$), 1732.1 (calculated: 1732.6 for $[M+H]^+$).

Vancomycin-spacer-tetraalkyne 7b

Boc-spacer-dendrimer-tetraalkyne[35] **6b** (50 mg, 0.052 mmol) was dissolved in DCM (10 mL)

and TFA (10 mL) was added and stirred at room temperature for 2.5 h. The solvents were removed *in vacuo* and the residue was dissolved in DMF (1.5 mL). The pH was adjusted to 8 using Et_3N. DMF (10 mL) was added to a mixture of vancomycin·HCl (230 mg, 0.155 mmol), EDC (20 mg, 0.104 mmol) and HOAt (14 mg, 0.104 mmol). The resulting slurry was added to the spacer-tetraalkyne solution and the reaction was stirred overnight at room temperature for 3 days. After this, DMF was removed *in vacuo* and the residue was purified with preparative HPLC and lyophilized to yield 87 mg of compound **7b** as white power (67 %). HPLC: t_R = 19.8 min (C_8). ESI-MS: *m*/*z* 1149.5 (calculated: 1150.1 for $[M+2H]^{2+}$).

TACzyme-vancomycin conjugate 10

Vancomycin-alkyne **7a** (5 mg, 2.9 μmol) and N_3-TACzyme **4** (3 mg, 2.9 μmol) were dissolved in H_2O:DMF 9:1 (1 mL). Then $CuSO_4$ (2 mg, 9 μmol) and NaAsc (3.5 mg, 18 μmol) were added and the solution was subjected to microwave heating for 20 min at a constant temperature of 80 °C. Buffer A (water/MeCN/TFA – 95/5/0.1, % (v/v)) was added (1 mL) and the crude mixture was purified by reversed phase preparative HPLC and lyophilized to afford 4.7 mg of pure (*figure 8*) conjugate **10** as white powder in a yield of 49%. ESI-MS: *m*/*z* 1378.2 (calculated: 1379.4 for $[M+2H]^{2+}$), 1838.6 (calculated: 1838.8 for $[2M+3H]^{3+}$).

$(TACzyme)_4$-dendrimer-vancomycin conjugate 11

Vancomycin-alkyne **7b** (5 mg, 2.9 μmol) and N_3-TACzyme **4** (3 mg, 2.9 μmol) were dissolved in H_2O:DMF 9:1 (1 mL). Then $CuSO_4$ (2 mg, 9 μmol) and NaAsc (3.5 mg, 18 μmol) were added and the solution was subjected to microwave heating for 20 min at a constant temperature of 80 °C. Buffer A (water/MeCN/TFA – 95/5/0.1, %, v/v) was added (1 mL) and the crude mixture was purified with preparative HPLC and lyophilized to give 7.3 mg of conjugate **11** as white powder in a yield of 39%. t_R = 14.27 min (C_8, see *figure 4*); MALDI-TOF *m*/*z*: 6397.40 (calculated: 6397.84 for $[M+H]^+$) (see *figure 3*).

$(TACzyme)_4$-dendrimer 9

Tetra-alkyne **8** (0.5 mg, 0.74 μmol) was dissolved in DMF (0.5 mL) and added to N_3-TACzyme **4** (4.6 mg, 4.4 μmol) dissolved in H_2O (0.9 mL). Then $CuSO_4$ (1.8 mg, 7.4 μmol) and NaAsc (3 mg, 15 μmol) were added and the solution was subject to microwave heating for 15 min at a constant temperature of 80 °C. Buffer A (water/MeCN/TFA – 95/5/0.1, %, v/v) was added (1 mL) and 3 drops of TFA. The crude mixture was purified with preparative HPLC and dried to afford 1.9 mg of dendrimer **9** as white powder in a yield of 53%. HPLC showed a product of high purity (*figure 9*). MALDI-TOF *m*/*z*: 4779.70 (calculated: 4779.28 for $[M+H]^+$) (*figure 10*).

5(6)carboxyfluorescein diacetate hydrolysis experiments

DOPE (0.12 mL, 20 mg/mL $CHCl_3$, 3.2 μmol) was added to 5(6)carboxyfluorescein diacetate *N*-succinimidyl ester (1.7 mg, 3 μmol). Et_3N (4.5 μL, 32 μmol) was added and the solution was left at room temperature for 45 min. 1:1 DOPC/DOPE-5(6)carboxyfluorescein diacetate LUV's (lipid content 10 mmol/L) with and without Lipid II (0.1%) were made by repeated (10 times) extrusion of multilaminar vesicles through an inorganic membrane filter (0.2 μm) in aqueous buffer (10 mM Tris, pH 7, ionic strength: 150 mM NaCl). The lipid concentration in the LUV's was determined to be 11.2 mmol/L after destruction of the vesicles and inorganic phosphate determination according to Rouser.[36] A hydrolysis experiment consisted of adding 5 μL vesicles to 1 mL buffer (10 mM HEPES, pH 7.5) in a fluorescence cuvette. The change in fluorescence (λ_{ex} = 492 nm, λ_{em} = 515 nm) was measured upon injection of hydrolytic compound (for a final concentration of 20 μmol/L TACzyme equivalents) over 3 minutes. The slope of the increase in fluorescence was determined after subtraction of a blank run.

7. Notes and References

1 J. Suh, *Acc. Chem. Res.* **2003**, *36*, 562.

2 For MRSA for instance: '*Lichte stijging MRSA in ziekenhuizen*', Bilthoven (ANP), **30 april 2006**, from http://www.allesovermrsa.nl/mrsa/Nieuws/. See also http://webcollect.rivm.nl/MRSA/ and W.J.B. Wannet, X.W. Huijdens, M.E.O.C. Heck, G.N. Pluister, M.G. van Santen-Verheuvel, E. Spalburg, M. van Luit, T. Bosch, A. Heanen, E.W. Tiemersma, A.J. de Neeling, *Infectieziekten Bulletin* **2007**, *18*, 347.

3 It has been estimated that only 0.24% of all possible small molecules – molecules with less than 11 atoms of C/N/O/F and which are feasible for synthesis – has been prepared. T. Fink, J.-L. Reymond, *J. Chem. Inf. Model.* **2007**, *47*, 342. See for modification of excisting drugs: H.G. Floss, *J. Biotechnol.* **2006**, *124*, 242; C.M. Huwe, *Drug Discovery Today* **2006**, *11*, 763; C.A. Lepre, J.M. Moore, J.W. Peng, *Chem. Rev.* **2004**, *104*, 3641.

4 See *Science (Special Issues: Drug Resistance)*, **2008**, *321*, 355.

5 B. Meunier, *Acc. Chem. Res.* **2008**, *41*, 69 and references cited therein. R. Morphy, Z. Rankovic, *J. Med. Chem.* **2005**, *48*, 6523. A related strategy is used for tumor-targetting: I. Ojima, *Acc. Chem. Res.* **2008**, *41*, 108.

6 For example bleomycin, an efficient anticancer agent: B. Meunier, *Acc. Chem. Res.* **2008**, *41*, 69 and references cited therein.

7 J. Suh, *Acc. Chem. Res.* **2003**, *36*, 562 and references cited therein.

8 P.M. Rendle, A. Seger, J. Rodrigues, N.J. Oldham, R.R. Bott, J.B. Jones, M.M. Cowan, B.G. Davis, *J. Am. Chem. Soc.* **2004**, *126*, 4750. This article was featured in Nature (P. Ball, *Nature*, **2004**, *428*, 907) and in the Financial Times (April 30, **2004**).

9 H.B. Albada, F. Soulimani, B.M. Weckhuysen, R.M.J. Liskamp, *Chem. Commun.* **2007**, 4895.

10 M.H. McCormick, W.M. Stark, G.E. Pittenger, R.C. Pittenger, G.M. McGuire, *Antibiot. Annu.* **1955-1956**, 606; M.P. Lechevalier, H. Prauser, D.P. Labeda, J.-S. Ruan, *Int. J. Sys. Bacteriol.* **1986**, *36*, 29.

11 C.W. Tornøe, C. Christensen, M. Meldal, *J. Org. Chem.* **2002**, *67*, 3057; V.V. Rostovtsev, L.G. Green, V.V. Fokin, B.K. Sharpless, *Angew. Chem., Int. Ed.* **2002**, *41*, 2596; V.D. Bock, H. Hiemstra, J.H. van Maarseveen, *Eur. J. Org. Chem.* **2006**, 51; M. Meldal, C.W. Tornøe, *Chem. Rev.* **2008**, *108*, 2952.

12 D.H. Williams, B. Bardsley, *Angew. Chem., Int. Ed. Engl.* **1999**, *38*, 1172; J.C.J. Barne, D.H. Williams,

Annu. Rev. Microbiol. **1984**, *38*, 339.
13 M. Nieto, H.R. Perkins, *Biochem. J.* **1971**, *123*, 773.
14 Structure obtained from the Protein Data Bank, PDB-code: 1FVM.
15 R. Kerns, S.D. Dong, S. Fukazawa, J. Carbeck, J. Kohler, L. Silver, D. Kahne, *J. Am. Chem. Soc.* **2000**, *122*, 12608. See also: S.J. Kim, J. Schaefer, *Biochemistry* **2008**, *47*, 10155.
16 J. Rao, J. Lahiri, L. Isaacs, R.M. Weis, G.M. Whitesides, *Science* **1998**, *280*, 708.
17 R. Breslow, *Artificial Enzymes*, 1st edn, Wiley: Weinheim, Germany, **2005**; H. Dugas, *Bioorganic Chemistry: A Chemical Approach to Enzyme Action*, 3rd edn, Springer: New York, **1996**; A.J. Kirby, *Angew. Chem., Int. Ed. Engl.* **1996**, *35*, 706; R. Breslow, *Acc. Chem. Res.* **1995**, *28*, 146; D.J. Cram, *Science* **1988**, *240*, 760; T. Darbre, J.-L. Reymond, *Acc. Chem. Res.* **2006**, *39*, 925.
18 A. Fehrst, *Enzyme Structure and Mechanism in Proteins Science: A Guide to Enzyme Catalysis and Protein Folding*, WH Freeman and Company: New York, **1999**; I. Bertini, H.B. Gray, E.I. Stiefel, J.S. Valentine, *Biological Inorganic Chemistry*, University Science Books: Sausalito, **2007**; H.-B. Kraatz, N. Metzler-Nolte, *Concepts and Models in Bioinorganic Chemistry*, Wiley: Weinheim, **2007**.
19 V.T. D'Souza, M.L. Bender, *Acc. Chem. Res.* **1987**, *20*, 146; R. Breslow, *Acc. Chem. Res.* **1995**, *28*, 146; J. Suh, *Acc. Chem. Res.* **2003**, *36*, 562; T. Darbre, J.-L. Reymond, *Acc. Chem. Res.* **2006**, *39*, 925.
20 M. Paetzel, R.E. Dalbey, *Trends Biochem. Sci.* **1997**, *22*, 29; G. Dodson, A. Wlodawer, *Trends Biochem. Sci.* **1998**, *23*, 347.
21 H.B. Albada, F. Soulimani, B.M. Weckhuysen, R.M.J. Liskamp, *Chem. Commun.* **2007**, 4895. See also chapter 6 and 7 of this thesis.
22 A.J. Barrett, N.D. Rawlings, J.F. Woessner, *Handbook of Proteolytic Enzymes, volume 1: aspartic and metallo enzymes*, 2nd edn, **2004**, Elsevier academic press, London.
23 U. Baumann, *J. Mol. Biol.* **1994**, *242*, 244. PDB-code 1SAT.
24 X. Zhu, M. Teng, L. Niu, *Acta Crystallogr., Sect. D* **1999**, *55*, 1834.
25 See ref. 21. See also: T. Opatz, R.M.J. Liskamp, *Org. Lett.* **2001**, *3*, 3499; T. Opatz, R.M.J. Liskamp, *J. Comb. Chem.* **2002**, *4*, 275; C. Chamorro, J.-W. Hofman, R.M.J. Liskamp, *Tetrahedron*, **2004**, *60*, 8691; M.C.F. Monnee, A.J. Brouwer, L.M. Verbeek, A.M.A. van Wageningen, R.M.J. Liskmap, *Bioorg. Med. Chem. Lett.* **2001**, *11*, 1521.
26 J.V. Staros, H. Bayley, D.N. Standring, J.R. Knowles, *Biochem. Biophys. Res. Commun.* **1978**, *80*, 568; I.L. Cartwright, D.W. Hutchinson, V.W. Armstrong, *Nucleic Acids Res.* **1976**, *3*, 2331. See also: J.W. Back, O. David, G. Kramer, G. Masson, P.T. Kasper, L.J. de Koning, L. de Jong, J.H. van Maarseveen, C.G. de Koster, *Angew. Chem. Int. Ed.* **2005**, *44*, 7946.
27 For instance, a positive dendritic effect was observed in dendrimer systems studied by the group of Reymond: E. Delort, T. Darbre, J.-L. Reymond, *J. Am. Chem. Soc.* **2004**, *126*, 15642.
28 Unfortunately, the effect of $ZnSO_4$ on the hydrolytic activity in the model membrane system could not be measured due to quenching of fluorescence.
29 R. Kerns, S.D. Dong, S. Fukuzawa, J. Carbeck, J. Kohler, L. Silver, D. Kahne, *J. Am. Chem. Soc.* **2000**, *122*, 12608; S.J. Kim, J. Schaefer, *Biochemistry* **2008**, *47*, 10155.
30 P. Charlier, J.-P. Wery, O. Dideberg, J.-M. Frere, *Handbook of Metalloproteins* **2004**, *3*, 164 (PDB-code: 1LBU); ref. 22, p. 251-252, 857-866.
31 M.C.F. Monnee, A.J. Brouwer, R.M.J. Liskamp, *QSAR & Combinatorial Sciences* **2004**, *23*, 546.
32 E. Kaiser, R.L. Colescott, C.D. Bossinger, P.I. Cook, *Anal. Biochem.* **1970**, *34*, 595.
33 T. Fukuyama, C.-H. Jow, M. Cheung, *Tetrahedron Lett.*, **1995**, 36, 6373.
34 R. Autar, A.S. Khan, M. Schad, J. Hacker, R.M.J. Liskamp, R.J. Pieters, *ChemBioChem* **2003**, *4*, 1317.
35 H.M. Branderhorst, R. Kooij, A. Salminen, L.H. Jongeneel, C.J. Arnusch, R.M.J. Liskamp, J. Finne, R.J. Pieters, *Org. Biomol. Chem.* **2008**, *6*, 1425. See also: D.T.S. Rijkers, G.W. van Esse, N.S.M. Merkx, A.J.

Brouwer, J.J.F. Jacobs, R.J. Pieters, R.M.J. Liskamp, *Chem. Commun.* **2005**, 4581; J.A.F. Joosten, N.T.H Tholen, F. ait el Maate, A.J. Brouwer, G.W. van Esse, D.T.S. Rijkers, R.M.J. Liskamp, R.J. Pieters, Eur. J. Org. Chem. **2005**, 3182.

36 G. Rouser, S. Fleischer, A. Yamamoto, *Lipids* **1970**, *5*, 494.

Appendix A

Supramolecular Chemistry of Peptidic TAC-based Amphiphilic Molecules

Surfactants are amphiphilic molecules that have found widespread application as drug delivery systems and therefore new and more sophisticated surfactants are continuously developed.[1] One of the main characteristics of surfactants is that they spontaneously aggregate in water to form well-defined supramolecular structures such as micelles, liposomes, and bilayers, among others.

During the course of our combinatorial search towards TAC-based serine hydrolase mimics (see chapter 3), we stumbled upon some interesting features of amphiphilic TAC-based molecules. In an attempt to further pre-organize the functionalities of some initial hits of the screening, *i.e.* receptors that contained the β-lactamase active site residues Asp-Lys-Ser, the aggregating properties of aliphatic hydrocarbon tails in aqueous solutions were employed (*figure 1*). The formation of supramolecular assemblies by these compounds was evaluated.

First vesicle formation was analyzed. For this, solutions of both of the two TAC-based surfactants (*figure 1*) were prepared. Initial dynamic light scattering (DLS) measurements of both species did not reveal vesicles with clearly defined structural properties, even not after filtration through a 200 μm filter. However, temperature annealing – heating the samples to 100 °C and cooling slowly it to room temperature – resulted in vesicles with improved structural properties of the 5 mg/mL solutions of both surfactant molecules (*table 1*).

The polydispersity index (PDI) of the vesicles measured was significantly lower than before heating, indicating the presence of vesicles with similar size. Even more

Table 1. Geometric properties of vesicles formed by TAC-based amphiphilic peptides.

	conc.	No treatment		200 μm filter		T_{anneal} (100 °C)		After 1 week	
		rad	PDI	rad	PDI	rad	PDI	rad	PDI
1-C_{14}	5	157.8	0.49	48.0	0.45	79.1	0.19	**83.1**[a]	**0.07**
	10	361.0	0.53	15.2	0.50	16.3	0.52	15.3	0.54
1-C_{18}	5	118.5	0.40	58.3	0.26	56.2	0.25	**58.2**[b]	**0.002**
	10	283.1	0.49	21.7	0.57	18.7	0.55	1414.8	0.15

Notes: conc. = concentration in mg/mL; rad = radius in nm; PDI = polydispersity index.
[a] $[\alpha]_D^{20}$ = 6.6 (c = 0.05); [b] $[\alpha]_D^{20}$ = -4.8 (c = 0.05).

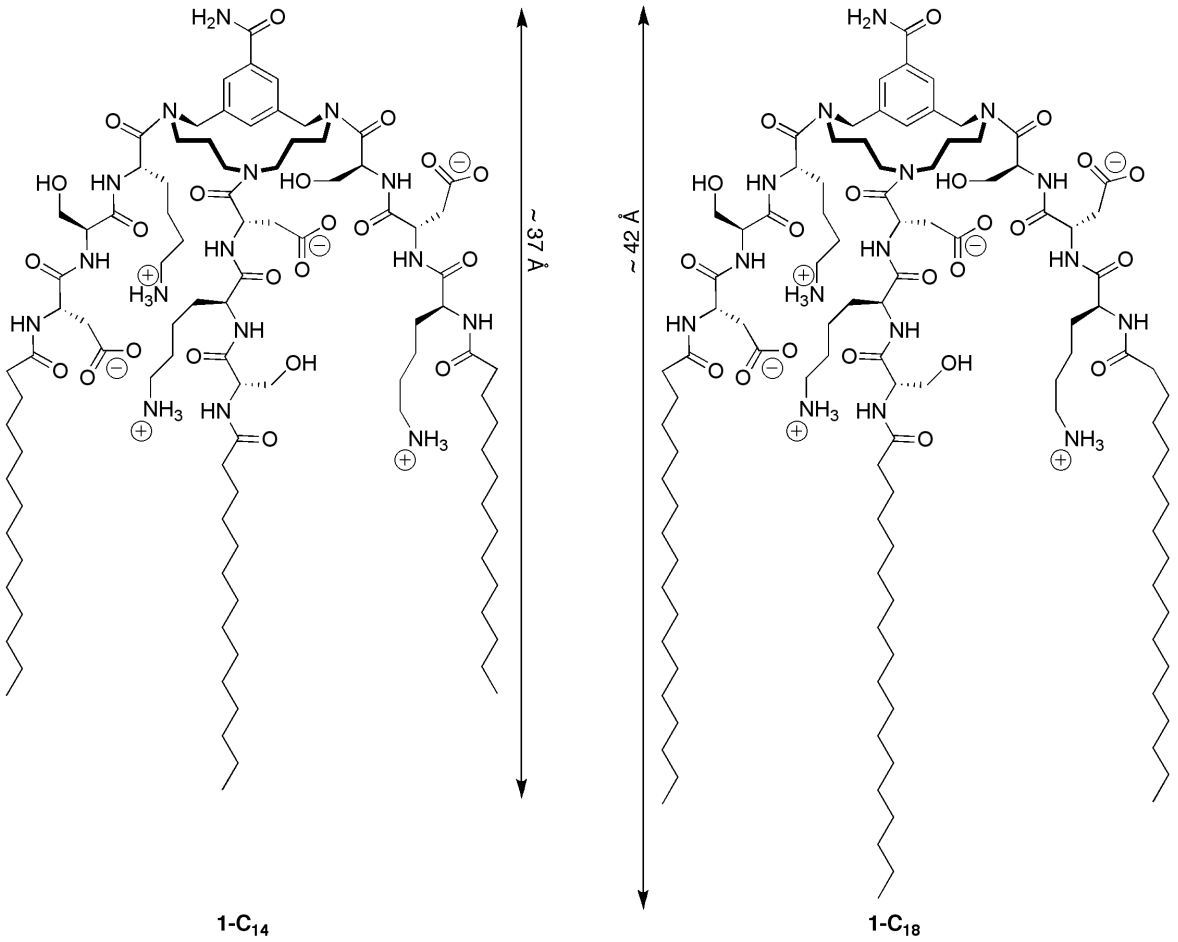

Figure 1. Structures of the two TAC-based β-lactamase triad containing surfactants.

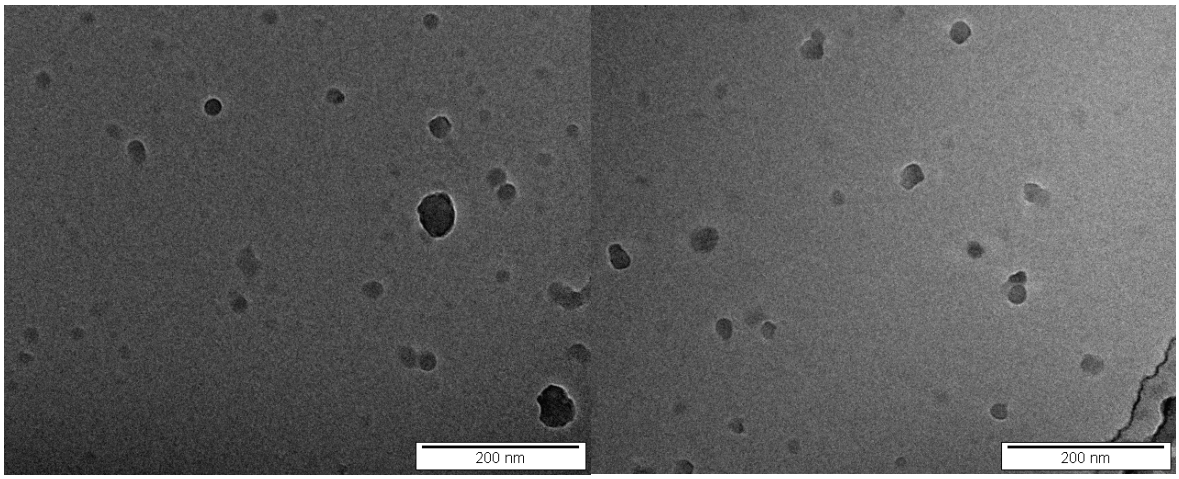

Figure 2. Cryo-TEM pictures of a freshly prepared 5 mg/mL solution of **1-C$_{14}$**.[3]

remarkable, after storing the sealed samples for one week on the bench, vesicles with remarkably low PDI values were detected. A low PDI is an indication for the presence of vesicles of which the distribution of the radius around an average value is narrow. The radii of the vesicles were 83 nm for **1-C$_{14}$** and 58 nm for **1-C$_{18}$**, which is within the range that is suitable for pharmaceutical applications: nanoparticles larger than

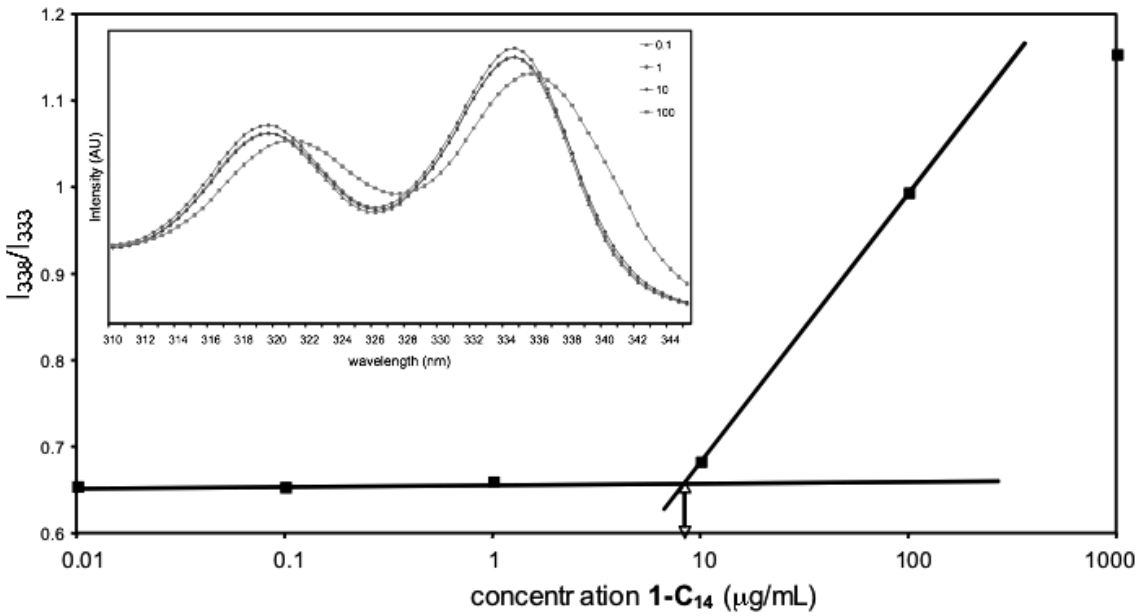

Figure 3. Determination of the critical micelle concentration for **1-C_{14}** using the pyrene-method. The insert shows parts of the fluorescence excitation spectra.

200 nm are removed by mechanical filtration by the inter-endothelial cell-slits in the spleen and particles smaller than 10 nm are subject to renal excretion.[2]

Unfortunately, transmission electron microscopic (TEM) and cryo-TEM analysis of these two solutions with extremely low PDI was not successful (bold values in *table 1*). Cryo-TEM analysis of a freshly prepared solution of **1-C_{14}** (5 mg/mL), with inferior structural properties as compared to the aged solution, could be performed (*figure 2*). This picture clearly showed the presence of vesicle-like supramolecular structures. The critical micelle concentration (CMC) for **1-C_{14}** was approximately 9 μg/mL, indicating that these surfactants easily form vesicles. This CMC-value corresponds to 4.7 μM[4], which is just above the range of CMC-values often measured for polymeric species (0.1-1 μM) but well below that of low molecular weight surfactants (0.1-1 mM). Therefore, these TAC-based vesicles might be useful candidates for drug delivery systems since a low CMC means that dissociation will be limited resulting from dilution that will take place upon administration of such a drug delivery system.

The properties of TAC-based amphiphilic molecules described here are promising enough to be explored further. Vesicles with well-defined structures were detected of which the properties are likely to fit pharmacokinetic demands. Synthetic modifications in order to adapt the compounds for specific purposes can easily be envisioned. A combination of biodegradability and high uniformity of the vesicles may make these constructs attractive candidates for drug delivering vesicles.

Experimental section

Dynamic light scattering (DLS) measurements were performed to determine the size of the micelles and the effect of certain sample-treatments on these micelles. DLS measurements were performed on a Malvern 4700 system (Malvern Ltd., Malvern, UK) consisting of an Autosizer 4700 spectrometer, a pump/filter unit, a Model 2013 air-cooler argon ion laser (75 mW, 488 nm, equipped with a model 2500 remote interface controller, Uniphase) and a computer with DLS software (PCS, version 3.15, Malvern). The temperature at which the measurements were performed was 37 °C and the angle under which the scattering was measured was 90°. The software corrected the change in solvent viscosity with temperature.

The method by which the CMC was determined was based on the differences in fluorescence of pyrene between an aqueous and an apolar environment.[5] Pyrene in water has a fluorescence maximum at 333 nm whereas in an apolar environment – for instance the fatty acid tails of a surfactant – this maximum is found at 338 nm (see *figure 3*, insert). By measuring this shift in fluorescence maximum at different concentrations of surfactant, the formation of vesicles can be monitored.

For this experiment, a stock solution of 2 mg/mL of the surfactant was prepared. This was used to prepare 4.5 mL solutions with concentrations ranging from 0.01 μg/mL – 1 mg/mL. In addition, a 180 μM solution of pyrene in acetone was prepared. 15 μL of this solution was added to 4.5 mL solutions of the different concentrations of surfactant. The resulting mixture was stored in open tubes overnight. Measurement of the excitation of pyrene as function of the surfactant concentration resulted in slightly different spectra for each concentration. From this data, a plot of I_{338}/I_{333} *vs* the concentration of **1-C$_{14}$** could be obtained, which gave the CMC (*figure 3*). Fluorescence excitation spectra of pyrene were obtained as a function of the surfactant concentration using a Horiba Fluorolog fluorometer (at a 90° angle). The excitation spectra were recorded at 37 °C from 300 to 360 nm with the emission wavelength at 390 nm. The excitation and emission band slits were 4 nm and 2 nm, respectively.

References and notes

1 V.P. Torchilin, *J. Contr. Rel.* **2001**, *73*, 137.

2 See G.S. Kwon, *Crit. Rev. Therap. Drug Carrier Syst.* **2003**, *5*, 357; S.M. Moghimi, A.C. Hunter, J.C. Murray, *Pharmacol. Rev.* **2001**, *53*, 283.

3 Courtesy of Johannes D. Meeldijk, Electron Microscopy Utrecht (EMU), Utrecht University, The Netherlands.

4 Assuming the presence of one TFA-counter ion for each lysine residue, the CMC is 4 μM.

5 M. Wilhelm, C.L. Zhao, Y.C. Wang, R.L. Xu, M.A. Winnik, J.L. Mura, G. Riess, M.D. Croucher, *Macromolecules* **1991**, *24*, 1033; G. Kwon, M. Naito, M. Yokoyama, T. Okano, Y. Sakurai, K. Kataoka, *Langmuir* **1993**, *9*, 945.

Summary and Outlook

1. Summary

Catalysts are molecules that assist the chemical transformation of other molecules. In the entire range of catalysts that are known to date, enzymes are the most interesting since they display unparalleled activity, the highest specificity and selectivity. In general, enzymes can be classified as either functional group enzymes or metalloenzymes: the first perform catalytic transformations by the action of cooperating functional groups, the latter by metal-ions that are immobilized in the protein scaffold. These two classes of enzymes are schematically depicted in *figure 1*, functionalities **X**, **Y**, and **Z** directly catalyze the transformation of A to B in functional group enzymes (*left*), or immobilize a metal-ion in a cavity in the protein in order to perform catalytic reactions at the metal-centre (*right*). One of the drawbacks of enzymes is their limitation in meeting the current desires of mankind for advanced materials. Nevertheless, enzymes have served as a tremendous source of inspiration for the construction of novel catalysts or enzyme mimics. Many approaches have been based on the synthesis of organic and inorganic molecules as mimics of functional group enzymes and metalloenzymes. The application of a synthetic scaffold molecule in the construction of peptide-based enzyme active site mimics that can serve as structural and functional models for an enzyme is relatively new. In this thesis, we describe our efforts in this area.

Initially, we decorated an orthogonally protected triazacyclophane (TAC) scaffold with the catalytic triad amino acid residues found in serine hydrolases: serine, histidine and aspartatic acid (chapter 2, see *figure 2*). Since the TAC-scaffold has two identical positions, three arrangements of the amino acid residues on the scaffold represented all three mimics. Kinetic analysis of these three mimics and comparison with two imidazole derivatives, *i.e.* 4-methylimidazole and Ac-His-diethylamine, showed that the activity towards hydrolysis of a *p*-nitrophenol ester was mainly caused by the isolated action of the histidine residue. We suspected that the high degree of flexibility present in the constructs resulted in this low activity. Therefore, we performed some NMR-studies on the constructs and indeed, this analysis showed the presence of at least 12 conformations. The inherent flexibility of the compounds prevented determination of the 3D-structures present in solution. By constructing small analogues of one of the three mimics, we showed that the attachment of already one amino acid residue resulted in complete loss of the symmetry of the TAC-core and resulted in the presence of multiple isomeric compounds. Based on these results we concluded that the pre-organizing ability of the

TAC-scaffold was insufficient and that other measures had to be taken in order to enforce the cooperative action of the functional groups that were attached to the TAC-scaffold.

In view of the chemical space that is offered by an orthogonally protected TAC-scaffold – the attachment of the 20 proteinogenic amino acid residues to the TAC-scaffold can lead to $20^3 = 8000$ different compounds – we decided to explore this space in a combinatorial fashion (chapter 3, see *figure 2*). Using combinatorial techniques, in which large libraries of compounds can be generated by combining several amino acid building blocks with a resin-bound orthogonally protected TAC-scaffold, we screened the chemical space offered by TAC-scaffolded peptides with respect to its possible applicability in the construction of hydrolytically active molecules. From a mixture of 19,683 potentially hydrolytic TAC-based tripodal receptor molecules, only a few showed hydrolytic activity in a screening assay. Resynthesis of the catalytically active hits revealed that hydrolysis of the *p*-nitrophenol ester was mainly mediated by the histidinyl imidazole ring, although subtle differences were shown to have effect on the catalytic activity. It was also shown that the receptors did not have significant substrate binding ability, indicating that a binding pocket for the substrate was not present in these constructs.

Based on these findings, it was concluded that the flexibility of the TAC-based tripodal peptidic constructs was disadvantageous for their catalytic activity including the hydrolysis of esters studied here. In order to decrease the flexibility of the TAC-based molecular constructs small serine hydrolase mimicking cryptand molecules were constructed. Cryptand molecules – which are often molecules with three arms or tentacles that are connected to each other at each end – are particularly known for their binding ability of guest-molecules. The construction of TAC-based cryptand

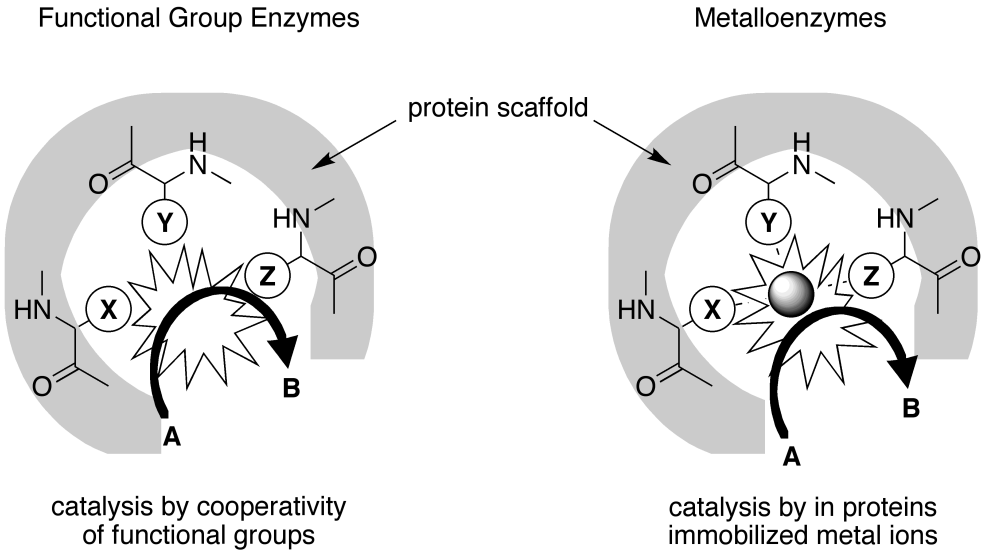

Figure 1. Schematic outline of the catalytic transformation of substrate **A** to product **B** by a functional group enzyme (*left*) or metalloenzyme (*right*).

molecules should lead to both an increased pre-organization of functional groups and an increased binding ability of the resulting molecules.

For the construction of these TAC-based cryptand molecules standard solid-phase peptide chemistry techniques and additional (protected) functional groups at the end of the arms attached to the TAC-scaffold were used. In one approach, these functional groups included two protected acid-functionalities and one bis-amine containing molecule of which the amine- and carboxylic acid groups were protected with trimethylsilyl-based protecting groups. These protecting groups were stable during the entire synthesis sequence and could be removed at the end of the synthesis by treatment with fluoride. After removal of the protecting groups, the two amine and carboxylic acid functionalities were linked together by a peptide coupling reaction under formation of an amide bond. Even though the amide-cyclized TAC-based peptidic cryptands could be constructed, the yields were very low and therefore unfortunately the hydrolytic activity of the construct could not be assessed. In addition, from NMR-

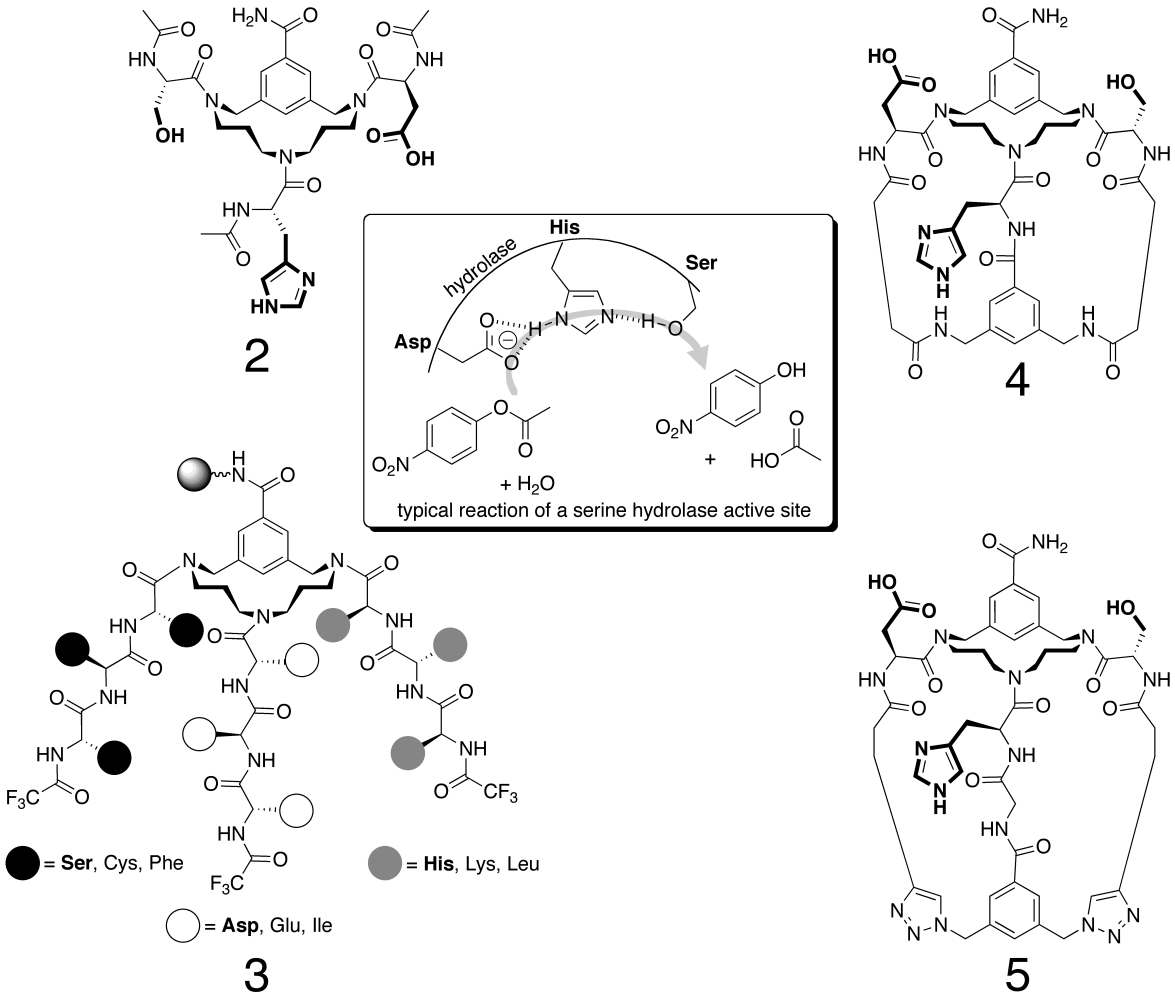

Figure 2. Overview of the approaches that were employed for the mimicry of the active sites and activity of serine hydrolases (chapters-numbers are given below the structures).

analysis of the obtained compound it was unclear whether pre-organization of the functional groups was achieved. To circumvent this somewhat cumbersome synthesis of the TAC-based peptidic serine hydrolase mimicking cryptand molecules using amide-bond formation, we also explored the applicability of the well-known copper-catalyzed alkyne-azide cycloaddition reaction to construct these molecules. By introducing two alkyne functionalities at the ends of the outer two arms of the TAC-based construct and a bis-azide group at the end of the middle arm, the feasibility of this synthetic approach could be evaluated. Although the solid-phase synthesis of the cyclized construct was convenient, the purification of the cleaved products was very tedious. Nevertheless, formation of the desired bi-cyclic construct was inferred from MS/MS analysis of the purified product. In this case as well, the amount of this construct was too small to undertake steps toward the elucidation of the structure or its activity.

The attempts described above concerned mimicry of the serine hydrolase class of functional group enzymes. As was also indicated, besides functional group enzymes, many enzymatic transformations are performed by metalloenzymes (*figure 1*). These enzymes are proteins that have included the properties of metal-ions for their catalytic purposes. Although enzymes can use prosthetic groups like heme functionalities to complexate these ions, many enzymes only use amino acid side-chain functionalities to realize this complexation. In particular, many metalloenzyme active sites use histidine and aspartic or glutamic amino acid side chain functionalities to immobilize metal-ions like copper, zinc, nickel, iron and manganese, in order to perform a broad spectrum of catalytic transformations. In view of this we assessed the applicability of our TAC-scaffold in the construction of novel metalloenzyme active sites mimics.

For the construction of TAC-based metalloenzyme active site mimics we therefore decorated a TAC-scaffold with histidine and aspartic amino acid residues. By doing this, mimics of three different frequently occurring metalloenzyme active sites were constructed, namely those having three histidine, two histidine and one aspartic, and one histidine and two aspartic amino acid residues in their active site (*figure 3*). Using appropriately protected TAC-scaffolds, TAC-based mimics of these active sites were constructed using solid-phase peptide synthesis techniques. The coordination chemistry of these three TAC-based mimics, also called TACzymes, was studied by UV-vis spectroscopic and ESI-MS spectrometric analysis of aqueous solutions of the Cu(II)-complexes. These techniques indicated that monomeric complexes were formed in which the copper(II)-ion was surrounded by the functional groups present in the side-chains of the amino acid residues. Infrared and Raman spectroscopic analysis of the dried complexes showed coordination of the N^{τ}-nitrogen atom of the histidinyl imidazole ring and monodentate coordination of the carboxylate functionality. Thus,

these data pointed to a close structural mimicry of many metalloenzyme active sites by these TAC-based constructs.

After establishing close structural mimicry, the applicability of these TAC-based mimics in biologically relevant chemistry was evaluated. For this two important reactions were selected: immobilization of molecular oxygen by copper(I)-complexes, as found in hemocyanin, and oxidation of olefins by iron(II)-hydrogen peroxide. Biological counterparts of this last reaction are found in Rieske dioxygenases like naphthalene 1,2-dioxygenase. With respect to the behavior of the TAC-based metalloenzyme active site mimics in Cu(I)-O_2 chemistry, all three copper(I)-complexes reacted with molecular oxygen from the air under the formation of dimeric bis(μ-hydroxo) dicopper(II) complexes. Infrared and Raman analysis of the dried complexes showed the formation of the bis(μ-hydroxo) dicopper(II) core in all three cases. These analyses also indicated that coordination of the histidinyl imidazole rings to the copper(II) centers mainly occurred by the N^{τ}-nitrogen atoms. Coordination of the carboxylate functionalities, present in two of the three mimics, was either monodentate to copper with the remaining carboxylate oxygen atom participating in hydrogen bond formation, or bridging mono- or bidentate. Be this as it may, the formation of biologically relevant dimeric complexes was shown, especially for the 3-histidine residue triad mimic. With respect to the applicability of the TAC-based metalloenzyme active site mimics in the Fe(II)-H_2O_2 catalyzed oxidation of olefins, it appeared that the presence of the mimics did not result in an increase in product formation. This showed that the mimics played at best a weak role in the catalytic reaction. The results obtained in these two biomimetic reactions indicated that TAC-based metalloenzyme active site mimics could be used as models for enzymatic activity even though improvements can be made.

Although the TAC-based mimic of the "3-histidine" triad found in many metalloenzyme active sites was initially constructed for the mimicry of those active sites, we were also interested in the behavior of these tri-dentate ligand systems in asymmetric catalysis. As was mentioned above, the chemical space that can be offered by an

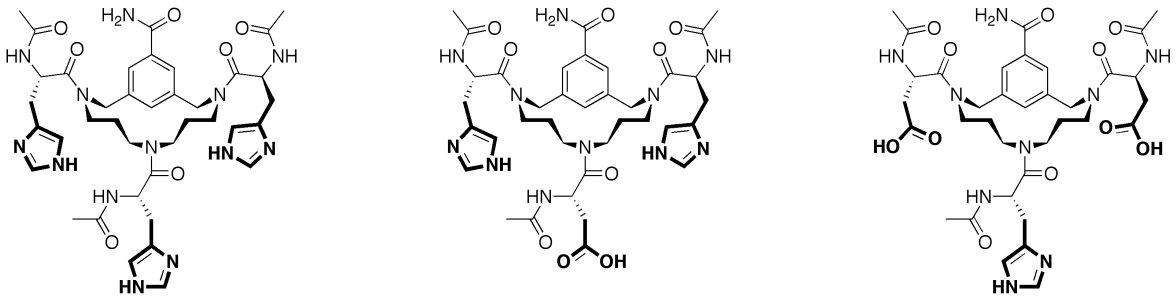

Figure 3. Overview of the TAC-based non-heme metalloenzyme active site mimics studied in this thesis.

orthogonally protected TAC-scaffold is very large and might be employed for the construction of numerous ligand-systems that can be used in asymmetric catalysis. Whereas the approaches described above were focused on the construction of enzyme active site mimics, this line of research could potentially lead to the construction of artificial enzymes. In view of these considerations, the enantiomeric excess of approximately 50% that was observed in copper-catalyzed Diels-Alder and Michael addition reactions, two important carbon-carbon forming reactions, is promising. The origin of the enantiomeric excess in these catalyzed reactions was the chiral centre of the amino acid residues. It was also shown that *N*-terminal extensions resulted in a complete loss of enantioselectivity.

Finally, even though enzyme active site mimics themselves are interesting objects to study, applications of such enzyme models make them even more interesting. In order to pursue a possible application, the TAC-based "3-histidine" triad mimic was conjugated to vancomycin using copper-catalyzed alkyne-azide cycloaddition chemistry. By conjugating a mimic of commonly observed metallohydrolase active sites to a powerful targeting device we whished to construct potential antibiotics with hydrolytic activity (*figure 4*). This might add to the repertoire of antibiotics for the ongoing fight against pathogens. For this, the TAC-based model of the 3-histidine triads was equipped with an azide functionality and vancomycin was outfitted with an alkyne functionality. Since multivalent effects are known to increase the hydrolytic activity of model-systems, also a tetravalent TACzyme-vancomycin conjugate was constructed. In a model-system, targeted hydrolysis was demonstrated. In addition, in a bio-activity test using bacteria, it was shown that the activity could be modulated by the addition of zinc(II). In this example, it was shown that TAC-based enzyme active site mimics can be modulated and conjugated to larger, biologically relevant, systems. It is anticipated that the addition of powerful hydrolysis catalysts to pathogenic targeting systems can lead to antibiotics with high activity, which will show additional activity for tackling resistance-generating mechanisms.

2. Outlook

The research described in this thesis dealt with the construction of enzyme active site models or mimics using a TAC-scaffold molecule. During the course of the experiments described in this thesis, insight about the possibilities and limitations of TAC-scaffolded peptides for the mimicry of enzyme active sites was obtained. Even though structural mimics of some important enzyme active sites have been prepared, functional mimicry was less successful. In order to possibly achieve this, some suggestions for future research will be given.
In the mimicry of functional group enzymes, for which the cooperative action of pre-organized functional groups is crucial, more effort has to be put in the rigidification

of TAC-based peptidic constructs. With respect to this, *N*-terminal double cyclization using copper-catalyzed alkyne azide cycloaddition chemistry (chapter 5) has already shown to be especially interesting since the construction of the desired compound can be performed on the resin from start till finish. This was also the case for the amide-bond rigidified mimic (chapter 4), but this procedure seemed to be more prone to side-product formation. Extension of the arms with a few bulky amino acid residues might allow the introduction of a substrate-binding pocket in close proximity of the catalytically active residues. The double cyclization could then serve two purposes: (1) pre-organization of the catalytically crucial residues, and (2) introduction of a substrate binding pocket in close proximity of the catalytic site. If successful, synthesis of highly active hydrolysis catalysts could then find their way, for example, for the synthesis of novel antibiotics, which was illustrated in chapter 9. In addition to the construction of enzyme active site mimics, the described double cyclization techniques might also be used for the construction of larger double cyclic peptidic constructs as mimics of discontinuous epitopes, which are crucial in protein-protein interactions.

For mimicry of non-heme metalloenzyme active sites, significant results have been obtained. Nevertheless, improvements are required. For instance, alkylation of the N^{π}-nitrogen atom of the histidinyl imidazole rings might help to increase the solubility of the histidine-containing constructs, which will allow the assessment of Cu(I)-O_2 chemistry in aprotic solvents and at low temperature. This seems to be a

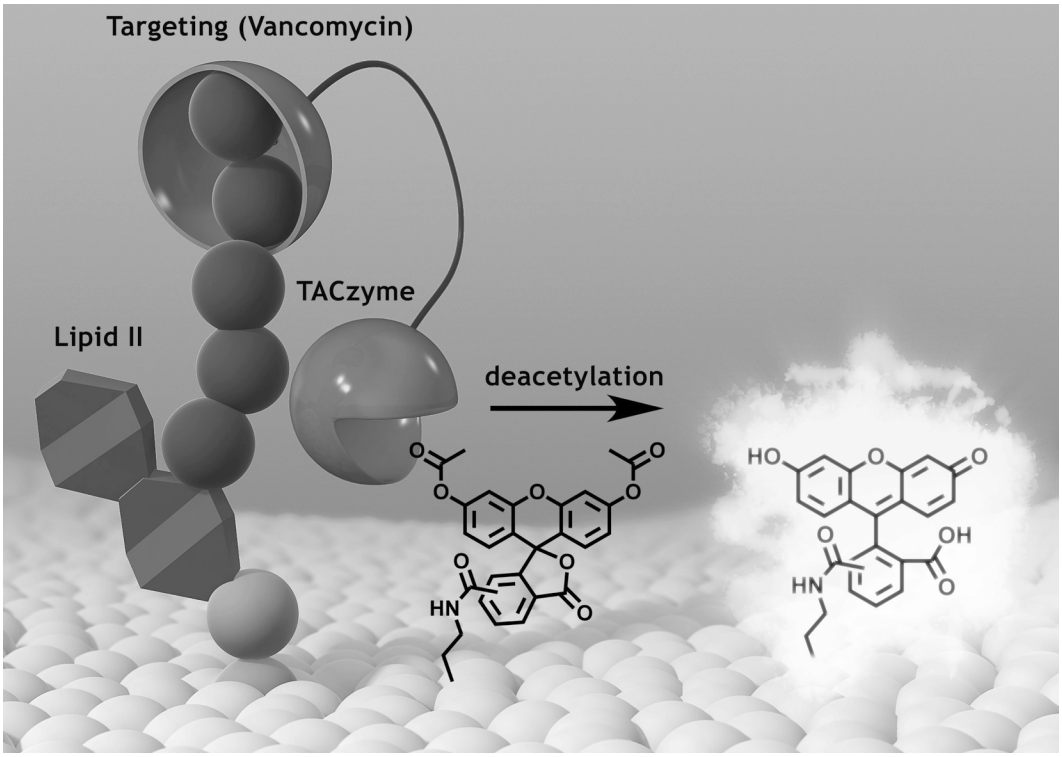

Figure 4. Schematic view of the mode of action of the constructed scorpionate antibiotic.

crucial aspect for the mimicry of biological Cu(I)-O_2 chemistry. Also, *N*-terminal hydrophobic extensions might have a beneficial effect on the stability of the CuO-species. In case of truly biomimetic Cu(I)-O_2 chemistry, study of the reactivity of the generated CuO-species with substrates would be the next step. Especially the construction of amphiphilic CuO-containing structures that might be capable of catalyzing reactions at the rim of vesicles is very interesting (see Appendix A). In addition to Cu(I)-O_2-chemistry performed by supramolecular structures, many other reactions are known to be catalyzed by metalloenzymes and several of them may be studied in such a supramolecular system. This might lead to catalytically active vesicles.

The application of TAC-based multi-dentate ligand systems in asymmetric catalysis also deserves to be explored more extensively. The results described in chapter 8 are very promising. It would be very interesting to investigate whether the enantiomeric excess might increase upon introduction of a combination of L- and D-amino acids. This would be indicative of some additional assistance of the scaffold molecule itself. Furthermore, incorporation of the azide-containing mimic in proteins, for instance, deserves exploration. This may lead to enzyme like proteins in which a novel catalytic site has been introduced. Some examples of this strategy have been described recently[1] and it would be worthwhile to assess the applicability of TAC-scaffolded ligands in this area.

Finally, the application of amphiphilic TAC-based peptidic constructs as drug-delivery systems may be very interesting (Appendix A). More efforts have to be put in the analysis of the supramolecular structures that can be obtained, but so far the preliminary results are promising. In addition, we recently discovered that TAC-based amphiphilic compounds can be used as anti-fungal agents which properties are determined by both the length of the fatty acids attached and the pH of the medium.[2]

Reference

1 See for instance: J. Steinreiber, T.R. Ward, *Topics in Organometallic Chemistry* **2009**, *25*, 93.

2 C.J. Arnusch, H.B. Albada, R.M.J. Liskamp, Y. Shai, "Nanostructure determines antifungal activity of *de novo* designed pH dependent histidine containing ultra-short lipopeptides" Abstracts of Papers, 54th Biophysical Society Annual Meeting, San Francisco, CA, United States, Feb. 20-24, 2010.

Nederlandse Samenvatting

Katalysatoren zijn chemische bestanddelen - (kleine) moleculen of oppervlakken bestaande uit een vaste stof - die in staat zijn chemische processen te versnellen. Met het versnellen van bepaalde stappen in een chemische transformatie, kunnen zij de uitkomst van een chemische reactie sterk beïnvloeden en ervoor zorgen dat de gewenste producten in grote mate vanuit het reactiemengsel tot stand komen. Ook zijn katalysatoren in staat de vorming van ongewenste producten te reduceren, zodat industriële processen gepaard gaan met een minimale hoeveelheid aan afval. Dit is niet alleen van belang vanuit een economisch oogpunt, maar is ook cruciaal voor een duurzame samenleving.

Van alle katalysatoren die op dit moment bekend zijn, hebben enzymen de beste eigenschappen wat betreft belangrijke katalytische parameters zoals activiteit, selectiviteit en specificiteit. Deze laatste twee eigenschappen, selectiviteit en specificiteit, hebben betrekking op de capaciteit van de katalysator om uit een verzameling van moleculen één molecuul te selecteren, en dit om te zetten in één specifiek product. Dit laatste aspect is met name belangrijk voor reacties waarbij één molecuul theoretisch in meerdere moleculen omgezet kan worden, bijvoorbeeld in reacties waarbij nieuw chirale centra worden gemaakt.

Enzymen zijn katalytisch actieve eiwitten, die over het algemeen zijn opgebouwd uit een aaneenrijging van aminozuren (*figuur 1*). Er zijn vele subtiele factoren van belang bij de totstandkoming van de totale activiteit van een enzym. Eén van de meest bepalende factoren voor deze activiteit is echter de plaatsing van specifieke functionele groepen in een speciaal daarvoor geoptimaliseerde uitsparing in het eiwit. In deze uitsparing heerst een soort van micro-klimaat, waarvan de eigenschappen fundamenteel verschillen van

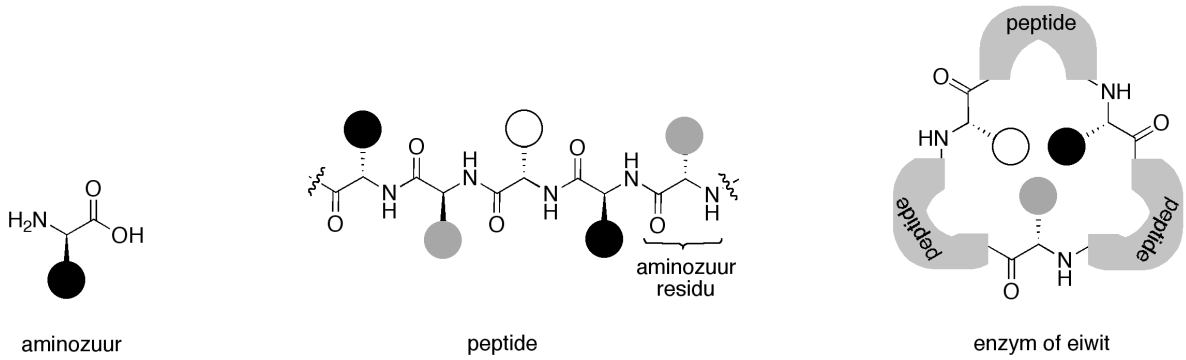

Figuur 1. Schematisch overzicht voor de opbouw van eiwitten uit aminozuur residuen.

die van de omringende oplossing. Door dit micro-klimaat én door de zeer precieze plaatsing van enkele functionele groepen, welke veelal afkomstig van aminozuur-residuen, kunnen de sterke covalente bindingen in reagerende moleculen onder milde condities verbroken of gevormd worden.

Dankzij de sublieme eigenschappen van enzymen zijn wetenschappers uitgedaagd om hun eigenschappen na te bootsen met kleine synthetische verbindingen, de zogenaamde modellen. Dit nabootsen van het actieve gebied en/of de activiteit van het enzym dient twee doelen. Aan de ene kant kunnen synthetische modellen gebruikt worden om de factoren die belangrijk worden geacht voor de reactie op waarde te schatten, en om zeer specifieke reactiestappen in een chemische transformatie te ontrafelen. In het verleden is aangetoond dat simpele moleculen als modellen voor enzymen kunnen helpen bij het ophelderen van de structuur van het katalytisch actieve deel van het enzym. Aan de andere kant dienen synthetische modellen als hulpmiddel bij het ontwikkelen van nieuwe katalysatoren die dezelfde chemische reacties kunnen katalyseren als enzymen. Want, hoe geschikt enzymen ook zijn voor veel reacties, hun beperkte stabiliteit in organische oplosmiddelen, en gevoeligheid voor temperatuur-schommelingen, additieven en pH-waardes zijn belangrijke beperkingen voor de toepassing van deze biologische katalysatoren. Synthetische modellen van enzymen hebben deze beperkingen vaak niet, en kunnen zodanig aangepast worden dat de chemische transformatie ook onder ruige condities gerealiseerd kan worden.

In het onderzoek dat beschreven staat in dit proefschrift, is op verschillende wijzen geprobeerd om de activiteit van enzymen na te bootsen met behulp van synthetische modellen. Zoals geïllustreerd in *figuur 1* bestaan enzymen uit een aaneenrijging van aminozuren, en wordt de katalytische activiteit voornamelijk bepaald door slechts enkele aminozuur-residuen die op hun plaats worden gehouden door de rest van het eiwit. Omdat de rest van dit eiwit vooral een ondersteunende rol heeft, is deze vervangen door een klein molecuul waaraan aminozuur-residuen gekoppeld kunnen worden (*figuur 2*). Dit kleine molecuul, dat fungeert als een soort kapstok waaraan

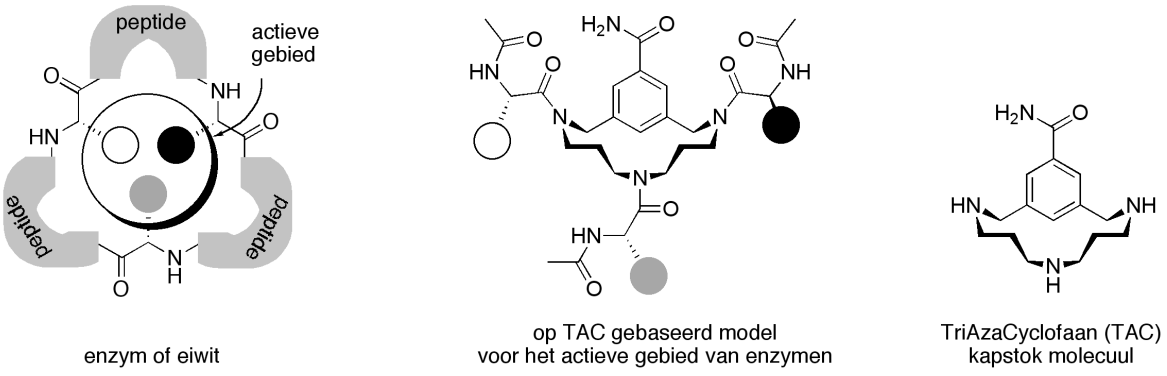

Figuur 2. Schematische voorstelling van het onderzoek beschreven in dit proefschrift.

aminozuren en peptiden gekoppeld kunnen worden, is TriAzaCyclofaan (TAC). Door dit TAC-molecuul te voorzien van drie verschillende beschermgroepen kunnen de amines selectief gekoppeld worden aan verschillende aminozuur-residuen.

Allereerst hebben we ons gericht op de nabootsing van één van de meest voorkomende categoriën enzymen, namelijk de serine hydrolasen. Deze enzymen hydrolyseren esters en peptiden door middel van het katalytische drietal van aminozuur-residuen Asp-His-Ser (*figuur 3*). In eerste instantie hebben we de drie katalytisch actieve aminozuur-residuen van deze enzymen op het TAC-molecuul geplaatst en de katalytische activiteit van de drie resulterende moleculen geanalyseerd door de hydrolysesnelheid van een actieve ester te meten (hoofdstuk 2 en *figuur 3*). Omdat deze hydrolysesnelheid niet veel sneller was dan de hydrolyse gekatalyseerd door een simpel imidazool derivaat, hebben we geconcludeerd dat er geen samenwerking is tussen de drie aminozuur residuen. Het is bekend dat deze samenwerking cruciaal is voor een hoge activiteit. Uit NMR-analyse is inderdaad gebleken dat de gemaakte modellen geen definieerbare structuur hebben.

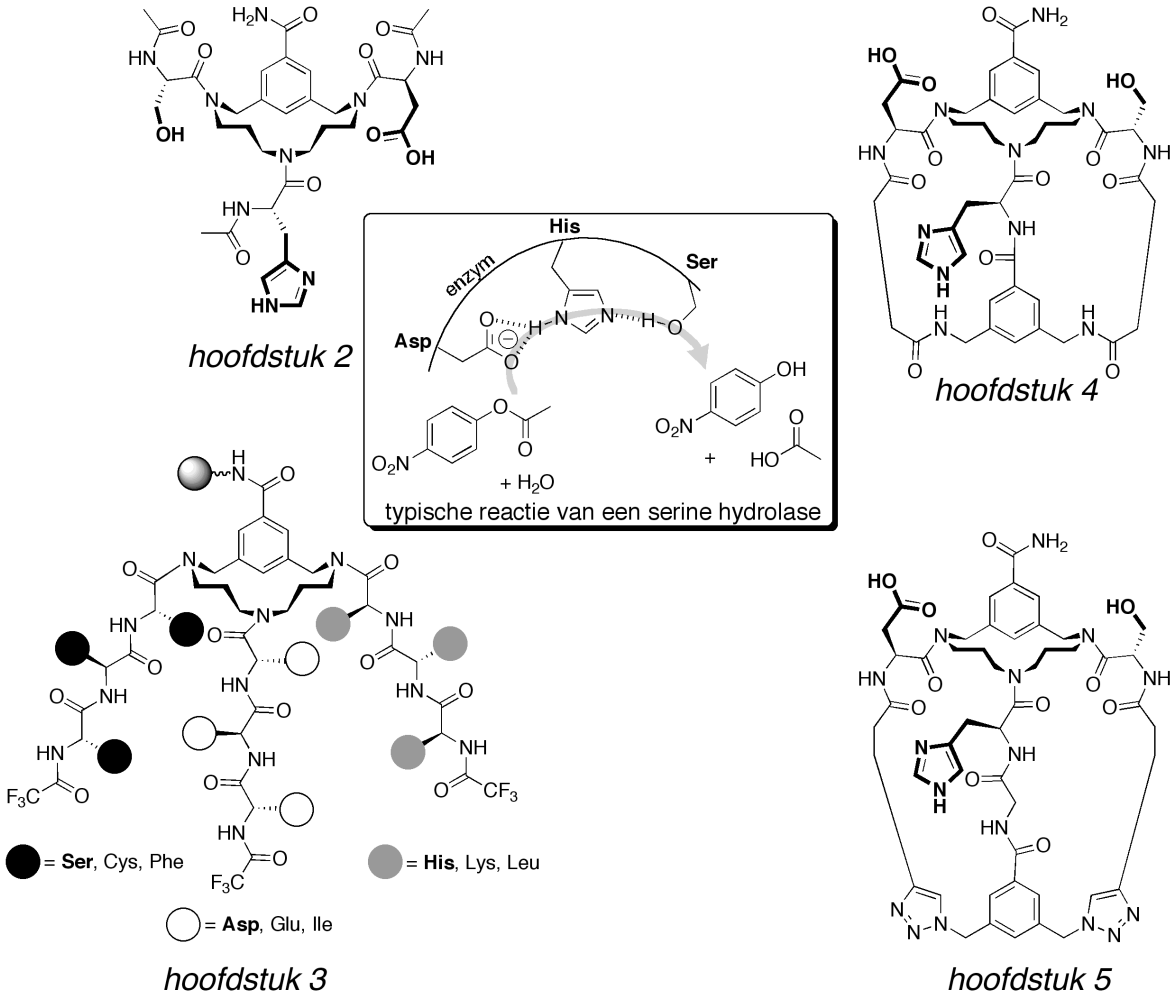

Figuur 3. Overzicht van de vier benaderingen die verkend zijn voor het nabootsen van serine hydrolasen.

Als gevolg van deze lage hydrolytische activiteit en het gebrek aan een gedefinieerde structuur van de gemaakte verbindingen, is er een aanpak verkend waarin een grote verzameling aan gewenste verbindingen gemaakt en getest kan worden op hydrolytische activiteit (hoofdstuk 3). Door gebruik te maken van combinatoriële chemie, is een grote zogenaamde bibliotheek van verbindingen gemaakt (*figuur 3*). Deze bibliotheek bestond uit bijna 20.000 verschillende moleculen, welke geïmmobiliseerd waren aan een vaste drager. Deze vaste drager bestaat uit kleine hars-bolletjes en elk hars-bolletje bevat een unieke verbinding. Omdat deze bibliotheek gemaakt was op hars-bolletjes was het analyseren van de katalytische activiteit (screenen) eenvoudig uit te voeren door een latent fluorescent molecuul of substraat toe te voegen. Actieve verbindingen zullen het latent fluorescente substraat omzetten in een fluorescent molecuul, hetgeen resulteert in een oplichtend hars-bolletje. Als gevolg van deze screening zijn verschillende actieve verbindingen geïsoleerd en geïdentificeerd. Hersynthese van enkele van de geïdentificeerde verbindingen en analyse van de kinetische parameters betreffende de hydrolyse van een substraat, heeft uitgewezen dat ook deze moleculen geen significant hogere activiteit vertonen dan simpele imidazool derivaten en de kleine modellen beschreven in hoofdstuk 2.

Door de beperkte activiteit van de gesynthetiseerde verbindingen en omdat deze lage activiteit waarschijnlijk het gevolg was van de hoge flexibiliteit van de verbindingen, zijn er vervolgens moleculen gemaakt waarin de flexibiliteit in grote mate is gereduceerd. Hiertoe zijn de uiteinden van de aminozuur-residuen die aan het TAC-molecuul gebonden zijn op covalente wijze met elkaar verbonden. In eerste instantie is deze verbinding van de uiteinden gerealiseerd met behulp van amide-binding vormende reacties (hoofdstuk 4). Hiervoor is er op elk van de buitenste aminozuur residuen een beschermd carbonzuur geïntroduceerd, en is er op het middelste residu een beschermde bis-amine geplaatst. Door zowel het bis-amine als de beschermde carbonzuren vlak voor het sluiten van de dubbele ring beschikbaar te maken, is het mogelijk gebleken een zeer compact kooi-molecuul te maken (*figuur 3*). In dit kooi-molecuul zijn alle functionele groepen aanwezig die ook gevonden worden in het active gebied van veel serine hydrolasen. Hoewel de uiteindelijk gemaakte en geïsoleerde hoeveelheid zeer laag was - hetgeen vooral veroorzaakt werd door de moeilijke dubbele ringsluitingsreactie en de zeer moeilijke zuivering - is het gelukt om een kleine en zeer compacte nabootsing van serine hydrolasen te maken.

Vanwege de lage opbrengst van de reactie is er vervolgens een andere methode verkend voor het sluiten van de dubbele ring (hoofdstuk 5). Een recentelijk populair geworden reactie is de door koper(I)-gekatalyseerde reactie tussen een eindstandig alkyn en een azide, die leidt tot vorming van een 1,4-gesubstitueerde 1,2,3-triazool ring. Door het plaatsen van twee eindstandige alkynen op de buitenste residuen en een bis-azide, alsmede het introduceren van een extra glycine residu in de middelste

arm van het TAC-molecuul, is het gelukt om een dubbel gesloten kooi-molecuul te maken (*figuur 3*). Ook voor dit molecuul was de uiteindelijke zuivering erg lastig. Er waren meerdere opeenvolgende zuiveringsstappen vereist, waardoor ook deze methode van ringsluiten in een lage opbrengst resulteerd. Desalniettemin is het gelukt om het gewenste product te vormen, hetgeen bewezen is door middel van analyse met fragmentatie massa-spectrometrie. Door een gebrek aan tijd en de lage hoeveelheid verzamelde eind-verbinding is het helaas niet mogelijk geweest de hydrolytische activiteit van de gemaakte verbindingen te bepalen.

De hierboven beschreven benaderingen resulteerden in modellen van slechts één groep enzymen, namelijk de serine hydrolasen. Deze groep enzymen valt onder de categorie van *functionele groep* enzymen en katalyseert chemische reacties door een subtiel samenspel van functionele groepen, die geplaatst zijn in het actieve gebied van het enzym. Naast de categorie van functionele groep enzymen, is er ook een grote categorie van enzymen die een katalytisch cruciaal metaalion bevatten. Deze categorie van enzymen, die circa eenderde van alle tot nu toe bekende enzymen beslaat, staat bekend als *metalloenzymen*. Kenmerkend voor deze categorie enzymen is dat de chemische reactie plaats vindt aan het metaalion (*figuur 4*). In aanvulling op boven genoemde studie, waarin het TAC-molecuul als hulpmiddel bij het nabootsen van *functionele groep* enzymen, is ook zijn toepassing in de nabootsing van *metalloenzymen* bestudeerd.

Veel van de bekende metalloenzymen gebruiken aminozuur-residuen voor het immobiliseren van de voor katalyse belangrijke metaal-ionen. Van de 20 meest voorkomende aminozuren worden vooral histidine (His) en asparaginezuur (Asp) of glutaminezuur gebruikt voor immobilisatie van metaalionen. Met behulp van deze drie aminozuur-residuen kunnen verschillende metaalionen gebonden worden, hetgeen

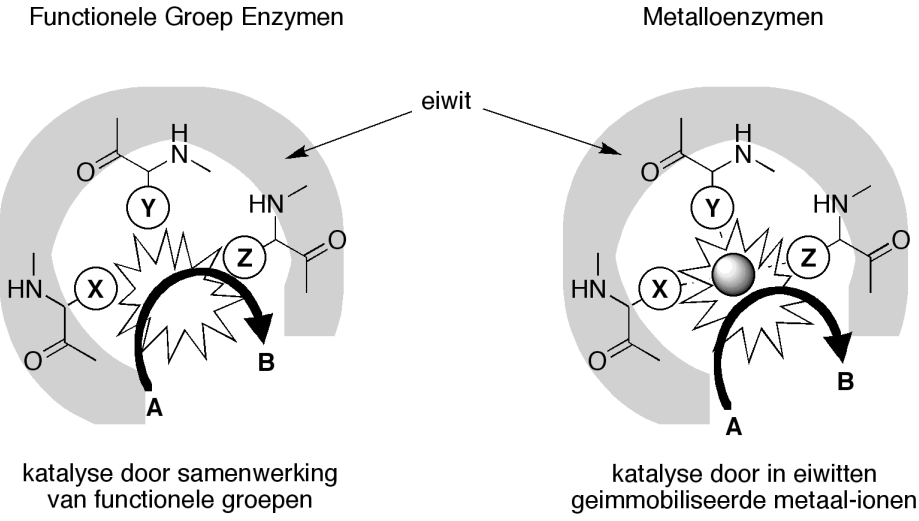

Figuur 4. Schematische vergelijking tussen functionele groep enzymen en metalloenzymen.

resulteert in een breed spectrum aan reacties die gekatalyseerd kunnen worden door metalloenzymen.

In eerste instantie hebben we drie op het TAC-molecuul gebaseerde modellen van drie veel voorkomende actieve gebieden van metalloenzymen gemaakt. Deze drie actieve gebieden bestaan uit 3-His, 2-His-1-Asp en 1-His-2-Asp, en kunnen onder andere koper, nickel, ijzer en zink immobiliseren.

Door het TAC-molecuul te voorzien van deze drie combinaties van histidine- en asparaginezuur-residuen, zijn drie structurele modellen van deze actieve gebieden gemaakt (hoofdstuk 6, *figuur 5*). Complexering van koper(II)-ionen aan deze drie modellen heeft aangetoond dat de interactie tussen het model en het ion plaatsvindt via de functionaliteiten in de zijketens van deze drie aminozuur residuen. Hoewel de twee modellen die asparaginezuur bevatten ook multimere complexen kunnen vormen, werden alleen monomere complexen aangetoond. Uit vibratie-spectroscopische studies is tevens gebleken, dat de imidazool ring van de histidine-residuen en de carboxylaat functionaliteit van de asparaginezuur-residuen op dezelfde wijze aan het metaal-ion binden als in het actieve gebied van metalloenzymen plaatsvindt.
Als vervolg op deze studie naar de coördinerende eigenschappen van de op TAC-gebaseerde metalloenzym modellen, is ook het gedrag van deze modellen in twee belangrijke biologische reacties bestudeerd (hoofdstuk 7). De natuur gebruikt veelvuldig metalloenzymen om zuurstofmoleculen te activeren en vervolgens in organische verbindingen te incorporeren. Met name ionen als koper(I), ijzer(II) en mangaan(II) worden gebruikt voor deze zuurstof-activering. In eerste instantie zijn

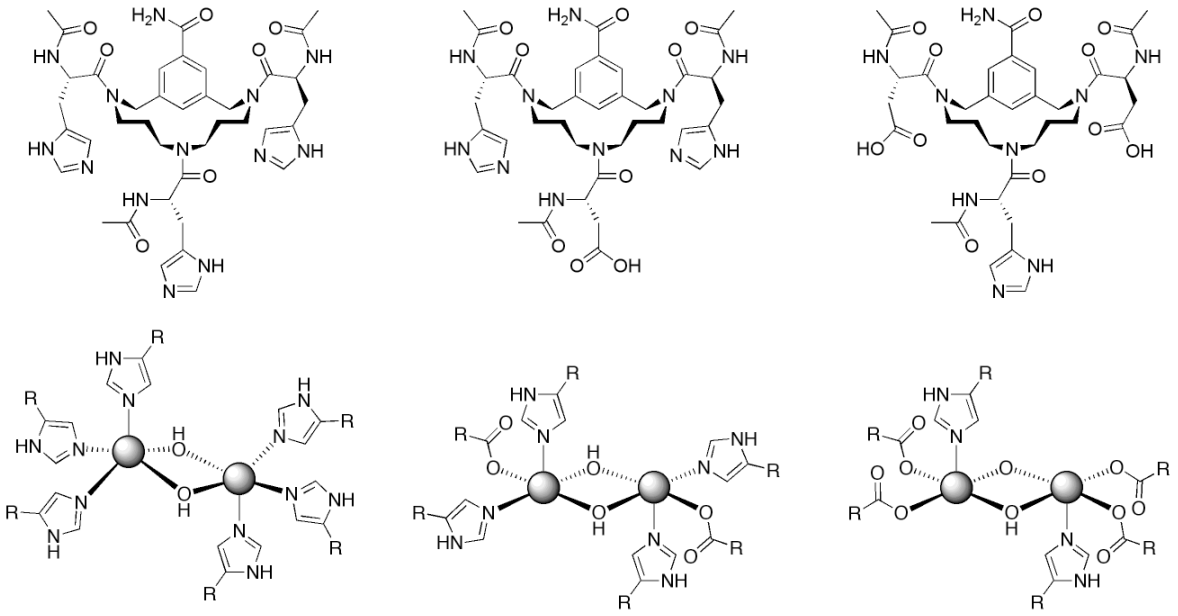

Figuur 5. Structuurformules van de drie modellen voor drie veel voorkomende actieve gebieden van metalloenzymen (*boven*) en de drie geïdentificeerde complexen welke gevormd werden door de reactie tussen de koper(I)-complexen van deze drie modellen met moleculair zuurstof (*onder*). De grijze bolletjes symboliseren de koper(II)-ionen en R de rest van de modellen.

de zuurstofbindende eigenschappen van de koper(I)-complexen van onze modellen bestudeerd. Vanwege de beperkte oplosbaarheid van onze modellen in aprotische of watervrije oplosmiddelen, resulteerde het binden van zuurstof in alledrie de gevallen in de vorming van dimere *bis(*μ*-hydroxo) dicopper(II)* complexen (*figuur 5*). Alledrie de eind-vormen van de complexen zijn uitvoerig gekarakteriseerd met behulp van UV-vis, infrarood en Raman spectroscopie. Hieruit kwam naar voren dat het complex dat gebaseerd is op drie histidine-residuen, een structurele nabootsing is van één van de meest voorkomende zuurstof-transporterende eiwitten en van enkele oxiderende enzymen welke een cruciale rol spelen in de bruining van fruit en van de huid. In een ander experiment is het gedrag van deze drie modellen in de door Fe(II)-H_2O_2 gerealiseerde oxidatie van alkenen bestudeerd. In geen van de gevallen hadden de modellen een positieve invloed op de activiteit.

Ondanks de teleurstellende activiteit in de ijzer-gekatalyseerde oxidatie van alkenen, zijn zowel de resultaten in de complexering van koper(II) als de zuurstofbindende eigenschappen van koper(I)-complexen veelbelovend. Toekomstig onderzoek naar de toepassing van dergelijke op TAC-gebaseerde nabootsingen van metalloenzymen, kan zeer goed leiden tot verbeterde eigenschappen van de modellen.

Hoewel het grootste gedeelte van dit proefschrift betrekking heeft op de nabootsing van het actieve gebied van zowel *functionele groep enzymen* als *metalloenzymen*, zijn ook twee andere toepassingen van op TAC-gebaseerde systemen bestudeerd.

Voor toepassing van op TAC-gebaseerde moleculen in katalytische reacties, is het gedrag van één zo'n modelverbinding in twee door koper(II)-gekatalyseerde koolstof-koolstof binding vormende reacties bestudeerd (hoofdstuk 8). Recentelijk is ontdekt dat koper(II) sommige Diels-Alder reacties en Michael additions kan versnellen. In afwezigheid van een ligand dat coordineert aan het koper(II)-ion, is de uitkomst van beide reacties een racemisch mengsel. Door gebruik te maken van het op TAC-gebaseerde model dat drie histidine-residuen bevat, is voor beide reacties vorming van een enantiomere overmaat 50% waargenomen. Dit wil zeggen dat voor elke uitgevoerde reactie drie van de vier geproduceerde moleculen dezelfde chiraliteit hebben. Door gebruik te maken van D- en L-histidine residuen is vervolgens gebleken dat de chiraliteit voornamelijk afkomstig is van de chiraliteit van de aminozuren. Daarnaast is gebleken dat residuen op de *C*-terminus van het TAC-molecuul of de *N*-terminus van de histidine-residuen de uitkomst van de reactie sterk kunnen beïnvloeden.

Tot slot is de mogelijke toepassing van op TAC-gebaseerde enzym modellen in de synthese van nieuwe antibiotica onderzocht (hoofdstuk 9). Hiervoor werd het antibioticum vancomycine - dat gebruikt wordt als laatste redmiddel en dat aan een

specifieke moleculaire structuur aan de buitenkant van de cellen van bacteriën bindt - gebonden aan een enzym model. Om dit te realiseren werd een op het TAC-molecuul gebaseerd model aan de *C*-terminus van het TAC-molecuul voorzien van een azide groep. Deze azide werd vervolgens covalent gebonden aan terminale alkyn-groepen die op vancomycine waren aangebracht. Op deze manier zijn zowel monovalente als tetravalente - met één of vier enzym modellen, respectievelijk - model-vancomycine conjugaten zijn gemaakt. Hoewel doelgerichte hydrolytische activiteit van de modellen is aangetoond, bleef de antibacteriële activiteit achter bij die van vancomycine.

Zowel voor de nabootsing van functionele groep enzymen als van metalloenzymen is gebleken dat op TAC-gebaseerde moleculen zeer bruikbaar zijn. Ook is gebleken dat deze moleculen gebruikt kunnen worden in asymmetrische katalyse en doelgerichte hydrolyse. Toekomstig onderzoek naar deze moleculen is dan ook zeer interessant en kan leiden tot nieuwe toepassingen in katalyse en de synthesis van nieuwe medicijnen.

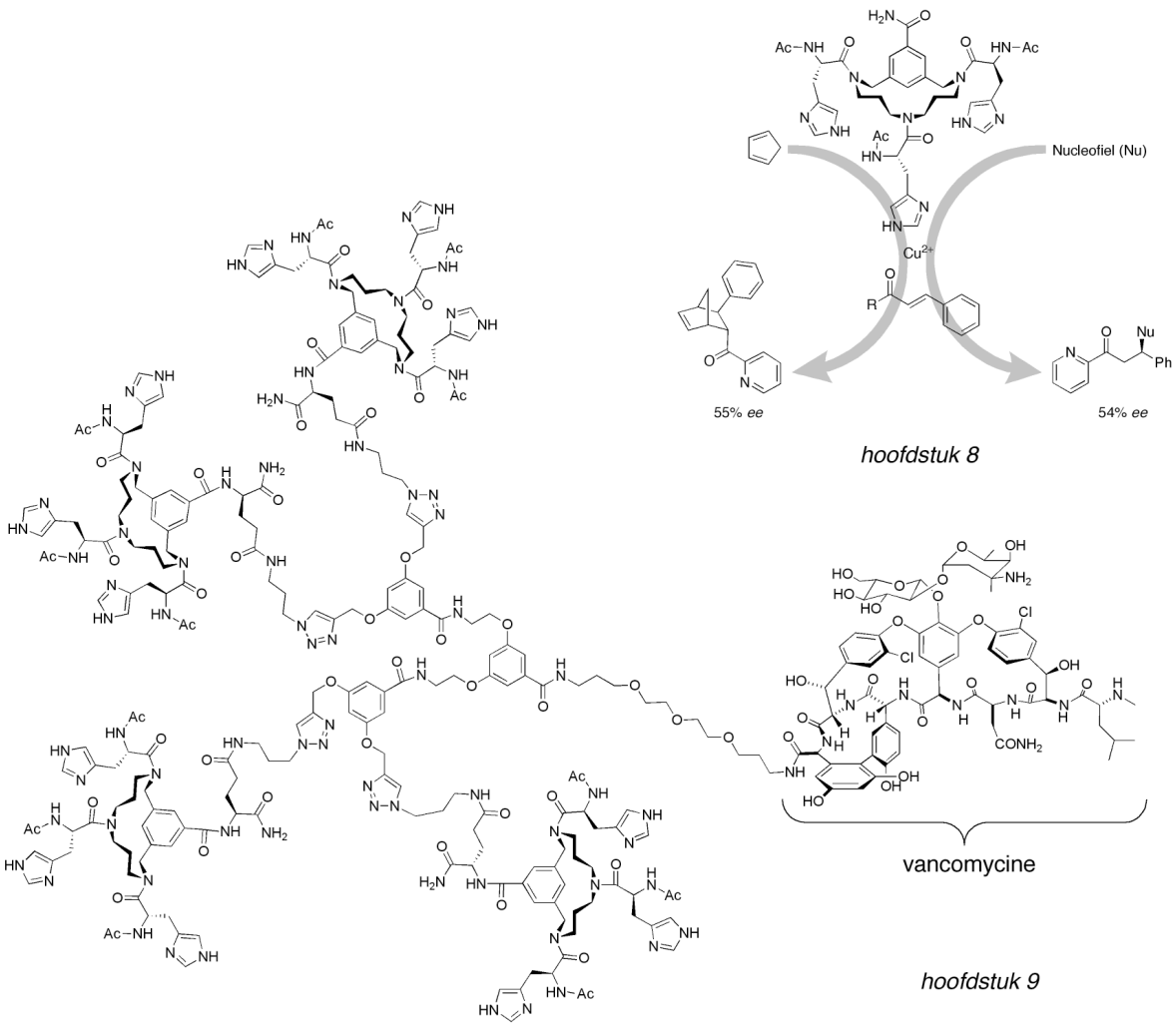

Figuur 6. Twee toepassing van op TAC-gebaseerde enzym modellen. Rechtsboven staat de toepassing in asymmetrisch gekatalyseerde koolstof-koolstof binding vormende reacties en linksonder de toepassing in de synthese van een nieuw type antibiotica.

List of Abbreviations

Amino Acids

Xxx	X	Full name
Ala	A	Alanine
Arg	R	Arginine
Asp	D	Aspartic acid
Cys	S	Cysteine
Glu	E	Glutamic acid
Gln	Q	Glutamine
Gly	G	Glycine
His	H	Histidine
Ile	I	Isoleucine
Leu	L	Leucine
Lys	K	Lysine
Met	M	Methionine
Nle	X	Norleucine
Phe	F	Phenylalanine
Pro	P	Proline
Ser	S	Serine
Thr	T	Threonine
Trp	W	Tryptophane
Tyr	Y	Tyrosine
Val	V	Valine

Solvents

DCM	dichloromethane
DMF	*N*,*N'*-dimethylformamide
DMSO	dimethylsulfoxide
EtOAc	ethylacetate
MTBE	methyl-*tert*-butyl ether
NMP	*N*-methylpyrrolidone
THF	tetrahydrofuran

Symbols

δ	chemical shift
Δ	difference
λ	wavelength
v	volume
w	weigth
s	singlet
d	doublet
t	triplet
q	quartet
m	multiplet
br	broad

Reagents/Chemicals

AIBN	2,2'-azobisisobutyronitril
BOP	benzotriazol-1-yl-oxytris-dimethylamino-phosphonium hexafluorophosphate
DBU	1,8-diazabicyclo[5.4.0]undec-7-ene
D*i*PEA	*N*,*N'*-diisopropylethylamine
DMAP	*N*,*N'*-dimethyl-4-pyridine
DMM	dimethyl malonate
DTNB	5,5'-dinitro-bis(2-nitrobenzoic acid)
DTT	dithiothreitol
EDC	1-ethyl-3-(3-dimethylamino-propyl)carbodiimide
EDTA	ethylenediaminetetraacetic acid
EtOTFAc	ethyl trifluoroacetate
HATU	2-(1H-7-azabenzotriazol-1-yl)-1,1,3,3-tetramethyl uronium hexafluorophosphate
HOAt	1-hydroxy-7-azabenzotriazole

HOBt	*N*-hydroxybenzotriazole
4-MeIm	4-methylimidazole
NBS	*N*-bromosuccinimide
NM	nitromethane
PTSA	anilinium *para*-toluenesulfinate
TBAB	tetrabutylammonium bromide
TBAF	tetrabutylammonium fluoride
TEA	triethylamine
TIS	triisopropylsilane
TMS	tetramethylsilane

Protecting groups

Ac	acety
All	allyl
Alloc	allyl-oxycarbonyl
Boc	*tert*-butyloxycarbonyl
Fmoc	9-fluorenylmethyl-oxycarbonyl
o-NBS	*ortho*-nitrobenzenesulfonyl
*t*Bu	*tert*-butyl
Te	2-(trimethylsilyl)ethyl
Teoc	2-(trimethylsilyl)ethyl-oxycarbonyl
TFAc	trifluoroacetyl
Trt	triphenylmethyl (also 'trityl')

Techniques

DLS	dynamic light scattering
ESI	electrospray ionization
GC	gas chromatography
HPLC	high pressure liquid chromatography
IR	infrared
MALDI	matrix assisted laser desorption ionization
MS	mass spectrometry
μW	microwave
TEM	transmission electron microscopy
TLC	thin layer chromatography
TOF	time-off flight
UV	ultra violet

Others (chemistry)

Ar	aromatic
Asc	ascorbate
BAMB	3,5-bis(aminomethyl)benzoic acid
BAzMB	3,5-bis(azidomethyl)benzoic acid
Bt	benzotriazole
Cp*	pentamethylcyclopentadienyl
DACF	di-acetyl carboxyfluorescein
dea	diethylamine
Im	imidazole
MeIm	4-methylimidazole
*p*NAc	acetyl *para*-nitrophenol
OSu	oxysuccinimide
PEG	poly ethyleneglycol
PS	polystyrene (resin)
Pyr	pyridine
Tf	trifluormethanesulfonate
TG	tentagel (resin)
TFA	trifluoroacetic acid or acetate

Others (terminology)

ATP	attached proton tes
CuAAC	copper-catalyzed alkyne-azide cycloaddition
DA	Diels-Alder
FC	Friedels-Craft
LUV	large unilamellar vesicles
MA	Michael addition
MIC	minimum inhibitory concentration
PDI	poly dispersity index
RuAAC	ruthenium-catalyzed alkyne-azide cycloaddition
TON	turnover number

List of Publications

H.B. Albada, C.J. Arnusch, H.M. Branderhorst, A.-M. Verel, W.T.M. Janssen, E. Breukink, B. de Kruijff, R.J. Pieters, R.M.J. Liskamp, "Potential scorpionate antibiotics: Targeted hydrolysis of lipid II containing model membranes by vancomycin–TACzyme conjugates and modulation of their antibacterial activity by Zn-ions", *Bioorg. Med. Chem. Lett.* **2009**, *19*, 3721-3724.

H.B. Albada, R.M.J. Liskamp, "TAC-scaffolded tripeptides as artificial hydrolytic receptors: a combinatorial approach toward esterase mimics", *J. Comb. Chem.* **2008**, *10*, 814-824.

H.B. Albada, F. Soulimani, B.M. Weckhuysen, R.M.J. Liskamp, "Scaffolded amino acids as a close structural mimic of type-3 copper binding sites", *Chem. Commun.* **2007**, 4895-4897.

J. van Ameijde, H.B. Albada, R.M.J. Liskamp, "A convenient preparation of several *N*-linked glycoamino acid building blocks for efficient solid-phase synthesis of glycopeptides", *J. Chem. Soc., Perkin Trans. 1* **2002**, 1042–1049.

In preperation:

C.J. Arnusch, H.B. Albada, M. van Vaardegem, R.M.J. Liskamp, Y. Shai, "Nanostructure determines antifungal activity of de novo designed pH dependent histidine containing ultra-short lipopeptides".

H.B. Albada, F. Rosati, D. Coquière, G.J. Roelfes, R.M.J. Liskamp, "Application of tris-Histidine Containing TACzymes in Asymmetric Copper(II)-Catalyzed Diels-Alder and Michael Addition Reactions". Chapter 8 of this thesis.

Curriculum Vitae

De auteur van dit proefschrift werd geboren op 1 november 1979 te Sneek. Na het behalen van zijn HAVO diploma in juni 1997 werd begonnen met de studie *Chemie* aan de Hogeschool Utrecht. De specialisatie *Organische Chemie* werd in 2001 afgerond na een onderzoeksstage bij de vakgroep Medicinal Chemistry (prof. dr. R.M.J. Liskamp). Tijdens deze stage is onderzoek gedaan naar de synthese van ureum peptidomimetica en glycopeptiden. In datzelfde jaar werd begonnen met een verkorte doctoraal studie *Scheikunde* aan de Universiteit Utrecht. In het najaar van 2003 werd deze studie afgerond (met genoegen) na een hoofdvak gedaan te hebben bij Medicinal Chemistry (prof. dr. R.M.J. Liskamp). Gedurende deze periode is onderzoek gedaan naar het gebruik van ring-sluiting metathese om starre synthetische receptoren te maken en is een begin gemaakt met de verwezenlijking van synthetische vaccins. Vanaf 2004 tot 2008 was hij werkzaam als AIO bij de vakgroep Medicinal Chemistry & Chemical Biology onder begeleiding van prof. dr. R.M.J. Liskamp. Het hierbij verrichte onderzoek is beschreven in dit proefschrift en is ondermeer gepresenteerd op het *EuroCombi-3* symposium in Winchester (Verenigd Koninkrijk) in 2005, de *IDECAT-meeting* in Toulouse (Frankrijk) in 2008 en het KNCV *Design & Synthesis* symposium in Lunteren (Nederland) in 2006. Van medio 2008 tot medio 2009 is hij werkzaam geweest als post-doc bij de groepen van prof. dr. P.C.J. Kamer (School of Chemistry, St. Andrews, Verenigd Koninkrijk), prof. dr. R.J.M. Klein Gebbink (Chemical Biology & Organic Chemistry, Universiteit van Utrecht) en prof. dr. R.M.J. Liskamp (Medicinal Chemistry & Chemical Biology, Universiteit van Utrecht). In deze periode is onderzoek gedaan naar de synthese van fosfine-peptiden en de toepassing van op TAC-gebaseerde enzym modellen in katalytische reacties.

Dankwoord

Een proefschrift is pas écht af als het dankwoord geschreven is. Net als vele andere proefschriften is ook dit proefschrift nooit tot stand kunnen komen zonder de hulp van collega's.

Als eerste wil ik mijn begeleider en promotor Rob Liskamp bedanken. Jouw onbegrensde enthousiasme, tomeloze geduld, enorme kennis van de meest uiteenlopende zaken die relevant zijn voor (chemisch) onderzoek en altijd bemoedigende opmerkingen. Je hebt mij gedurende mijn promotieonderzoek gaande gehouden door mij steeds weer te motiveren en te voorzien van nieuwe ideeën. Ook heb je mij voortdurend gestimuleerd om met ideeën te komen. Ik denk met veel genoegen terug aan de afgelopen jaren.

Naast de begeleiding van Rob, hebben ook enkele vaste krachten binnen *MedChem* geholpen bij dit onderzoek. Allereerst zijn de commentaren en hulp van John Kruijtzer en Dirk Rijkers, dé peptide-chemici (zonder daarmee te willen beweren dat zij alléén verstand hebben van peptide-chemie) van Nederland, zeer behulpzaam geweest bij mijn onderzoek. Kort daarachter (òf daarvoor) komt Hans Jacobs. Hans, enorm bedankt voor alle hulp die je geboden hebt bij alle praktische problemen in het lab, het jarenlang regelen van de bestellingen en de altijd blijmakende humor. Voor de NMR-studies aan de verbindingen in hoofdstuk 2 en 4 ben ik Hans Ippel zeer erkentelijk, helaas hebben we het nog niet op kunnen schrijven maar hebben we een goed idee voor de richting die toekomstig onderzoek moet krijgen. Gwenn Mulder, jij hebt me meer dan goed geholpen bij het doen van massa analyses van de cryptanden uit hoofdstuk 5 en dankzij jouw hulp is het gelukt om de verbindingen te vinden en het hoofdstuk af te maken. Ook ben ik je zeer dankbaar voor het lezen van enkele teksten.

Onze secretaresses Paula en Natatia: jullie zijn onmisbaar voor de groep en hebben ook mij gedurende de jaren met allerhande advies en praktische hulp bijgestaan. Enorm bedankt daarvoor, zonder jullie was het allemaal nog lastiger geworden.

En dan zijn er nog twee mensen die ooit bij *MedChem* werkten (zoals Hans Ippel en Hans Jacobs) maar die inmiddels elders een onderkomen hebben gevonden. Laat ik beginnen met Annemarie ("hoe-zeg-je-je-achternaam-ook-alweer") Deschesne: dankzij de vele massa's die jij gemeten hebt is het onderzoek naar de cryptanden goed van de

grond gekomen. Vervolgens my friend Chris Arnusch (aka 'Cwis Awnusch'): we started almost simultaneously at *MedChem*, had loads of fun in and outside the lab, did a project together that cumulated into a sweet paper and the other one is being worked on as we speek (right?).

Ronald Elgersma, we zijn samen begonnen bij de (toen nog) HvU en jij hebt eerder dan ik het hele traject afgelegd. Nu is het mijn beurt. Ik kan me een jaar geleden nog goed voor de geest halen. Ik ben blij dat je me bij wilt staan en dat we dit samen mogen afronden.

Dan is er nog een flink aantal studenten die ik heb mogen begeleiden. In chronologische volgorde. Steffen van der Wal, je hebt het spits mogen afbijten en gelukkig heeft het je goed gedaan want je bent nu AIO bij 'ons'. Martin van Vaardegem, jij hebt als eerste gewerkt aan de cryptanden, en de door jou gemaakte amfifiele TAC-moleculen blijken ineens actief te zijn tegen schimmels! Evan Johnson, thanks for giving me the shocking thrill of your nicotine chewing gum. Dan mijn drie Chinezen: Yanmei, Lifan Zeng en Shaoxu Huang. You all did great work: Yanmei on the phosphine-peptide-TAC constructs and Lifan and Huang contributed significantly to the work described in chapter 5. Tot slot Geertje van Hal, we hebben leuk aan fosfino-aminozuur bouwstenen gewerkt en ook nog kunnen kijken naar de synthese van fosfine-peptiden op de vaste drager. Hoewel het niet af is, hebben we toch leuke ontdekkingen gedaan voor de toekomst.

Mijn huidige directe labgenoten Nathaniel Martin, Timo Koopman en Peter 't Hart, en de inmiddels lang vertrokken Chantal Appeldoorn, Reshma Autar, Magali Dousset: jullie hebben het tot een memorabele periode gemaakt. Bedankt voor de goede sfeer, toffe grappen en het fiepjes-kanon. Ik wil Jeroen van Ameijde apart bedanken voor het mij leren van de 'ropes', dankzij het fundament dat ik onder jouw begeleiding heb gelegd heb ik dit boek kunnen produceren. Dan zijn er nog voor de 'algemene sfeer en dagelijkse discussies': Hilbert Branderhorst, Monique van Scherpenzeel en Monique Mulder, Marjolein van de Kaaden, Nuria Parera Pera, Francesca Pertici, Loek van Wandelen (moeten wel opschieten met vissen, maar dat is mijn fout), Raymond 'Braking Bad' Kooij, Hilde van Hattum, Rik Cleophas, Cheng (wat doe jij hier?), Alex Poot, en Joeri Kuijl: jullie hebben allemaal bijgedragen aan de goede sfeer en ook in gesprekken/ discussie bijgedragen aan mijn ontwikkeling. Dank! Natuurlijk geldt dit ook voor de 'oude' labs met Anton Bunschoten, Arwin Brouwer, Maarten van Dijk, Remco Merckx, Jing Zhang en Jack Slootweg: bedankt alles. Aan de nieuwelingen Thierry, Helmus en Jacqueline: succes!

Voor het mij bijbrengen van enkele modelling-principes wil ik Ed Moret en Hans Hilbers bedanken, hoewel ik dergelijke modellen slechts gebruik als een luxe of drie-dimensionale ChemDraw heb ik de kunst toch fijn bij jullie af kunnen kijken. Roland

Pieters (en ook Eefjan Breukink) wil ik bedanken voor de kritische doch zeer behulpzame discussies omtrent het in hoofdstuk 9 beschreven onderzoek. Ik wil Cristina Chamorro bedanken voor alle discussies, jouw werk aan receptoren hebben (samen met het werk van Menno Monnee en Jan-Willem Hofman) aan de basis gestaan van dit onderzoek. Johan Kemmink, bedankt voor de hulp bij het doen van MAS-NMR aan beads en algemene hulp bij de NMR.

Ook collega's waar ik dagelijks minder mee te maken heb gehad, wil ik bedanken. Allereerst voor de verassende en goede opmerkingen tijdens de verschillende besprekingen, maar ook voor de goede sfeer. Bert van den Berg, Cees ('volleybal') Beukelman, Marcel (you have mail, master) Fischer, Bart Halkes, Burt ('kart-en-laserquest') Kroes, Nico de Mol, Edwin van Kampen tot van den Worm, Rob Ruijtenbeek, Hans Hilbers, Linda Quarles van Ufford.

Naast de directe collega's zijn er ook enkele collega's uit andere vakgroepen die significant bijgedragen hebben aan dit onderzoek. Allereerst Fouad Soulimani en Tom Visser van vibratie spectroscopie. Fouad, we hebben een mooi stukje vibratie spectroscopie gedaan en samen met Tom hebben we de interpretatie mooi rond gekregen. Het was de tompouchen meer dan waard. Voor het meten dan de UV-vis diffuse reflectie ben ik Marianne Kox en Inge Buurmans dankbaar. Met name wil ik ook Bert Weckhuysen bedanken voor de behulpzame discussies die mij op gang hebben gebracht voor het werk beschreven in hoofdstuk 6 en 7. Cees Versluis wil ik bedanken voor het meten van talloze massa's en goede conversaties. Bert Klein Gebbink, Marcel Moelands en Harm Dijkstra ben ik dankbaar voor de discussies en hulp bij de door ijzer(II)-gekatalyseerde oxidatie van alkenen. Gerard Roelfes, David Coquière en Fiora Rosati bedank ik voor hun werk dat beschreven is in hoofdstuk 8, we gaan er een mooi verhaal van maken. Arie Schouten en Mark van Raaij (Santiago de Compostela) wil ik bedanken voor zijn inspanningen voor het kristalliseren van TAC-verbindingen. Martin Lutz voor het ophelderen van de structuur van het TAC-molecuul. Myrra en Mies van Biopharmacy wil ik bedanken voor de instructes voor de DLS. Hans Meeldijk wil ik bedanken voor de interessante middag bij de cryo-TEM. Paul Kamer wil ik bedanken voor het mogelijk maken van mijn verblijf in St. Andrews en de nuttige discussies die we hebben gevoerd voor het maken van op TAC-gebaseerde peptide-fosfine conjugaten. Ook mijn collega's in St. Andrews wil ik bedanken voor deze discussies en ook voor het aangename verblijf dat ik on Schotland heb gehad. Crina Balog (LUMC), ik wil jou bedanken voor de vriendschap en de goede gesprekken. Ik ben blij dat je één van mijn paranimfen wil zijn.

Dan zijn er ook nog heel-heel-heel lang geleden vertrokken labgenoten die, hoewel niet direct bij dit onderzoek waren betrokken, toch bijgedragen hebben aan het totale labgebeuren. Ik noem Frank Dekker, Ingrid Dijkgraaf, Laurence de Fays, Nourdin Ghalit,

John Joosten Menno Monnee, Jan Tois, Pieter van der Veken, Yannis Vrasidas, Eelco Ruijter, Bas Wels en Dirk-Jan van Zoelen. Tot slot de van het Iberische schiereiland afkomstige Miriam Alías, Lluis Ballell, Ana Hernandez Higueras en Olga Familiar: muchos gracias.

Dat waren alle aan dit werk gerelateerde bedankjes, nu de persoonlijke. Als eerste wil ik Gwenn (nogmaals) bedanken. In drie, nee, vier gescheiden periodes hebben we samen op het lab gestaan, waarvan de laatste zonder meer de meest interessante. Ik zal mijn best doen om net zo'n goede hulp voor jou te zijn als jij voor mij bent geweest, zonder jouw inzet was hoofdstuk 5 nooit afgekomen. Je bent ontzettend belangrijk voor me! en ik kijk uit naar wat de toekomst ons gaat brengen.

Tot slot mijn directe familie. Peter en Wendy (en Robin), Fennie en Sjanet: bedankt voor jullie begrip voor mijn drukte. Ik ben enorm blij met jullie aanwezigheid in mijn leven en hoop dat we nog veel mooie momenten samen mogen beleven, waaronder de 21e van december. Heit en mem, het is vast lastig geweest om een zoon te hebben die onbegrijpelijke dingen doet. Ik ben jullie zeer dankbaar voor de liefde die jullie altijd voor me hebben gehad en het geduld waarmee jullie mijn drukte tolereerden. Nu is het klaar, vier het met me mee, het is ook jullie succes!